Design And Control of a Photovoltaic-Based Standalone Off-Grid Electric Vehicle Charging Station

Divya Krishnan Nair

A Thesis submitted to

Auckland University of Technology

In fulfilment of the requirements for the degree of

Doctor of Philosophy (Ph.D.)

2023

School of Engineering, Computer and Mathematical Science

Abstract

The use of petroleum for transportation has resulted in significant environmental concerns such as fuel shortages and price surges, air pollution, climate change, etc. Consequently, many governments worldwide are promoting eco-friendly and low-emission alternatives such as electric vehicles (EVs), to reduce the dependence on fossil fuels and limit greenhouse gas (GHG) emissions. However, achieving sustainable transportation requires the integration of renewable energy sources and EVs, and a reliable and efficient charging infrastructure is crucial.

The exclusive reliance of EV charging systems on the grid as the sole power source poses a significant ecological challenge. Off-grid EV charging stations that depend on standalone renewable energy sources such as photovoltaic (PV) panels for power supply are gaining attention. However, uncontrolled charging can have a negative impact on the operation of the utility grid. Therefore, developing an effective and reliable off-grid EV charging infrastructure that can be deployed in remote areas or regions with limited access to the utility grid is necessary.

This study aims to design an efficient off-grid EV charging system powered by solar energy. The system will also achieve Zero Voltage Switching (ZVS) and Zero Current Switching (ZCS) by incorporating snubber circuits in bidirectional DC-DC converters (BDC). The research involves developing an optimal system for charging and discharging the standalone PV-based EV charging station, identifying problems to enhance the efficiency of standalone EV charging station, and exploring control techniques to optimize the performance of the charging station.

The off-grid EV charging system proposed in this work incorporates a BDC with the snubbers, a solar array, a boost converter, and an energy storage unit (ESU). This charging station uses droop and master-slave control techniques to manage the charging of multiple EVs while maintaining stable voltage and frequency levels. The combination of these control techniques simplifies the operation and maintenance of the charging system, resulting in a more cost-effective solution. The results show that the proposed system achieves ZVS and ZCS, improving the efficiency of the charging system while reducing switching losses.

The results of the study are essential for creating a reliable and efficient off-grid EV charging infrastructure, particularly in remote locations or areas with limited grid access. Additionally, the results from this study support the shift towards a more sustainable future by decreasing reliance on fossil fuels and reducing GHG emissions.

Declaration of Authorship

I hereby confirm that this work is entirely my own and was conducted during my enrolment at Auckland University of Technology. Additionally, I have appropriately acknowledged and referenced any information or ideas obtained from external sources. I assert that this thesis has not been previously submitted for any other degree or diploma at any other institution of higher education, to the best of my understanding.

Divya Krishnan Nair

June 2023

Acknowledgement

I am sincerely grateful to Auckland University of Technology (AUT) for the invaluable opportunity to pursue my doctoral studies. The exceptional academic environment, state-of-the-art facilities, and supportive faculty have shaped my research journey. The resources and opportunities provided by AUT were crucial to the successful completion of my PhD thesis.

I am sincerely grateful to Professor Krishnamachar Prasad, my primary supervisor, for his exceptional guidance, unwavering support, and commitment to academic excellence. His expertise and extensive knowledge have greatly influenced the direction and outcomes of my research, and his constructive feedback and dedication to my success have been invaluable. I would also like to express my heartfelt appreciation to Professor Tek Tjing Lie, my secondary supervisor, for his continuous support, valuable contributions, and insightful guidance that have enhanced the quality and depth of my work. Their presence has been instrumental in my journey towards achieving excellence.

I would like to express my sincere appreciation to the faculty members and staff at the School of Engineering, Computer and Mathematical Sciences at AUT. Their resolute dedication to excellence, collaborative ethos, and invaluable support have greatly enriched my academic journey and fostered my personal growth.

I cannot overstate the importance of my family, who have been a steadfast source of support, love, and understanding. Their belief in my abilities and the sacrifices they have made have been the pillars of my success. Their constant encouragement and unyielding strength have played a pivotal role in enabling me to pursue and complete this transformative doctoral journey.

Lastly, I am profoundly grateful for the blessings and divine guidance that have accompanied me on this journey, providing me with unwavering strength, wisdom, inspiration, and the determination to overcome obstacles and achieve my goals.

Table of Contents

List of Figures

List of Tables

List of Symbols and Abbreviations

K	Boltzman Constant
V_o	Output Voltage
ΔI_{EV}	Output of the Droop Control
H	Battery Efficiency
η_{ch}	Charging Efficiency
η_{dis}	Discharging Efficiency
Δi_L	Ripple Current
$\Delta V_0/V_0$	Output Voltage Ripple
C or C_s	Snubber Capacitor
$C_{BATTERY}$	EV Battery Capacitance
C_{EV}	Capacitor in the EV charger converter
C_0	DC Capacitor Bank
C_f	Capacitor in the Flyback Converter
C_1 and C_2	Buffer Capacitors
C_{f1} and C_{f2}	Filter Capacitors
C_c	Clamping Capacitor
C_{PV}	Array Capacitor
D	Converter's Duty Ratio
D_C	Duty Ratio Derived from Capacitors
D_{PV}	Duty Ratio Derived from Solar Panel
D_{clamp}	Clamping Branch Duty Ratio
E_{PV}	Solar Energy
E_{TOT}	Total Energy Capacity of all the Connected EVs
f_s	Switching Frequency
G	Solar Irradiance
G_{avg}	Average Solar Irradiance
i_{in}	Input Current

I_{EV}	Current in the EV charger converter
I_0	Diode Saturation Current
$i_{battery}$	Current Flowing through the Battery
I_d	Diode Current
$I_{ESU\text{-}ref}$	Reference Charging Current of ESU
$I_{EV\text{-}ref}$	Reference Charging Current of EV
i_L	Inductive Current
I_{PV}	Array Current
K_{droop}	Droop Gain for EV Charger Converter Control
K_{ESU}	ESU Droop Gain
L	Inductor
L_{boost}	Inductor in Boost Mode
L_{buck}	Inductor in Buck Mode
L_{EV}	Inductor in the EV charger converter
L_k	Leakage Inductance
L_{PV}	Array Inductor
l_r	Critical Point of Leakage Inductance
N	Transformer Turns Ratio
n_1	Diode ideality factor
N_{cell}	Number of Serial Cells in a Module
N_P	Number of Turns in the Primary Winding of the Transformer
N_S	Number of Turns in the Secondary Winding
$P_{BATTERY}$	Instantaneous Battery Power
P_{ESU}	ESU Power
P_{EV}	EV Consumption Power
P_{EV_i}	Demand of EV power at time slot i
$P_{EV_{req}}$	Maximum required EV power
P_{mpp}	Maximum PV Output Power

Q	Electronic Charge
Q	Battery Capacity
Q_0	Battery Initial Charge Stored
R_C	Resistor For Charging
R_D	Resistor For Discharging
R_S	Series Resistor
R_P	Parallel Resistor
S_i	EV connectivity status at time slot i,
SOC	State of Charge
SOC_0	Current State of Charge
SOC_{ESU}	SOC of ESU
$SOCL$	Lower SOC Limit
$SOCU$	Upper SOC Limit
t_d	Dead Time
T	Cell Temperature
T_{DR}	Conducting Time of Rectifier Diode
T_t	Total Period of the Switching Cycle
T_s	Period Of the Driving Signal for Each Bridge Switch
V_{bat}	Battery Voltage
V_{bus}	Nominal DC Bus Voltage
V_C	Capacitor Voltage
V_d	Diode Voltage
V_{f1} *and* V_{f2}	Voltages of the Capacitors (C_{f1} and C_{f2}) in the Boost Mode
V_{in}	Input Voltage of BDC
V_{OC}	Battery Open Circuit Voltage
V_{pri}	Volatage at primary side of the transformer
V_{PV}	PV Voltage
$V_{PV\text{-}ref}$	Reference PV Voltage

V_{ref}	Reference Voltage of the Isolated BDC with Snubbers
V_{sec}	Volatage at secondary side of the transformer
w_i	EV charging status at time slot *i*
^{0}C	Degree Celsius
A	Ampere
AC	Alternating Current
Ah	Ampere-Hour
AI	Artificial Intelligence
AM	Ante Meridiem
APF	Active Power Filtering
BDC	Bidirectional DC-DC Converter
BESS	Battery Energy Storage System
BESU	Battery Energy Storage Units
BEV	Battery Electric Vehicle
BIPV	Building-Integrated Photovoltaic
BMS	Battery Management System
BMW	Bayerische Motoren Werke Aktiengesellschaft
BSS	Battery Swapping Stations
CAN	Controller Area Network
CCM	Continuous Conduction Mode
CCS	Combined Charging System
CHAdeMO	Charge De Move
CO_2	Carbon dioxide
D1 - D8	Diodes
DAB	Dual Active Bridge
DC	Direct Current
ESU	Energy Storage Unit
EV	Electric Vehicle

EVCS	Electric Vehicle Charging Station
EVSE	Electric Vehicle Supply Equipment
FC	Fuel Cell
FCEV	Fuel Cell Electric Vehicles
G2V	Grid To Vehicle
GHG	Greenhouse Gas
HEV	Hybrid Electric Vehicles
HV	High Voltage
ICE	Internal Combustion Engines
ICEV	Internal Combustion Engine Vehicles
IEA	International Energy Agency
IEC	International Electromechanical Commission
IEEE	Institute of Electrical and Electronics Engineers
IGBT	Insulated-Gate Bipolar Transistors
K	Kelvin
LV	Low Voltage
M1-M8 and M_c	MOSFET Switches
MATLAB	Matrix Laboratory
MOSFET	Metal-Oxide-Semiconductor Field-Effect Transistor
MPC	Model Predictive Control
MPP	Maximum Power Point
MPPT	Maximum Power Point Tracking
MW	Megawatt
NREL	National Renewable Energy Laboratory
NZD	New Zealand Dollars
OBC	On-Board Charger
OCV	Open-Circuit Voltage
OGCS	Off-Grid Charging Station

P&O	Perturb and Observe method
PCC	Point Of Common Coupling
PEV	Plug-In Electric Vehicles
PHEV	Plug-In Hybrid Electric Vehicles
PI	Proportional Integral Control
PIC	Power Information Collector
PID	Proportional Integral Derivative Control
PV	Photovoltaic
PWM	Pulse-Width Modulation
RCD	Resistor-Capacitor-Diode
RES	Renewable Energy Sources
REV	Range-Extended Electric Vehicles
S or S_1 and S2	Switches
S2G	Station to Grid
SAE	Society Of Automotive Engineers
SCC	Short-Circuit Current
UK	United Kingdom
US	United States
V	Volt
V2G	Vehicle To Grid
VMM	Virtual Machine Monitor
W	Watts
Wh	Watt-hour
W_p	Watts peak
ZCS	Zero Current Switching
ZVS	Zero Voltage Switching

Chapter 1 Introduction

1.1Background

The concept of Electric Vehicles (EVs) can be traced back to 1832, when the first prototypes were developed. During the early 1900s, EVs gained significant popularity, particularly in commercial settings. They were quieter, cleaner, and easier to operate than vehicles with internal combustion engines (ICEs). However, factors such as the rapid improvement of ICE technology, the cheap and abundant availability of fossil fuels, and the limitations of battery technology contributed to the decline of EVs in the following decades. EVs became less competitive and less attractive to consumers who preferred faster, cheaper, and more powerful vehicles [1].

However, in recent years, EVs have experienced a resurgence of interest and demand due to growing awareness and concern about the environmental and economic impacts of fossil fuel consumption [2]. The electrical and transportation industries are the two largest sources of CO_2 emissions globally, accounting for 13.13 billion metric tons and 7.29 billion metric tons, respectively in 2021[3], [4]. Greenhouse gas (GHG) emissions, which are primarily caused by CO_2 emissions, are a significant factor in the acceleration of global warming and the resulting climate change. Moreover, fossil fuel dependence poses serious challenges for energy security and geopolitical stability as many oil-producing countries are politically unstable or hostile.

The electrification of transportation, enabled by EVs, has the potential to offer a solution to transportation challenges. EVs can effectively reduce CO_2 emissions by utilizing electricity from sustainable sources such as wind or solar power, rather than relying on fossil fuel combustion. Additionally, EVs can enhance energy independence by reducing reliance on foreign oil imports.

Governments, automakers, and researchers have recognized the benefits of EVs and have invested heavily in developing and promoting them. In 2020, the International Energy Agency (IEA) reported that 10 million EVs were sold worldwide, with China having the largest fleet of 4.5 million EVs, followed by Europe with 3.2 million EVs. The IEA projects that if the newest cars sold after 2040 are electric, there could be more than one billion EVs on the road by 2050 [3].

The rise of EVs presents numerous opportunities for the power industry as they are gaining popularity as a means of reducing emissions and saving energy. Developing and building EV Charging Stations (EVCS) provide a significant potential for power storage. The transport sector contributes 23% to worldwide GHGs emissions, making EVs a viable alternative. A strategic approach must be considered when constructing charging infrastructure, including where charging stations will be placed, what technologies will be used, and how slow-smart charging can be maximized to serve consumers efficiently [5].

Compared to vehicles powered by an ICE, EVs offer several benefits, including high engine efficiency (90-95% for EVs compared to 17-21% for ICE vehicles), zero tailpipe emissions, less maintenance, and economic savings (EVs cost $3 for a 100 km journey compared to $40 for ICE cars in New Zealand). However, the scarcity of charging infrastructure is a significant challenge, preventing widespread adoption of EVs [6].

The New Zealand government has launched an NZD 70 million sustainable development plan to promote the adoption of EVs and phase out fossil fuel vehicles by 2050. The plan includes measures such as providing zero-cost overnight charging, improving accessibility of charging infrastructure, equipping parking lots with charging stations, and building homes suitable for EVs. While the government's efforts support EV adoption, the increasing demand for EV charging puts pressure on the electric grid, leading to undesirable peaks, transformer overload, increased losses, voltage deviations, and operational costs. A possible solution to this problem could be the development of standalone off-grid EVCS that can significantly reduce CO_2 emissions [7].

The transportation sector is a major contributor to GHG emissions and air pollution in New Zealand, contributing to around 17% of the country's total GHG emissions and 39% of its domestic CO_2 emissions. Encouraging the adoption of EVs can result in a variety of benefits, including a decrease in emissions, enhanced travel choices and accessibility, improved health and safety, and alleviated traffic congestion. The New Zealand government has partnered in the co-funding of 1,000 public chargers and is actively working on enhancing the charging infrastructure to make it accessible, affordable, convenient, secure, and reliable for all residents of New Zealand. In addition, the government is working on a program to improve EV-charging infrastructure,

which involves coordinating policy, investment, and stakeholder engagement, devising a national strategy for EV-charging infrastructure, and reviewing safety regulations associated with charging EVs [7].

The environmental impact of EVs largely depends on how they are charged, with emissions not being zero if charged from a grid mostly fueled by fossil fuels. EVs can be powered by various renewable energy sources (RES) such as solar, wind, hydropower, geothermal, biogas, or tidal energy. Among these, using photovoltaic (PV) panels to fuel EVs is an attractive solution for several reasons such as low maintenance, quiet operation, and no moving components. PV power is highly accessible to EV owners since solar panels can be installed on roofs and in parking lots, close to where EVs would be parked. Solar energy's cost per kWh has been steadily declining over the past few decades and is currently quite low when compared to other RES and is shown in Fig. 1.1. In 2021, the five major renewable sources produced around 28 percent of the world's power altogether, with solar finally surpassing the 3.7% share barrier. New solar plants are now substantially cheaper to build and operate over a longer period than new coal plants with the cost of energy of solar plants being almost one-fifth that of coal plants ($167 per MWh) [8].

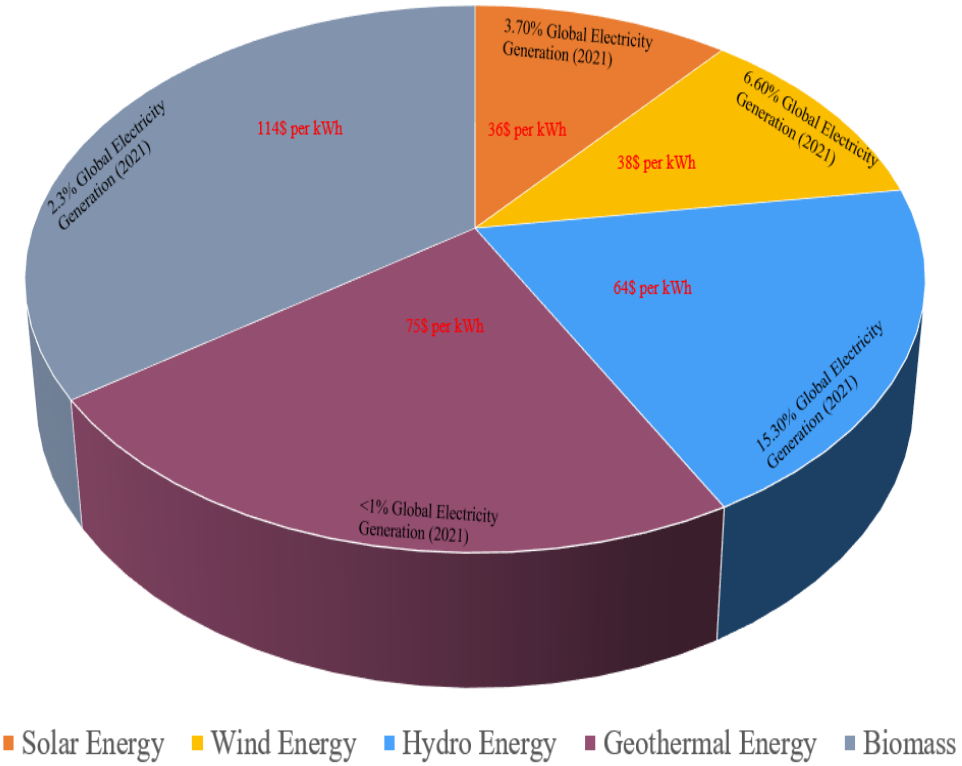

Lead Source: Global Electricity Review, 2022, U.S. Department of Energy, Our World in Data, IEA

Figure1. 1 Cost per kWh and Global Electricity Generation by different RES [8].

In conclusion, the promotion of EVs and the development of EV charging infrastructure by the government can significantly contribute to reducing GHG emissions and promoting a greener future. However, it is crucial to ensure that the electricity used to charge EVs is sourced from RES. The concept of PV-based stand-alone off-grid EVCS can be a viable solution as it offers several benefits such as low maintenance, accessibility, and cost-effectiveness. As the world shifts towards a more sustainable future, it is essential to adopt innovative solutions like PV-based stand-alone off-grid EVCS to promote sustainable transportation and reduce our carbon footprint.

1.1.1 The Concept of PV-based Stand-alone Off-grid EVCS

Access to energy is a basic human right, but about a billion people in Sub-Saharan Africa and Asia lack access to electricity due to limited traditional power sources. Off-grid technology can address these challenges and promote the growth of rural communities. Renewable energy technologies are increasingly becoming more affordable and the sun, as an abundant source of energy, can be captured sustainably for power generation and transportation. The combination of off-grid EVCS and PV-based RES has enormous potential to reduce CO_2 emissions and promote the adoption of EVs worldwide. PV-based EVCS are more promising than wind-based stations, with several advantages such as being cost-effective, having limited power electronic devices, and enhanced reliability. Consequently, the increasing demand for sustainable charging solutions has resulted in a significant trend towards the deployment of PV-powered DC fast-charging stations. Such stations usually consist of several components, such as an Energy Storage Unit (ESU), multiple DC-DC power converters, EV chargers, and PV arrays. Standalone solar-powered charging stations are the most practical way to increase EV adoption internationally in an environmentally friendly manner without impacting the current power infrastructure [9], [10].

Off-grid charging stations, such as the DeGrussa Solar Farm and Robben Island's Microgrid, have demonstrated their effectiveness in providing EV charging services while reducing diesel consumption and CO_2 emissions [11]. In the United Kingdom, "pop-up" charging centres powered by solar farms and energy storage technology will be tested in remote locations as part of a £6.6 million collaborative effort [12]. Solar energy and off-grid EVCS are an ideal combination, especially with the expected rise in electricity costs. The Tesla, BMW, and Sun

Power aims to promote electric mobility, with solar energy and off-grid EVCS being a noteworthy undertaking [13]–[15].

The New Zealand Government has plans to accelerate the development of renewable electricity generation. This will involve generating more electricity from low-emission technologies such as wind and solar. Several key initiatives have been put in place, including the review of national direction tools, the development of regulatory settings, the support of renewable and affordable energy in communities, and the ensuring of the electricity system and market can support high levels of renewables [16].

In conclusion, off-grid technology powered by RES such as solar energy has enormous potential to provide energy access to remote communities and promote sustainable transportation. Pairing off-grid EVCS with PV energy presents an affordable and eco-friendly approach to encourage the use of EVs on a global scale. The development of renewable electricity generation and low-emission technologies can accelerate the transition toward a cleaner and more sustainable future.

1.1.2 An Efficient Framework for Off-grid EV Charging Using PV Energy

A standalone PV-fed charging station, as shown in Fig. 1.2, can provide remote charging facilities for EVs, making it an excellent solution for long-distance travelers and tourists in areas without grid infrastructure.

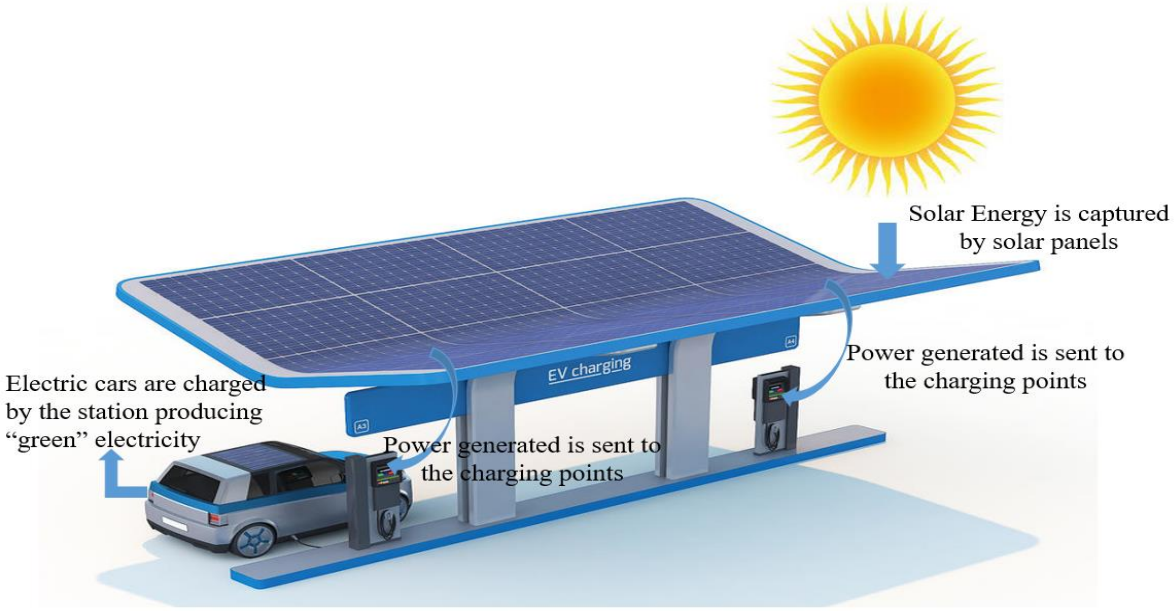

Figure1. 2 PV-based off-grid EVCS.

The PV-based off-grid EVCS operates entirely on renewable energy, making it completely independent of possible power disruptions from power companies and their potential price increases. Solar energy from the sun is harnessed by the solar panels, which then transmit the generated power to the charging points located at the EVCS. EVs are charged at these points, utilizing the green electricity produced by the PV system.

Figure 1.3 illustrates the complete framework of the PV-based off-grid EVCS, used in this research, which showcases its ability to accommodate up to five EVs simultaneously. As a self-sustaining off-grid power plant, the proposed EVCS consists of a battery and a solar power system that can provide the necessary energy for EV charging. It comprises a battery and a solar power system, connected to the common bus through an isolated bidirectional DC-DC converter (BDC) and a boost converter. While the PV panels serve as the main energy source, the battery also acts as a backup source, storing excess energy from the PV panels and providing energy to the EV load.

Since the solar irradiation is unpredictable, the energy available for EV charging can be erratic and inconsistent. The most effective way to solve this issue is by deploying ESUs to store surplus energy and ensure that charging continues even during situations when there is no energy generation due to insufficient sunlight or dark conditions. The ESU is refueled by solar energy when no EVs are present and charged and discharged using a power electronic circuit employed in the EVCS.

The connection between the PV system and the 400V DC bus is established through a DC-DC boost converter, as shown in Fig. 1.3. Power transfer between the battery and the solar panel system is facilitated by an isolated BDC equipped with both active and passive snubbers. In addition, an isolated BDC, which includes a battery storage system and active and passive snubbers, is used to maintain the DC bus voltage close to its nominal value under varying operational conditions [17].

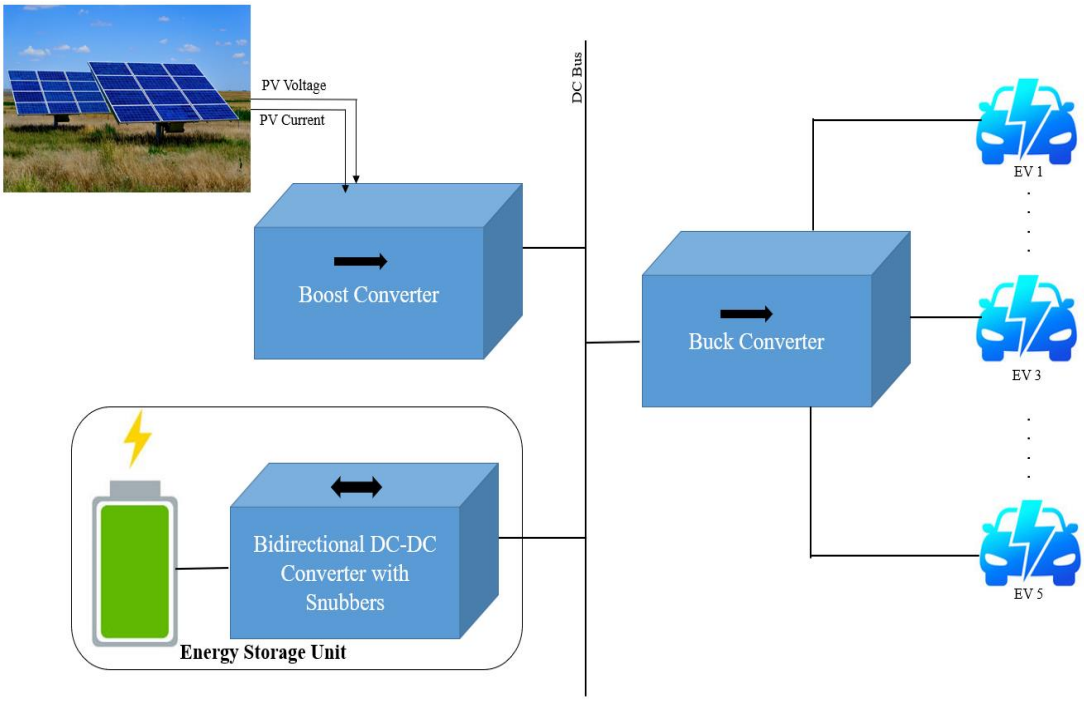

Figure1. 3 Comprehensive Model of the PV-based off-grid EVCS.

The charger circuit's performance is influenced by several factors such as the converter type, components, control strategies, switching methods, and overall implementation cost. An isolated BDC is utilized, equipped with snubbers, to control the charging and discharging process of the battery within the ESU. However, most BDCs that use a transformer and soft-switching techniques suffer from limitations such as increased switching loss and current stress. This will lead to difficulties in achieving near Zero Voltage Switching (ZVS) and Zero Current Switching (ZCS), thereby leading to reduced overall efficiency.

In this thesis, the issue is addressed by the design of a new BDC that incorporates both an active snubber and two passive capacitive-diode snubbers. This design allows for near ZVS and ZCS on the switches located on either side of the transformer, resulting in reduced voltage and current stresses, and improved overall efficiency for the EVCS. By utilizing different current densities of the leakage inductance and low-voltage side-fed inductor currents, the proposed system configuration clamps the rail voltage and minimizes current spikes at the converter switches.

While EVs offer a greener and more sustainable transportation option, charging stations can pose several challenges. The charging of EVs can potentially strain the current grid infrastructure and result in a substantial increase in carbon emissions, depending on the charging source employed.

Developing an off-grid charging infrastructure combined with PV panels is a potential solution to tackle these inadequacies. Nevertheless, the limited adoption of PV-ESU-EV systems can be attributed to challenges such as limited access to charging infrastructure and increasing concerns about range anxiety. Moreover, the development and proliferation of these technologies in the broader market face obstacles due to political and societal factors, especially in developing countries with diverse applications.

Despite the obstacles, developing a distributed PV-ESU-EV infrastructure seems to be the most viable solution to drive economic growth, create employment opportunities, promote sustainability, and enhance the global climate. As they say, the night is darkest before sunrise, and this applies to the EV industry as well. Therefore, it is crucial to address the challenges and overcome them to fully realize the benefits of EVs and PV-ESU-EV systems [5], [17], [18].

1.2 Motivation

The demand for petroleum for transportation has caused serious environmental concerns due to fuel price surges, air pollution, and climate change. Governments have urged automobile manufacturers to create eco-friendly and low-emission alternatives like EVs, which reduce dependence on fossil fuels and minimize GHG emissions. Many countries are encouraging EV adoption through funding and policies. It is projected that by 2050, all EV fleets will be powered by RES, and the growing popularity of EVs can be attributed to advancements in battery technology and charging infrastructure.

However, the overall charging infrastructure is critical to promoting the use of EVs. One significant drawback of EV charging systems is their dependence on the grid as the sole power source, and this is not eco-friendly. RES, on the other hand, provides a distributable and time-bound energy source that can be used to power EVs. Thus, the integration of RES and EVs is essential to ensure a sustainable future for transportation.

While many studies have investigated the impact of large-scale implementation of EVs on the utility grid, off-grid EVCS remains an area of research that is still vastly under explored. These charging stations are not connected to the utility grid and rely on standalone RES, such as PV

panels, for their power supply. The use of off-grid EVCS will limit the grid's influence, but high penetration of uncontrolled charging can increase peak power demand and affect the utility grid's operation.

Majority of existing research on PV-EV-based charging stations mostly focuses on theoretical studies with few demonstrations where they have implemented PV array-based EVCS [10], [19]. Most studies that have investigated PV-EV-based charging stations have assumed ideal ZVS and ZCS characteristics, which is far from reality.

Research work done in this thesis seeks to bridge these research gaps by examining the effectiveness of a self-contained solar-powered EV charging station in achieving ZVS and ZCS features at the primary switches of the bidirectional converter. The research involves implementing an active and passive snubber system in the BDC of an EVCS to minimize both voltage and current stresses at the primary switches, with the aim of achieving ZVS and ZCS properties.

Such a study has not been carried out to the best of our knowledge, and it is believed that the proposed research will lead to improved performance of bidirectional converters used in EVCS. By investigating the use of snubber circuits to improve off-grid PV-based EV charging, the proposed research aims to develop a more efficient and reliable charging infrastructure that can be deployed in remote locations or areas with limited access to the utility grid.

The proposed study has three main research questions to achieve its goals. The first question pertains to designing an optimal system for charging and discharging a standalone PV-based EV charging station. This question involves exploring the design of a solar PV-based charging station that can efficiently charge and discharge EVs while minimizing the impact on the utility grid.

The second research question is focused on improving off-grid PV-based EV charging by incorporating snubber circuits for BDCs. The objective of this work is to explore the utilization of active and passive snubber circuits for the purpose of diminishing voltage and current stresses at the primary switches of the BDC. The study will assess the feasibility of using such circuits in

practical applications and explore their impact on the performance and efficiency of the charging station.

The third research question concerns the identification of problems that could be addressed to improve the efficiency of a standalone EVCS and the exploration of control techniques that can be used to enhance its performance. This question involves exploring various control techniques, such as droop and master-slave control, to enhance the efficiency and effectiveness of the charging station. The study will investigate the impact of these control techniques on the charging station's stability, reliability, and efficiency.

In summary, the proposed research aims to develop a more efficient and reliable off-grid EV charging infrastructure that can be deployed in remote locations or areas with limited access to the utility grid. The study's findings will contribute to the development of sustainable transportation systems and support the transition toward a cleaner and greener future.

1.3 Thesis Contribution

The primary focus of this thesis is to explore the potential of off-grid EV charging infrastructure using standalone solar-powered EVCS equipped with snubber circuits for BDCs. The proposed research aims to assess the viability of integrating active and passive snubber circuits for BDCs as a means of improving the efficiency and reliability of off-grid EV charging. Furthermore, this study strives to design a charging and discharging system for a standalone PV-based EV charging station, analyze the effects of integrating snubber circuits on off-grid PV-based EV charging, and detect potential issues that could be resolved to enhance the effectiveness of a standalone EVCS. Additionally, the research will investigate several control techniques, including droop and master-slave control, to optimize the performance of the charging station. This study uses MATLAB/Simulink for modeling and simulation to ensure that the off-grid EVCS is designed and optimized in accordance with the research objectives. The discoveries made in this study will aid in the advancement of eco-friendly transportation systems and facilitate the shift towards a more sustainable and environmentally conscious future. This thesis will contribute to fundamental academic knowledge in the area of off-grid EV charging infrastructure. The results from this work/thesis have led to the publication of following articles in peer-reviewed journals.

Krishnan Nair, D.; Prasad, K.; Lie, T.T. "Standalone Electric Vehicle Charging Station Using An Isolated Bidirectional Converter With Snubber," Energy Storage, p. e255, 2021, https://doi.org/10.1002/est2.255.

Krishnan Nair, D.; Prasad, K.; Lie, T.T. "Implementation of Snubber Circuits in a PV-Based Off-Grid Electric Vehicle Charging Station—Comparative Case Studies". Energies 2021, 14, 5853. https://doi.org/10.3390/en14185853.

Krishnan Nair D, Prasad K, Lie TT. "Design Of A PV-Fed Electric Vehicle Charging Station With A Combination Of Droop And Master-Slave Control Strategy". Energy Storage. 2023; e442. https://doi:10.1002/est2.442.

1.4 Objectives of the Thesis

The primary objectives of this thesis can be listed as follows:

• To create a solar-powered charging station for EVs that can effectively charge and discharge EVs while reducing its impact on the utility grid.

• To evaluate the feasibility of using active and passive snubber circuits in BDCs to minimize voltage and current stresses and determine their practical application.

• To analyze control techniques like droop and master-slave control to enhance the efficiency and performance of the charging station and simulate the design using MATLAB/Simulink to optimize the system.

1.5 Thesis Organization

This thesis is divided into multiple chapters.

Chapter 1 is an introduction to the thesis and outlines the research objectives and motivations behind the study. It helps readers quickly grasp the challenges and difficulties involved in off-grid EVCS.

Chapter 2 presents a literature review on EVCS, analyzing earlier works and considering related factors such as PV panels, maximum power point tracking (MPPT) models, BDCs, battery models, snubbers, and control techniques like droop and master-slave control.

Chapter 3 covers the various types of charging stations for EVs. This chapter also delves into charging levels and the corresponding charging times, as well as the different designs of charging stations. The information provided in this chapter is crucial for understanding the infrastructure required to support the widespread adoption of EVs.

Chapter 4 examines the environmental consequences of EVs and the grid infrastructure and suggests an alternative approach that employs solar energy-based charging infrastructure for EVs. In particular, a fast-charging station that comprises a PV system, a boost converter, a BDC that integrates snubber circuits, and an ESU. The chapter details how the inclusion of snubber circuits can increase converter efficiency and achieve near-zero voltage and current switching. The effectiveness of the proposed system is demonstrated through simulation results.

Chapter 5 describes the importance of utilizing solar-based charging infrastructure for EVs and proposes an off-grid charging station that incorporates a bidirectional converter with a zero-voltage switching snubber, a solar array, a boost converter, and an ESU. In this chapter, various types of snubbers such as resistive-capacitive-diode snubbers, active clamp snubbers, and flyback snubbers are investigated, and the results are described in detail.

Chapter 6 presents a unique control scheme for EVCS that combines droop and master-control strategies to enhance their effectiveness. It also introduces a bidirectional isolated DC-DC converter with snubber circuits and a three-level booster converter that incorporates a capacitance-voltage control design to improve the system's stability. The proposed design is verified through simulations, and a comprehensive discussion is provided. The EVCS design is formulated and validated using MATLAB/Simulink.

Chapter 7 summarizes the main contributions of the research work conducted and draws conclusions from this research. The chapter concludes by presenting potential future work in the field of off-grid PV-based EVCS.

Chapter 2 EV Charging Infrastructure – A Literature Review

In recent times, the increasing apprehensions about climate change and environmental sustainability have led to a surge in the utilization of RES. Among these sources, PV technology has become increasingly popular for capturing solar energy. The proposed research work aims to investigate the feasibility of using PV technology for EV charging infrastructure. An extensive review of recent academic and commercial literature will be conducted as a first step in achieving this goal to determine the advantages and disadvantages of PV-powered charging systems for EVs. The ultimate objective is to identify the most efficient system architecture, power converter topology, modularity implementation, and EV charging standards. The results from the proposed research will contribute to the expanding knowledge base on environmentally friendly EV charging infrastructure and facilitate the development of more sustainable transportation networks.

2.1 EV Technology

EVs have been in existence since the 19th century when Davidson invented a non-rechargeable electric carriage in 1832 [1][20]. In 1859, rechargeable lead-acid batteries were developed by French scientists, which opened new opportunities for EV development. However, the commercial use of EVs declined with the rise of gas-powered cars in the 1920s [1][20]. Battery technology limitations also hindered EV adoption until nickel-metal hydride and lithium-ion batteries were developed [1][20].

For more than six decades, gas-powered cars continued to progress as gasoline was cheap and readily available. But in the late 1960s, gas prices surged, and there was a growing awareness of air pollution. Concerns about energy crises and environmental pollution spurred R&D efforts in EV technology. In 1975, the US Postal Service promoted the use of EVs by introducing 350 electric delivery jeeps from the company AM General. Though Americans tried to incorporate electric power into automobiles in the form of hybrids, the breakthrough in EV adoption came from Japan with the introduction of the commercially mass-produced and marketed hybrid car, Toyota's Prius, in 1997. Other manufacturers followed suit, and hybrids became increasingly popular [1][20].

The emergence of Tesla's Roadster in 2008, along with the progress in battery technology, has expedited the growth of Battery Electric Vehicles (BEVs) in recent times. Major automotive manufacturers like BMW, Nissan, and Mitsubishi have made significant strides in EV development. Nissan introduced the Leaf, the world's best-selling EV in 2009. Tesla, on the other hand, has become a key player in the EV market by introducing a new model every year. In 2021, the company unveiled the Model Y, the world's best electric compact crossover utility vehicle [1][20].

Despite having a long history, EVs are still regarded as an innovation in the automobile industry. With sustainability becoming a top priority, the adoption of EVs is expected to rise rapidly in the coming years.

2.2 EV Architectures

EVs of today utilize different architectures in their construction and design for power generation. The four main types of EVs are BEVs, Plug-in Hybrid Electric Vehicles (PHEVs), Hybrid Electric Vehicles (HEVs), and Fuel Cell Electric Vehicles (FCEVs) as shown in Fig. 2.1. It is important to note that each architecture is unique in its features and advantages, making it suitable for various applications and uses. Generally, BEVs are ideal for short-distance commutes and city driving, while PHEVs are more suited to longer-distance driving. FCEVs are a new technology that use hydrogen fuel cells to generate electricity, providing zero-emissions driving.

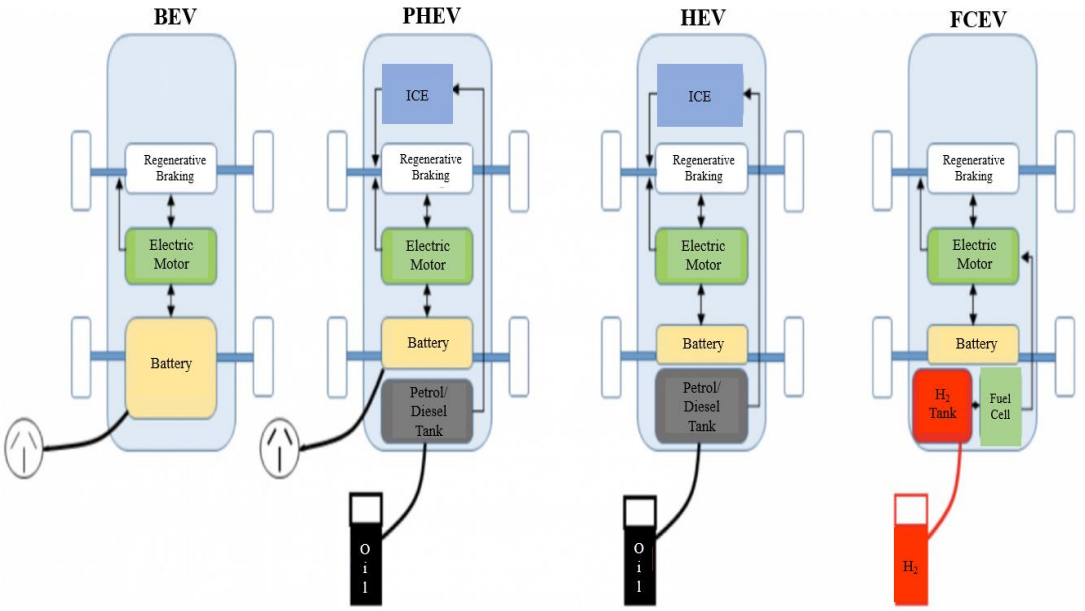

Figure 2. 1 EV Topologies available today [21].

BEVs rely entirely on battery technology to store energy, resulting in zero emissions during operation. However, the current limitations of on-board battery technology make BEVs less attractive than Internal Combustion Engine Vehicles (ICEVs) in terms of economics and driving range. This is because batteries with high power densities, but low energy densities, require longer charging times, even with fast charging technologies. The primary hurdles that BEVs face are a restricted driving range, a high initial cost, and inadequate charging infrastructure.

In PHEVs, an ICE or another propulsion source is used in conjunction with batteries and other fuels such as gasoline or diesel. The charging equipment, along with regenerative braking, can effectively charge the batteries of the PHEVs. This leads to a decrease in fuel consumption and operating expenses when compared to traditional ICE vehicles. The amount of emission produced by PHEVs depends on the electricity source and the frequency of operation in all-electric mode. It is possible that PHEVs may result in lower emissions.

HEVs combine both gasoline/diesel-powered ICEs and electric motors as driving power sources. HEVs can be categorized into two types: conventional HEVs and grid-HEVs, which are distinguished by their respective refuelling or recharging methods. Conventional HEVs can be further categorized as micro, mild, or full HEVs based on the combination level, while grid-able HEVs include PHEVs or range-extended electric vehicles (REV).

FCEVs emit zero pollutants during operation due to the use of fuel cell (FC) technology. FCs are electrochemical devices that produce DC electrical energy through a chemical reaction. FCEVs are comparable to ICEVs in terms of driving range and can be applied in various scenarios from small-scale plants to small power plants. However, the high initial cost and lack of refuelling stations are significant challenges for the success of FCEVs. Additionally, the reliability of electricity supply from FCs is lower than that of conventional batteries used in EVs [21].

EVs contain many internal components, and it is important to understand the precise location of the charger before discussing charging stations. EVs are equipped with an On-Board Charger (OBC) and a charger designed for use by the customer to charge their EV at home or from a power outlet. These chargers are often basic and can take up to 8 hours to charge an EV [22], [23].

2.3 Electric Vehicle Charging Station (EVCS)

Multiple research studies have been conducted to analyze the influence of EV charging infrastructure on the power grid and the integration of RES. According to these studies, the amount of power taken from the grid is reliant on factors such as the number of EVs being charged, charging rates, charging start and end times, and the initial state of charge (*SOC*) of EV batteries.

The uncertainty associated with the initial *SOC* and charging start times can pose challenges for the grid's existing infrastructure as the increase in power demand can cause voltage imbalances, harmonics, and voltage sags. Upgrades to transformers, power transmission lines, and security settings are necessary to meet power transfer constraints. However, some research studies have proposed solutions such as optimal distribution of EV loads during off-peak periods to reduce the impact on the grid. Additionally, using the electric grid power for both grid to vehicle (G2V) and vehicle to grid (V2G) technology can also help to alleviate the grid impact. To perform both modes of operation, a bidirectional charger is necessary for the grid-connected EV charger [24]. Fig. 2.2 shows the typical configuration of an EV connected to the grid.

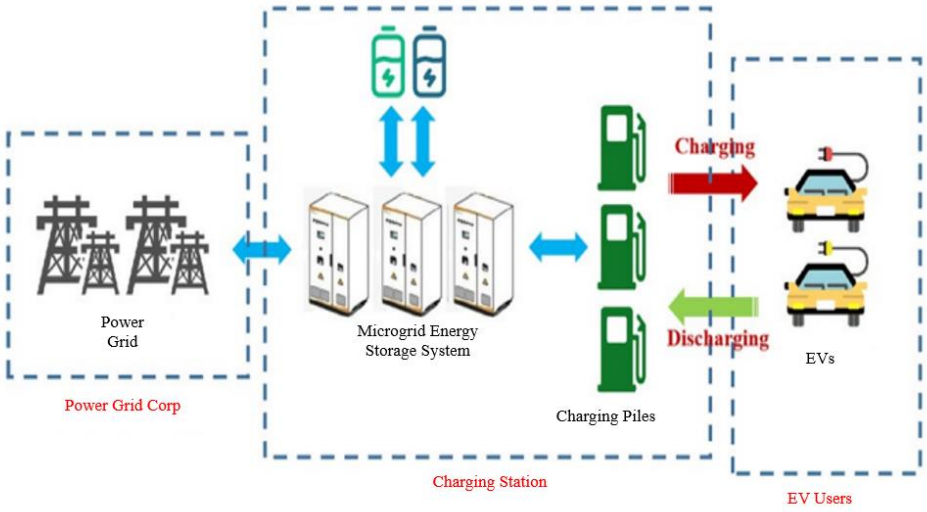

Figure 2. 2 Grid-connected EV Charging Station [24].

The usage of fossil fuels for grid-connected bidirectional chargers results in environmental pollution [25]. It is a misconception that people believe EVs have zero CO_2 emissions. However, generating electricity from carbonizing sources, such as coal and gas, results in significant CO_2 emissions. Using RES as a charging strategy for EVs could potentially transform the process into an economically and environmentally sustainable option, thereby reducing its negative impacts [26].

According to Biya *et al.*[27], the rise of global warming has made EVs a popular choice as a replacement for ICEs. However, the conventional method of charging EVs with fossil-fuel-based grid power is becoming less efficient and less cost-effective as the number of EVs on the road increases. Therefore, it is essential to explore renewable energy-based EV charging stations that can optimize power management. One potential solution to address the challenges associated with EV charging infrastructure on the power grid is the implementation of a charging station that integrates PV power and a Battery Energy Storage System (BESS) along with grid support. Incorporating various strategies, including MPPT, Proportional Integral Derivative Control (PID,) and current control, a charging station design can effectively manage the power supply and utilization between solar, BESS, grid, and EVs, thereby ensuring uninterrupted power supply and a seamless charging experience for EVs. MATLAB/Simulink simulations have been performed

to validate the power management and design of the station, considering two EV charging scenarios and five modes of operation. The proposed charging station design is robust, and the algorithm is scalable and can be adapted for use in larger power ratings and capacities, making it an ideal solution for EV charging in workplaces and parking lots.

Feasibility studies conducted by Tang *et al.*[28] concluded that grid connected EVs have cost compensations in the short term. According to a study conducted by Bokopane *et al*. [29], designing a charging station that relies on RES was the most effective solution for a remote area in the Democratic Republic of Congo. The study also found that charging multiple vehicles consecutively at full capacity was the optimal functional scenario. According to Richardson's analysis of current research on EVs, electric grids, and renewable energies, the increased use of EVs could have a positive impact on the electrical network by reducing negative consequences and increasing the use of renewable energy [30].

Several publications support PV-based EV charging stations. Khan *et al.*[31] proposed analytical approaches for collecting data on EV charging patterns, charging station operational modes, and the geographical locations of charging station users. Tulpule *et al.* [32] proposed a profitable PV-based charging station that utilizes solar energy to reduce the grid burden on charging. Zhang *et al.* [33] and Zhao *et al.* [34] have documented a PV-driven charging station equipped with a BESS. However, all these research works fail to address the potential voltage and current stresses that may and will impact the main switches.

Chowdhury *et al.* [35] conducted a life cycle assessment of an EV-PV charging station and reported positive results, indicating that it is an effective strategy for reducing GHG emissions. One common strategy recommended by these researchers to address the uncertainties associated with PV involves the use of a battery storage system that is separate from the EV batteries [36]. Castello *et al.* [37] conducted a comparative analysis of various algorithms to optimize the battery storage system's operating parameters. They concluded that the best approaches include utilizing a sigmoid function-based discharging algorithm and charging EVs during the night while storing excess PV.

Kumar *et al.* [38] introduced an off-grid charging station (OGCS) to increase the utilization of EVs in remote locations and reduce the burden on urban grids. The OGCS obtains energy from RES, with PV being the most suitable due to its abundance and ease of installation. Nevertheless, PV energy production is subject to fluctuations in irradiance and cannot provide a constant energy output. Therefore, they incorporated an energy storage system alongside the PV source and EV charger. This setup consists of a PV array integrated with a boost converter, as well as two bi-directional converters and an energy storage system. The bi-directional converters play a vital role in enabling the charging and discharging of both the EV and the energy storage system. Additionally, the energy storage system serves to fulfill energy demands when the PV generation is inadequate. Conversely, excess energy generated by PV is stored in the BESS, making the system more stable. However, the researchers utilized a bridge-type bi-directional converter that failed to achieve near ZVS and ZCS. As a result, the converter's main switches were subjected to voltage and current stresses, ultimately diminishing the EV charging station's overall efficiency. The results of this study are described in detail in Chapter 4.

Doubabi *et al.* [39] examined the importance of charging infrastructure as a key factor for promoting the adoption of EVs. The researchers proposed an off-grid charging infrastructure powered by PV energy for e-scooters. Six charging stations were installed at Cadi Ayyad University in Marrakesh, Morocco, as part of their proposal. The EV charging station relied on solar power, making it an eco-friendly and sustainable choice for transportation.

The authors explained the EV charging station's components and presented a power management approach that effectively allocated energy among the PV array, battery storage, and loads, even under diverse operating conditions. They utilized MATLAB/Simulink simulations to demonstrate the energy management strategy's efficacy. The study showed that the charging station can reduce CO_2 emissions by almost 1154.21kg/year.

Atawi *et al.* [40] proposed an EVCS that operates independently and uses solar energy as a power source. The operation of charging stations may place considerable pressure on the utility grid. An approach to address this issue involves implementing independent charging stations that utilize RES. However, designing these systems can be complex. Their work introduces a straightforward

design for a standalone PV-powered charging station. The design encompasses equations for each system component, accompanied by case-study design calculations. They used MATLAB/Simulink to model and simulate the system, and an experimental setup was constructed to validate the simulation results. The set-up includes a PV panel, a boost converter, an energy storage system with batteries, two DC-DC charging converters, and an EV battery. Three controllers, including the MPPT, an EV charger, and a storage converter controller, are used to control the system. The simulations and experimental results demonstrated the consistent charging process of the EV battery even in the presence of PV insolation fluctuations. Additionally, the energy storage system battery exhibited excellent responsiveness in storing and compensating for variations in PV energy. The effectiveness of the design was demonstrated by the efficient current and voltage control of the converters, along with the precise tracking of peak PV conditions by the MPPT controller. Energy and power analyses were presented as helpful tools during the design phase and closed-form equations were derived to facilitate system design. The results demonstrated that their system was efficient and effective at different insolation levels.

Krim *et.al*. [41]studied the advantages of implementing solar energy in charging stations for EVs, with an emphasis on improving energy management. The objective of the research was to evaluate the economic feasibility and requirements of PV-powered charging infrastructures for EVs, as well as to propose a techno-economic tool to help local stakeholders manage and determine the size of the charging stations. The tool was developed in such a way that it can be easily used by individuals with varying levels of expertise. The optimization of PV-powered charging stations can be enhanced by exploring forecasting techniques and maximizing the utilization of PV energy. Their methodology and tool provide a valuable contribution to the development of sustainable and efficient charging infrastructure for EVs.

Mohamed *et al.* [42] proposed a new approach to overcome the technical limitations and take advantage of opportunities for renewable-powered EVCS in the UK. Their work highlights the importance of sustainable transportation to combat air pollution stemming from the transport sector and examines the challenges and benefits of EVs in reducing carbon emissions. They introduced two reflector-based solar PV systems for EVCSs, including a dual mono-facial PV

design with reflectors and a bi-facial PV design with parallel reflectors that can handle the solar radiation levels. They suggested an off-grid, self-sufficient DC mini-grid configuration powered mainly by RES, especially solar PV, to address the disruptions caused by significant loads with high power requirements, which can impact the stability of the grid. In addition, they suggested a fast-charging DC charging topology for two PV array configurations that use reflectors to enhance PV power generation. Their designs offer better conversion efficiency in terms of effective surface area and are suitable for PV-complemented EVCSs.

Existing literature on PV-based off-grid EV charging stations mainly focuses on system design [28]–[35], [37]–[42], V2G operations [24], [43], [44], energy management [35]–[37], [45], [46], and reducing electricity costs in smart homes [35]. However, these strategies do not consider abrupt system disturbances such as rapid changes in irradiance. Thang *et al.* [47] proposed a sliding mode control approach to address fast dynamic response issues and regulate the DC-bus output voltage in the presence of sudden system disturbances. However, the coordination of ESU and EV was not mentioned. Wu *et al.* [48] presented a coordinated control strategy to prevent ESU over-charging and over-discharging in standalone mode. However, the strategy did not account for any short-term disruptions in PV generation that could lead to insufficient charging power for EVs, which could potentially cause instability in the system. Some studies have put forth a decentralized control method that aims to synchronize the PV generation with ESU charging and discharging [49]–[52]. However, these studies did not analyze the impact of EV outages. Table 2.1, shows a summary of the main findings from various works discussed above.

Table 2. 1 Summary of Key Findings from References on Renewable Energy-Based EV Charging Stations.

Author(s)	**Main Findings**	**Reference**
Biya *et al.*	Renewable energy-based EV charging stations integrating solar power, BESS, and grid support can optimize power management and minimize environmental impacts.	[27]
Tang *et al.*	Grid-connected EVs have cost compensations in the short term.	[28]
Bokopane *et al.*	Charging multiple vehicles consecutively using a renewable energy charging station at full capacity was the best functional scenario.	[29]

Richardson	The use of EVs could promote renewable energy utilization while mitigating adverse effects on the power grid.	[30]
Khan *et al.*	Analytical methods have been proposed to gather data on EV charging patterns, charging station operation modes, and the location of charging station users for PV-powered EV charging facilities.	[31]
Tulpule *et al.*	A profitable PV-based charging station that utilizes solar energy to reduce the grid burden on charging has been proposed.	[32]
Zhang *et al.*; Zhao *et al.*	A charging station with solar panels and a BESS been proposed.	[33] and [34]
Chowdhury *et al.*	The life cycle analysis of an EV-PV-based charging station is positive, depicting a promising and effective GHG emission reduction strategy.	[35]
Castello *et al.*	PV uncertainty can be mitigated by implementing a sigmoid function-based discharging algorithm and charging EVs during the night while storing excess PV.	[37]
Kumar *et al.*	Proposed an OGCS that utilizes PV as the primary RES due to its abundance and easy installation. The system comprises a PV array with a boost converter, two bi-directional converters, and an energy storage system to meet energy demands when PV generation is inadequate.	[38]
Doubabi *et al.*	Proposed OGCS for e-scooters using solar power and power management strategy for efficient energy distribution.	[39]
Atawi *et al.*	Standalone PV-powered EV charging station proposed with efficient design: PV panel, boost converter, energy storage system, 2 DC-DC charging converters, EV battery, and 3 controllers. Effective at different insolation levels according to simulations and experiments.	[40]
Krim *et al.*	Proposed a user-friendly techno-economic tool to evaluate the benefits of solar PV for EV charging infrastructure and help stakeholders manage and size their charging stations.	[41]
Krim *et al.*	Reflector-based PV systems proposed for EVCSs in Leeds, UK, along with a self-sufficient DC mini-grid powered by renewables to address grid stability issues caused by concentrated loads.	[41]
Thang *et al.*	A sliding mode control was proposed to regulate DC-bus output voltage for fast dynamic response to sudden system disturbances, such as fast irradiance changes.	[47]
Wu *et al.*	Coordinated control to prevent overcharging and over-discharging of ESU but did not address transient PV generation disruption leading to inadequate EV charging power and system instability.	[48]

Xia *et al.*; Zhang *et al.*; Alam *et al.*; Hleihe *et al.*	Proposed coordination of PV generation and ESU charging and discharging in some studies, but without analyzing the impact of outages from the EV side.	[49]–[52]

2.4 PV Panels and Arrays

In the late 1950s, the first conventional PV cells were produced primarily for providing electrical power to orbital satellites [53]. However, recent advancements in design, manufacturing, and performance have led to significant improvements in the quality and reduced costs of solar cells and modules [54]. Off-grid EV charging stations primarily rely on PV arrays as their energy source. The solar cell, which is a PN junction diode, converts solar energy into electrical energy [55], [56].

Figure 2.3 illustrates a solar cell's equivalent circuit, which incorporates an internal series resistor, R_s, and a parallel resistor, R_p [57].

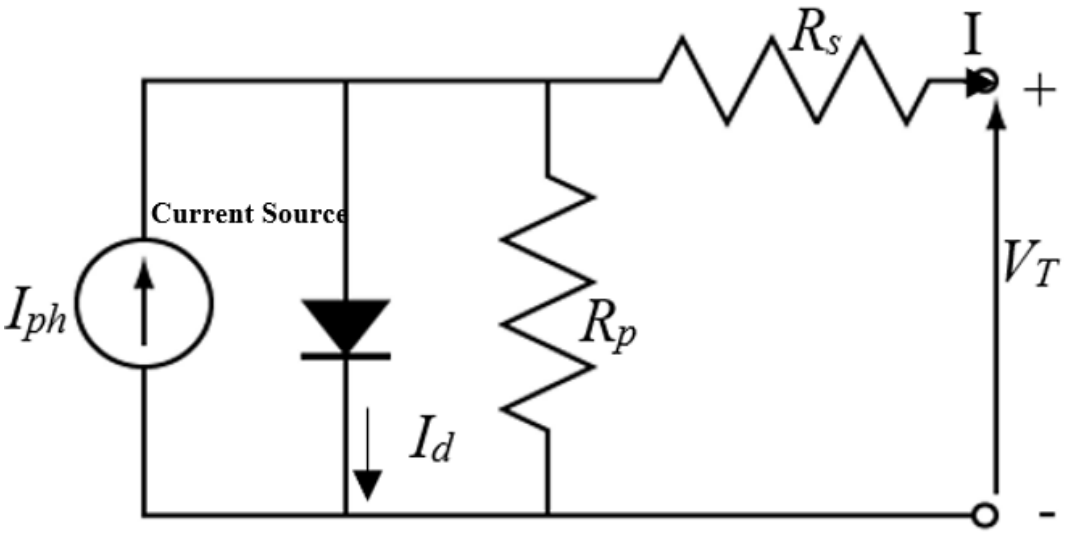

Figure 2. 3 Solar Cell Equivalent Circuit [57].

The following equations define the VI characteristics of a single PV module:

$$I_d = I_0 \left[exp\left(\frac{V_d}{V_T}\right) - 1 \right], \quad (2.1)$$

where

$$V_T = \frac{kT}{q} * n_1 * N_{cell}. \quad (2.2)$$

where the diode current and voltage are represented by I_d and V_d,respectively. I_0 is the diode saturation current, n_1 is the diode ideality factor (which is typically chosen close to 1), k is the Boltzman constant (8.617×10^{-5} eV/K) , q is the electronic charge (1.6×10^{-19} Coulumbs), T is the cell temperature in K, and N_{cell} is the number of serial cells in a module [57].

2.4.1 Maximum Power Point Tracker (MPPT)

PV-based EV charging stations commonly employ MPPT controllers to optimize the power and efficiency output of solar panels [58]. There are several MPPT techniques available: they are the Open-circuit voltage (OCV) technique, temperature method, Short-Circuit Current (SCC) technique, Perturb and Observe (P&O) method, and Incremental Conductance method.

1. OCV technique: This method determines the maximum power point by measuring the OCV of the PV module. The OCV technique is simple, and it works well in clear weather conditions. However, this method is not accurate under partial shading and variable temperature conditions [59]–[62].
2. Temperature method: This method determines the maximum power point by measuring the temperature of the PV module under OCV conditions. The temperature method is simple and accurate. However, it requires additional temperature sensors to measure the module's temperature, making it more complex and expensive [60].
3. SCC technique: The maximum power calculation technique utilized by this method involves utilizing the short-circuit current of the PV module. The SCC technique is simple and works well in most weather conditions. However, like the OCV method, it is not accurate under partial shading and variable temperature conditions [59], [63], [64].
4. P&O method: This method is the widely used MPPT technique and involves perturbing the solar panel's operating point and observing the corresponding changes in power output. In P&O, the controller adjusts the operating point to increase or decrease the power output. The fluctuations in power are used to determine the maximum power point [65]–[67]. There are three types of P&O techniques:

   P&O fixed step size [68]: In this technique, the perturbation is a fixed increment in the duty cycle.

P&O variable step size [69]: In this technique, the perturbation size is dynamically adjusted according to the rate of change in power output.

Three-point weighted P&O [70]: This technique evaluates three duty cycles at each step and selects the ideal duty cycle based on a weighted average of the power output at these three points.

5. Incremental Conductance method: This technique traces the maximum power point by utilizing the slope of the PV curve. The controller adjusts the operating point until the slope of the PV curve equals the incremental conductance. The Incremental Conductance method is more complex than other techniques, but it provides accurate and reliable results under variable conditions [71]–[73].

2.5 Battery Model Used in EVCS

The battery model, as shown in Fig. 2.4, is an essential component in EVCS.

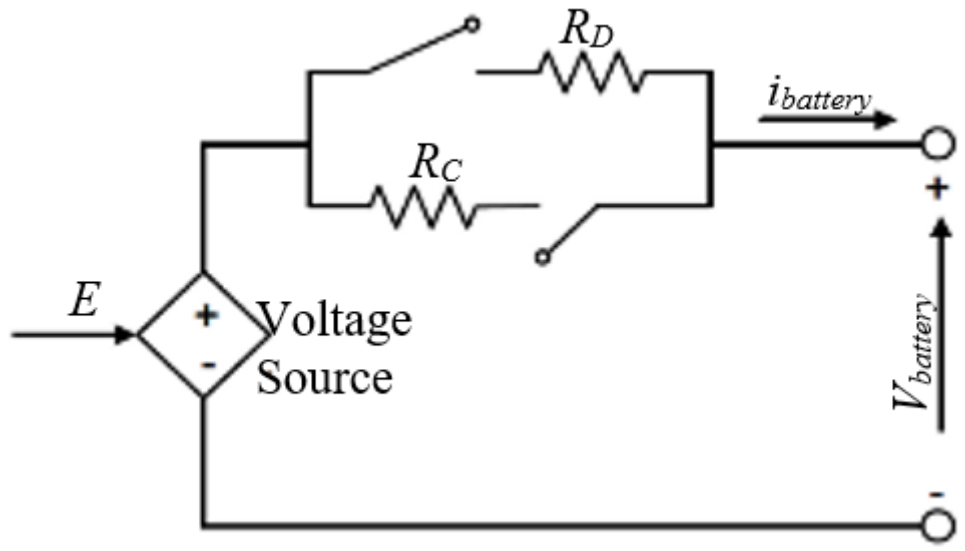

Figure 2. 4 Model of a Battery [74]–[76].

In this model, the *SOC* of the battery is determined by a controlled voltage source that is connected in series with the specific resistors (R_C for charging and R_D for discharging) during their respective cycles. The *SOC* of the battery during the charging and discharging process is calculated using the following equation:

$$SOC = \frac{Q_0 - \int \eta \, i_{battery} \, dt}{Q} , \qquad (2.3)$$

where Q_0 is the initial charge stored in Ah (Ampere-hour), η is the battery efficiency, $i_{battery}$ is the current flowing through the battery, and Q is the battery capacity. Battery efficiency is determined by the interplay between the voltage and current within the battery. The following equations estimate the charging efficiency (η_{ch}) and discharging efficiency (η_{dis}).

$$\eta_{ch} = \frac{V_{OC}}{V_{OC} - R_C i_{battery}}, \tag{2.4}$$

$$\eta_{dis} = \frac{V_{OC} - R_D i_{battery}}{V_{OC}}, \tag{2.5}$$

where V_{OC} is the battery open circuit voltage [74]–[76].

2.6 BDC

High-power applications commonly use BDC topologies, which can be classified either as current-fed, or voltage-fed, or a hybrid of both. The isolated full-bridge BDC is shown in Fig. 2.5. The inductor L functions as an output filter in buck mode, enabling power to move from the high-voltage side towards the batteries. Conversely, in boost mode, the converter operates when power is transmitted from the batteries to the high-voltage side. A BDC comprises a high-frequency inverter, high-frequency transformer with leakage inductance (L_k), and a high-frequency rectifier. The converter is directly connected to either the voltage source or the DC capacitor bank, shown in the Fig.2.5 as C_0. This converter can perform both the charging and discharging processes of the battery and is available in full-bridge topology and single-stage buck/boost type. The full-bridge topology offers a substantial boost ratio and provides electrical isolation between the input and output[77]–[79]. Additionally, the voltage stress on the switches remains consistent with that of half-bridge configurations, but the current stress in the switches is only half of that in half-bridges. Thus, full-bridge BDCs are often the preferred choice for high-power energy storage applications due to their ability to use voltage-fed full-bridge on the high voltage DC-link side and a current-fed full-bridge with an inductor on the low voltage battery side [80]–[83].

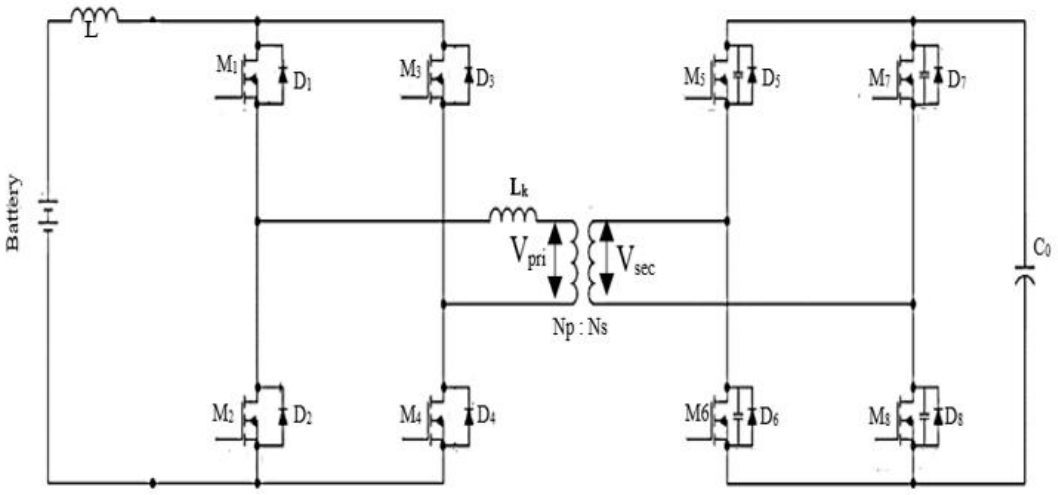

Figure 2. 5 Isolated full-bridge BDC [83].

The dual active bridge (DAB) DC-DC converter is another widely used BDC. The conventional modulation strategy produces a square wave output of both full bridges, with a phase shift controlling the power's direction and amplitude. A drawback of this topology is its limited suitability for wide voltage range applications due to its narrow optimal operating voltage range when under full load with ZVS and reactive power considerations. An approach that has been suggested to address this challenge involves the use of a combined triangular and trapezoidal modulation method. This method effectively minimizes losses across a broad operating voltage range. Moreover, in DAB isolated BDCs, a dual-phase-shift modulation approach can be employed to decrease current stress and reactive power [84].

The use of isolated full bridge BDCs is common in off-grid EVCS because they offer bidirectional power transfer, galvanic isolation between the primary and secondary sides, and high efficiency. Among full-bridge BDCs, the isolated bidirectional dual active full-bridge converter has several advantages over other DC-DC converters. Dual active-bridge converters are symmetrical and easy to analyze and control[85]–[88].

A variety of isolated dual active-bridge converters have been studied, including both voltage-fed non-resonant [85], [89]–[92] and resonant [85], [93]–[97] converters. Voltage-fed converters [90], [91] employ a discontinuous mode of operation to mitigate circulating current, temporarily interrupting power transfer to the load during certain intervals. The series-resonant DAB

converter is a proposed solution to address several issues related to full-bridge BDCs. Its design aims to reduce current stress, extend the soft-switching range, improve efficiency, and minimize the impact of dead-time on power transmission and soft-switching [85], [98]

One proposed converter topology aims to integrate both a PV system and the grid without the use of an isolation transformer. However, it should be noted that this design lacks the protection provided by isolation, despite its compact size [99]. A proposed solution for integrating the DC bus and energy storage system is the hybrid bridge topology, which offers high efficiency and soft switching even when the transformation ratio '*n*' is far from unity [100].

A controller has been introduced in to regulate power transmission and reduce losses using a minimum-current-point-tracking method [101]. This controller is generic in design and is independent of circuit parameters and complicated circuit modeling. A recent study [102] presented a new topology that can transfer more power compared to a traditional DAB converter. This topology has a power transmission capacity twice that of conventional DAB converters and has been successfully applied in electric-powered aircraft.

A topology with a high step-down ratio involves stacking inverter bridges in series using a capacitor, while rectifier bridges are connected in parallel. This configuration enables the series-connected bridges to add voltage at the input, while the parallel-connected bridges at the output reduce voltage and increase current. The converter employs GaN semiconductor switches and is capable of achieving efficiencies ranging from 97.5% to 99% [103], [104]. According to a previous study [105] , a new scheme has been developed to improve the dynamic response of power systems, particularly in the face of wide-ranging load changes. This topology is versatile and can be effectively utilized in a variety of applications, including distributed energy systems, solid-state transformers, and energy storage.

A hybrid-switching scheme has been proposed to minimize losses for a DAB converter with advanced switching devices like SiC, achieving 98.96% efficiency [106]. Previous research, as documented in [107]–[109], has examined voltage-current-fed isolated BDCs that do not utilize a resonant network. However, these converters are susceptible to current stress and losses that can

result from magnetizing current. Voltage-current-fed isolated BDCs with resonant networks have been proposed in [110]–[112] as a potential solution to the issue of high current stress and conduction losses. These converters are designed to provide nearly sinusoidal current, which can result in lower current stress and reduced conduction losses. However, the extra inductors on one of the bidirectional operations in voltage-current-fed converters make them unsymmetrical structures, resulting in uneven distribution of current on the switches. In contrast, current-fed isolated bidirectional DC-DC resonant converters are symmetrical in both forward and reverse modes of operation, requiring less gate drive than voltage-fed converters. This feature makes them suitable for low-voltage applications due to their inherent boosting capability [113].

2.7 Snubbers

Snubbers are small networks of electrical components used in power converters to clamp voltage and current spikes when a switch is turned off or on. There are two types of snubbers: passive and active. Passive snubbers use elements like resistors, capacitors, inductors, and diodes, while active snubbers include transistors and other active components, making them more complex and expensive [114]–[116]

When a switch is turned off, parasitic inductance can trap energy that is then transferred to the output capacitance of the converter, creating a voltage spike that may exceed the switch's peak rating and damage it. A capacitor connected in parallel with a switch can limit the voltage across it and prevent voltage spikes. Similarly, connecting an inductor in series with a switch can limit the sudden current rise when the switch is turned on [114].

Snubber circuits play a crucial role in bidirectional converters and can take the form of (resistor-capacitor-diode) RCD snubbers, active clamping snubbers, or flyback snubbers. An RCD snubber is a straightforward solution to the issue of circulating current, where the clamping capacitor discharges through a resistor. However, traditional RCD-based BDCs are generally inefficient due to the resistor's dissipative energy element, leading to a voltage spike caused by parasitic properties of high-frequency transformers that frequently damage power electronic devices [113], [117], [118].

Active clamp converters were introduced as an alternative solution, but they suffer from poor efficiency at light load conditions and cannot actively eliminate the circulating current. Therefore, the circulating current flows through the low-voltage (LV) side inverter bridge's semiconductor devices, increasing the converter's conduction losses. A novel active clamp-based BDC with a symmetrical structure has been developed to achieve high static gain and reduce switching stress and switching loss of the converter, although it possesses a complex structure with a high number of semiconductor devices, leading to higher conduction loss and cost [113], [119], [120].

Researchers have proposed the flyback snubber as a solution to transfer circulating energy from the primary to the secondary side of a BDC, which can help reduce power losses [107], [114]. In [121], a flyback snubber-based DAB-BDC topology is presented. This topology utilizes a capacitor-diode circuit to clamp the voltage spike across the switches and recover energy through a flyback converter. By reducing circulating current, this converter can help decrease power losses. In step down and step-up modes, phase shift control and (pulse-width modulation) PWM control are used, respectively. However, this converter does have some disadvantages, such as the added complexity of the control circuit due to an extra switch in the active snubber circuit and hard switching of the active snubber switch. In [122], the DAB-BDC consists of a flyback snubber and two diode-capacitor snubbers. This converter reduces the voltage spikes across switches and provides ZVS conditions at both low and high voltage sides. However, an auxiliary circuit with an additional three winding auxiliary transformer is required.

A CLLC resonant DAB converter was used by Jung *et al.* [123] , where the resonance circuit provides a ZVS condition for switches at the primary side and soft commutation for output rectifiers. The abbreviation "CLLC" denotes the presence of two coils and two capacitors, with "*L*" representing a coil and "*C*" representing a capacitor. The CLLC resonant converter is a commonly employed DC transformer for linking AC/DC to the DC bus in electronic systems. This converter provides soft switching in a vast range of input and output voltages, and voltage stress is reduced without the need for a snubber. However, the converter is controlled using variable switching frequency method, and the control algorithm is not simple.

Various snubber configurations to achieve soft switching have been proposed. Soft switching reduces the voltage and current stresses on the main switch. For example, Wang *et al.* [124] proposed a bidirectional dual full-bridge DC-DC converter with a unified soft-switching scheme and soft-start capability. Their configuration includes a voltage-clamp branch to limit the transient voltage across the current-fed bridge and achieve ZVS in boost mode. In buck mode, they achieve ZVS and ZCS for the voltage-fed bridge. Wu *et al.*[125] presented a soft-switching boost converter with a flyback snubber for high-power applications. Their configuration reduces voltage and current stresses on the main switch by achieving near-ZVS and ZCS. They reviewed several passive and active snubber configurations associated with boost converters and proposed a boost converter with a flyback snubber. Experimental results from a 5-kW boost converter confirmed the feasibility of their configuration for high-power applications.

2.8 Optimal Control Strategies

The primary objective of the control tactics is to stabilize the DC bus voltage in DC microgrids through the application of distributed ESUs. These tactics comprise the adjustment of droop coefficients, coordination of multiple ESUs for efficient load current distribution, and management of battery ESUs' charge and discharge power to maintain power equilibrium in the microgrid and regulate DC bus voltage fluctuations. The techniques employ droop control methods that facilitate the sharing of a common load by various parallel converters in the microgrid, along with outer voltage restoration loops that correct voltage deviations caused by droop control. These control methods ensure reliable operation of the DC microgrid, facilitate power management, and surplus power sharing among microgrids, and improve the smart charging infrastructure's scalability and speed of plug-in electric vehicles (PEVs).

Zhang *et al.* [126] propose a strategy to stabilize the DC bus voltage in DC microgrids by using distributed ESUs. They suggest designing the BDC in the energy storage system based on voltage level and electromagnetic isolation requirements, and coordinating multiple ESUs for load current distribution according to the *SOC*. The proposed *SOC* power index droop control strategy uses communication lines to distribute load current among multiple ESUs, and quickly converges the *SOC* between ESUs to a consistent state. The study also proposes an improved *SOC* power index

droop control to overcome communication line failures. Connecting ESUs in layers in the DC microgrid is necessary to optimize resource allocation due to the high cost of these units. The study also discusses the quantification standards of the DC bus fluctuation range and the working range of each converter to maximize the stability of the DC bus voltage and grid-connected power fluctuation. The study presents a distributed drooping control of *SOC* power exponents, which considers emergency situations during communication faults. The proposed approach is effective and has been confirmed by both simulation and experimental results.

Jiechao *et al.*[127] proposed a control strategy to maintain *SOC* balance among battery energy storage units (BESUs) in an islanded DC microgrid. The control strategy involves adjusting the droop coefficient in real-time and controlling the charge and discharge power of the BESU. The aim of the strategy is to achieve power balance in the microgrid, control DC bus voltage fluctuations within 4.5%, and suppress power fluctuations using the ESU as the main controlled unit. In their research, they also analyzed and improved the traditional energy storage system control strategy to complete the *SOC* balance between the ESUs. They designed an operation control strategy based on the *SOC* of the energy storage system to coordinate the control methods of the distributed power generation units and ensure the power balance of the DC microgrid. Their simulation results demonstrated that the proposed energy storage system control strategy based on the *SOC* of the ESU can complete the *SOC* balance among the ESUs and maintain the smooth switching of various modes. The designed operation control strategy based on the *SOC* of the energy storage system can control the fluctuation range of the DC bus voltage within 4.5%, ensuring the stable operation of the islanded DC microgrid.

Zammit *et al.*[128] presented a control system for buck and boost converters that can be extended to other similar applications. The converters can interface PV panels or wind turbine systems to a DC microgrid. The authors modelled both converters in continuous conduction mode (CCM) and derived the small signal equivalent circuit to obtain transfer functions for the design of the current and voltage controllers of the converters. They utilized a droop control method to enable sharing of a common load by multiple paralleled converters in the microgrid, and an outer voltage restoration loop to correct voltage deviations caused by the droop control method. The study

tested the control system through simulations of two paralleled buck converters sharing a common resistive load.

Haghmaram *et al.* [129] investigated the use of a modular-isolated BDC in a PV-based DC microgrid connected to other microgrids in a DC distribution network. The modular converter allows for bidirectional power flow between the microgrid and distribution network, even in islanding mode. A power management strategy is employed to ensure reliable power exchange and surplus power sharing among the microgrids. The authors demonstrate the simple control and reliable operation of the modular converter through both low-power experimental testing and software simulations. The results confirm the converter's bidirectional power transfer capability and its ability to inject surplus power into the distribution network and absorb shortage power from the microgrid. The modular converter's extendable configuration and operation principles make it suitable for high-power applications and a valuable tool for DC microgrid power management.

Abraham *et al.* [130]present a comprehensive analysis of current research on EV charging stations that rely on RES for power. The authors discuss the importance of different charging station designs that incorporate RES, categorized according to their integration with DC, AC, or hybrid microgrids. They also explore the available charging converter topologies, including bidirectional power flow options to regulate the DC bus voltage. One of the main challenges in charging stations is connecting the DC and AC loads, especially at DC charging points. Their study examines various control strategies that can help choose the most appropriate technology. The AC microgrid-based charging station utilizes droop control characteristics, which enhance the stability at higher gains compared to frequency droop control. However, this approach necessitates a communication channel. In contrast, the DC microgrid-based charging station employs a straightforward DC-DC conversion that provides fast charging and reduces conversion losses.

Chung *et al.* [131] have introduced a master-slave control approach for smart charging infrastructure of PEVs. The approach involves adding a power information collector (PIC) to level one electric vehicle supply equipment (EVSE) to enhance scalability and speed, enabling

the level one charger to perform operations within the EVSE itself. This allows the level 1 EVSE to locally execute simple charging algorithms such as round-robin. The updated hardware of level 2 EVSE includes the removal of the redundant ZigBee communication system and the installation of a more robust microprocessor. This update facilitates the implementation of a power-sharing algorithm locally and enables the execution of a fair charging algorithm that is calculated on the server side with minimal instructions on the EVSE side. The virtual machine monitor (VMM) system is also enhanced with algorithms that automatically authenticate and authorize each PEV approaching the EVSE, simplifying the charging process for the user. These enhancements to the WINSmartEV system (is a comprehensive software solution for monitoring, controlling, and managing PEVs) increase its ability to service multiple PEVs, aiding in the proliferation of PEVs and contributing to the larger push towards energy independence and reduced GHG emissions.

Table 2.2 provides a summary of the control strategies discussed earlier in the paper for DC microgrids with distributed ESUs.

Table 2. 2 Control Strategies for DC Microgrids with Distributed ESUs.

Author(s)	**Control Strategy**	**Results**	**References**
Zhang *et al.*	*SOC* power index droop control	Distribute load current among multiple ESUs and converge *SOC* to consistent state using communication lines. Improved droop control to overcome communication line failures. Effective approach confirmed by experimental and simulation results.	[126]
Jiechao *et al*.	Adjust droop coefficient in real-time, control charge and discharge power of BESUs	Proposed ESU control strategy balances *SOC* and maintains smooth switching. Designed operation control strategy maintains stable operation of islanded DC microgrid with 4.5% fluctuation range of DC bus voltage.	[127]

Zammit *et al.*	Utilize droop control method to share a common load by multiple paralleled converters in the microgrid, and an outer voltage restoration loop to correct voltage deviations caused by the droop control method	Control system tested through simulations of two paralleled buck converters sharing a common resistive load.	[128]
Haghmaram *et al.*	Utilize modular-isolated BDC, power management strategy to ensure reliable power exchange and surplus power sharing among microgrids	Converter successfully transfers power bidirectionally and can inject surplus power into the network and absorb shortage power from the microgrid, as confirmed by experimental tests and software simulations.	[129]
Abraham *et al.*	Examine charging station designs that incorporate RES, categorize according to integration with DC, AC, or hybrid microgrids	Paper explores charging converter topologies and control strategies for regulating DC bus voltage.	[130]
Chung *et al.*	Add power information collector to level one EVSE to enhance scalability and speed, enabling level one charger to perform	Proposed approach improves scalability and speed of EV smart charging infrastructure.	[131]

2.9 Summary

The review of literature highlights the potential of PV-based EV charging stations as a sustainable and low-carbon transportation solution. Integrating solar PV systems with EV charging infrastructure has numerous advantages such as reducing GHG emissions, enhancing energy efficiency, and improving grid reliability and resilience. Nonetheless, several challenges must be addressed. These are the high initial costs of PV systems, grid integration challenges, and variability in solar energy production, *etc.* Innovative business models and continued research in PV technology can aid in overcoming these challenges and increasing the use of PV-based EV charging stations. This chapter presented detailed literature reviews on a variety of important topics related to EV charging stations.

Chapter 3 Empowering Sustainable Transportation: Inside A PV-Powered Off-Grid EV Charging Station

3.1 Introduction

The global community continues to grapple with the impacts of climate change and there is an ever-growing interest in sustainable modes of transportation. The adoption of EVs is being seen as an important way to help reduce GHG emissions, but they are only as sustainable as the electricity that is used to charge them. The sustainability of EVs depends on the sustainability of the electricity used to charge them. The solution to this issue lies in the implementation of PV technology that can provide a sustainable and renewable source of energy to power EVs [17].

Off-grid PV-based EVCS is an innovative and sustainable solution for EV charging, particularly in remote locations where traditional power grids are inaccessible. These charging stations utilize PV panels to generate electricity from the sun, which is subsequently stored in a battery bank for later use. By providing EV charging without relying on traditional power infrastructure, off-grid PV-based charging stations offer a way to bring sustainable mobility to areas that may have been previously underserved. This can be particularly beneficial in remote and rural areas, where access to traditional power grids is limited or non-existent [5], [17].

The use of off-grid PV-based charging stations is a step towards a more sustainable future, as it reduces the reliance on fossil fuels and promotes the use of RES. Off-grid charging stations can contribute to reducing GHG emissions, as EVs charged using solar-generated electricity have a significantly lower carbon footprint than those charged using electricity from non-renewable sources [5], [17].

The inner workings of an off-grid PV-based EVCS are complex, and understanding the key components is essential to appreciating their potential for sustainable transportation. At the heart of any PV-based charging station are the PV panels, which convert sunlight into electricity that charge the EVs. The number and size of these panels will depend on the charging station's power demand and the amount of sunlight available in the area [5], [17], [18].

The charge controller is the next critical component of the PV-based charging station. This device regulates the flow of electricity from the PV panels to the battery bank, ensuring that the battery is neither overcharged nor undercharged. The battery bank, in turn, stores the electricity generated by the PV panels for later use when there is no sunlight. This means that EVs can still be charged even when the sunlight is absent, making the off-grid PV-based charging station a viable option for 24×7 charging [5].

This chapter provides an in-depth examination of the various components and control techniques used in this research on off-grid PV-based EVCS. These charging stations rely on PV panels, charge controllers, and battery banks to ensure reliable and uninterrupted charging. The charging stations offer a sustainable solution for EV charging in remote areas by utilizing solar energy generated by PV panels and stored in a battery bank. This reduces dependence on non-RES, promotes sustainable transportation, and helps to decrease GHG emissions. The control techniques have been developed to optimize the performance and efficiency of the PV panels, charge controller, and battery bank.

3.2 PV Panels

The main component of off-grid EVCS are PV panels that convert sunlight into usable electrical energy for charging EVs. These panels consist of solar cells connected and mounted on a framework that faces the sun. When the sun shines on the solar cells, it creates an electrical charge that is collected by wiring within the panel and transported to the charge controller. The effectiveness of a PV panel in generating electrical energy from sunlight depends on its conversion efficiency. The most widely utilized solar cells are those composed of silicon, as they are highly durable, reliable, and require minimal maintenance. However, alternative technologies such as thin-film solar cells and organic solar cells are gaining attention as substitutes for silicon-based panels due to their advantages in terms of flexibility, cost-effectiveness, and higher efficiencies [132]–[134].

PV systems offer various advantages, such as their ability to generate electricity silently and without causing pollution. Additionally, these systems are known for their relatively affordable operation and maintenance requirements. However, it is essential to recognize that PV systems

also come with certain disadvantages that should be considered. These include the need for high upfront investment and their reliance on sunlight to generate electricity [132]–[134].

PV panels are the basic building blocks of a PV array. These cells are usually sandwiched between a layer of glass and a durable material, forming a sealed unit that is designed to resist moisture. As solar radiation interacts with the semiconductor layers of a solar cell, it induces the movement of electrons, leading to the generation of an electric current. Multiple solar cells within a panel are typically connected in a series-parallel configuration to produce a desirable current and voltage output. The rating of a PV panel power output is usually measured in Watts peak (Wp) according to standardized testing conditions. PV panels come in various output capacity sizes, with some models capable of producing up to 350 Wp. These panels can be configured into arrays of any size depending on the specific application requirements. On sunny days with optimal solar gain, an array of panels rated at 2,000 Wp has the potential to generate a daily energy output ranging between 4 kWh and 10 kWh [132]–[134].

The energy output of a PV system is directly linked to the amount of sunlight it captures, which in turn depends on several factors such as the solar irradiance, the area of the solar panel, the orientation of the panel, and the tilt angle of the panel. The level of solar irradiance is typically greater in regions located further north, during the summer season, in areas with less air pollution, and with minimal shading. The power output of an entire PV panel can be significantly reduced by just a small amount of shading on one of its individual solar cells. Although PV cells can generate electricity even in cloudy conditions, their energy output will be lower than in direct sunlight conditions. The area of solar panels required to generate 1 kWp of electricity can range from 5 to17 m^2, depending on the specific type of panels used. In New Zealand, solar panels are generally recommended to face northward, as the sun's path follows an arc towards the northern part of the sky. The optimal tilt angle for solar panels varies depending on the type of system and the intended use. For a grid-connected system that aims to maximize energy production throughout the year, the recommended tilt angle is typically 10 degrees less than the local latitude. On the other hand, off-grid systems are usually designed to generate the most energy during winter months when power demand is highest, and as such, the recommended tilt angle is often

the local latitude plus 10 degrees. Array frames are support structures that enable PV panels to be adjusted to the ideal tilt angle for maximizing solar energy absorption. PV array frames provide a structure for mounting solar panels at the optimal angle for receiving solar energy, and they can be either fixed or adjustable. These frames must be installed in a way that meets the necessary wind and seismic loading requirements. Additionally, they must be isolated to prevent any electrochemical corrosion between different metals in the solar panels or building materials. It is also important to allow adequate airflow behind the panels for cooling purposes. PV panels come in two main types: crystalline silicon panels or thin film amorphous silicon panels. Crystalline silicon panels use a crystalline silicon wafer as the semiconductor, while amorphous silicon panels use a thin film of silicon deposited on a low-cost substrate such as glass or a thin metal foil. PV panels mounted on array frames are the conventional choice in New Zealand, but building-integrated photovoltaics (BIPVs) are gaining popularity. BIPV refers to the integration of solar cells into building elements such as roof cladding and/or wall cladding, enabling them to serve both as PV panels and building materials [132]–[134].

3.3 Boost Converter

Boost converters play a crucial role in the operation of off-grid EVCS. These stations rely on RES like PV panels to provide low voltage DC power, which is then converted into a higher voltage level suitable for charging EVs. In this context, two-level and three-level boost converters are often utilized. The choice of converter type primarily depends on the specific needs and constraints of the charging station setup. The two-level boost converter is a basic design that uses a single power switch and a diode to regulate the voltage. In contrast, the three-level boost converter employs an additional power switch and a capacitor to achieve a higher efficiency and reduce the voltage ripple [5], [10], [17], [18], [27], [31].

The two-level boost converter consists of a single power switch *S*, a diode *D*, an inductor *L*, a capacitor *C*, and a load as shown in Fig. 3.1. The inductor in a boost converter stores energy in its magnetic field when the power switch is closed. Upon opening the switch, the inductor discharges its stored energy to the load and capacitor, thereby charging the capacitor. The diode ensures that the capacitor and the load do not discharge back to the inductor when the switch *S* is

off. Although this converter is less expensive and less complex to build, it has a lower efficiency than the three-level boost converter. The voltage gain of a two-level boost converter can be very high. However, this type of converter encounters challenges as the switching duty cycle approaches zero, mainly due to parasitic components such as the inductor's equivalent series resistance and the switching transistor, and the limited switching speed of the transistor [135].

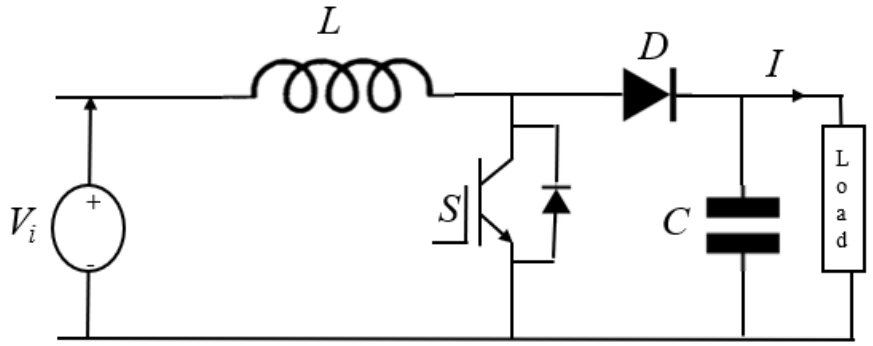

Figure 3. 1 Two level Boost Converter [135].

The three-level boost converter is an advanced and efficient design that incorporates two power switches and two capacitors. By operating in a complementary manner, the power switches generate a voltage level that exceeds the input voltage, while the capacitors play a crucial role in energy storage and current flow during the switching cycle. This configuration effectively reduces voltage ripple and enhances the overall efficiency of the converter. However, it is important to note that this intricate design may require additional components, potentially increasing the converter's cost and size.

Within the realm of PV systems, the three-level boost converter is widely utilized to maximize power extraction while adapting to varying operational conditions. It offers notable advantages over conventional boost converters by reducing the size of the inductor and the switch voltage rating. Operating in a cascaded configuration, this converter enables high voltage gain and efficient power conversion by incorporating three voltage levels: the input voltage, the output voltage, and the voltage at the center point of the converter. The inclusion of capacitors at the center point serves to minimize voltage stress on the switching devices.

Figure 3.2 illustrates the configuration of the three-level boost converter, highlighting crucial components such as an inductor L_{PV}, two IGBTs with antiparallel diodes S_1 and S_2, two capacitors

C_{f1} and C_{f2}, and two diodes. These components work harmoniously to generate output power at each of the three levels. An efficient three-level boost converter can outperform traditional boost converters in terms of efficiency and voltage gain, achieving a double increase [136]–[138]. For a more detailed explanation, please refer to Chapter 6 for an extensive analysis.

The converter operates in four distinct modes:

Mode 1: In this mode, both power switches are turned ON, and the inductor operates in the charging mode. The input voltage charges the inductor, storing energy in its magnetic field.

Mode 2: In this mode, one power switch is ON while the other is OFF, and the inductor can be in either the charging or discharging mode. When the inductor is in the charging mode, energy is transferred from the input source to the inductor. Conversely, when the inductor is in the discharging mode, the stored energy is transferred to the output.

Mode 3: Similar to Mode 2, one power switch is OFF while the other is ON, and the inductor can be in either the charging or discharging mode. The energy flow is similar to Mode 2 but in the opposite direction.

Mode 4: In this mode, both power switches are turned OFF, and the inductor operates in the discharging mode. The energy stored in the inductor's magnetic field is transferred to the output.

The converter utilizes duty cycle control to ensure voltage balancing across the capacitors. This duty cycle is determined by a MPPT control algorithm, which continually tracks and adjusts to the maximum power output of the PV system, accounting for various environmental conditions [139].

In off-grid EVCS, the three-level boost converter is often preferred over the two-level converter due to its higher efficiency and superior voltage regulation. This converter enables the charging station to draw power from RES and efficiently charge EVs without relying on the grid. Moreover, the converter allows for energy storage, which proves crucial in scenarios where the renewable energy source is intermittent or unavailable [5].

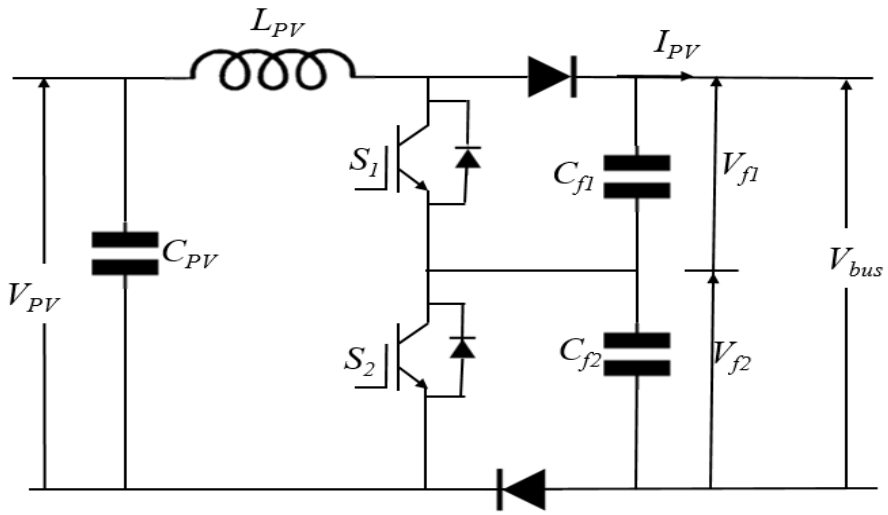

Figure 3. 2 PV boost converter.

3.4 BDC

The isolated bidirectional full-bridge DC-DC converter is a power electronic converter commonly used in off-grid EVCS (see Fig. 2.5). It can transfer power bidirectionally between two DC sources or loads, thereby facilitating an efficient and flexible energy management system [5], [17], [18].

In a bridge converter, power transfer between two DC sources or loads is regulated and controlled using four power switches, with two situated on each side of the bridge. Additionally, the converter utilizes a transformer to ensure that the input and output sides of the converter are electrically isolated from one another. The transformer is an essential element of the bridge converter, which transfers energy between two sides of the circuit. The primary side of the transformer is connected to one of the DC sources or loads, while the secondary side is connected to the other, ensuring efficient power transfer between the two sides of the circuit [5], [17], [18].

The charging of an EV involves the use of a bidirectional full-bridge DC-DC converter. This converter is responsible for transferring power from a PV panel to the battery of the vehicle. It connects the PV panel to one side of the converter and the battery to the other side. The converter ensures the charging process is safe and efficient by regulating the power transfer between the solar panel and the battery [5], [17], [18].

When the EV is not linked to the charging station, the isolated bidirectional full-bridge DC-DC converter can be used to transfer power between two DC sources, such as the PV array and a

battery bank. This enables excess energy generated during the day to be stored and used to power the charging station and/or other loads during the night or when there is insufficient sunlight [5], [17], [18].

The isolated bidirectional full-bridge DC-DC converter offers several benefits for the off-grid EVCS. They include efficient power transfer between two DC sources or loads, minimizing energy losses and improving the overall system efficiency. It also provides electrical isolation between input and output sides of the converter, ensuring safe and reliable charging station operation. Furthermore, it enables flexible energy management by facilitating power transfer in both directions, allowing energy to be stored and used as required [5], [17], [18].

However, there are also challenges associated with the use of isolated bidirectional full-bridge DC-DC converters in off-grid EVCS. These include complexity and cost in design and manufacturing, necessitating advanced knowledge of power electronics and control systems. Additionally, customization for specific applications may be required, increasing costs and lead times.

3.5 Snubbers

Snubbers are electronic devices used to shield switches and other components in power circuits from sudden voltage surges. These surges can cause high-frequency oscillations and vibrations, leading to excessive stress on the components [5], [17], [18].

Snubbers function by providing a channel for the energy stored in parasitic inductances to be released. A snubber often contains a combination of a resistor, capacitor, and diode, arranged either in parallel or series with the component being protected. Three common types of available snubbers are RCD snubbers, active snubbers, and flyback snubbers, each with its own unique features that suits different applications [5], [17], [18]. For a more comprehensive understanding, which includes detailed explanations and diagrams, please refer to Chapter 5.

RCD snubbers (see Fig. 5.2) are often used in DC-DC converters and are constructed with a resistor, capacitor, and diode connected in parallel with the switch. When the switch goes off, the capacitor charges with the energy stored in the parasitic inductance, resulting in a voltage surge

across it. This surge is released when the capacitor discharges through the resistor and diode. In contrast, active snubbers employ active components such as transistors to create a route for energy dissipation. Active snubbers (see Fig. 5.3) are superior to RCD snubbers because they can switch on and off faster, resulting in more efficient energy dissipation [5], [17], [18].

Flyback snubbers (see Fig. 5.4) are commonly implemented in flyback converters, which utilize transformer leakage inductance to store energy which is returned back to the input when the switch is turned off. A flyback snubber comprises a capacitor and a diode that are connected in series with the transformer. When the switch turns off, the capacitor discharges through the diode, returning the energy to the input [5], [17], [18].

3.6 EVCS

EVs require a reliable and secure source of electricity to recharge, without overloading the system or causing power surges [140]–[142]. Several types of EVCSs have been developed to fulfill this requirement, and they are categorized as follows.

3.6.1 Residential Charging Station

A residential charging station is an ideal solution for EV owners who want to charge their vehicles at home during off-peak hours. This will reduce the demand on the electrical grid and provide a more cost-effective charging option. However, it is worth mentioning that the charging time for a full charge at a residential station can take up to 17 hours, depending on the specific EV and charging equipment used. Despite the longer charging time, many EV owners find the convenience and accessibility of a home charging station to be a significant advantage, as it eliminates the need for frequent trips to public charging stations and ensures that the vehicle is always ready for use. Additionally, using a residential charging station may also allow EV owners to take advantage of time-of-use electricity pricing, which can result in lower charging costs [141]–[143]. Section 3.7.1 will discuss the various charging levels in detail.

3.6.2 Parking Charging Station

Parking charging stations provide a convenient and accessible way to charge EVs while they are parked for extended periods of time, such as while the driver is at work or running errands.

According to the National Household Travel Survey, vehicles are frequently parked for over five hours daily at workplaces, presenting an excellent opportunity to charge EVs and alleviate the pressure on public charging stations and the electrical grid during peak hours [144]. Parking charging stations can be installed in a variety of locations such as restaurants, shopping malls, and libraries, following established infrastructure guidelines [145], [146].

Smart charging spaces with internet and Wi-Fi facilities can be created to allow for slot booking and traffic inquiries, making it easier for EV owners to plan their charging needs and access the charging station when they need it. Parking charging stations typically offer both single and three-phase supply. It takes approximately 7 to8 hours to fully charge an EV battery, depending on the specific vehicle and charging equipment used [145]–[147].

Overall, charging stations for parked vehicles provide a practical and accessible solution for EV owners to charge their cars while conducting their daily routines, contributing to the reduction of pressure on public charging infrastructure and promoting the shift towards a more sustainable transportation system.

3.6.3 Public Charging Station

Public charging stations are essential for EVs to travel longer distances, as they provide fast charging capabilities that significantly reduce charging time. Standard charging can take several hours and is not practical for EV drivers on the move. Public charging stations employ fast charging techniques, such as polyphase supply, which can charge an EV in approximately half an hour, making it a more convenient and practical solution for the drivers. These charging stations are strategically located at convenient locations, such as gas stations, and public parking lots, to make them easily accessible to the public. They can be equipped with advanced features such as smart charging capabilities, to optimize charging times and reduce the burden on the grid during peak hours. Public charging stations are an essential part of the EV infrastructure, as they allow EV drivers to travel longer distances without worrying about range anxiety [143], [147]–[149].

3.6.4 Battery Swapping Station (BSS)

BSS are designed to overcome the lengthy charging times associated with EVs. Instead of waiting for the battery to charge, a fully charged battery can be exchanged with a depleted one. However, the implementation of BSS poses several challenges that need to be addressed. One major challenge is the compatibility of battery modules with different EV models, brands, and battery designs. To address this, manufacturers need to agree on standardized battery modules, which will help ensure compatibility across different EV models [143], [150]–[152].

Another challenge with BSS is battery degradation. As batteries age and degrade over time, the performance and capacity of the battery will decrease. This could lead to issues with battery swapping, as the swapped battery may not have the same level of performance as the original battery. To address this, BSS operators need to carefully monitor battery performance and replace degraded batteries to maintain high levels of service quality [143], [148], [151], [152].

Overall, while BSS present a promising solution to lengthy charging times, significant challenges remain that need to be addressed. With the implementation of standardized battery modules, careful monitoring of battery performance, and clear ownership guidelines, BSS could become a practical solution to support the widespread adoption of EVs.

3.7 Features of EVCS

Charging an EVSE or EVCS is essential for connecting a battery storage system to the grid [153]. Specific requirements are necessary for the station to operate. They are :

Supporting Grid Factors Reactive power from the charging station injected back to the grid eliminates the high-power demand from charging vehicles, thereby maintaining the Point of Common Coupling (PCC) voltage and preventing voltage instability. Additionally, the Station to Grid (S2G), V2G, and Active Power Filtering (APF) technologies have played a significant role in highlighting the significance of charging stations to utility owners, leading to increased investor interest [154].

Incorporation of RES

Incorporating RES into the charging station can resolve issues related to EV charging, such as peak loading, overload, and voltage drop. This, in turn, can reduce the amount of power that needs to be drawn from the grid [5], [10], [17], [18], [155]

Incorporation of BESS

When a BESS is integrated into the charging station and RES, it can mitigate the problems associated with charging an EV. The recurrence of RES improves when a BESS is deployed in the charging station [5], [10], [17], [18], [156].

Power Density

The term "power density" describes the amount of power that can be accommodated within a given area of a charging station. In areas with high density, such as urban areas, the charging station's footprint is kept minimal [143], [152], [155], [157].

Accuracy

The complexity of control strategies and numerous power electronic components in the charging station can reduce the station's accuracy [143], [152], [155], [157].

Charging Time

The charging time of EVs is the primary challenge in EV charging technology. Four crucial aspects impact fast-charging stations, which are summarized below.

Battery size: The charging time of the battery is proportional to its size. The larger the battery, the longer it takes to recharge.

SOC: The *SOC* determines whether the battery is fully or partially charged or discharged and will influence the charging time.

Maximum charging rate of the vehicle: The rate of charge for an EV is predetermined and cannot be exceeded during charging.

Charging rate of the charge point: The outlet's rating, where the battery is connected, affects the charging time [143], [152], [155], [157].

3.7.1 Types of Charging

Various standard codes such as the Society of Automotive Engineers (SAE), IEA, Institute of Electrical and Electronics Engineers (IEEE), International Electromechanical Commission (IEC), and International Organization for Standardization offer guidelines and voltage levels to charge EVs based on their rated capacity [158]–[162]. Charging EVs is classified into three types:

Conductive Charging [143], [152], [155], [157], [162], [163] : The SAE divides charging into three different levels, while the IEC 62196 defines four charging modes based on power supply levels, protection systems, and connector types.

- Level 1: These chargers are designed for residential purposes and are not typically used in public charging stations. Manufacturers provide Level 1 chargers with the EV, which can be charged from a standard house power outlet. With an output current of 12A-16A and compatibility with a single-phase AC supply, the Level 1 charger can charge an EV with 24kWh in approximately 17 hours.
- Level 2: The Level 2 charger is an improved version of the Level 1 charger. These chargers can be installed in houses with split-phase power supplies and public charging stations. The charging stations can deliver an output current of up to 80A, enabling them to charge an EV with 24kWh in about 8 hours.

Both Level 1 and Level 2 charging stations are AC charging stations. In both the cases, AC power from the grid is supplied to the EV, and an On-Board Charger then converts the AC into DC to charge the vehicle (see Fig. 3.3).

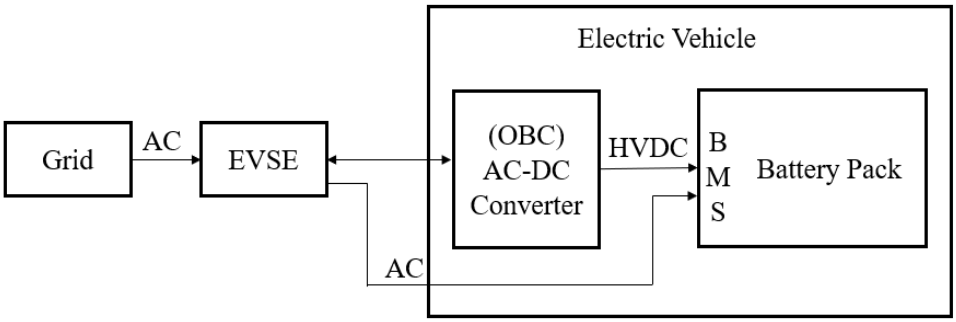

Figure 3. 3 AC Charging Station: Levels 1 and 2 [143], [152], [155], [157].

- Level 3: The Level 3 chargers, also known as DC charging stations, convert AC power from the grid to DC and then charge the battery directly, bypassing the On-board Charger. Chargers operating on a polyphase supply can provide an output current of up to 400A and a voltage of up to 600V, enabling EVs with 24kWh to be charged in under 30 minutes (Fig. 3.4). Level 3 chargers are also referred to as DC Fast Chargers or Super Chargers.

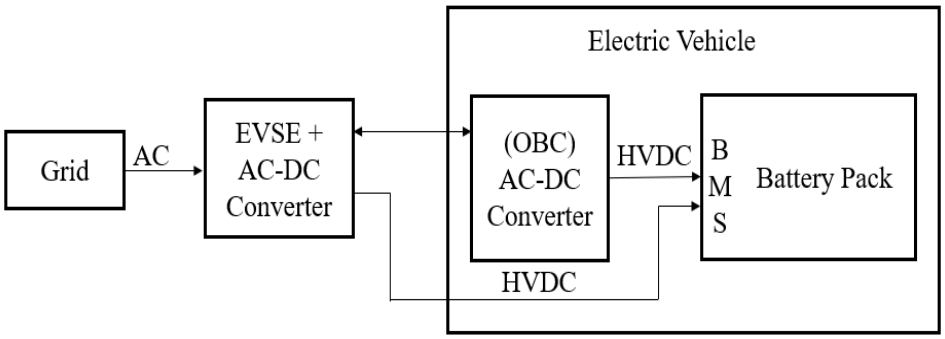

Figure 3. 4 DC Charging Station: Level 3 [143], [152], [155], [157].

Table 3.1 provides information on charging levels and types of chargers as per SAE and IEC standards, as well as the CHAdeMO (CHArge de MOve) charging standard:

Table 3. 1 Charging Levels.

Level of Charging	Phase	Type of Charger	Usage & Location	Power(kW) and Current(A)
Level 1 (SAE)	Single-Phase	On Board	Residential and Office	1.4kW/12A, 1.9kW/20A
Level 2 (SAE)	Single or Three Phase	On Board	Public and Private	4kW/17A, 8kW/32A
Level 3 (SAE)	Three Phase	Off-Board	Commercial and Filling Station	50kW, 100kW
DC Power Level 1 (SAE)	Poly Phase	Off Board	Dedicated Charging Station	40kW/80A
DC Power level 2 (SAE)	Poly Phase	Off-Board	Dedicated Charging Station	90kW/200A
DC Power level 3 (SAE)	Poly Phase	Off-Board	Dedicated Charging Station	240kW/400A
AC power level 1 (IEC)	Single-Phase	On Board	Residential and Office	4-7.5kW/16A
AC Power level 2 (IEC)	Single or Three Phase	On Board	Public and Private	8-15kW/32A
AC power level 3 (IEC)	Three Phase	On Board	Commercial and Filling Station	60-12kW/250A
DC rapid charging (IEC)	Poly Phase	Off-Board	Dedicated Charging Station	1000-2000kW/400A
DC rapid charging (CHAdeMO)	Poly Phase	Off-Board	Dedicated Charging Station	62.5kW/125A

Source: SAE J1772™: SAE EV Conductive Charge Coupler, and IEC 61851-1:2017 EV conductive charging system – Part 1: General requirements.

Inductive Charging [143], [152], [155], [157], [162], [163]

Wireless Power Transfer Charging, also known as Inductive charging, provides an innovative solution to traditional conductive charging. This charging process is based on magnetic coupling between two coils, with one connected to the power grid and the other to the EV battery, as shown in Fig. 3.5. The SAE is aiming to standardize inductive charging for various charging scenarios and levels with its SAE J2954 standard. The market offers several inductive charging topologies, each with unique limitations and categorized into three charging scenarios.

Static Charging is a user-friendly scenario that occurs when the EV is parked and unoccupied, such as at home or work, eliminating the need for handling cords and reducing the risk of electric shock. Stationary Charging is another scenario that takes place when the vehicle is stationary, and the driver is inside, such as at a traffic light, bus stop, or delivery truck. Dynamic Charging is a scenario where the vehicle is in motion, usually on a designated road or highway. Stationary and

Dynamic charging offer the advantage of continuously recharging the EV's battery while the vehicle is in use. However, inductive charging has some drawbacks such as limited energy efficiency, higher cost, issues with exposure to the magnetic field, and complexity of design.

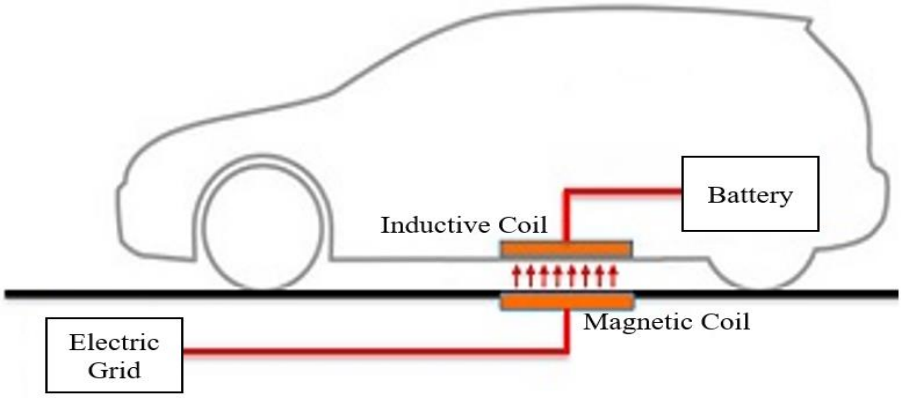

Figure 3. 5 Inductive Charging [143], [152], [155], [157], [163].

Battery Swap

Section 3.6.4 provides detailed information about battery swapping, which is one of the methods for EV charging.

3.7.2 Current Technologies for Effectual EV Charging

The proliferation of EV charging stations has created a significant need for electrical power, imposing challenges on the power grid. These challenges encompass various aspects of power quality such as voltage variations, regulatory compliance, peak demand management, system reliability, and load prediction. Several technologies have been identified for overcoming these challenges.

One such technology is smart grid technology [163]–[165], which involves self-sufficient structures that use automation to improve the communication, automation, and connectivity of the power network components. This technology facilitates the establishment of a communication link between the power grid and the users to monitor the area's load effectively. Furthermore, the technology automates remote terminals that correspond to their respective feeders. These terminals transmit any incorrect state information and report the power usage at each feeder. The use of this technique can help in providing preliminary information on the load conditions, which can ultimately eliminate potential reliability issues in the power grid. Additionally, this technique

also has a valuable role in load forecasting linked with the vehicle, and in this manner, the *SOC* of the battery can be shared with the grid. On the other hand, the adoption of smart grid technology is not without drawbacks. These include challenges in terms of regulations, data security and vulnerability, technical requirements, integration complexity, high installation costs, and potential communication issues.

Another technology that can help is the V2G technology [163], [166], [167], which facilitates the bidirectional flow of energy between EVs and the power grid. The use of this technology enables the charging and discharging of an EV battery to be adjusted based on the nearby energy production or consumption. Maintaining a balance between active power and frequency is crucial in preventing overloading and underloading, which can result in a frequency mismatch and potentially impact the power system. Hence, it is recommended to implement a bidirectional energy flow system, where the power grid supplies energy to the EV when needed, and during idle or surplus periods, the EV can feed power back to the grid.

Renewable energy technology [5], [10], [17], [18], [163] is an essential tool in the shift towards sustainable energy. It harnesses energy from renewable sources such as solar, wind, hydro, wave, heat exchange, tidal, and bioenergy to generate electricity, heat, and fuel. The rapid expansion of RES would lead to significant energy security and economic benefits while reducing environmental pollution caused by burning fossil fuels and improving public health. Currently, 26% of electricity from renewable sources is expected to reach 30% by 2024. RES provides a highly beneficial option for charging EVs due to its ability to significantly reduce carbon emissions and minimize the impact on the grid. Mounting a solar plant at residential places is also a harmless and an easy way to produce electricity. Solar panels mounted on the rooftops of shopping malls, public charging stations, offices, and libraries can also reduce the direct load on the grid. The installation cost of solar panels can be expensive, but the running cost is very inexpensive, and therefore it moderates the running cost of EVs compared to gasoline vehicles.

3.7.3 Types of EV Connectors

EV charging is categorized as slow, fast, or rapid with each type having specific connectors for either low or high-power applications [162], [163].

The slow charger operates between 2.3kW and 6kW, with the most common rating being 3.6kW, 16A. This method is widely used by owners to charge their EVs at home overnight, but it takes 6-12 hours to fully charge the vehicle. Due to the long charging time, slow chargers are becoming less popular and are considered outdated. These chargers use a standard residential three-pin socket [168].

The fast charger typically operates at 7kW at single-phase and 22kW at three-phase, both with a current rating of 32A. Fast chargers are commonly found in car parks, supermarkets, or leisure centers where cars are parked for more than an hour. The charging time for a 7kW charger is typically 4-6 hours, while with a 22kW charger, it is only 1-2 hours [168].

Rapid AC chargers, deliver a power output of 43 kW (three-phase, 63A). These chargers have the capability to charge an EV to approximately 80% of its battery capacity within a time range of 20-40 minutes. The charging duration may vary based on the specific model's battery capacity and initial *SOC*[168].

Rapid DC chargers, which utilize either the CHAdeMO or Combined Charging System (CCS) charging standards, provide a power output of 50 kW (125A), enabling charging to around 80% of an EV's battery capacity within a time frame of 20 minutes to an hour [168].

Unfortunately, there are several standards worldwide regarding the socket and corresponding connectors.

AC Charging Socket: There are three common sockets available for AC charging: Yazaki Socket- SAE J1772, Mennekes Socket, and Le-grand socket [169] (see Fig. 3.6). Among these, SAE J1772 (Type 1) is the most used in North America, providing a power output of 7.4kW and charging up to 32A in a single-phase AC supply. The charging connector has various connections for phase, neutral, and ground, along with two small pins to facilitate communication between the EV and the charger [169], [170].

Mennekes (Type 2) is popular in European countries and outputs up to 44kW employing a three-phase power system. This socket charges up to 63A in a three-phase AC supply, providing a power output of 44kW [169]–[171].

Le-grand or Type 3 is similar to Type 2 and has a protection shield to prevent from any debris. This socket charges up to 22A in a three-phase AC supply and outputs a power of 22kW. It is commonly used in France and Italy [169], [170].

Yazaki Socket

7.4kW,32A,
Single-phase

Mennekes Socket

44kW,63A,
Three-phase

Le-Grand Socket

22kW,32A,
Three-phase

Figure 3. 6 AC Charging Socket [169].

DC Charging Socket: DC charging sockets can be categorized into three types: CHAdeMO, CCS-1, and CCS-2 charging sockets (see Fig. 3.7). CHAdeMO sockets are particularly popular and are used by Nissan Leaf and KIA EV models. These sockets have two large pins that are used for DC power rails and communication pins for the Controller Area Network (CAN) protocol. The CAN protocol enables communication between the battery pack of the EV and the charger, allowing for the proper flow of current and voltage to charge the battery pack [169], [170].

CHAdeMO

400kW,1000V,
400A

CCS-1

2237.5kW,950V,
250A

CCS-2

135kW,410V,
330A

Figure 3. 7 DC Charging Socket [169].

Tesla Supercharger Socket: The Tesla Supercharger Socket (see Fig. 3.8) is the primary charging method for Tesla cars. The socket is designed to be versatile, combining both AC and

DC chargers in a single unit, offering flexibility during the charging process. With this socket, drivers can charge their Tesla vehicles using both AC and DC power sources. The socket delivers a power output of up to 43kW for AC charging and up to 400kW for DC charging, which is significantly more than other charging sockets available in the market [172].

Figure 3. 8 Tesla Supercharger Socket [172].

With the ongoing EV revolution, it is crucial to continually improve charging technology. One of the biggest obstacles that EV customers face is the absence of a uniform charging system. A potential solution to this problem is the creation of a universal design that resembles the size of ICE model vehicle fuel nozzle inlets. This standardization would allow EV owners to cross international borders without difficulty in charging their vehicles. Moreover, standardized devices could include features to notify EV drivers about energy sources and demands that have a negative impact on the grid.

3.8 Control Techniques Used

Off-grid EVCS commonly use droop and master-slave control techniques as control strategies. These techniques are used to manage the charging of multiple EVs simultaneously while maintaining stable voltage and frequency levels in the off-grid system [5], [138].

Master-slave control involves designating one charger as the primary charger ("master"), which regulates the charging current and voltage to maintain stable voltage and frequency levels in the off-grid system. The other chargers ("slaves") are then controlled based on the instructions from the master charger to adjust their charging current and voltage to match the master charger's output, ensuring that all EVs receive the same charging power [173][174].

Master-slave control allows for precise control of the charging process resulting in more efficient and reliable charging. It can ensure that each EV receives the same amount of charging power, regardless of the *SOC* of the EV's battery, which is particularly important when some EVs have more discharged batteries than others. Additionally, master-slave control can prioritize the charging of certain EVs over others based on factors such as EV owner's preferences or battery capacity [173][174].

However, master-slave control has some disadvantages. It requires a central control unit (the master charger) to manage the charging process, which can introduce additional complexity and expenses to the charging system. The slave chargers must also be compatible with the master charger, which limits the flexibility of the charging system. Additionally, if the master charger fails, the entire charging system may be affected, leading to charging delays or disruptions [175].

On the other hand, droop control is a decentralized technique commonly used in power systems to manage the distribution of power among multiple loads. In the context of off-grid EV charging stations, droop control manages the charging current based on the *SOC* of each EV battery [173][176].

Utilizing a voltage or current sensing circuit, droop control monitors the *SOC* of each EV battery. This circuit can be placed either at the charging station or directly within each individual EV. By continuously monitoring the *SOC*, the charging current can be dynamically adjusted for each EV. A feedback loop is employed in droop control to regulate the charging current. The loop is made up of a sensor that measures the voltage or current of the EV battery, a comparator, and a control element. The measured voltage or current is compared to a reference voltage or current using the comparator. Based on this comparison, the control element adjusts the charging current by evaluating the measured voltage or current against the reference value. The reference voltage or current is determined based on the *SOC* of the EV battery. As the battery approaches its maximum capacity, the reference voltage or current is gradually reduced. Consequently, the charging current is also reduced. Conversely, when a battery is depleted and requires a significant recharge, the charging current is increased. This approach ensures that each EV receives a charging experience tailored to its specific requirements. By adjusting the charging current based on the *SOC*, droop

control optimizes the charging process and guarantees that each EV is charged at a rate that aligns with its individual needs [176], [177].

Droop control has several advantages. It allows for efficient charging of multiple EVs simultaneously while ensuring that each EV is charged at the appropriate rate, maximizing the utilization of the charging station's capacity, and minimizing the time required for charging. It is also a cost-effective solution for off-grid EVCS, as it can be implemented using simple voltage or current sensing circuits [176].

However, droop control also has limitations. It is sensitive to changes in the system parameters such as the resistance of the charging cable or the battery's internal resistance, which can affect the accuracy of the *SOC* measurements and lead to errors in the charging current adjustment. Additionally, droop control may result in slower charging times for EVs [178].

When it comes to managing the charging of multiple EVs in off-grid charging stations, combining both droop and master-slave control techniques offers several advantages. One of these advantages is increased flexibility in managing the charging process. The droop control technique can regulate the overall voltage and frequency levels in the off-grid system, while the master-slave control can ensure that each EV receives a consistent level of charging power. This enables the efficient utilization of available power and can lead to faster charging times.

Another benefit of combining these control strategies is more precise control over the charging process. The droop control mechanism ensures consistent voltage and frequency levels, while the master-slave control system enables customization of charging current and voltage to meet the individual needs of EVs. This combination promotes efficient charging and enhances the longevity of EV batteries.

Furthermore, incorporating droop and master-slave control methods can simplify the charging system's overall complexity. Utilizing droop control to regulate the voltage and frequency levels and master-slave control to manage the charging of individual EVs eliminates the need for a complex central control unit. This can simplify the operation and maintenance of the charging system and reduce costs.

In short, combining droop and master-slave control techniques in off-grid EV charging stations provides several benefits, including improved flexibility, reliability, precision, and cost-effectiveness compared to using either control strategy alone. This technique is used in this research.

Table 3. 2 Comparison of Control Strategies for Off-Grid EV Charging Stations.

Control Strategy	Advantages	Disadvantages
Master-slave control	More precise control, consistent charging power, prioritize certain EVs	Requires central control unit, limits flexibility, system-wide failure risk
Droop control	Efficient charging, cost-effective, simple implementation	Sensitive to system changes, slower charging times
Combined (droop + master-slave) control	Increased flexibility, more precise control, reduced complexity, and costs	None mentioned

3.9 Summary

In this chapter explores the potential of off-grid PV-based charging stations as a sustainable solution for EV charging. These charging stations offer a promising alternative, especially in remote areas where traditional power grids are unavailable. By using PV panels to generate and store solar energy in a battery bank, the need for fossil fuels is reduced, thus promoting sustainable transportation, and lowering GHG emissions. The chapter also describes the critical components of PV-based charging stations, such as PV panels, charge controllers, and battery banks, and how they work together to ensure reliable and uninterrupted charging. Additionally, the control techniques used in off-grid PV-based charging stations, such as master-slave and droop control, are also described.

Chapter 4 Enhanced Efficiency and Reliability of Standalone EV Charging Stations through Isolated Bidirectional Converter with Snubber

The work and results presented in this chapter was published in a peer-review journal in which the author of this thesis (D.K. Nair) was the principal author. The details of the publication are as follows: D. K. Nair, K. Prasad and T.T. Lie (2021), "Standalone Electric Vehicle Charging Station using an Isolated Bidirectional Converter with Snubber", *Energy Storage 3*, https://doi.org/10.1002/est2.255.

4.1 Introduction

As the world becomes increasingly concerned with reducing GHG emissions and promoting eco-friendly transportation, EVs have provided a much needed and a popular solution. However, in remote areas, the availability of off-grid EV charging stations is essential to encourage EV usage. One promising solution to this problem is the use of solar energy. However, solar energy is not constant throughout the day, which means that an ESU is necessary for energy storage in addition to a PV array. In tackling this challenge, the research work described in this chapter presents a design approach that involves the utilization of a fast-charging station. This approach integrates key components such as a boost converter with MPPT, a BDC featuring a snubber circuit, and an ESU. By effectively combining these elements, the design presented in this chapter aims to optimize power management and provides a viable solution for addressing the challenge. Power electronic converters, with an active snubber and two capacitive-diode snubbers, act as the energy sources that interface with the ESU, resulting in near-ZVS and ZCS for the converter, thus leading to improved overall efficiency. The ESU can meet EV energy demands when there is insufficient generated solar energy and uses excess solar energy to develop an optimal power management system. Ultimately, this results in a green, reliable, and efficient off-grid EV charging station. A MATLAB/Simulink environment was used to validate the system performance of the proposed method.

EVs offer a viable solution for reducing GHG emissions and addressing fossil fuel depletion on a large scale. Currently, ICEs remain the most used form of propulsion for vehicles. However, it is critical to find sustainable alternatives to non-RES. An ideal solution can leverage electricity

generated from renewable sources such as solar, wind, nuclear, geothermal, natural gas, and fossil fuels. The transport sector is the second-largest contributor to carbon emissions and global warming. By extracting electricity from renewable sources, EVs offer a means of overall emission-free transportation. While EVs have been around since the early 20th century, the shift from gasoline to EVs became more pronounced in the 21st century due to increased global concerns about climate change and rising crude oil prices. Despite the clear benefits of EVs, there are still significant challenges that hinder their widespread adoption, with one of the most significant being the lack of infrastructure for fast charging of EVs [179].

Addressing the existing infrastructure deficit necessitates the establishment of an ample number of charging stations that effectively deliver significant climate benefits, generate economic profits, and garner widespread public acceptance. Charging stations that use RES, particularly solar energy, can make EVs entirely free from exhaust gases. Therefore, for non-urban and farm areas, a solar-based remote EV charging station can be considered, especially in areas where grid availability is absent. However, the available power for charging EVs may be uncertain and unreliable due to the inconsistency of solar irradiance. Hence, during uneven solar irradiance conditions, it is necessary to implement a PV source with an ESU to efficiently manage the power supply. During excess power conditions and the absence of EVs, the ESU can be charged from solar energy. The power electronic equipment used in the EV charging station is responsible for charging and discharging the ESU. Batteries are essential to back-up power, and BDC used in this system can execute the charging and discharging of ESU.

EV charging stations with bridge-type bidirectional converters have been widely used in previous research [38]. However, the efficiency of this type of converter was found to be reduced due to voltage and current stresses on the converter's main switches, as it did not achieve near ZVS and ZCS. A proposal for a new off-grid EV charging station is presented in this chapter with specific aim to achieve near ZVS and ZCS. The proposed system utilizes a BDC with an active snubber and two passive capacitive-diode snubbers, allowing for near ZVS and ZCS for the switches on both sides of the transformer. It was also possible to have an optimized energy extraction by developing and simulating various EV charging stations, confirming that PV-enabled EV

charging stations were the best choice. Ultimately, it is shown that the new off-grid EV charging system has the potential to reduce stresses and improve efficiency in the long run, outperforming many existing charging facilities.

4.2 The System Architecture

The proposed charging station is intended for use outside of urban areas where grid infrastructure is not readily available to support the charging activity. An overview of the PV-charged EVCS proposed in this study is shown in Fig. 4.1. An integrated solar power system with a total capacity of 100 kW is utilized to power the plant. The PV station continuously monitors the maximum output of the system and ensures that the maximum output is fed to the integrated DC bus for optimum performance. Accordingly, the charging station operates as a DC microgrid to provide power to the charging station while also storing power generated by the PV system. A maximum of 80 kW of power will be available from the proposed ESU. The charger is connected to the EV load with the aid of a BDC via an active and passive snubber. As their name suggests, bidirectional converters control how much power is conveyed from the ESU during the charging and discharging processes. The following section outlines the modelling of each component of the proposed system.

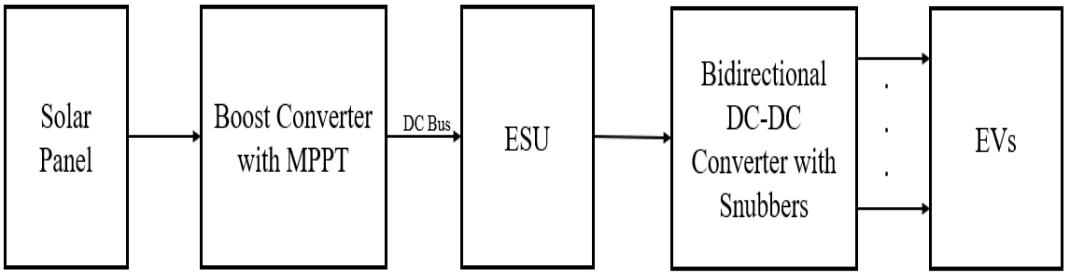

Figure 4. 1 Schematic of the proposed charging station.

4.2.1 PV Panels with Boost Converters

This scheme utilizes a PV array as the primary source of energy for the system. A calibration of the real-time output power is conducted prior to the simulation of a charging station. The output power of the PV cell is predicted using a single diode model [180]. Therefore, the model makes use of PV module parameters such as solar irradiance (G) and module temperature (T) to simulate the PV module performance. Several meteorological data sets are obtained from the National

Renewable Energy Laboratory (NREL) to extract the various parameters that govern the PV model's operation [181]. Boost converters boost the PV array voltage to the DC voltage required to load two EVs.

4.2.2 Energy Storage Unit

A backup option is provided by the ESU when the PV array is not able to provide sufficient power. During this study, a lithium-ion battery pack is used as the ESU. *SOC* constraints are set at 95% and 20%, respectively, to circumvent over-charging and over-discharging of the battery pack, such that.

$$SOCL \leq SOC \leq SOC, \quad (4.1)$$

where the lower *SOC* limit of 20% is specified by *SOCL*, and an upper *SOC* limit of 95% is specified by *SOCU*. As long as the PV array's *SOC* reaches the upper limit (*SOCU*) of 95%, the battery pack will provide the energy needed to charge EVs until the lower limit (*SOCL*) of 20%. In the proposed work, *SOC* is initially assumed to be a random value between *SOCL* and *SOCU*, which is routinely updated as the charging process progresses. It is from the *SOC* of the ESU that the estimate of the energy that can be obtained from the battery pack is derived. The ESU can provide energy to EV loads when the current *SOC* is higher than the *SOCL* at the time of delivery [182].

4.2.3 BDC with Snubbers

If an EV load is connected to an ESU, the ESU will start to discharge. A total of two charging units are used in the system, each of which acts as a current source to regulate the EV charging current and forms the charging circuit. In this manner, the charging and discharging of a unit connected to an ESU is controlled by a current control strategy. It is the case that while the ESU is charging, the BDC will enable the user to use the buck mode, whereas user uses the boost mode when the ESU discharges and the EV loads need to be powered. During transitions between the on and off states of the converter, an active snubber, as well as two passive capacitor-diode snubbers, can help reduce the high current and high voltage stress encountered at the main switches of the converter [120]. As a result of the snubber circuits on either side of the BDC, one

can achieve both ZVS and ZCS on either side of the converter, thereby enhancing the reliability of the entire system significantly. A diagram of the overall arrangement is shown in Fig. 4.2.

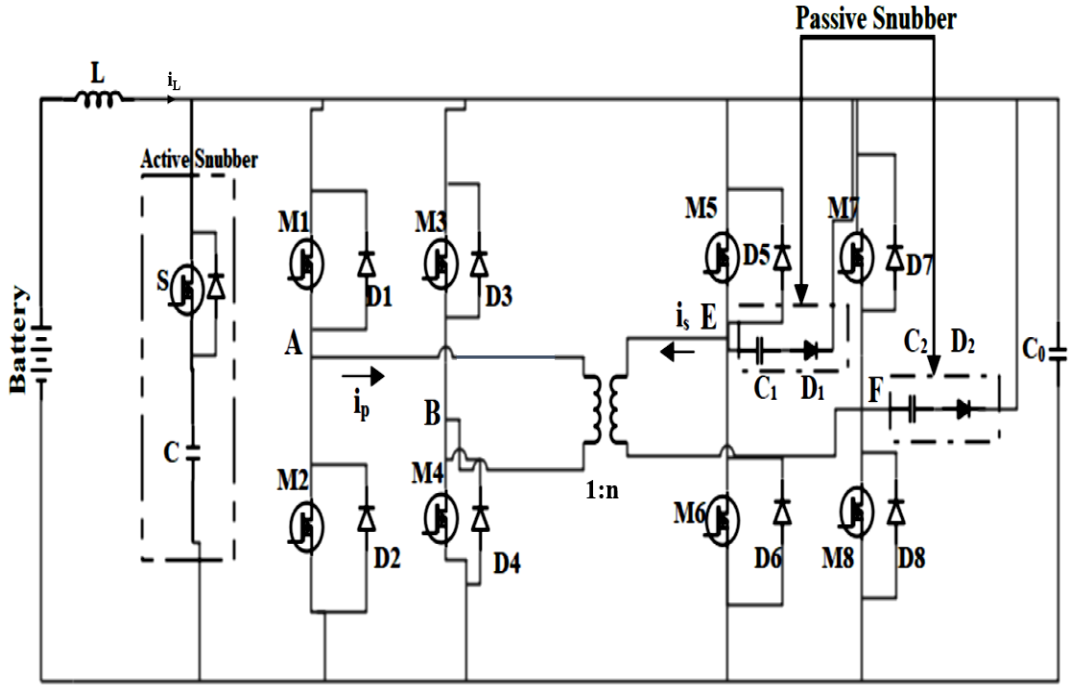

Figure 4. 2 Combined active and passive snubber circuits in a BDC.

Essentially, the converter consists of four parts: a current-fed bridge, an active snubber circuit on the low-voltage side of the converter and a voltage-fed bridge and a pair of passive snubbers on the high-voltage side. The circuit is in buck operation mode, where power flows from the high voltage side to the low voltage side through inductor *L*, through which output filtering is carried out. Meanwhile, when power is transferred from the low-power side of the circuit to the high-power side of the circuit, it is in boost mode. The snubber capacitor *C*, readily absorbs and stores the energy absorbed by the transformer as the voltage across the low end of the transformer starts to rise. Also, it clamps the voltage at a level just above the voltage across the lower side of the transformer, thereby increasing its effectiveness. When a heavy load is applied to the main switches, there can be reductions in the current stress across the main switches since the snubber current cannot circulate through the main switches when the load is high.

Ensuring switches S, M1, and M4 are switched on is the first thing to perform the boost mode operation. M2 and M3 have been switched off. The output receives the energy released from the inductor and clamp capacitor. When S is abruptly turned off, the transformer leakage current rises

above the inductive current, i_L. The clamp branch voltage resonates down to zero because of the excess current discharging the capacitor across the clamp branch and switches M2 and M3. The switches M2 and M3 are switched on with ZVS characteristics when the transformer current equals i_L because of conducting antiparallel diodes. The transformer current reduces to zero with all switches on, charging the inductor L. The clamp branch voltage is then charged until the clamping capacitor clamps it after M1 and M4 are switched off. The leakage inductance, L_k of the transformer is influenced by the voltage differential between the clamp capacitor and the reflected output voltage. When the clamp switch S is shut off, the subsequent half-cycle of operation will start.

The load current may now freely flow across the current-fed bridge, as the circuit is currently operating in buck mode. The output voltage is delivered to the transformer once M8 is activated. The whole voltage is applied to the leakage inductance while the opposite side of the transformer is short circuited, increasing the current. The voltage between the transformer terminals on the low voltage side instantaneously changes to the reflected voltage from the high voltage side as the transformer current increases linearly to the load current. The clamp branch voltage increases to the reflected voltage after the transformer current meets the load current. The leakage inductance and clamping capacitor begin to carry the resonant current via the clamp switch's antiparallel diode, which charges the inductor L. M5 is now switched off. Following that, D7 begins to conduct the freewheeling leakage current.

As the switch S is activated, the clamp branch voltage is maintained at a high level. The voltage fed side of the transformer's terminals experience this reflected voltage, which exerts pressure on the leakage inductance and causes the current to decrease. Eventually M7 conducts in conjunction with ZVS. Starting to reversal block, D1 and D2 stop leakage current from flowing in the other way. The load current is increased by the clamp branch. As soon as S is switched off, the clamp branch voltage falls to zero. During this period, there is no current freewheeling on the high voltage side, and M8 is shut off with zero-current switching. The circuit then resumes its previous

half-activity cycle's when M7 is switched on. Transformers reverse their polarity in order to maintain flux balance by reversing their voltage [120], [183].

When switching commutation is being performed, the *C* absorbs the difference in current between the current fed into the inductor and the current flowing through the leakage inductance of the isolation transformer. Furthermore, the active snubber provides an initial charge to the capacitor's high-voltage side during the start-up process, essentially preventing any unforeseen inrush current from being caused by the capacitor during this period. A consequence of this design is that the high-voltage side switches experience a hard switching shut-off when operating in step-down mode. Consequently, two capacitor diode snubbers are connected in parallel with the voltage-fed bridge as a preventative measure. As a result, the main switches will operate close to the point of transition between ZVS and ZCS in the programme. Snubber capacitor of the active snubber is used to transmit the energy stored in it to buffer capacitors C_1 and C_2. This decrease in snubber capacitor voltage occurs as a consequence of this [120].

Table 4. 1 Switching Condition of the Proposed Converter.

Switches	**ZVS turn ON**	**ZCS turn ON**	**ZCS turn OFF**
M1-M4	YES	YES	NO
S	YES	NO	NO
M5-M8	YES	NO	YES

Table 4.1 shows the switching state of the proposed converter. The table shows that all switches accomplish ZVS turn-on features for the proposed converter. It is also clear that switches M1-M4 accomplish ZCS turn-on characteristics, whereas switches M5-M8 obtain ZCS turn-off characteristics. The inductor is intended to be big enough to limit the exciting current and decrease transformer loss as calculated by the following equation,

$$l_r = \frac{i_{in} * {}^{V_0}/_n}{t_d}, \qquad (4.2)$$

where l_r is the critical point of leakage inductance to achieve ZVS, i_{in} is the input current, V_0 is the output voltage, n is the transformer turns ratio, and t_d is the dead time (500ns).

There are two voltage stress terms that are used in the proposed converter: the voltage stress on the rectifier diodes is the actual output voltage, and the voltage stress on the primary side switches is the reflecting output voltage of the converter ($^{V_0}/_{n}$). It is not commercially possible to find inductors which are ready-made for the application at these power levels; thus, these components must be designed to perform the job. It is assumed that the maximum discharge current will be 2A. In terms of ripple, the allowed amount is about 10% of the maximum discharging current. Accordingly, the value of the inductor can be given as follows:

$$L = \frac{[|V_{bat} - V_c|(1-D)T_S}{\Delta i_L}, \qquad (4.3)$$

where $|V_{bat} - V_c|$ represents the absolute difference between the battery voltage (V_{bat}) and the capacitor voltage (V_c). The duty cycle D is calculated as $\frac{2\Delta t}{T_s}$, with Δt representing the time when the primary side voltage across the transformer is equal to $\pm V_{in}$ and T_s denotes the period of the driving signal for each bridge switch. Finally, Δi_L represents the ripple current through the inductor.

A resonant transition switching between the leakage inductance and the output capacitor enables a large ringing voltage spike across the switches. Using a snubber resistor equivalent to the characteristic impedance of the ringing will effectively dampen or eliminate the ringing. A snubber capacitor is used to minimize dissipation at the switching frequency, but still maintain the electrical characteristics of the resistor at the ringing frequency by minimizing dissipation at the switching frequency. For designing purposes, it is best to start with when the capacitor's impedance at the ringing frequency is equal to the value of the resistor [183].

Clamping capacitor, $C \geq \frac{(T_S/4\pi)^2}{L_k}$, (4.4)

where T_s denotes the period of the driving signal for each bridge switch and L_k is the leakage inductance of the circuit.

Transformer turns the formula gives the ratio as

$$\frac{N_p}{N_s} = \frac{V_{in}}{V_0}, \quad (4.5)$$

where N_p represents the number of turns in the primary winding of the transformer, N_s represents the number of turns in the secondary winding, V_{in} is the input voltage, and V_0 is the output voltage of the circuit.

T_{DR} is the conducting time of rectifier diode and is given by,

$$T_{DR} = \frac{V_{in}}{2fs\,{}^{V_0}/_n}, \quad (4.6)$$

where V_{in} is the input voltage, V_0 is the output voltage of the circuit, f_s is the switching frequency and n is the transformer turns ratio.

The clamping branch ensures a safe path for the stored energy in inductive or capacitive elements, thereby preventing spikes and safeguarding the circuit components. The duty ratio, D_{clamp}, corresponds to the duration in the switching cycle when the main switching devices are active, determining their on-state timing and duration. By modifying the duty ratio, the bidirectional converter gains the capability to regulate power flow, controlling the output voltage or current. The duty ratio, D_{clamp} can be calculated using the formula:

$$\left(1 - D_{clamp}\right)T_t + \frac{2i_{in} * l_r}{{}^{V_0}/_n} = T_{DR}, \quad (4.7)$$

where i_{in} is the input current, T_t denotes the total period of the switching cycle, l_r is the critical point of leakage inductance to achieve ZVS, V_0 is the output voltage and *n* is the transformer turns ratio.

4.2.4 EV Load

A wise precaution should be taken when modelling the power demand of an EV to avoid damage to the batteries. In this regard, we assume that the battery should have 80% *SOC* at the time of departure and that there should not be any over-discharge of the EV battery. In this way, the EV ceases to use the electric energy available from the EV battery as soon as the battery *SOC* reaches 10% of its rated battery capacity. During the next charge from the ESU, when the *SOC* of the battery achieves 70% of its total capacity, the EV will start utilizing electric energy for its own generation. The power demand for an EV can be calculated as

$$P_{EV_i} = P_{EV_{req}} * S_i * w_i \,, \quad (4.8)$$

where P_{EV_i} is the demand of EV power at time slot *i* in kW, $P_{EV_{req}}$ is the maximum required EV power in kW at the time of plug-in, corresponding to the maximum *SOC* difference (80%) and current SOC_0. S_i is the EV connectivity status at time slot *i*, and w_i, the EV charging status at time slot *i*. The required EV power, $P_{EV_{req}}$ is calculated as

$$P_{EV_{req}} = (SOCU - SOC_0) * C_{battery} \,, \quad (4.9)$$

where *SOCU* is the maximum *SOC* required by each EV and $C_{battery}$ is the EV battery capacitance [154].

4.3 Formulation and Control of the Proposed Converter

Solar panels will supply a maximum power output of 100kW at a solar irradiance of 1000W/m^2 and a temperature of 40°C. Approximately 64 parallel strings of 5 SunPower SPR-315E modules are used in this PV block. A common DC bus of 400V connected to the PV array output and the boost converter. A DC-DC converter uses MPPT, particularly the P & O technique, to achieve maximum power by variably controlling the voltage across the PV array terminals [184]. Over the DC bus, the ESU consists of the lithium-ion battery that inputs the energy from the boost converter with MPPT. Battery life is prolonged by maintaining the battery's *SOC* between 20% and 95%. The following are possible scenarios for an operational ESU.

- *Scenario 1: $E_{PV} > E_{TOT}$ and $SOC_{ESU} \geq max\ SOC_{ESU}$*

  It is great to see EVs get charged with solar energy E_{PV}, however when the *SOC* of ESU (SOC_{ESU}) reaches its maximum, the E_{PV} disconnects from the DC bus to maintain a balanced power grid. It is the total energy capacity of all the connected EVs which is expressed as E_{TOT}.

- *Scenario 2: $E_{PV} > E_{TOT}$ and $SOC_{ESU} < max\ SOC_{ESU}$*

  It is important to understand that if the delivered solar energy E_{PV} exceeds E_{TOT}, then EVs can be charged from this energy. The additional power provided by solar power is used

to recharge the ESU if the current *SOC* of the charging station battery is lower than its maximum *SOC*.

- *Scenario 3:* $E_{PV} \leq E_{TOT}$ *&* $SOC_{ESU} > minSOC_{ESU}$

  As a result of the solar output in the charging station being reduced or zero during the night or in rainy/cloudy conditions, the ESU supplies the energy for charging the EVs in the charging station by keeping the battery at a minimum *SOC*.

With the aid of the BDC as well as the snubber circuits, the ESU can be charged or discharged quickly. A BDC with snubber circuitry at a switching frequency of 50 kHz serves as the unit for charging batteries. It is expected that the battery will provide the nominal input voltage, and that the EV voltage will be in the range of 250-450 volts. It is estimated that the EV current will be between 200 and 500A. EVs are connected to the DC bus by each of the two charging units. The DC-DC converter is used to feed energy to the EV loads when they are connected to the charging station. In such a case, each charging unit acts as a current source for controlling the EV charging to balance the supply of power with the demand of power.

If we assume that the charging current of the 100Ah battery is 11A, the charging time of the battery would be 9.09 hours when operated under ideal circumstances. The Nissan Leaf Acenta Auto model, for instance, comes with a 40kWh battery and it can be charged in between 29 minutes and 5 hours, depending on the charging method it uses at a public charging station, usually a DC fast charger, or a DC rapid charger [185].

This chapter aims to analyze the performance of the proposed charging station in relation to the assumed scenarios and a set of recommendations. The following sections discuss and describe what are the characteristics of the station and their subsequent analyses.

4.4 Simulation Results

A PV-based off-grid EVCS has been offered for evaluation including 100 kWh solar generation for the charging of an EV battery of 40 kWh capacity and an ESU of 80 kWh capacity. This ESU

supports the EV batteries during times when there is an insufficient output of solar energy and saves power during times when solar energy is in peak production. The simulation study for the proposed charging station is conducted using MATLAB/Simulink and is made up of considering three cases of EV requirements - EVs are charged either via a PV array alone, a PV array and an ESU together, or ESU only. A change in power demand can lead to a change in the performance of the ESU and the solar generation system. It is estimated that the Maximum Power Point (MPP) of the system is 96.24kW when solar irradiance is 1000W/m^2 and the temperature is 40^0C.

Usually, the DC-link voltage is higher than the voltage levels of the batteries. As a result, the BDC is useful in many EVs and charging stations for charging and discharging batteries. An evaluation of the performance of the proposed converter with and without the use of snubber circuits has been carried out. An illustration of the voltage waveform that is generated on the transformer's primary side of the BDC is shown in Fig. 4.3. In the case of a BDC without a snubber, there is parasitic ringing associated with voltage spikes. These spikes can damage the BDC. Using a snubber circuit, voltage clamping of the BDC can be achieved, and the voltage spikes are eliminated as shown in Fig. 4.3. It is beneficial in selecting lower-rated diodes for the BDC, and this can contribute to a longer lifespan of the diodes when compared to the case of a BDC without a snubber circuit [186].

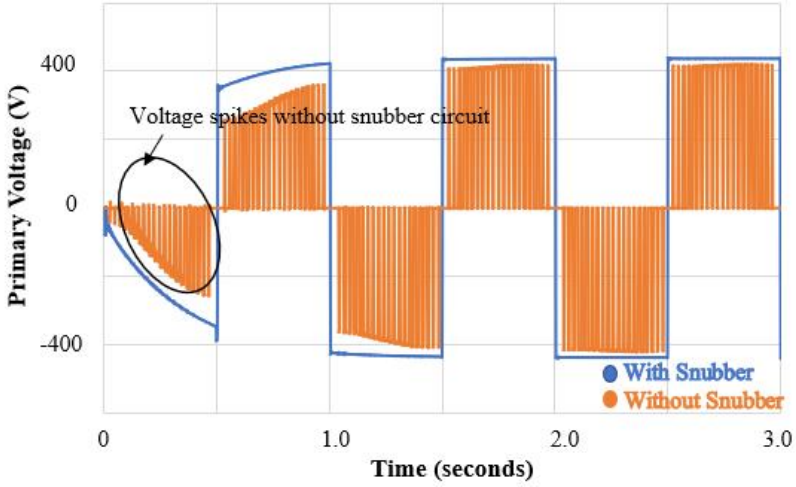

Figure 4. 3 Voltage across the primary side of the transformer of the proposed BDC.

4.4.1 EV charging with PV array only

A solar irradiance graph and the power response curve of the PV panel are shown in Fig. 4.4 for the purpose of generating the solar irradiance test data at 1000W/m^2. EV batteries are being charged exclusively by solar power, in this scenario, to make them fit for use. There is a constant DC voltage that is supplied to the terminals of the EV to provide the required terminal voltage continuously [186].

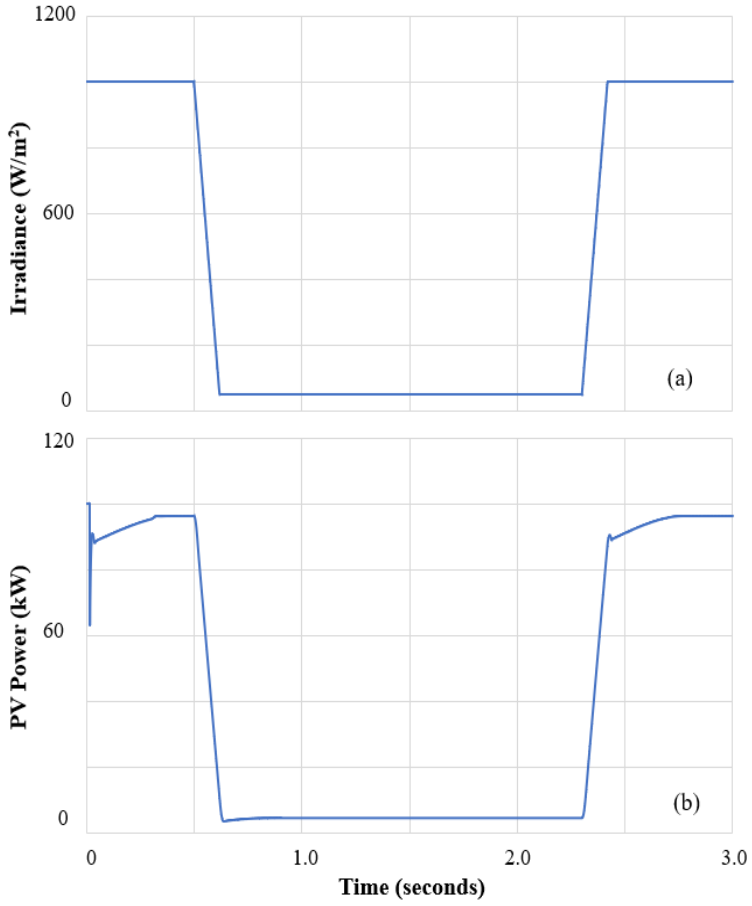

Figure 4. 4 (a) Solar irradiance data used for generating the test data and (b) power response curve of PV.

Figure 4.5 shows the *SOC* of the EV load as well as the power response curve of the EV load with the BDC and with and without snubber circuits. By using a BDC with a snubber circuit, it appears that the output power of the BDC is obtained according to the amount of solar irradiation available. Besides clamping the voltage and removing the spikes, this converter can also be

utilized to increase the lifecycle of the converter as well as its overall efficiency by reducing power losses.

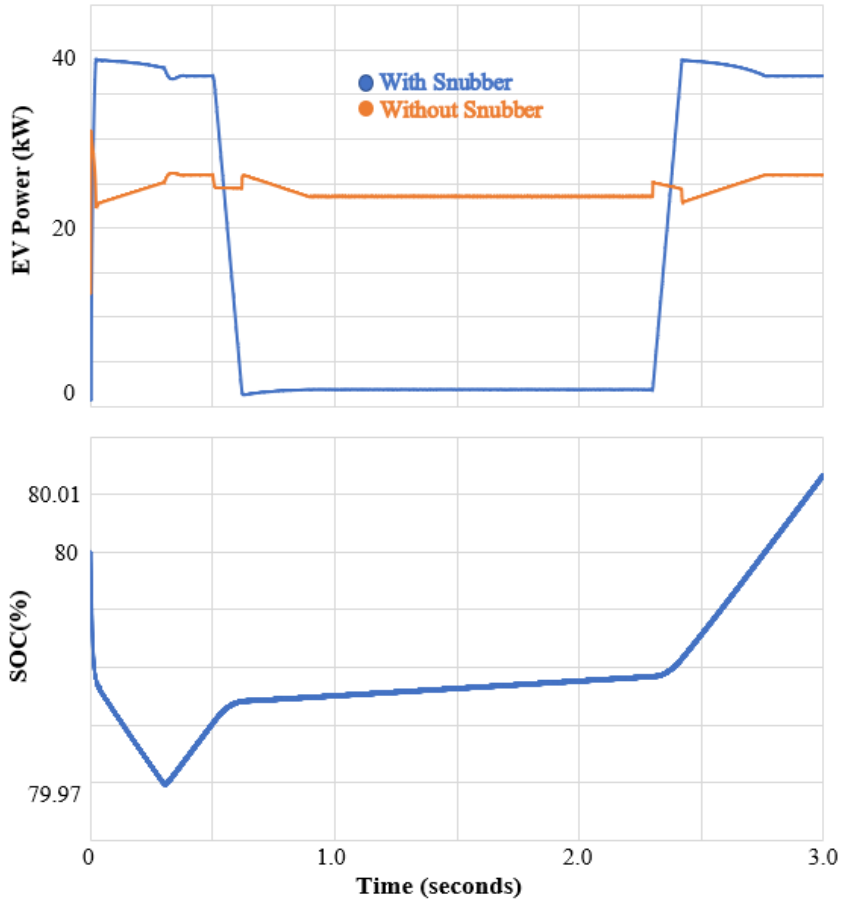

Figure 4. 5 (a) Power response curve for EV load with and without snubber circuit and (b) *SOC* of EV load.

4.4.2 EV charging with both PV array and ESU

Solar energy is advantageous in this scenario if it can adequately charge both EVs and the ESU. It has been found that excess solar energy is mainly utilized for the purpose of generating electricity in residential or commercial buildings. As soon as there is insufficient PV generation to meet the EV charging demand, the ESU will start discharging the stored energy. It will then feed it to the charging units in the vehicle, ensuring that the batteries are constantly being charged. A BDC, which features snubber circuits, allows the charging and discharging of the ESU in a highly efficient manner. Figure 4.6 shows the response curves for both *SOC* and ESU. Figure 4.7 shows the power response curve of an EV load, using a BDC with and without snubbers. EV loads are less affected by the ringing associated with the output power in the power response curve

when the BDC is used without a snubber circuit, which means the ringing attenuates more rapidly for fewer seconds. EVCSs must deal with a ringing or surge to be as efficient as possible. A smooth output power like that shown in Fig. 4.7 is achieved by the implementation of a BDC with active and passive snubbers. The worst-case scenario is, without a doubt, one in which solar power generation is entirely absent. In this scenario, ESU alone is expected to provide the energy needed to drive the EV's.

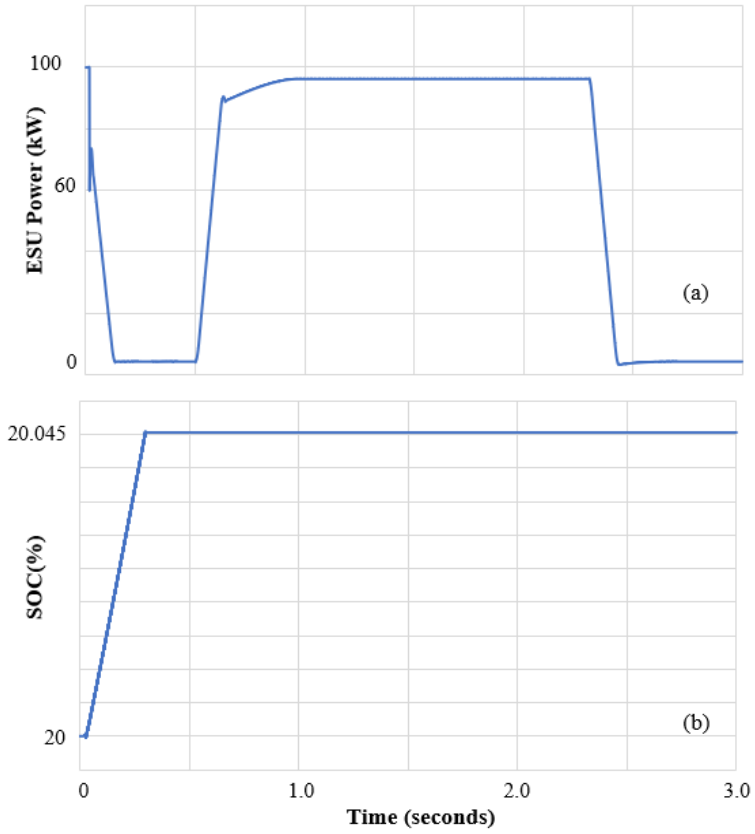

Figure 4. 6 (a) Power response curve of ESU and (b) *SOC* response of EV load.

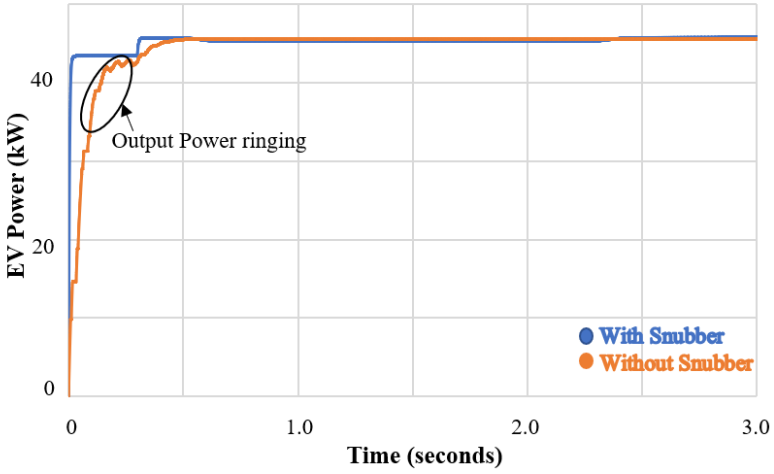

Figure 4. 7 Power response curve of EV load with and without snubber circuits.

4.4.3 EV charging with ESU only

This is a scenario in which EV loads are solely charged by the ESU. At this point in time, the ESU is the only source of power for EV loads. It is the ESU that discharges the stored energy to provide a continuous energy supply to the load when electricity is needed. Figure 4.8 shows the power response curves for the PV and *SOC* response of the EV load. Figure 4.9 shows the power response curve of the EV load with and without snubber circuits, and the response of the ESU. The output power ringing can also be observed in this scenario of a BDC without snubber circuits. With both active and passive snubber circuits, the BDC eliminates the ringing, thereby improving the converter's lifecycle and improving the overall efficiency of the EVCS.

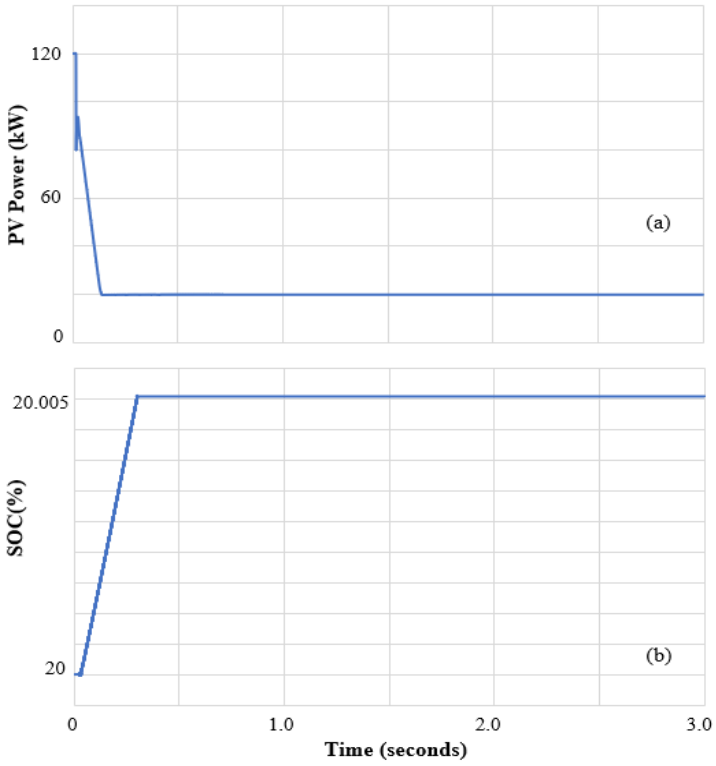

Figure 4. 8 (a) Power response curve for PV and (b) *SOC* response of EV load.

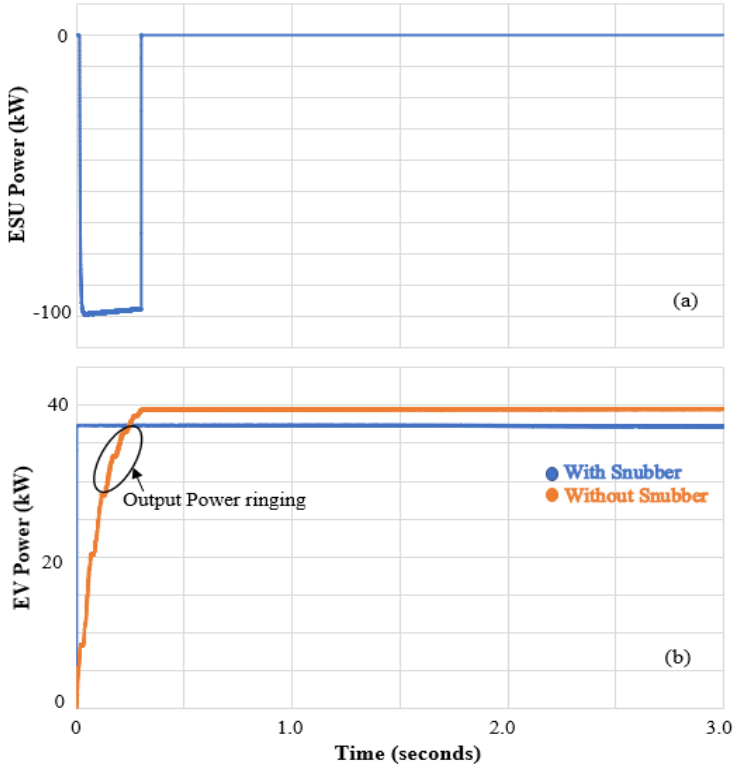

Figure 4. 9 (a) Power response curves of ESU and (b) EV load using BDC with and without snubber circuits.

Based on these scenarios, it can be concluded that the proposed off-grid EVCS based on PV generation is able to provide sufficient power for charging EVs in any situation. This design of the BDC, which uses snubber circuits to protect the charging station and its components from high voltages and high currents, has also proved to be very energy-efficient and protects the system from damage. An efficiency curve is obtained by retaining the input voltage constant throughout the calculation. With a fixed value of input voltage of 400V, Fig. 4.10 shows the efficiency curves for the inductor current variation ranging from 5-30A. BDCs that are not equipped with a snubber circuit are considered to have a maximum efficiency of ~88.7%, while BDCs that are equipped with snubbers have a maximum efficiency of ~92%. Clearly, a BDC that includes active and passive snubber circuits achieves higher efficiency than a BDC without snubber circuits.

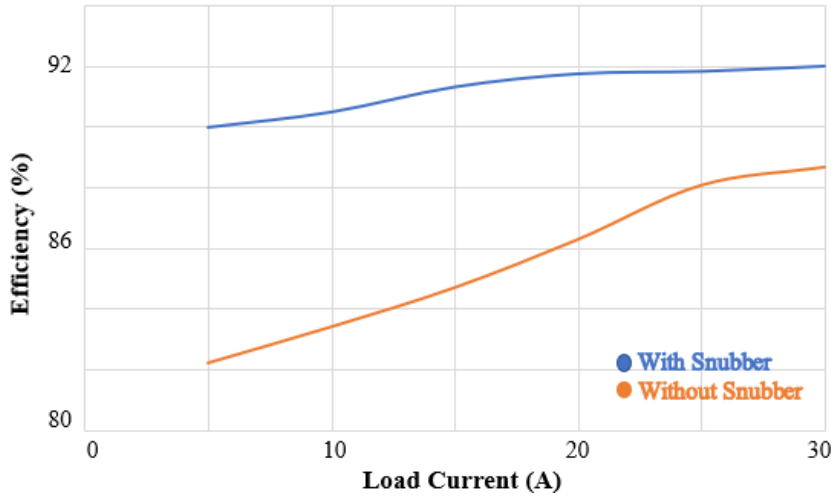

Figure 4. 10 Plot of conversion efficiency of the proposed converter.

4.5 Comparitive Analysis

In Table 4.2, a comparative analysis of different converter topology models for DC fast chargers is presented. As is evident from the table, most of the converter topologies that are described are bidirectional, provide grid support, and use battery storage as a power source. Thus, when the decision is being made about which topology is most suitable, other factors need to be considered. These factors include the realization of zero-voltage and zero-current switching, the number of passive components, conduction losses, and the complexity involved. In terms of complexity, the non-isolated three-port BDC is the simplest of all the converters. Compared to all other converters, it has fewer diodes and switches as it is powered by a dissipative energy element, and it offers lower efficiency than the others. In contrast to all the other converters proposed in the literature, the proposed converter offers and realizes both zero-voltage and zero-current switching simultaneously. The system is subject to conduction losses due to the circulation of current. Nevertheless, the proposed converter effectively reduces the circulating current and voltage spikes to a specified level.

Table 4. 2 Comparitive Analysis Between Different Converter Topologies for DC Fast Chargers.

References	[187]	[188]	[38]	This study
DC-DC Converter	Phase-shift full-bridge unidirectional	Non-isolated	Non-isolated BDC	Isolated BDC with active and

	DC-DC converter	three-port BDC		passive snubber
Use of snubber circuit	Clamp diode at primary side	No	No	Active clamp snubber circuit at LV side and Passive snubber circuits at HV side
Grid support	Yes	Yes	No	No
BESS Integration	No	Yes	Yes	Yes
RES Integration	No	Yes	Yes	Yes
Number of switches/diodes/capacitors	8/1/7	3/1/3	7/1/3	8/2/4
Conduction loss	high	High	high	low
Realization of ZVS and ZCS	ZVS	Near ZVS	No	Both ZVS and ZCS
Complexity	very high	Low	high	medium
Features	Due to the presence of circulating current, conduction loss is high. Low efficiency at light load conditions	Due to the presence of circulating current, conduction loss is high.	Due to the presence of circulating current, conduction loss is high.	Low conduction loss using the snubber circuit. Less switching stress

Kumar *et al.* [38] proposed a system that utilizes renewable energy resources to the maximum extent possible and can recharge the batteries of EVs under any circumstances. Using this system, grid burden could be minimized since no grid energy is required to charge the batteries. Despite this, it did not demonstrate any results in terms of the ability to eliminate any voltage stress that may develop within the BDC operated by the charging station. Consequently, these stresses have a negative effect on the overall efficiency of the converter. There are several advantages to the converter in the present work, due to the use of an additional active snubber circuit:

1) ZVS is automatically turned on for the main switches of the converter, which eliminates the reverse recovery problem.

2) Conduction losses are zero.

3) Energy transfer from the clamp capacitor does not cause a loss in duty cycle.

4) Higher efficiency, and

5) Switching and control scheme is extremely simple.

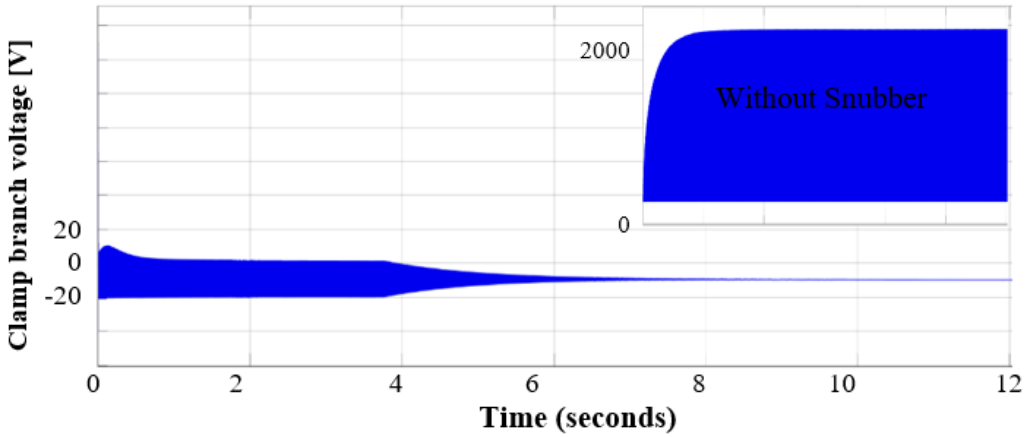

Figure 4. 11 Clamp branch voltage of BDC with active clamp snubber (inset shows the clamp branch voltage without snubber).

It is possible to obtain a zero voltage as short as 4-6 seconds after the BDC is turned on by using the clamp branch voltage obtained from a clamp snubber, as shown in Fig. 4.11. An effective snubber can be implemented to eliminate the stresses. With ZVS characteristics, the converter in this study has the capability of effectively reducing losses and is also capable of enhancing the power of the EVCS.

4.6 Summary

This chapter presents MATLAB/Simulink simulations to validate the performance of a stand-alone EVCS based on PV generation. The following summarizes the study:

1) A configuration for an isolated BDC has been developed, which incorporates both active and passive snubber circuits placed between the EV and ESU to enhance energy efficiency.

2) The active clamp and passive snubber utilized in the present converter have been used to minimize spikes at the primary side of the transformer and quickly achieve ZVS and ZCS characteristics.

3) It is clearly demonstrated that the proposed converter with a snubber circuit, when compared to an existing off-grid EVCS design, can reduce the stresses across the main switches, thus increasing the charging station's efficiency. Combining active and passive snubbers with a BDC and an additional energy storage device allows the solution to be an excellent option for PV-dependent EVCSs, resulting in an improved conversion efficiency of 92% compared to passive models.

4) The proposed EVCS will also help alleviate the grid burden and enable EV charging in remote areas that are challenging to access. In the absence of solar energy or a decrease in solar energy, the PV array and ESU are equipped with a suitable system to supply power to the EV loads. As a result, a PV-based EVCS is a more environmentally friendly and energy-efficient alternative.

Chapter 5 Optimizing Efficiency and Performance of Off-Grid EV Charging Stations: Comparative Analysis of Snubber Circuit Configurations

The work and results presented in this chapter was published in a peer-review journal in which the author of this thesis (D.K. Nair) was the principal author. The details of the publication are as follows: D. K. Nair, K. Prasad and T.T. Lie (2021), "Implementation of Snubber Circuits in a PV Based Off-Grid Electric Vehicle Charging Station — Comparative Case Studies", *Energies* 2021, *14*, 5853, https://doi.org/10.3390/en14185853.

The introduction of EVs has brought a significant change to the transportation industry, which was previously unimaginable. Although EVs are frequently hailed as a sustainable choice for the road ahead, there is a concern that they may cause a strain on the grid infrastructure and result in a notable surge in GHG emissions. This outcome largely depends on the electricity source utilized to power the vehicles. The ideal solution for EVs would be a solar-powered charging infrastructure that integrates sun power into the charging process.

In this context, an off-grid EVCS is presented in this chapter. This EVCS offers fast battery charging through a ZVS snubber-based BDC. The system comprises an ESU, a PV array, a boost converter, and a BDC equipped with various types of snubber circuits, namely RCD snubbers, active clamp snubbers, and flyback snubbers. Performance evaluation is carried out in terms of the use of different types of snubbers.

It is worth mentioning that the extent of leakage inductances varies depending on low-voltage side-fed inductor currents. Therefore, the system layout is designed to clamp the voltage on the rail and reduce the peak current at the converter switches, resulting in enhanced efficiency of EVCS. The MATLAB/Simulink environment is utilized to develop and validate a snubber-based off-grid EVCS to guarantee optimal system performance.

5.1 Introduction

EVs are an eco-friendly alternative to traditional ICE vehicles, emitting significantly fewer GHG gases. The transition to EVs is a positive step towards renewable energy for the transportation

sector. Nevertheless, EVs can still put pressure on the power grid despite their lack of emissions while in use. A solution to mitigate the strain on the power grid caused by EVs is coupling PV with EV charging stations. This method enables greater use of solar energy and EVs without overburdening the grid. This coupling is particularly beneficial for charging EVs in remote areas, although it can create unpredictability and instability due to variable solar irradiation [189].

Recent research has placed emphasis on the advantages offered by snubber-based BDCs when applied to EVs. Kumar *et al.* [38] conducted a study proposing a PV-based OGCS that effectively integrates a solar source with an ESU to accommodate varying irradiance conditions. While this system enhances the reliability of the off-grid charging stations for EVs, the non-isolated BDC utilized in their study lacks the capability to achieve ZVS, which negatively impacts the charging station efficiency. Considering this, this chapter introduces a BDC that incorporates snubber circuits, demonstrating near ZVS characteristics across BDC switches. This integration significantly enhances the overall efficiency of PV-based charging stations for EVs.

Given that EVs operate at low voltage levels, an interface between the BDC and the charging station becomes necessary. An isolated BDC surpasses a non-isolated BDC due to its bidirectional energy flow, electrical isolation, and heightened reliability. We will employ this BDC to facilitate both voltage step-up and step-down processes, thus enabling charging and discharging within a single circuit topology. Among the various BDC configurations available, the full-bridge BDC stands out due to its ability to handle high power. However, the leakage inductance of the isolation transformer leads to increased voltage and current spikes during switching transitions. Additionally, the freewheeling current contributes to conduction losses and reduces the effective duty cycle due to the leakage inductance effect. An alternative approach involves charging the leakage inductance to match the current level of the current-fed inductor, thereby minimizing current discrepancies, as well as voltage and current spikes. Nevertheless, achieving optimal synchronization between these two currents proves challenging as the current level varies with load conditions [17].

Various types of snubber circuits can be implemented to address the above-mentioned challenges. These circuits offer an alternative pathway for circulating current across BDC switches, effectively managing the impact of circuit reactance. This, in turn, enhances the overall performance and increases the converter's reliability [190], [191]. Snubbers can be categorized as either passive or active networks, with passive snubbers comprising of resistors, inductors, capacitors, or diodes, while active snubbers utilize transistors or other active switching elements.

A commonly used passive approach to clamp the voltage and restrict capacitor discharge current is through the implementation of an RCD snubber. Active clamped snubbers recycle energy stored in leakage inductance, leading to improved converter efficiency. The flyback snubber utilizes a capacitor-diode circuit to clamp the voltage spike across the switches and recover it. This snubber configuration proves highly effective in reducing circulating current across BDC switches [113].

Previous research has focused on the benefits of utilizing snubber based BDCs in EVs [113], [121]. However, little information exists on the use of snubber-based BDCs in off-grid charging stations for EVs. Kumar *et al.* [38] discussed a charging station that did not incorporate any snubber circuit, while a prior study [17], also discussed in Chapter 4, highlighted the beneficial effects of employing a flyback snubber. However, a comprehensive performance comparison of off-grid EVCS with various snubber circuit configurations has not been conducted. Therefore, work presented in this chapter aims to compare RCD, active clamp, and flyback snubbers for the BDC in terms of overall performance in off-grid EV charging stations.

Although BDCs in EVs operating at low voltage levels have been studied [113], [121], there is a lack of data for both off-grid and grid-connected EV charging stations. paperwork presented in this chapter recommends integrating snubber circuits into BDC configuration to effectively mitigate the impact of circulating current on the main switches, resulting in efficient clamping of voltage spikes across the switches. This, in turn, improves the off-grid EVCS's performance. Furthermore, implementing a single snubber circuit in the charging station is more cost-effective than having one in each EV. As a result, conducting a performance study of EV charging stations with different snubber circuit configurations is significant and necessary.

5.2 Analyses of the Snubbers

The study in [38] uses a BDC which consists of metal-oxide-semiconductor field-effect transistor (MOSFET) switches for step-up and step-down modes and a DC link capacitor that serves as the voltage source. Since the converter functions as a voltage source, the load source is inductive. However, there might be a time delay during the transition from turn-off to turn-on or vice versa which can cause an overvoltage condition. Additionally, the free-wheeling diode's reverse recovery leads to a current spike during turn-on, which results in significant switching losses, particularly during turn-off. A viable strategy for addressing these concerns involves the utilization of snubber circuits. By incorporating snubber circuits, the issues mentioned earlier can be minimized or eliminated.

Figure 5.1 portrays the proposed system, as outlined in [38], which includes a BDCs model that can function in both charging (buck) and discharging (boost) modes concurrently. During the charging process, the DC-link functions as the input for the BDCs, while the battery serves as the output load. The buck mode, which employs an inductor (L_{buck}), is utilized at the output side of the BDCs to attain the battery's voltage level. The value can be computed using the equation

$$L_{buck} = \frac{[|V_{DC} - V_{bat}|(1-D)]}{\Delta i_L f_s} \ , \qquad (5.1)$$

where Δi_L and f_s are the ripple current and switching frequency of the buck mode, respectively, V_{DC} and V_{bat} are input and output voltages of the BDC, respectively, and D is the converter's duty ratio.

If the battery has been depleted, the input should be linked to the battery terminals while the output should be linked to the DC-link. This is because the voltage at the DC-link exceeds that of the battery terminals. The calculation of the component inductor (L_{boost}) in boost mode uses the equation

$$L_{boost} = \frac{V_{bat} D}{\Delta i_L f_s} . \qquad (5.2)$$

The BDC operates in both boost mode and buck mode - so it is necessary to choose the value of inductor, L accordingly as

$$L = \max(L_{buck}, L_{boost}). \quad (5.3)$$

The equation 5.3 represents a mathematical function that calculates the maximum value between two variables, L_{buck} and L_{boost}. This function employs the "max" function to determine and output the larger value from the two variables. Simulations of converters with passive snubbers, active clamping circuits, and flyback snubbers were conducted for the purpose of comparison.

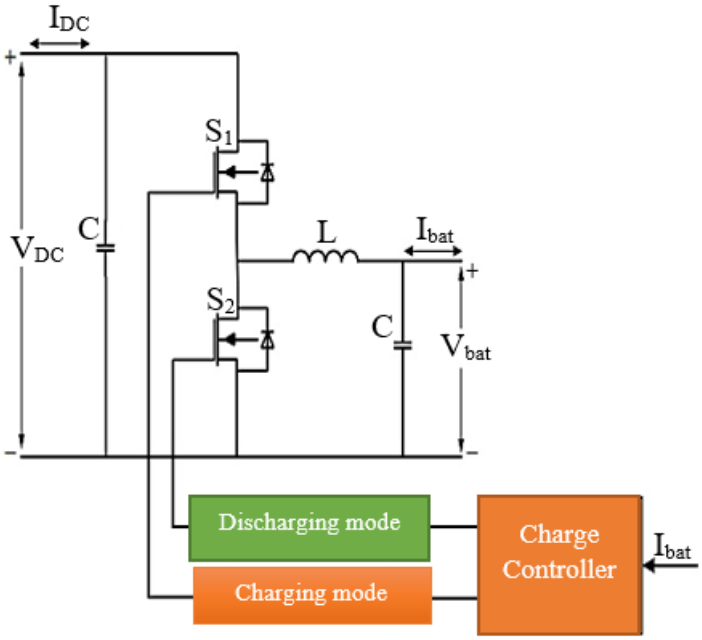

Figure 5. 1 Circuit diagram of the BDC used in [38].

5.2.1 RCD Snubber

Figure 5.2 depicts the three key components of RCD snubbers: the resistor R_s, the capacitance C_s, and diode D_s. RCD snubbers or RCD clamps can prevent sharp voltage fluctuations across the switches. The capacitor functions as a filter and helps to maintain a low-ripple DC source by dissipating the stored leakage energy through the resistor. Meanwhile, the diode is a switch that can only operate in one direction at a time. RCD snubbers measure the characteristic impedance of the resonant circuit, which can be determined by the following equation, to clamp spikes.

$$Z = 2\pi f_s L, \quad (5.4)$$

where f_s represents the switching frequency of the converter and L is the inductor value derived from equation 5.3. Setting the snubber resistor at a value equivalent to the characteristic impedance of the device can effectively reduce the ringing effect to an acceptable level. Therefore, to determine the resistor to be used, the following equation must be used.

$$R_s = Z. \tag{5.5}$$

The snubber capacitor, C_s, ensures that dissipation at the switching frequency is kept to a minimum, allowing the resistor to function at its peak efficiency at the ringing frequency. The capacitor is made to have a clamping frequency impedance that is equal to that of the resistor, according to the equation

$$C_s = \frac{1}{2\pi f_s R}, \tag{5.6}$$

where f_s is the switching frequency of the converter.

The purpose of this circuit is to absorb the current that flows through the inductor when the voltage at the switch's drain exceeds that of the clamp capacitor. As a result of the relatively large capacitor, this circuit can sustain a consistent voltage throughout the switching cycle. Additionally, increasing the capacitor value increases peak power and reduces switching loss [192].

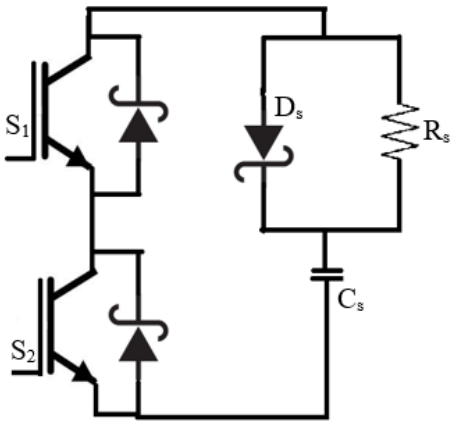

Figure 5. 2 Circuit diagram of the RCD snubber [192].

5.2.2 Active Clamp Snubber

For higher power applications of BDCs, an active clamp is a highly effective choice. The objective of this component is to restrict the turn-off voltage overshoot of the bridge switch, which facilitates energy storage for ZVS. Utilizing a suitable leakage inductance design can help overcome part of the reverse-recovery problem associated with the output diode. It's important to note that these converters use switches that operate under hard switching conditions, which means that passive lossless clamp circuits are replaced by active clamp circuits. Using parallel capacitors results in a ZVS condition where both the primary and clamp switches turn on, and this reduces turn-off losses significantly.

As shown in Fig. 5.3, this topology utilizes a coupled inductor to recycle the energy produced by the leakage inductances, which helps to achieve the ZVS condition for both the main and clamp switches. By implementing this approach, switches and diodes are subjected to lower voltage stresses than those resulting from the output voltage. In addition, to decrease conduction losses and lower the cost of the circuit, an active clamp circuit is incorporated, consisting of an active switch M_c, and a capacitor, C_c.

The resonant tank circuit can be constructed using the clamping capacitor C_c and the leakage inductance L_k. Off-stage resonance occurs during the operation of the boost mode. The following criteria should be considered when selecting C_c.

$$C_c \geq \frac{(T_s/4\pi)^2}{L_k}, \tag{5.7}$$

where, T_s represents the period of the driving signal for each of the bridge switches [193], [194].

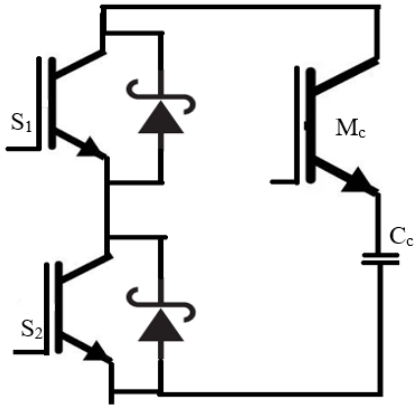

Figure 5. 3 Circuit diagram of the active clamp snubber [193], [194].

5.2.3 Flyback Snubber

The flyback snubber, shown in Fig. 5.4 is ideal for high-power applications. It is possible to achieve a ZVS turn-on process or a ZCS turn-off process with the use of a snubber circuit, which occurs when there is a brief period between the ZVS or ZCS characteristics in the main switch. The application of a series inductor slows down the reverse recovery current of the diode. However, the downside of this is that it can increase the voltage stress on the main switch during the transition between turn-on and turn-off operations, which results in higher switching losses. The purpose of using snubber capacitors is to limit the switch voltage by dissipating the stored energy of the snubber inductors. However, it is important to note that the snubber capacitor's function of recirculating energy through the main switch can lead to higher current stress, which can ultimately impact the reliability and lifespan of the converter. One way to mitigate the issue of high voltage and current stress on the main switch caused by snubber capacitors is to implement flyback snubbers that enable soft-switching capabilities. This approach can significantly reduce both voltage and current stress, which can help to improve the reliability and longevity of the converter. Furthermore, the flyback snubber can attain close to ZVS and ZCS conditions while also considerably reducing voltage and current stress on the main switch. The output voltage ripple in the flyback converter is computed by the equation

$$\frac{\Delta V_0}{V_0} = \frac{DT_s}{C_f}. \qquad (5.8)$$

This equation must be utilized to determine the snubber capacitor for the flyback snubber, taking into consideration the C_f capacitor in the flyback converter and a 3% output voltage ripple ($\Delta V_0/V_0$) [195], [196].

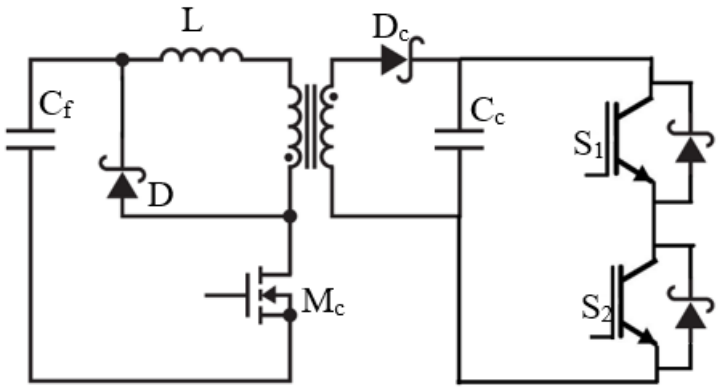

Figure 5. 4 Circuit diagram of the flyback snubber [195], [196].

5.3 Simulation Results

5.3.1 Case 1: Model proposed by Kumar *et al.* [38]

In a study presented in [38], a 24 kW PV-based generation system was used to power a 15 kWh battery of an EV that was coupled with an ESU of 15 kWh. The ESU serves as a backup source for the EV battery during times of low PV generation, and also stores any excess energy produced during times of high PV generation. This helps to ensure a steady and reliable power supply to the EV, while also maximizing the use of RES. Three modes were considered for charging the EV battery, which were (i) by PV energy alone, (ii) by both PV energy and ESU energy, and (iii) by ESU energy alone. MATLAB/Simulink was employed to simulate the three modes of operation for the BDC used in the charging station. Subsequently, the results for each snubber circuit were analysed and compared in the following sections to evaluate the converter's performance.

5.3.1.1 Charging Battery of EVs with PV Energy Only

As shown in Fig. 5.5, it appears that PV generation alone is enough to charge the EV batteries in a timely manner. The DC-link voltage is maintained at a level that can continuously supply the

battery terminal voltage. Figure 5.6 shows the power variations of the EV using three different types of snubber circuits with the BDC that can be used with the EV.

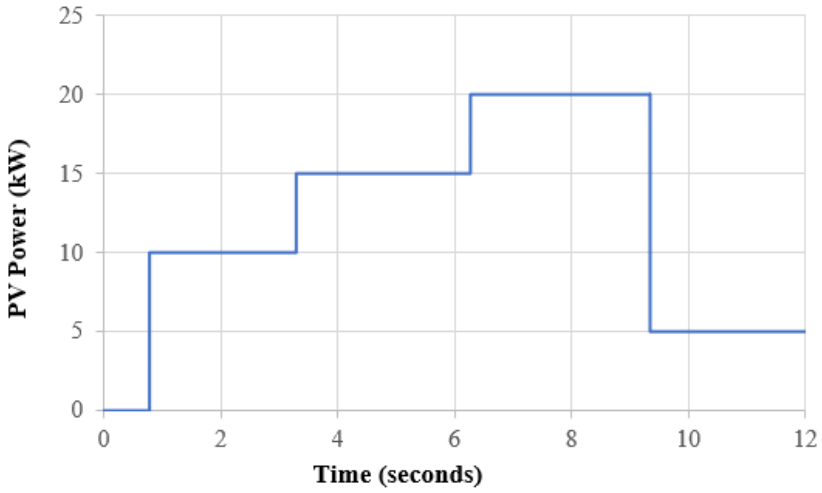

Figure 5. 5 Power response curve of PV.

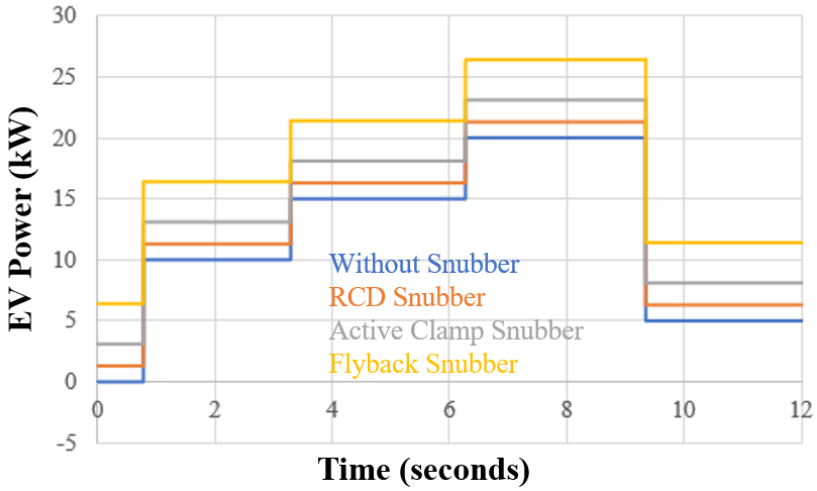

Figure 5. 6 Power response curve of EVs.

5.3.1.2 Charging Battery of EVs with PV Energy and ESU Energy

As shown in Fig. 5.7, it becomes apparent that relying solely on PV energy is not enough to charge EVs in a timely manner. Instead, ESUs are utilized to provide any additional energy required to charge the EV battery when needed. Figure 5.8 displays the power fluctuations of EVs when operating in this mode, utilizing three distinct snubber circuits alongside the BDC.

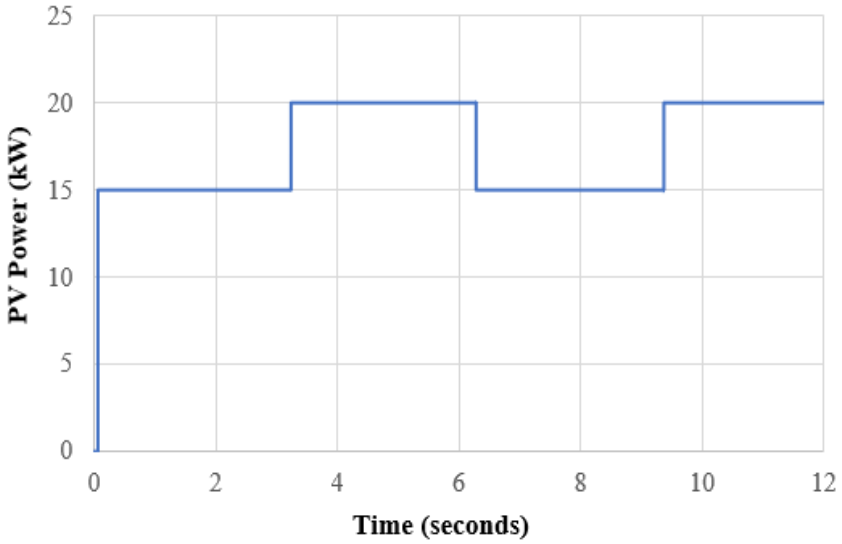

Figure 5. 7 Power response curve of PV.

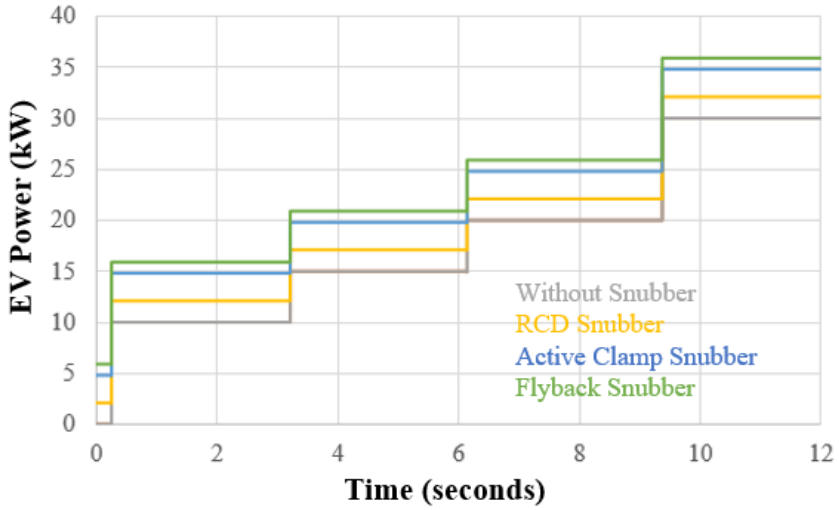

Figure 5. 8 Power response curve of EVs.

5.3.1.3 Charging Battery of EVs with ESU Only

During this mode of operation, the EV battery is solely recharged using the ESU since the PV generation is negligible. Figure 5.9 illustrates the power fluctuations of EVs in this mode, which utilize three distinct snubber circuits in conjunction with the BDC.

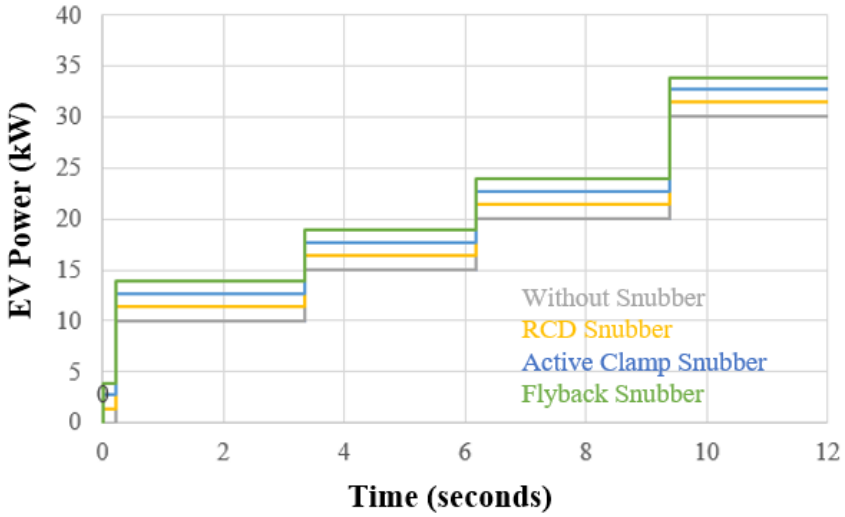

Figure 5. 9 Power response curve of EVs.

The charging station is fully capable of charging an EV battery under any circumstance, as shown by the results presented in these three cases. The concept of harnessing renewable energy in this manner is quite attractive. The voltage across the main switches of the BDC's clamp branch is shown in Fig. 5.10. From the figure, it can be inferred that achieving ZVS without a snubber circuit is unattainable due to the significant voltage stress observed across the switch. However, all three snubber circuits proposed in the study were able to achieve ZVS quickly. The RCD snubber circuit achieved this in just 6 seconds, while both the active clamp snubber and flyback snubber significantly reduced the voltage stress on the circuit and achieved almost instantaneous ZVS. Based on the data depicted in the graph, it can be concluded that the flyback snubber is the most appropriate option as it effectively reduces voltage stresses and facilitates ZVS. Moreover, Figures 5.6, 5.8, and 5.9 demonstrate that implementing snubber circuits in EVs can significantly increase power in those vehicles. Furthermore, the power waveforms reveal that the implementation of the flyback snubber in the charging station results in the highest output power compared to the other two snubber circuits tested.

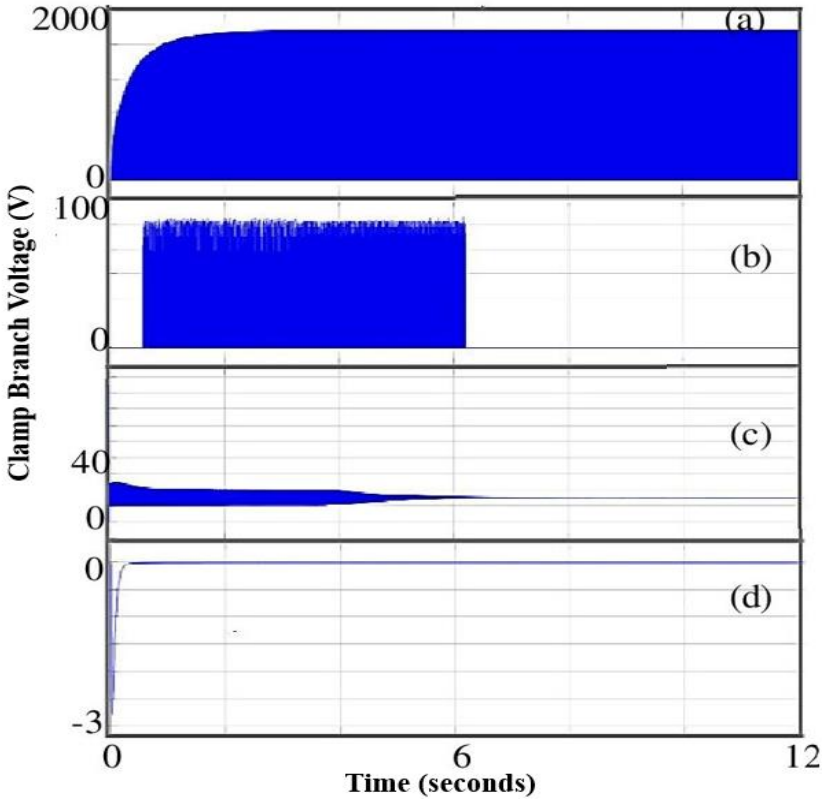

Figure 5. 10 Clamp branch voltage of BDC (a) without snubber (b) RCD Snubber (c) active clamp snubber (d) flyback snubber.

5.3.2 Case 2 : Model proposed us in this thesis and [17]

A charging station was utilized to charge EVs, which operated as a standalone EVCS [17]. The PV panel was connected to the EVs acting as a load, and a BDC with a snubber circuit was connected to the ESU. The charging system relied on a 100kWh solar panel to supply clean energy to the EVCS. The ESU had a capacity of 80 kWh, which was enough to store sufficient power to charge 40 kWh EVs. The charging station's efficiency was evaluated using MATLAB/Simulink, and three scenarios were tested [17] -PV array alone, followed by PV array and ESU together, and then ESU alone. The voltage across the clamp branch for each active snubber circuit is demonstrated in Fig. 5.11. The resistor of the RCD snubber generates power dissipation, resulting in a reduction in efficiency. Active clamp snubber circuits are not suitable for use in BDC topologies because they experience high current stress and thermal problems since they switch at twice the frequency of the switch. BDC based on RCD snubber and active clamp snubber differ significantly based on the voltage-clamp branch waveform. The BDC with the flyback snubber is

the best circuit for clamping voltage, eliminating transients from the circuit. Figures 5.12 and 5.13 present a comparison of the power output obtained from EVs and the output voltage of the BDC with the use of three different snubber circuits. It is clear from the figures that the steady-state behaviour of the BDC improved significantly when using the flyback snubber circuit compared to other circuits with snubbers. The flyback snubber was the most efficient circuit for the charging station when compared with the other snubbers used, resulting in higher output power.

When using a BDC for off-grid EVCS, the selection of a snubber circuit is crucial. Table 5.1 provides a comparative analysis of the different snubber circuits, which shows that all three are successful when combined with the converter. The decision of which snubber to use depends on voltage ripples, ZVS capability, and conduction losses. The flyback snubber is the optimal solution, considering these factors, as it offers superior performance compared to other snubbers. However, it has some drawbacks, such as its complex structure, difficulty in integration with the converter, and higher cost. Despite these drawbacks, the flyback snubber provides excellent ZVS performance, mitigates voltage spikes, and offers higher efficiency compared to other circuits.

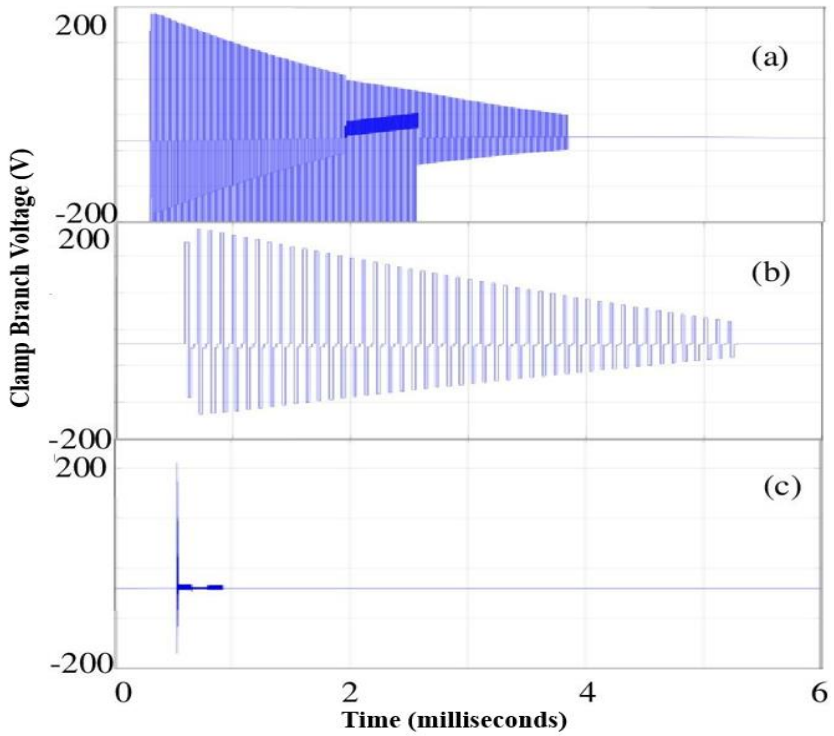

Figure 5. 11 Clamp branch voltage of BDC (a) RCD Snubber (b) active clamp snubber (c) flyback snubber.

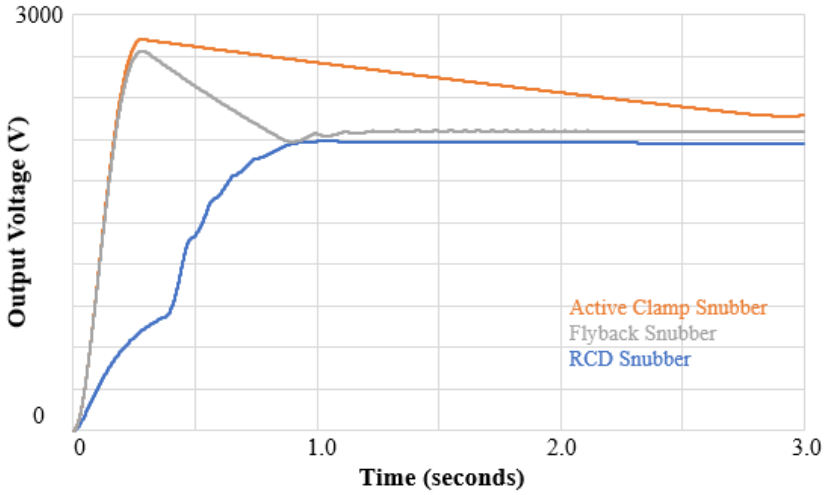

Figure 5. 12 Output voltage of bidirectional converter, using three different snubber circuits.

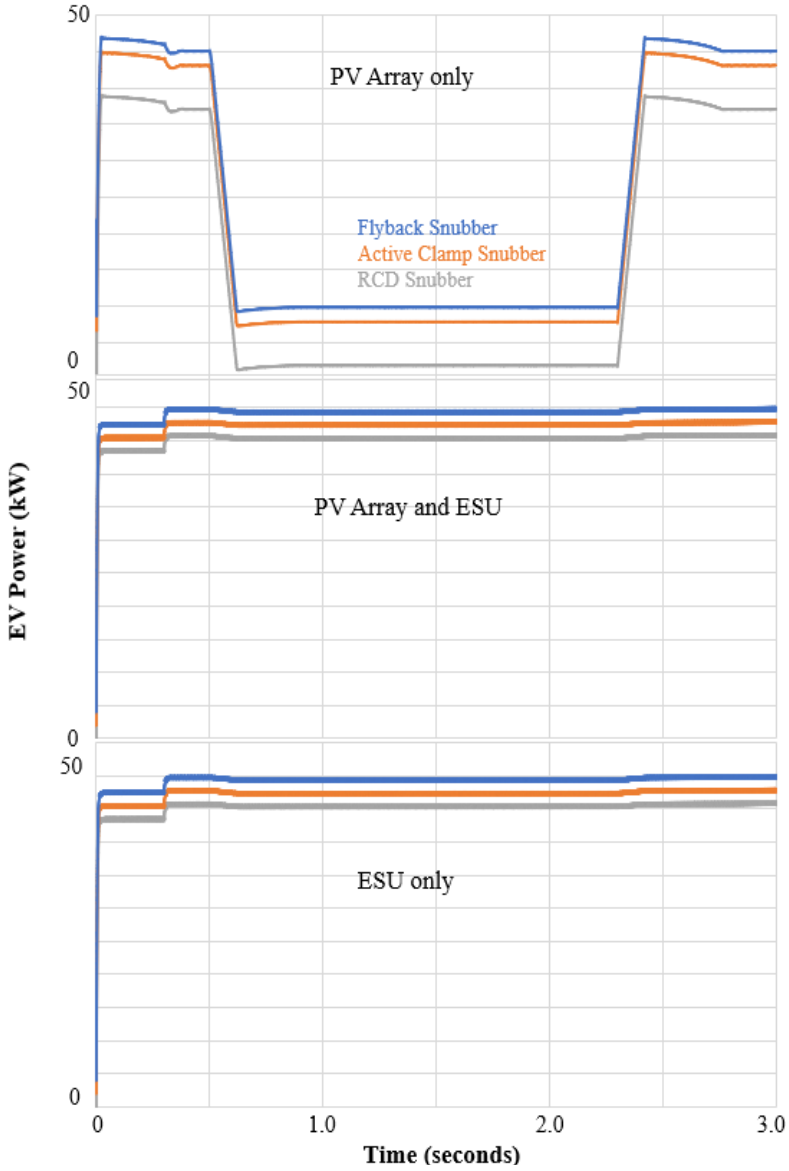

Figure 5. 13 EV power using three different snubber circuits.

Table 5. 2 Comparative analysis of various snubber circuits.

Parameters	**RCD Snubber**	**Active clamping snubber**	**Flyback Snubber**
Number of switches/diodes/capacitors	0/1/1	1/0/1	1/1/2
Conduction loss	Moderate	Low	Very low
Voltage ripple	Moderate	Low	Negligible
Attaining speed of ZVS	Very slow	Slow	Fast
Ease of implementation in BDC	Much easier	Easy	Difficult
Complexity	Smooth	Bit complex	Complex
Cost	Inexpensive	Reasonable	Bit expensive
Efficiency	Low	Moderate	High

Various scenarios clearly demonstrate the successful charging capability of a standalone PV-based charging station for EVs. By integrating a snubber circuit into the BDC, the system becomes free from high voltage stresses, ensuring energy efficiency. The proposed isolated BDC configuration, equipped with flyback and passive snubbers, provides an effective solution to minimize circulating current issues and voltage spikes. Conversely, using a BDC without a snubber circuit results in persistent voltage spikes caused by the presence of the inductor. The flyback snubber proves to be both reliable and efficient in mitigating these voltage spikes, offering the additional benefit of controllable soft start-up functionality.

Figure 5.14 presents the efficiency curve for two case studies, where the input voltage is kept constant at 400 V. Case 1, featuring a BDC with flyback and passive snubbers, achieves a maximum efficiency of 90%, while case 2 achieves an efficiency of approximately 92%. It was shown in chapter 4 [17]that a BDC without a snubber circuit exhibits lower efficiency compared to its snubber-equipped counterpart. The efficiency curves displayed in Fig. 5.14 emphasize the advantages of employing a BDC with snubber circuits in off-grid charging stations for EVs.

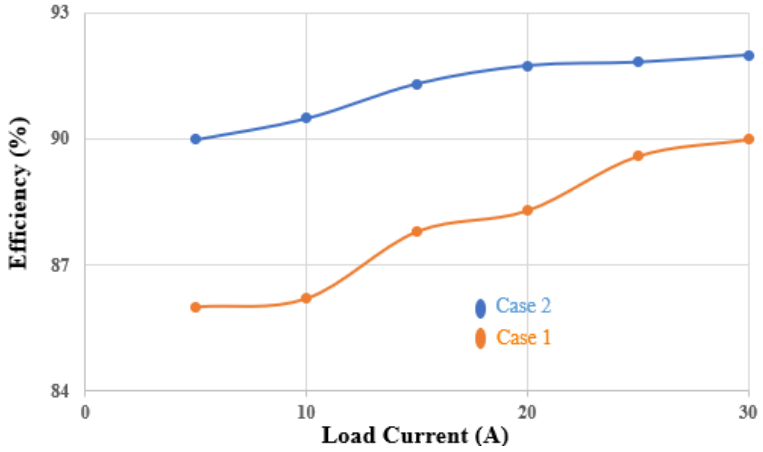

Figure 5. 14 Plot of conversion efficiency of the proposed converter.

5.4 Conclusions

This chapter discusses the validation and explanation of a design for an off-grid EVCS that uses various snubbers, which was carried out through MATLAB/Simulink simulation. Several snubber circuits were implemented and studied to improve the performance of the BDC. Compared to other charging stations, the proposed station demonstrated superior performance, making it a promising solution for off-grid EV charging.

1. The use of solar panels in an OGCS is a valuable tool in meeting the EV charging industry's demand for clean energy while reducing the system's load. Additionally, the development of charging stations in remote locations could further expand the use of EVs in areas where they were previously impractical.
2. One approach to mitigate voltage spikes caused by the current-fed inductor in BDCs is to utilize snubber circuits. Three snubber circuits, namely RCD snubber, active clamp snubber, and flyback snubber, were proposed. These circuits were shown to effectively reduce voltage stresses across the main switch and enable ZVS, thereby improving the overall performance of the converter.
3. A reliable and robust method was demonstrated by successfully testing it on two independent models. The integration of snubber circuits in the proposed converter leads to improved efficiency compared to the proposed converter without snubber circuits in

both cases. The converter is more likely to reach ZVS more rapidly than one without a snubber.

The proposed charging station's reliability and efficiency can be improved by utilizing an appropriate snubber. The study found that the flyback snubber proved to be the most effective solution for both the models presented in this chapter. It not only produced the highest output power but also mitigated voltage stress on the switches and enabled ZVS. Moving forward, the next chapter (Chapter 6) will focus on a master-slave control scheme combined with a droop control scheme to enhance stability in an isolated BDC equipped with active and passive snubber circuits.

Chapter 6 Enhancing PV-fed Electric Vehicle Charging Stations: Leveraging Droop and Master-Slave Control Strategies for Optimal Performance and Stability

The work and results presented in this chapter was published in a peer-review journal in which the author of this thesis (D.K. Nair) was the principal author. The details of the publication are as follows: D. K. Nair, K. Prasad and T.T. Lie (2021), "Design of a PV-fed Electric Vehicle Charging Station with a Combination of Droop and Master-Slave Control Strategy", Energy Storage. 2023; e442. doi:10.1002/est2.44.

6.1 Introduction

EVs have fundamentally transformed the transportation and power industries. With the transportation sector contributing to 23% of worldwide GHG emissions associated with energy, EVs have rapidly emerged as a viable alternative in recent years. Renewable energy is undergoing a notable shift in the transportation sector, with EVs gaining considerable momentum. This transformation is particularly evident in the realm of EVs, where they are making significant strides in the wagon category [197].

According to reports from the IEA discussed in Chapter 1, the increasing deployment EVs in the industry is expected to bring various benefits, particularly in terms of reducing emissions and conserving energy [3], [198].

Charging infrastructure is essential to meet the needs of the growing EV industry. EVCS that use PV panels to support charging have gained attention due to their minimal cost and the increasing awareness of environmental concerns. The EVCS holds the potential to be an extremely efficient way to store large quantities of electrical energy. However, the uncontrolled charging of many EVs can lead to an excessive load on the power grid. Additionally, it may be necessary to increase the capacity of the generation system to meet the growing demand for EV charging [199], [200].

This chapter introduces an innovative control scheme that combines the benefits of droop and master-control strategies to optimize the efficiency of EVCS. Additionally, a bidirectional isolated DC-DC converter, along with snubber circuits and a three-level booster converter with

capacitance-voltage control design, is implemented to ensure system stability. The design is developed and verified using a MATLAB/Simulink program.

Private investment plays a crucial role in the development of charging infrastructure for EVs. However, the current landscape lacks viable business models that can attract such investments. EVCS can be deployed in various environments, including both residential and public settings. Incentives and support from governmental bodies play a crucial role in promoting the establishment of EV charging infrastructure in these diverse locations. Therefore, effectively optimizing the charging and integration of EVs into the grid, as well as efficiently managing the overall vehicle grid integration, remains a critical and persistent challenge. Strategic decision-making is crucial during the establishment of charging infrastructure for EVs. Factors such as the placement of charging stations, the use of appropriate technologies, and the optimization of slow smart-charging and rapid charging are key considerations to ensure that consumers are provided with the most convenient and accessible service [201].

The increasing number of EVs presents challenges related to the demand for charging infrastructure and its impact on the grid. The charging patterns of EVs are unpredictable and erratic, further intensified by using rapid charging systems that draw significant grid power for shorter durations. Consequently, extensive and expensive renovations to the transmission, distribution systems, and other energy network components become necessary [200]–[202].

An investigation by Zou *et al.*[203] focused on the effects of EV charging on the low voltage network, revealing that overloading transformers adversely affect power quality. Effective management of EV charge characteristics, including timing and demand, is crucial for grid charging points to ensure network stability when vehicles arrive for charging. However, predicting and assessing these responses proves challenging [204].

In addition, Girard *et al.* [205] discovered that charging EVs through the grid does not yield environmental benefits, whereas utilizing off-grid methods significantly reduces CO_2 emissions. Thus, constructing stand-alone off-grid charging stations emerges as an ideal approach to

promoting global EV adoption while minimizing the impact on the current power grid. This strategy effectively addresses the growing demand for charging infrastructure, alleviates strain on the grid, and contributes to a reduction in CO_2 emissions [17].

In Chapter 5 (and our paper published elsewhere [18]), it was demonstrated that EVCSs powered by PV energy can effectively cater to the charging needs of EVs in remote locations where access to the power grid is limited or unavailable. Solar and wind energy are widely recognized as two of the most prevalent and popular RES available today. However, there are many stages of conversion and a great deal of effort involved in using wind energy compared to PV energy, making PV-based EVCS more feasible.

DC off-grid connected EVCS offers several advantages over the more common AC grid-connected EVCS. These benefits include [206], [207]:

• DC sources with minimal energy conversion losses.

• Reliable, continuous power supply without skin effect or reactive power losses.

• Fewer electronic gadgets and lower prices, and

• Grid synchronization need not be considered.

As is evident from the literature, there has been a recent surge in the popularity of PV-fed DC fast-charging stations. These stations usually include solar arrays, charging units for EVs, ESU, and multiple DC-DC converters. Installing a microgrid charging station in remote areas can provide the opportunity to recharge EVs. Off-grid charging stations have been utilized for various purposes. The DeGrussa Solar Farm, situated in Australia, holds the distinction of being the largest off-grid solar farm globally. With an impressive capacity of 10.6MW for solar PV panels and a 6MW battery system, this solar farm plays a crucial role in supporting a 23MW diesel-fired power station. By doing so, it effectively reduces diesel fuel consumption by an estimated five million liters annually. This program also allows the company to cut down on 12 million tons of CO_2 emissions. The combination of solar power and battery storage enables the solar farm to

provide a reliable and sustainable source of electricity, contributing to significant environmental and economic benefits [11].

Robben Island (South Africa) has been operating independently from the mainland's electricity grid since 2017. It relies on a robust energy system comprising a 666.4kW solar PV system and a battery energy storage microgrid. This sustainable solution has had a profound impact on the island's environmental footprint. By harnessing solar power and utilizing energy storage, the system eliminates the need for approximately 275,000 gallons of diesel fuel each year, resulting in a significant reduction of ~820 tonnes of CO_2 emissions annually. This shift to renewable energy has played a vital role in preserving the island's delicate ecosystem and protecting its diverse wildlife [11].

PV-fed DC fast-charging stations have become increasingly popular, as discussed in a collection of papers on PV-based charging systems. The papers delve into various aspects related to the V2G system, encompassing its design, operation, power management strategies, and approaches to reduce power consumption in smart homes [207]– [212]. Nevertheless, these techniques demand a stringent level of accuracy and consistency over an extended duration, making them susceptible to unforeseen disturbances like sudden fluctuations in irradiance.

A method was shown to enhance the resilience of the DC bus output voltage using a sliding-mode control technique [47]. Furthermore, a coordinated control system was introduced for the optimal operation of the ESU in island mode [48]. Another approach aimed to synchronize solar power utilization with ESU operations, but it did not consider EV charger integration or assess potential EV-side failures [49]. The findings and discussions presented in these works and in Chapter 2, serve as a basis for further exploration and analysis, which will be presented in this chapter.

In recent years, the escalating awareness of the environmental impact, the finite nature of fossil fuel resources, and the remarkable progress in battery technology have fuelled a surge in the development of cutting-edge EV models. The GHG emissions produced by EVs are typically

lower when compared to cars powered by ICE. Countries around the world are encouraging the use of EVs by introducing incentives such as tax breaks and reduced parking fees to promote their use [42].

One significant issue that hinders widespread adoption of EV is range anxiety, which refers to the limited range of a fully charged battery. Typically, the range of a battery-powered vehicle falls within the range of 100km to 500km, and the duration of the charging process varies depending on the quality of the charging station, spanning from 30 minutes to 10 hours. A fast-charging station that can offer a charge duration of 30-60 minutes would be an effective solution to this problem [42].

The battery charging profile is influenced by several factors such as the charging time, battery lifespan, and overall efficiency, all of which are determined by the characteristics of the charger circuit. The charger circuit's effectiveness, in turn, is influenced by several factors such as the specific type of circuit used, the components utilized, the chosen control strategies, the switching methods employed, and the overall cost associated with implementing the converter circuit. Therefore, it is important to carefully consider and optimize these aspects to ensure an efficient and cost-effective charging system [42].

In this regard, a snubber has been installed on the isolated BDC in the control circuit of the ESU, which regulates the charging and discharging of the battery. The proposed design effectively limits the rail voltage, mitigating the occurrence of current spikes at the switches of the converter. This is achieved by compensating for variations in leakage inductance and the currents fed to the low voltage side inductor. By implementing this clamping mechanism, the system ensures smoother operation and minimizes potential issues caused by abrupt current fluctuations. The details regarding the installation of the snubber, its effectiveness in limiting rail voltage and mitigating current spikes, were discussed in Chapter 4 and 5.

The concept of charging stations is undoubtedly beneficial but can vary depending on the source of electricity generation. Overloading the existing grid infrastructure and an increase in carbon

emissions can be a result if the grid is not designed properly. Developing an off-grid charging infrastructure, which incorporates the utilization of PV panels, can be a viable approach to overcome these limitations [138].

Decentralized control plays a crucial role in managing islanded EV charging infrastructure, addressing two key aspects: coordination between PV-ESU-EV systems and the integration of snubbers in isolated BDC. However, there is a scarcity of research publications dedicated to this specific topic, indicating that it has not received significant attention in the academic and/or research community over the years [138].

The widespread adoption of PV-ESU-EV systems has faced challenges primarily due to limited availability of charging infrastructure and increasing concerns regarding the driving range of private EVs. Societal constraints and political repressive policies are further hindrances, especially in developing countries where applications range from diverse to advanced [138].

In recent years, various studies have focused on addressing the challenges associated with the adoption of PV-based charging infrastructure installations. These studies have explored different charging system designs and solutions to overcome the barriers and promote the widespread implementation of PV-based charging infrastructure. The implementation of a distributed PV-ESU-EV infrastructure has the potential to make substantial contributions to various areas such as enhancing economic growth, fostering job creation, promoting sustainability, and improving climate conditions [138].

Sophisticated management techniques are necessary to maintain the stability of the DC system during irregular operating conditions. Effective management of these transient conditions in the converter controllers necessitates the coordination of their operations, employing a combination of droop and master-slave control approaches. However, ESUs play an important role in maintaining the stability and reliability of the overall system [138].

A control scheme that merges the benefits of droop and master-slave control systems, effectively addressing the issue of rapid connection and disconnection of EVs from the bus would be an ideal

solution and is the topic of this chapter. This innovative approach overcomes the challenges posed by frequent disruptions, ensuring seamless integration of EVs into the system. This will prevent the possibility of EVs being damaged in such an operating mode.

This chapter delves into the integration of PV arrays in an EVCS and the utilization of droop and master-slave control techniques to maintain system stability. The primary focus is on coordinating PV arrays, EVs, and ESUs to optimize power management and ensure reliable operation of the EVCS. By examining the design and implementation of this system, we gain valuable insights into the effective utilization of PV energy in EV charging infrastructure and the significance of control techniques in maintaining system stability. Additionally, the proposed ESU incorporates a BDC that is isolated from each other with passive and active snubbers. By implementing this particular configuration, it becomes possible to attain ZVS conditions for all switches within PV-based EVCS. This achievement of ZVS conditions across the switches leads to notable enhancements in the overall performance of PV-based EVCS devices. The utilization of ZVS conditions significantly reduces switching losses and enhances the efficiency of the charging process, thereby improving the overall effectiveness and reliability of PV-based EVCS systems.

Combining PV arrays, EVs, and ESUs into an off-grid EVCS can be managed through hybrid control, as proposed by Huang *et.al*. [138]. Various control schemes, such as master slave and droop, are employed to ensure stability of the system and prevent recurrences. However, the non-isolated BDC used in this application is likely to decrease the overall efficiency of the EVCS.

This chapter also proposes a BDC that consists of both active and passive snubber circuits, a master-slave control scheme in combination with a droop control scheme. This allows the main switches to be operated with minimal circulating current and clamp voltage spikes across the switches for efficient operation. Through the integration of both drooping control and master-slave control techniques in PV-based EV systems, along with the incorporation of snubber circuits, the DC bus voltage exhibits minimal fluctuations. This stability in voltage levels enables the system to support a maximum number of charge and discharge cycles, consequently extending the lifespan of the EV and the battery.

The primary objective of this research is to encourage the global adoption of EVs by implementing a self-sufficient off-grid EV charging system. The key focus is to minimize any adverse effects on the existing power grid, ultimately leading to a reduction in CO_2 emissions. MATLAB/Simulink is used to simulate and validate the proposed work in this chapter.

6.2 DC Off-Grid Structure

The off-grid DC system powered by a PV system incorporates two control schemes: droop control and master-slave control. These control schemes effectively coordinate the PV arrays, EVs, and the ESU within the system. Ensuring a continuous power supply to consumers off-grid necessitates the utilization of a battery storage system. This system serves as a reliable backup, providing uninterrupted power during periods of low or fluctuating PV generation. By implementing control schemes and integrating the battery storage system, the off-grid DC system maintains a stable and reliable power supply, meeting the energy demands of consumers even in challenging conditions. This system is crucial in providing energy when there is a drop in PV array power. It also stores excess power generated by the solar panels when the amount of power generated is more than what is required for off-grid operation. Figure 6.1 shows the architecture of an off-grid EVCS based on PV.

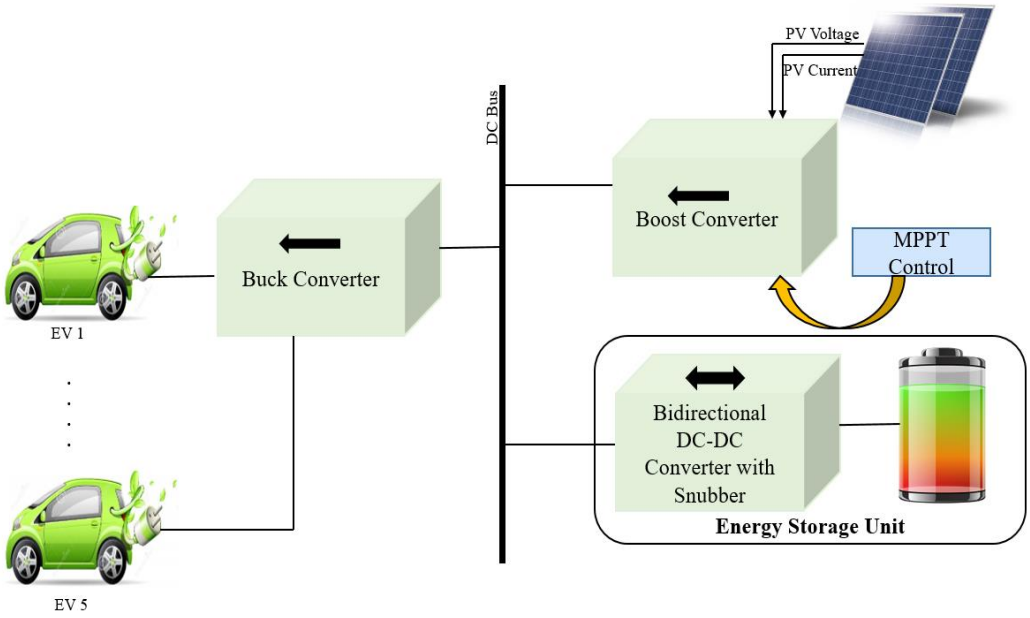

Figure 6. 1 Architecture of the off-grid EVCS.

6.2.1 System Power and Energy Analysis

In the design phase of the system, careful calculations of energy and power relationships are performed to facilitate the system's design process [10], [214]. The following are some of the specific premises used:

- A storage battery's initial energy is measured in the form of watt-hour (Wh) and is referred to as "E_t".
- A PV panel's ability to emit solar power, "P_{PV}" varies over time and is influenced by several factors:

$$P_{PV} = \frac{P_{mpp}}{36}(36 - t^2)\,, \tag{6.1}$$

where P_{mpp} is the maximum power output from the PV, and "t" refers to the time in hours. In Fig. 6.2, the time axis is commonly aligned with noon, which corresponds to the peak irradiation level. Solar energy is considered to be accessible for a duration of 12 hours, starting from 6:00 a.m. and continuing until midnight. In accordance with the principle of power balance, the EV's power consumption, P_{EV} is calculated as follows:

$$P_{EV} = P_{PV} - P_{BATTERY}, \tag{6.2}$$

where $P_{BATTERY}$ is the instantaneous battery power [10].

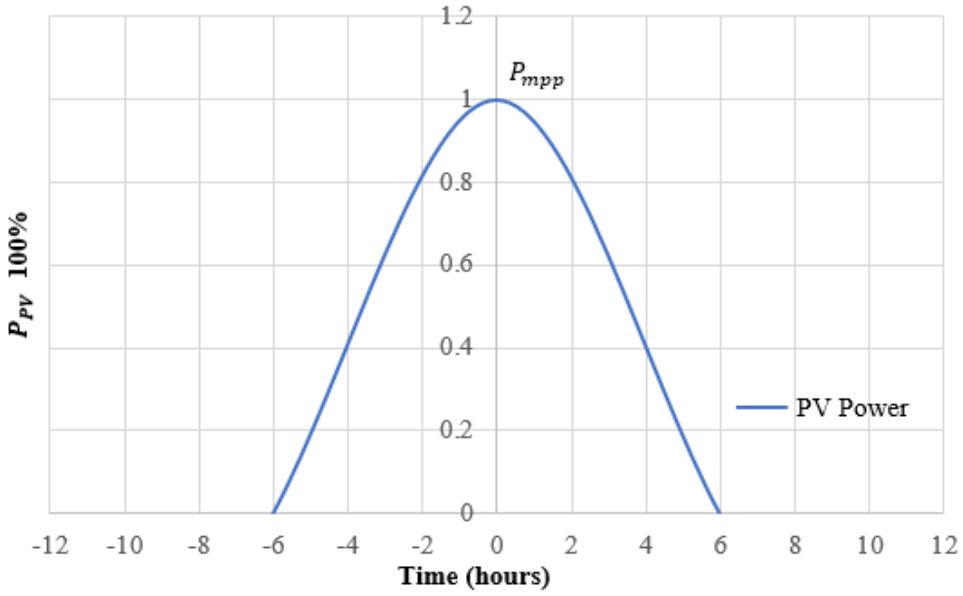

Figure 6. 2 PV power distribution for a day [10].

A day is assumed to have zero battery power during the course of a day (T is equal to 24 hours).

Therefore,

$$\int_0^T P_{BATTERY}\,dt = 0. \qquad (6.3)$$

Hence,

$$\int_{-6}^{6}\left[\frac{P_{mpp}}{36}(36 - t^2) - P_{EV}\right]dt - \int_6^{18} P_{EV}\,dt = 0, \text{ which gives} \qquad (6.4)$$

$$P_{mpp} = 3P_{EV}\ . \qquad (6.5)$$

This EV charging station is equipped with the capacity to simultaneously charge up to five EVs. The PV systems are connected to a 400V DC bus via a DC-DC boost converter. An isolated BDC, incorporating both active and passive snubbers, is employed to facilitate efficient power transfer between the battery and PV system.

The ESU, in conjunction with the battery storage system, features an isolated BDC equipped with both active and passive snubbers. This configuration enables simultaneous storage and release of energy within the system. Regulating and maintaining the DC bus voltage within an optimal range is critical for ensuring system stability and reliable operation, irrespective of the prevailing

operating conditions and variations. The primary source of energy for the off-grid DC system is the PV system, which uses 50 kW PV panels, providing a total of 100 kW of electricity. The maximum power generated by the PV system is actively monitored and then utilized within the DC bus, optimizing the distribution of solar energy resources. The ESU has a maximum capacity of 80 kW to store or release energy from the PV system. The charging station consumes an estimated 24 kW of power.

6.2.2 PV Panel with a Boost Converter

A three-level boost converter can be employed to establish a direct connection between the solar array and the DC bus, facilitating the switching between three distinct output levels, as discussed in Chapter 3. The PV boost converter works by tracking the MPPT. The MPPT control architecture of the PV system, as shown in Fig. 6.3, utilizes the incremental conductance method to monitor and assess the current and voltage of the PV arrays. This enables the system to determine the maximum power point and optimize the PV system's performance [136], [137]. An efficient three-level boost converter can surpass conventional boost converters in terms of efficiency and voltage gain by providing a double increase (see Fig. 3.2) [136]–[138].

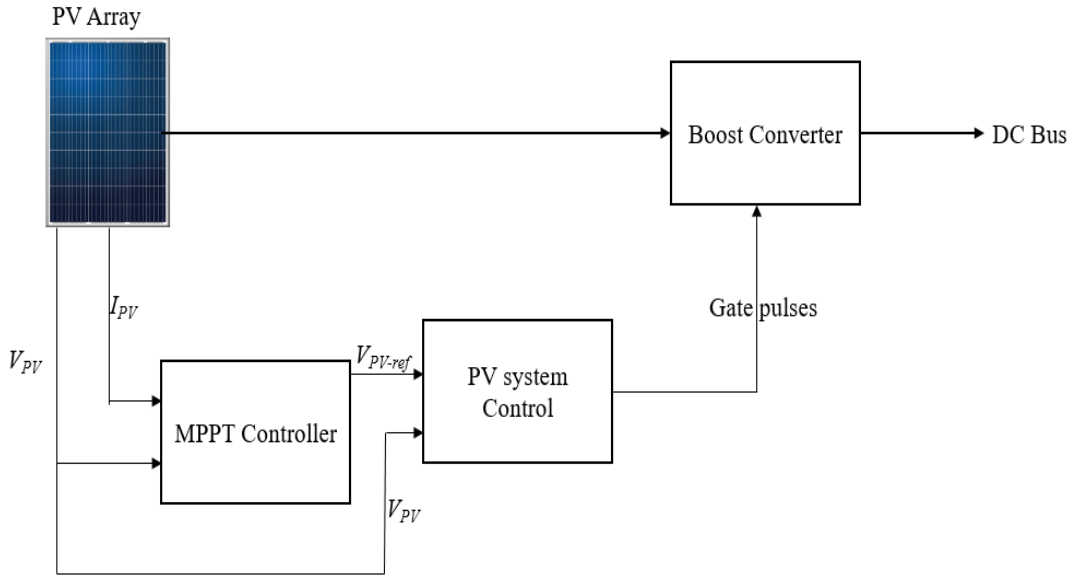

Figure 6. 3 Block Diagram of PV System Control.

6.2.3 Energy Storage Unit Converter

The ESU comprises two primary elements: a battery and an isolated BDC equipped with a flyback circuit and a passive snubber circuit (see Fig. 6.4). These components synergistically contribute to the functionality and performance of the ESU [17], [18].

The BDC serves a dual purpose by facilitating battery charging in the buck mode and battery discharging in the boost mode, simultaneously supplying power to the EV loads. This versatile operation of the converter ensures efficient energy transfer between the battery and the EV system [17], [18].

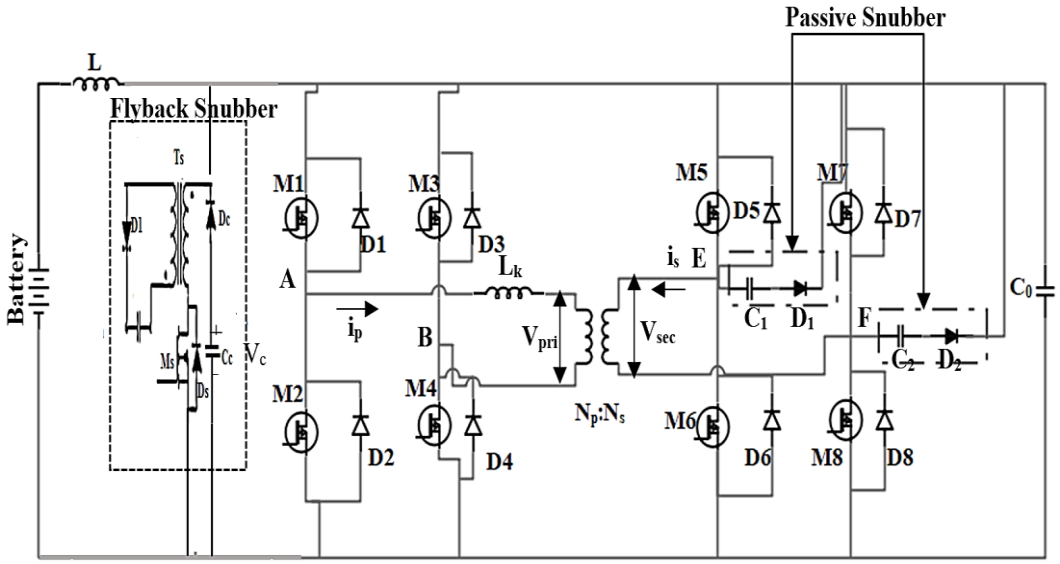

Figure 6. 4 Isolated BDC with a flyback snubber and a passive snubber.

ESUs play a critical role in charging systems by enabling the recharging of batteries when the power generated by the system surpasses the power consumed by the loads. This allows for efficient utilization of excess power generated by the system and ensures the effective storage and availability of energy for future use. ESUs come into play when the generated power is not sufficient for charging EVs. Incorporated with a flyback and passive snubber circuit, an isolated BDC is utilized to ensure the smooth functioning of the system. By mitigating the impact of circulating current on the main switches, the voltage spikes across these switches are effectively suppressed. This safeguarding mechanism ensures that the main switches are protected from

excessive voltage fluctuations, thereby promoting their stable operation, and preventing any potential damage.

The BDC incorporates two passive capacitor-diode snubbers, which effectively alleviate the high current and voltage stresses experienced by the main switch during the mode transition. These snubbers play a crucial role in mitigating the potential detrimental effects of abrupt voltage and current variations, ensuring the smooth and reliable operation of the converter. By reducing stress on the main switch, the snubbers contribute to its longevity and overall system performance. A converter equipped with a snubber circuit is much more efficient than one without it, as it achieves ZVS conditions faster. With this design, off-grid EVCS performs better than traditional ones, making it a cost-effective and efficient solution [17], [18].

6.2.4 EV Charger Converter

The schematic diagram for the buck converter (EV charger) is presented in Fig. 6.5, comprising a MOSFET switch *S*, an inductor L_{EV}, a diode, and a capacitor C_{EV}. The charging unit serves a pivotal function in establishing a connection between the DC bus and the terminals of the EV batteries, while simultaneously overseeing the regulation of the charging current, I_{EV}. In this investigation, a maximum charging current of 100A has been employed to facilitate efficient and reliable charging of the EV batteries [138].

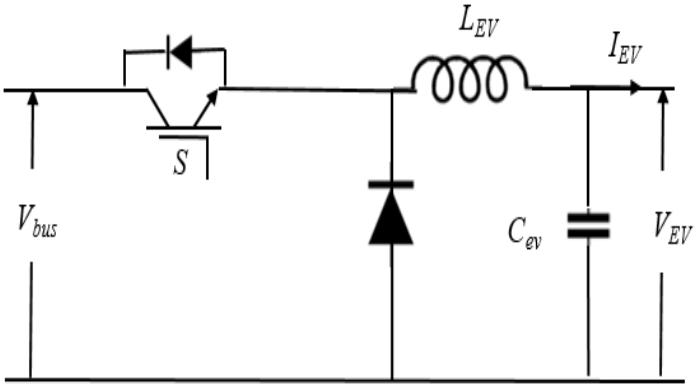

Figure 6. 5 EV Buck Converter.

6.3 Control Structure

The DC off-grid system's control structure consists of three primary algorithms. The following subsections detail the PV system droop control, ESU converter control, and EV charger control, which collectively form the control system.

6.3.1 PV System Droop Control

The PV system droop control uses a three-level boost converter to manage the voltage of the PV array terminal for maximum power extraction. The MPPT algorithm determines the reference PV voltage, $V_{PV\text{-}ref}$ by employing the incremental conductance method, which calculates the droop reference voltage. This method enables accurate tracking of the maximum power point, ensuring optimal operation of the PV system. By subtracting PV voltage, V_{PV} and reference voltage $V_{PV\text{-}ref}$, the difference is utilized to compute the error term. This error term is then fed into the Proportional Integral (PI) controller, resulting in the determination of the duty ratio, D_{PV}. The duty ratio is crucial for regulating the operation of the boost converter in the PV system [136], [137].

Based on the error term, the duty ratio D_C is adjusted and passed to the secondary PI controller. This secondary controller is responsible for maintaining balance between the voltages of the capacitors in the boost converter, namely V_{f1} and V_{f2}. The PI controller ensures that the voltages across the capacitors remain at desired levels for optimal operation of the boost converter [136], [137].

Figure 6.6 shows the control algorithm optimization for the PV boost converter. With the implementation of this advanced control system, the droop control of the PV system effectively maximizes power extraction from the PV arrays [138].

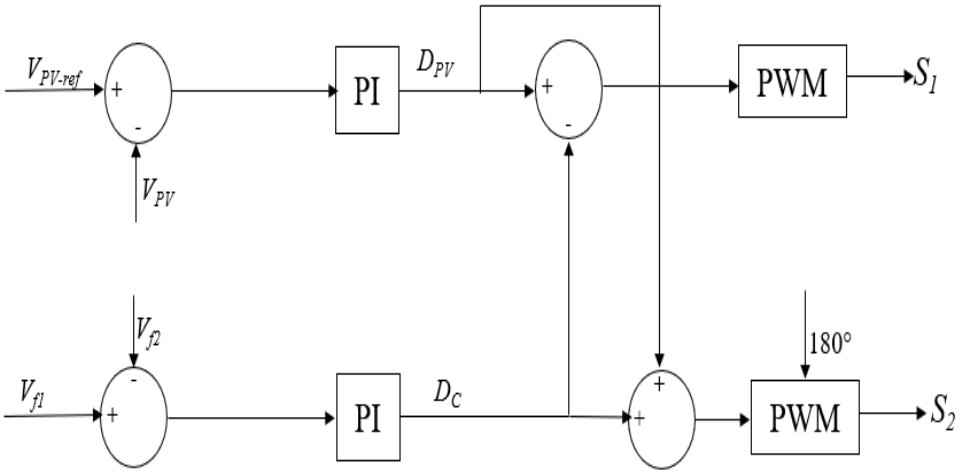

Figure 6. 6 Control Algorithm of PV Boost Converter.

6.3.2 ESU Converter Control

The ESU BDCs is responsible for regulating the nominal DC bus voltage, V_{bus}, by employing a boost or buck mode for charging and discharging the battery, respectively. Figure 6.7 presents a flow chart that outlines the process for switching between these two modes and managing the system [138].

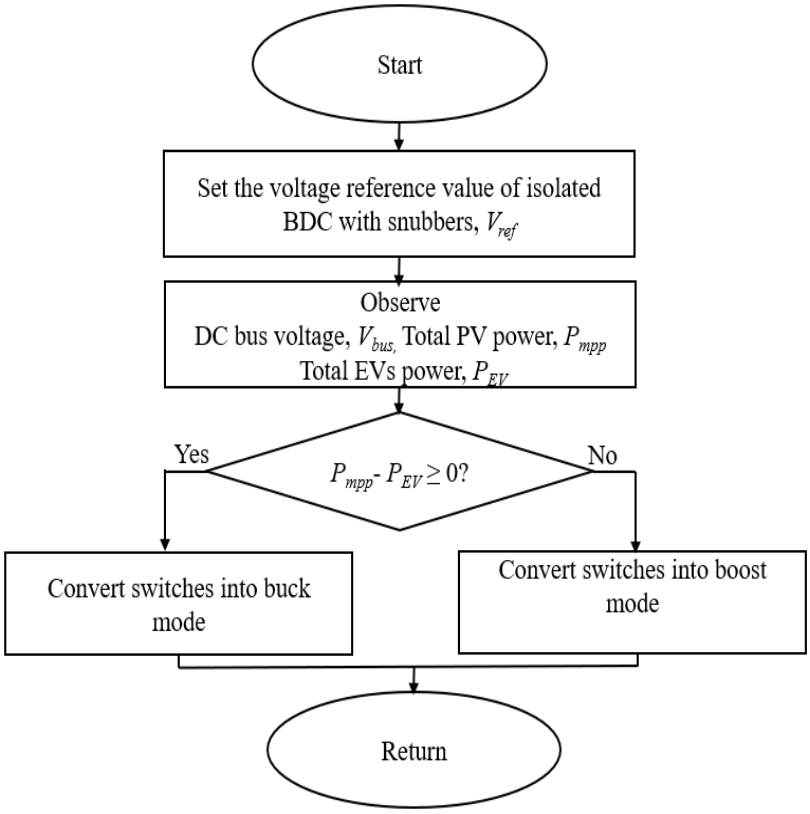

Figure 6. 7 Flowchart for the detection of buck/boost mode in isolated bidirectional converter.

The system aims to evaluate the power output from the PVs in relation to the maximum power consumption of the EVs. By determining the operating scheme of the converter based on the ratio between maximum PV output power (P_{mpp}) and EV consumption power (P_{EV}), it can be determined if the converters are operating at maximum efficiency.

In Fig. 6.8, a control model for ESU converter control is presented, and includes a reference charging current, $I_{ESU\text{-}ref}$, and a "disable" function based on the average solar irradiance, G_{avg}, for the day. The "disable" function allows for the limitation of the ESU discharging current and coordination with the EV charger. If the ESU drops below the minimum *SOC* level, all EV chargers will be immediately turned off, and G_{avg} will remain at zero until the PV arrays are able to generate power again. Given the importance of the ESU in maintaining system stability and reliability, it remains operational without the ability to be switched off or have its current flow adjusted, regardless of the *SOC* falling below a specific level or exceeding a predefined threshold. This ensures that the ESU continuously supports the system's functioning and prevents any compromise in its overall performance.

Droop control can be combined with master-slave technology to provide variable current sharing and a high level of reliability, which can help overcome this issue. Therefore, the additional droop control adjusts to the slope of the solar irradiance, $G'\left(\frac{dG_{avg}}{dt}\right)$, changes in the *SOC*, and the system's demands. The updated storage current reference, $I_{ESU\text{-}ref}$, is calculated using the following formula:

$$I_{ESU-ref} = \frac{P_{mpp}-P_{EV}}{V_{ref}} \times K_{ESU}\ , \qquad (6.6)$$

where K_{ESU} stands for the ESU droop gain, which ranges from 0 to 1. A look-up table is used to calculate the droop gain based on the G' and *SOC* levels.

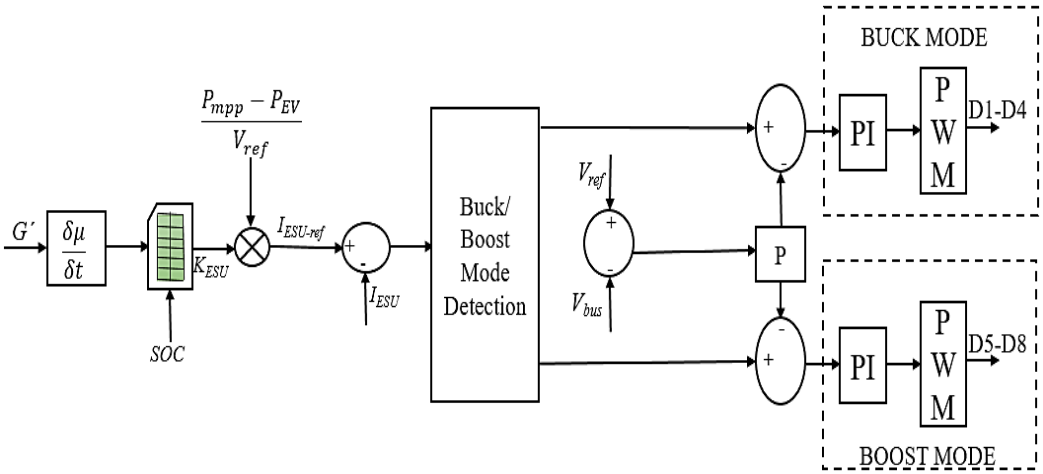

Figure 6. 8 ESU Converter Control.

6.3.3 EV Charger Converter Control

The control mechanism of the EV charger converter utilizes a voltage-based droop control structure, illustrated in Fig. 6.9. This control scheme effectively regulates the DC-bus voltage, ensuring optimal operation of the EV charger. The reference charging current is $I_{EV\text{-}ref}$, and the "disable" function is controlled using the average solar irradiation, G_{avg}, as a parameter of the controller. As the "disable" function is triggered at a predetermined threshold, the charger undergoes a smooth disconnection from the DC bus. This disconnection occurs gradually as $I_{EV\text{-}ref}$ approaches zero and G_{avg} falls below the specified threshold again. However, as G_{avg} drops, the number of unconnected EVs increases. K_{droop} stands for the droop gain, which ranges from 0 to 1. The output of the droop control, ΔI_{EV}, can be expressed as follows:

$$\Delta I_{EV} = K_{droop}(V_{ref} - V_{bus}), \quad (6.7)$$

Where K_{droop} represents the EVs adaptive droop gain calculated from G' and SOC.

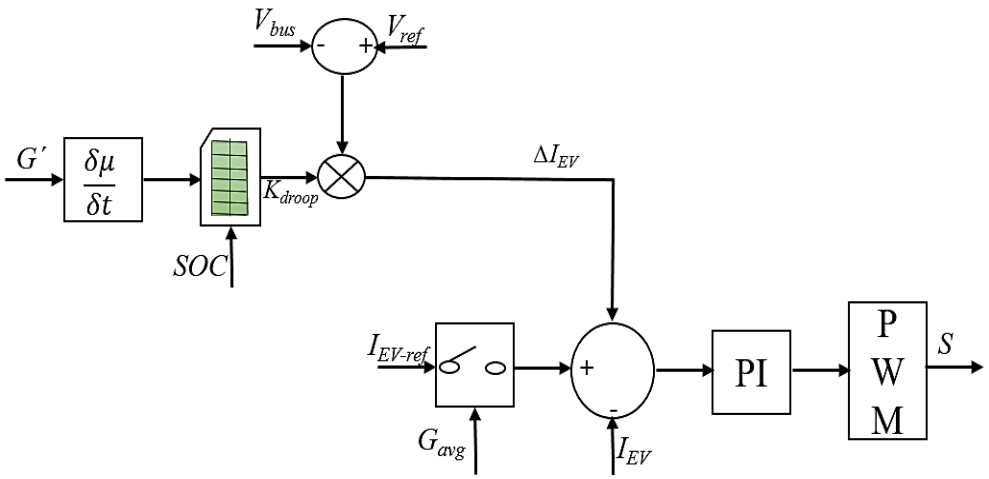

Figure 6. 9 EV Charger Converter Control.

6.4 Modes of Operation

Mode 1: $P_{mpp} > P_{EV}$ and $K_{ESU} = 1, K_{droop} = 0$, *SOC and G'* are within the specified limits.

When the power provided by the PV panels exceeds the power required by all connected EVs, the EVs are charged solely from the PV panels. The surplus power from the PV panels is used by the isolated BDC to charge the batteries. The excess energy can be utilized for various purposes, both domestic and commercial, depending on its usage and requirements.

Mode 2: $P_{mpp} < \sim 0$ and $0 \leq K_{ESU} \leq 1, 0 < K_{droop} \leq 1$ and *SOC and G'* fall outside the specified limits.

During rainy weather or low sunlight conditions, when the output power from the PV panels falls short of meeting the power demand for charging EVs, the additional power needed is sourced from the battery. An isolated BDC is used to maintain a minimum battery charge during charging.

Mode 3: $K_{ESU} < 1$ *and* $K_{droop} = 0$ and *SOC* reaches the maximum limit

When there are no EVs connected to the charging station and the battery has reached its maximum *SOC* of 90%, the PV panels are disconnected from the bus to maintain the stability of the overall system.

Therefore, the EVCS comprises three main components: PV system boost converter droop control, EV charger buck converter droop control, and ESU isolated bidirectional converter,

which utilize both droop and master-slave control methods. Additionally, the system implements PV-ESU-EV coordination to ensure optimal performance. These three components work in harmony to provide a reliable and efficient charging solution for EVs.

6.5 Simulation results

Simulation of the EVCS system is conducted using MATLAB/Simulink platform to obtain simulated results for various modes of operation. Figure 6.10 shows the configuration of the overall control strategy.

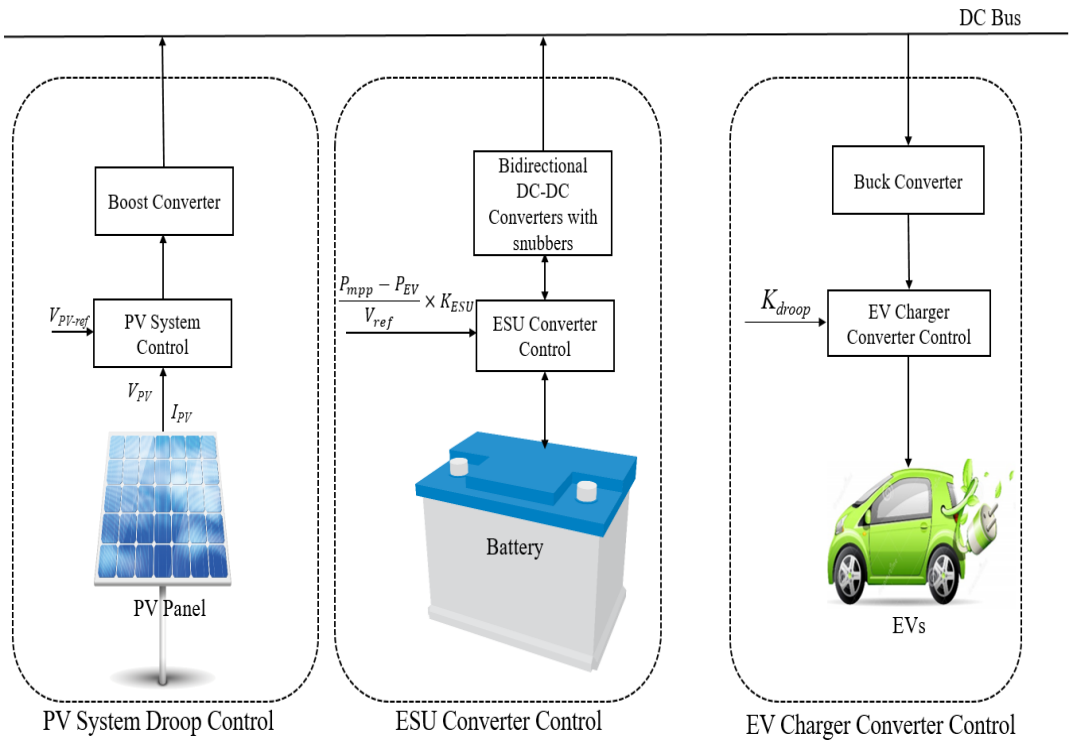

Figure 6. 10 Schematic view of the overall control strategy of the off-grid EVCS.

During the installation process, the battery's initial *SOC* is configured to 20%, establishing the starting point for its operation. The battery is designed to operate within a nominal range of 20% to 80% *SOC*, ensuring optimal performance and longevity. As there are no EVs connected to the PV panels, the panels continue to generate their rated electricity. Consequently, the maximum power tracked from the boost converter is directed towards the ESU.

One of the most crucial factors that affect the overall stability of a system is the rate of change of irradiance, *G'*. Initially, it is assumed that the irradiance *G* at the outset is 1kW/ m^2, which

gradually decreases over three seconds to 600W/ m^2, and eventually drops to 0kW/ m^2 at 5 seconds, as shown in Fig. 6.11.

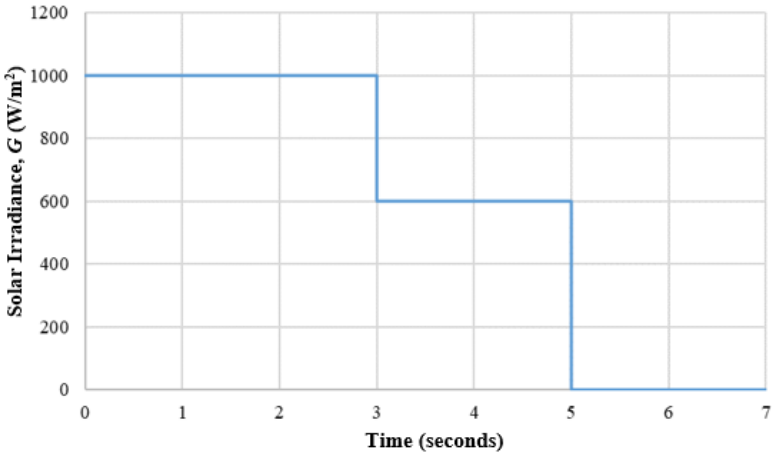

Figure 6. 11 Solar irradiance data.

6.5.1 Mode 1

The *SOC* of EVs can vary widely, ranging from 20% to 90%. During operation in Mode 1, the power output of the PV system surpasses the total power demand of the EV fleet. In this scenario, the excess power is efficiently utilized to recharge the battery. This is achieved through a isolated BDC, which is connected to the PV boost converter. This method is reliable and helps to reduce battery degradation. The extra power generated from the PV array is utilized to charge the battery until it reaches the maximum *SOC*.

Master-slave controls and droop controls are implemented to maintain the solar array current at 650A and the DC bus voltage at 400V during operation. Figure 6.12 shows a drop in array current, $I_{PV,}$ when the irradiance increases from 1kW/m^2 to 600W/m^2 at t=3s, with the current level of activity similar to MPPT conditions. In this mode, *SOC* and *G'* are defined within the limits, respectively, and K_{droop} = 0 and K_{ESU} = 1.

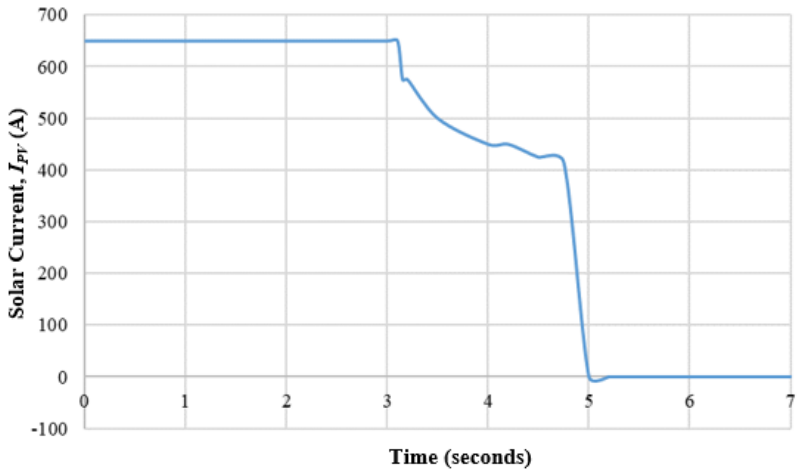

Figure 6. 12 Solar array current.

The surplus energy produced by the PV panels is harnessed to charge the batteries until they reach their maximum state of charge. The ESU charges from 20% to 34% *SOC* when there is surplus supply power, P_{ESU}, *i.e.*, 2500W - 400W = 2100W, as shown in Fig. 6.13(a). The EV batteries are gradually charged from 20%, 30%, 50%, and 70% to 80% of their total capacity, as shown in Fig. 6.13(c). As the EV battery is charging, the current is negative, as seen in Fig. 6.13(d).

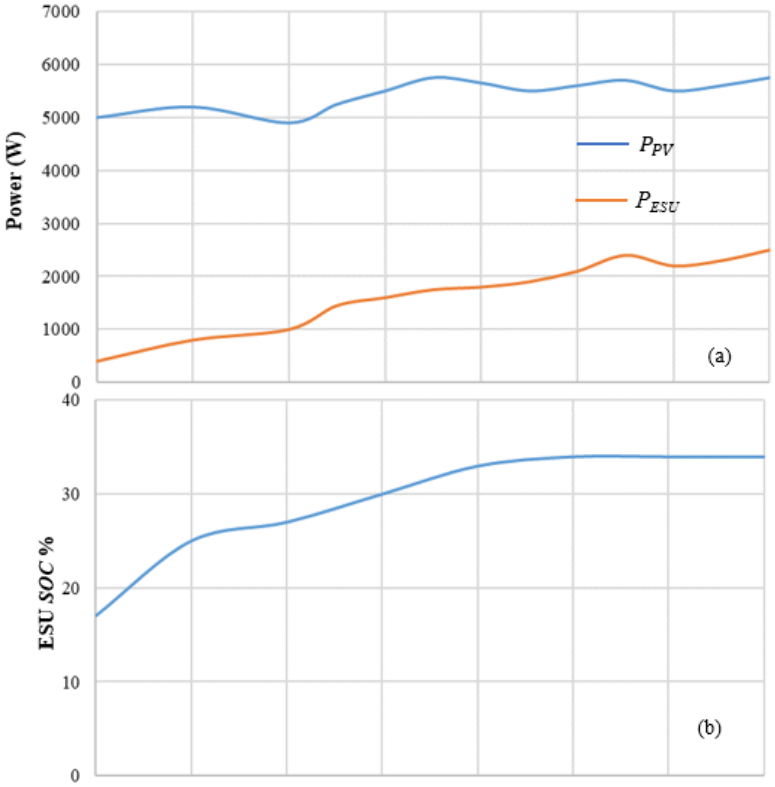

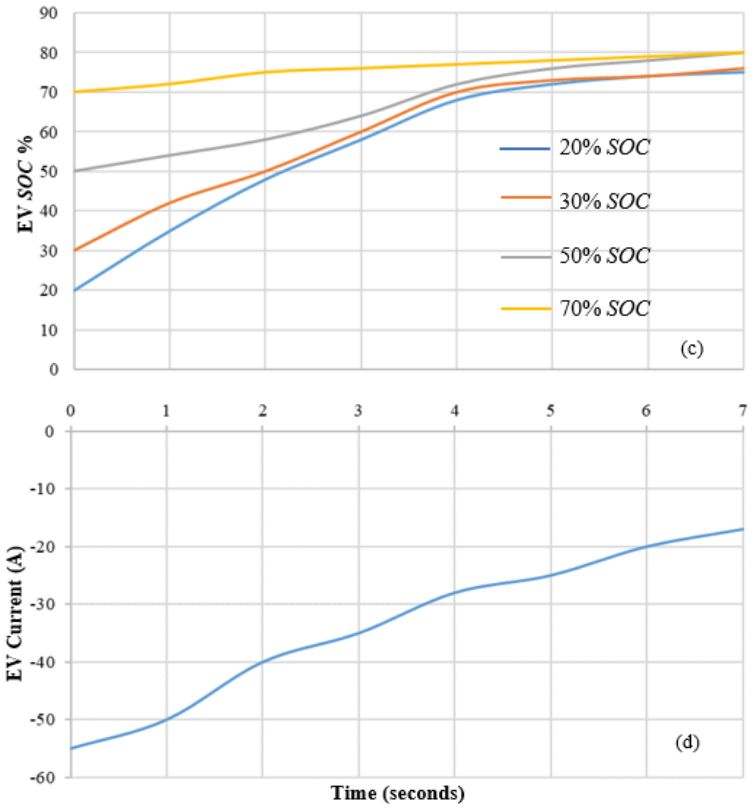

Figure 6. 13 **(a)** Solar power and ESU power **(b)** *SOC* of ESU **(c)** *SOC* of EV charging **(d)** Current drawn by EV Schematic view of the overall control strategy of the off-grid EVCS.

6.5.2 Mode 2

In the event of insufficient solar power, the system allows for discharging the battery from its maximum state of charge, which enables the energy to be utilized for charging EVs, as indicated in Figs. 6.14(a) and (b). Droop control is implemented in the EV converter control to maintain voltage stability during the charging process. The gain droop, K_{droop}, is set to switch from 0 to 1 whenever there is a significant change in irradiance G'. The combined droop and master-slave control are activated for ESU converter control. At this point, the gain K_{ESU} and K_{droop} are changed from 1 to 0.9 and 0 to 1, respectively, as shown in Fig. 6.14 (d). This setup allows the ESU to share the PV power with all connected EVs, and therefore the charging current supplied to the ESU is reduced, as can be seen in Fig. 6.14(c).

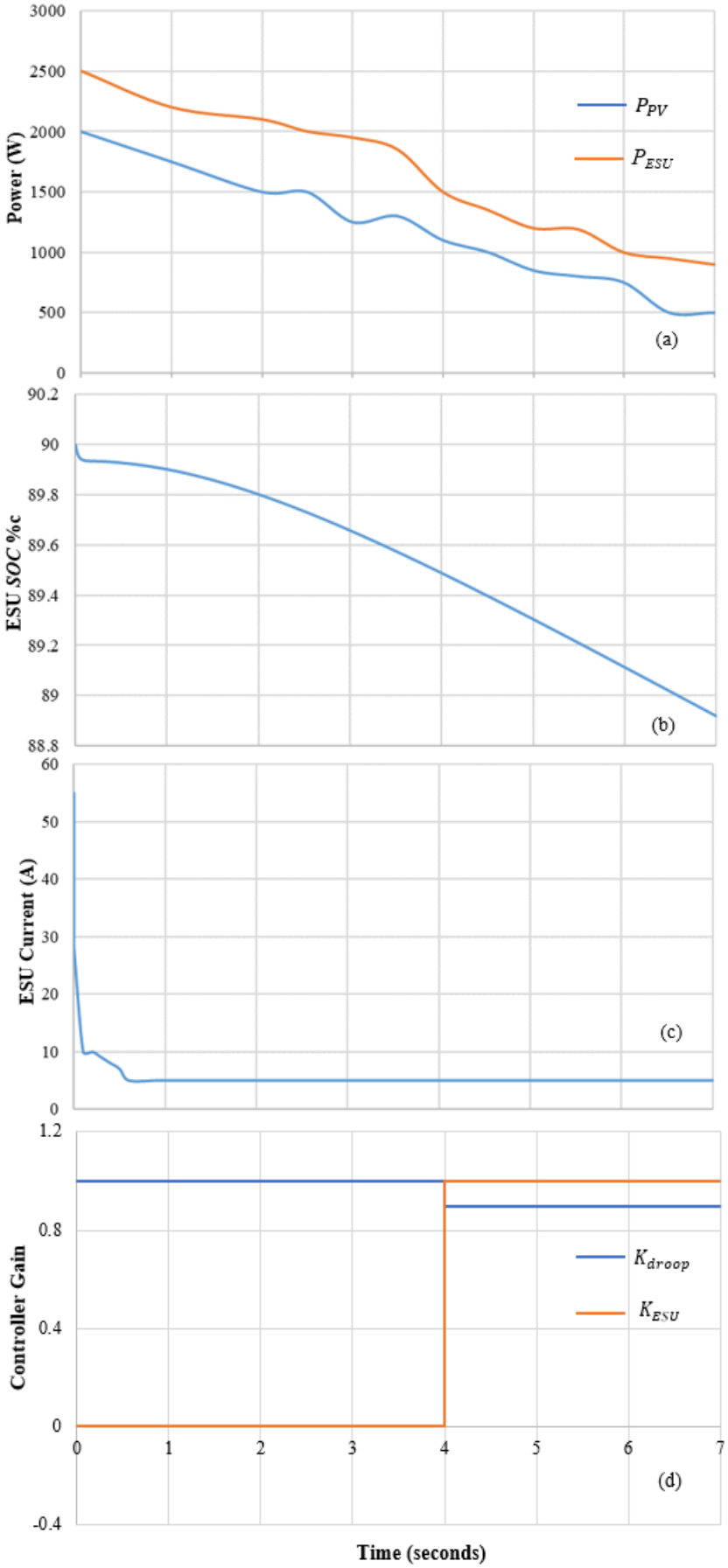

Figure 6. 14 **(a)** Solar power and ESU power **(b)** *SOC* of ESU **(c)** Charging Current of ESU **(d)** Controller Gain, K_{ESU} and K_{droop}.

6.5.3 Mode 3

When the battery system is not connected to any EVs, the *SOC* of the battery reaches its maximum of 90% as shown in Fig. 6.15. This is because the PV array is supplying energy, and the gain K_{ESU} is less than 1 while K_{droop} is equal to 0. At this stage, the system ensures stability by disconnecting the PV panels from the system.

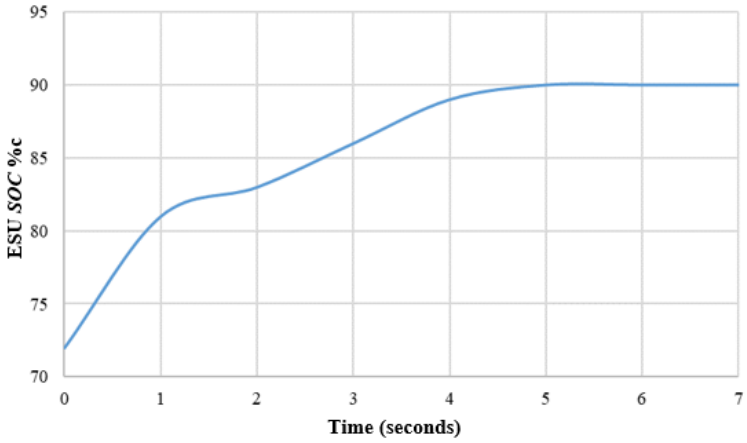

Figure 6. 15 *SOC* of ESU.

6.6 Comparitive Analysis

The ESU is a crucial component in maintaining the stability of the power supply voltage in the proposed PV-based EVCS. In the ESU, a BDC is employed to regulate the voltage level within a specific range determined by *SOC* and *G'*. However, simply using a droop control or master-slave control alone, along with *SOC* outside the limits, cannot effectively regulate the voltage or current through the ESU. A higher gain in the control technique can cause a larger deviation in voltage, so an additional control loop is necessary to address these issues.

Therefore, in the proposed PV-based EVCS, both droop control and master-slave control techniques are employed, as both have their advantages. The PV-based EVCS uses both control schemes without compromising either of them. This approach ensures that the ESU can maintain voltage stability under various conditions and improve the overall performance of the system.

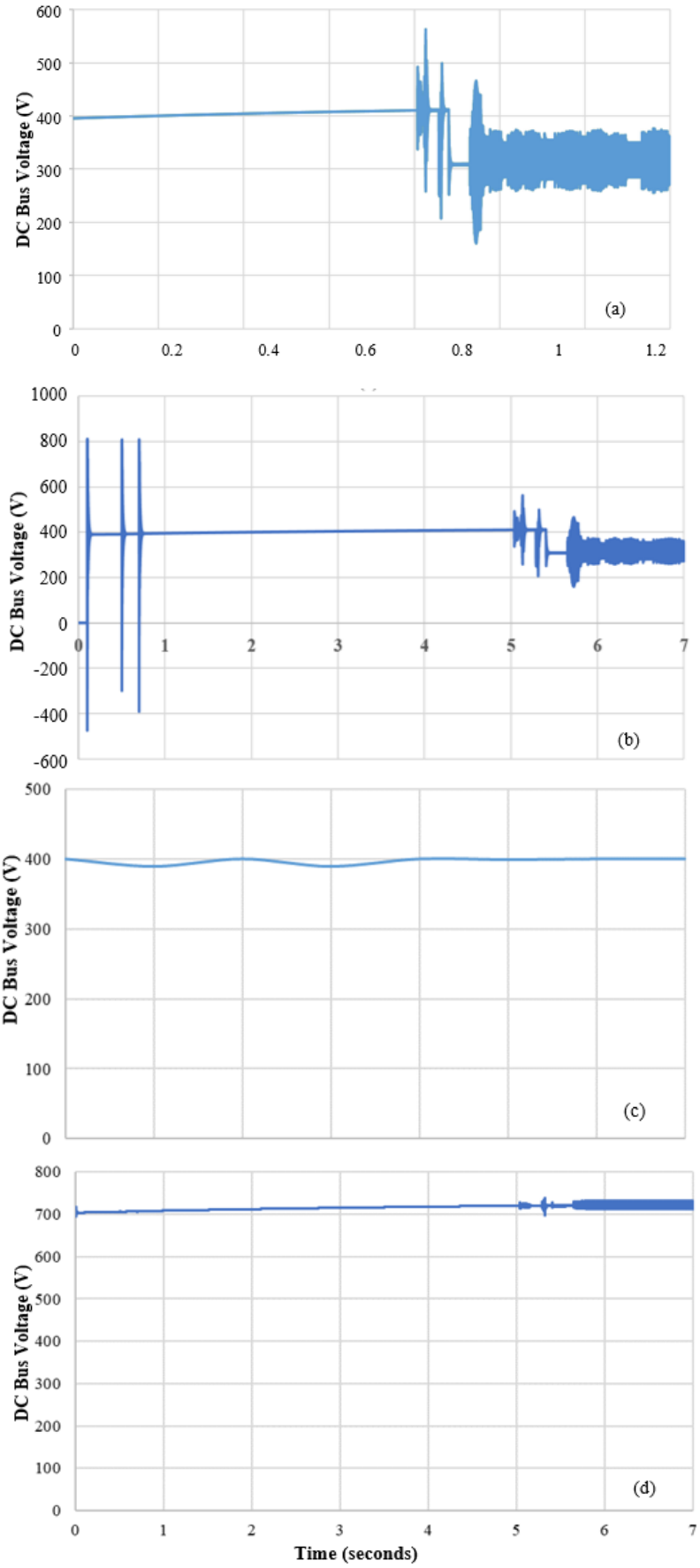
DC Bus Voltage (V)
600
500
400
300
200
100
0
0
0.2
0.4
0.6
0.8
1
1.2
(a)
DC Bus Voltage (V)
1000
800
600
400
200
0
-200
-400
-600
0
1
2
3
4
5
6
7
(b)
DC Bus Voltage (V)
500
400
300
200
100
0
(c)
DC Bus Voltage (V)
800
700
600
500
400
300
200
100
0
0
1
2
3
4
5
6
7
(d)
Time (seconds)

Figure 6. 16 **(a)** DC Bus voltage with master-slave control with active and passive snubber 1circuit in the proposed work **(b)** DC Bus voltage with droop control with active and passive snubber circuit in the proposed work **(c)** DC Bus voltage with the combination of master-slave and droop control with active and passive snubber circuit in the proposed work **(d)** DC bus voltage without active and passive snubber circuit used by Huang *et.al.* [138].

Figures 6.16 (a) and (b) show DC bus voltage variations under master-slave and droop control, respectively, along with active and passive snubber circuits. Figure 6.16 (c) shows a combination of master-slave and droop control approaches, in combination with active and passive snubber circuits, which is used to adjust the DC bus voltage. Utilizing either the master-slave control technique or the droop control technique alone leads to a decrease in the bus voltage from its rated value, leading to fluctuations in the DC voltage. Combining both the master-slave and droop control techniques along with the implementation of active and passive snubber circuits leads to a consistent and stable DC bus voltage.

The combination of droop and master-slave control techniques, along with active and passive snubber circuits, minimizes the voltage fluctuation of the DC bus in the PV-based EVCS. This approach extends the service life of the ESU by maximizing the number of charge-discharge cycles supported by the system. In contrast, Huang *et al.* [138]encountered difficulties in achieving a stable and uniform DC bus voltage, as shown in Fig. 6.16 (d). Consequently, the ESU's service quality experienced a gradual deterioration over time.

The BDC is the crucial device that links the ESU and the DC bus, and it requires a stable, reliable, and efficient architecture. Huang *et al.*'s[138] BDC was characterized by significant spikes in voltages and currents during the connection and disconnection of the EVs from the system, leading to increased conduction losses and a decrease in the effective duty cycle. However, by using an isolated BDC with active and passive snubber circuits, ZVS conditions can be achieved quickly, leading to a better job of clamping voltage spikes at the switches and enhancing the overall efficiency of the PV-based EVCS based on PVs.

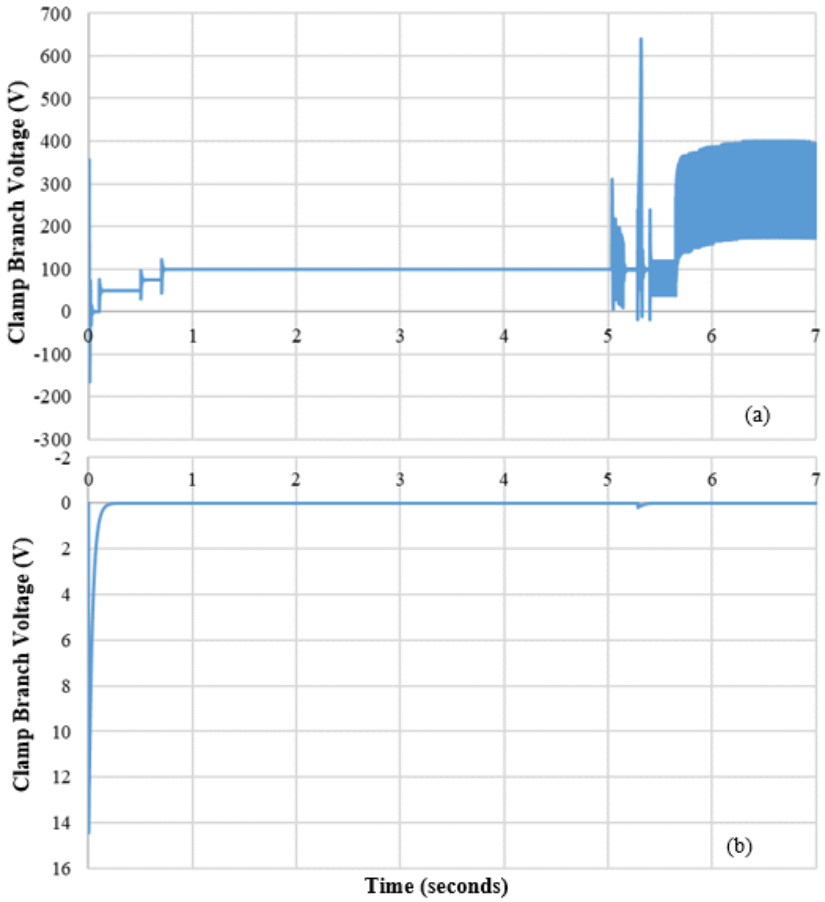

Figure 6. 17 **(a)** Clamp branch voltage of the bidirectional converter used by Huang *et al.* **(b)** Clamp branch voltage of the isolated bidirectional converter with active and passive snubber circuits in this work.

In Fig. 6.17 (a and b), the clamp branch voltages of the BDCs employed by Huang *et al*. [138]and the present study are presented, respectively. Notably, Fig. 6.17 (a) demonstrates that the BDC utilized by Huang *et al.*[138] does not attain ZVS conditions, primarily due to the inclusion of an inductor. As a result, significant stress is imposed on the switch, limiting its effectiveness. However, Fig. 6.17 (b) shows our results with snubber circuits where ZVS conditions were achieved in a fraction of a second after the usage of an isolated BDC. Isolated BDCs with snubber circuits, therefore, eliminate voltage stress across the main switches and are the best option in terms of ZVS.

The proposed EV charging station operates off-grid and utilizes PV generation, ensuring continuous charging service for EVs regardless of weather conditions. Snubber circuits are employed in the BDC to enhance energy efficiency and protect the system from issues related to high voltages and currents during high-rate charging. Figure 6.18 illustrates the efficiency curves

obtained by maintaining a constant input voltage of 400 V and considering inductor current fluctuations ranging from 2 to 40 A.

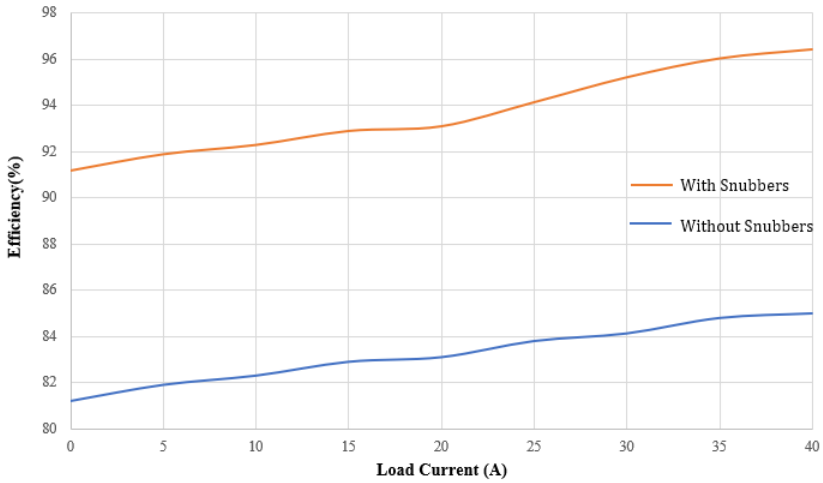

Figure 6. 18 Plot of conversion efficiency

The analysis demonstrates that the integration of snubber circuits significantly improves the efficiency of the BDC. Without snubber circuits, the converter achieves a maximum efficiency of approximately 85%. However, when active and passive snubber circuits are combined with dual control schemes, the efficiency increases to 96.4%. This enhancement ensures that the BDC with snubber circuits operates at a higher efficiency level compared to its snubber-less counterpart.

6.7 Summary

In this chapter, a new control scheme is proposed for a PV-based EVCS that enhances system stability compared to conventional methods. The key findings and contributions of the study are summarized as follows:

1. The proposed control scheme combines both master-control and droop control approaches, resulting in improved system stability. By utilizing a hybrid approach instead of relying solely on one scheme, a stable and consistent DC bus voltage of 400 V is maintained while achieving the desired power output.

2. The system incorporates a three-level boost converter optimized for efficient PV generation. The converter is regulated using incremental and conductance MPPT methods, ensuring optimal power extraction from the PV panels.
3. An in-depth explanation of the control schemes implemented for EV chargers and the ESU, utilizing an isolated BDC along with active and passive snubber circuits, has been presented. This integration enhances overall system reliability and facilitates quicker attainment of ZVS conditions.
4. The effectiveness of the proposed design is validated through simulation using MATLAB/Simulink, considering three distinct modes of EV operation. The obtained results showcase the robustness and reliability of the system, confirming its ability to provide stable and efficient EV charging.
5. The performance of the EVCS systems is thoroughly assessed. The inclusion of snubber circuits in the isolated BDC results in quickly reaching ZVS conditions, significantly enhancing system reliability. The combination of active and passive snubbers, BDC, master-slave droop control technique, and energy storage device presents an outstanding solution for PV-dependent EV charging stations. The system achieves an impressive conversion efficiency of 96.4%, emphasizing its efficiency and effectiveness.
6. The proposed design takes into consideration the utilization of solar energy for powering EVs, particularly in remote rural areas with limited access to conventional power grids. It highlights the advantages of employing DC supply technology in EVCS, emphasizing lower conversion losses. The inclusion of an ESU in the charging station optimizes the utilization of solar energy while enabling continuous EV charging.
7. The integration of innovative technologies such as off-grid EVCS, smart charging techniques, and EV control systems allows the energy sector to achieve a harmonious balance, maximizing the utilization of renewable sources like solar energy These advancements facilitate effective communication with clients, ensuring their satisfaction and providing cost-effective charging rates. An optimized charging system minimizes EV charging time and ensures a stable DC bus voltage.

8. The promotion of a stable, DC-based off-grid EVCS system that primarily utilizes renewable energy generation is of utmost importance in reducing our reliance on fossil fuels. By embracing such a system, we can effectively decrease our carbon footprint and contribute to a cleaner and more sustainable environment. This approach not only facilitates the provision of emission-free electricity but also caters to the growing demand for dynamic electrical loads, particularly the surging popularity of EVs.

Chapter 7 Conclusion and Scope for Further Work

7.1 Conclusions

Through extensive investigations and simulations, a charging and discharging system was successfully designed for a standalone PV-based EV charging station. The effects of integrating snubber circuits on off-grid PV-based EV charging was analyzed, and potential issues that could be resolved to enhance the effectiveness of a standalone EVCS were identified. Both droop and master-slave control techniques were implemented to optimize the performance of the charging station.

The findings of this study contribute to the development of sustainable transportation systems and support the transition toward a cleaner and greener future. By embracing innovative technologies like off-grid EVCS, smart charging techniques, and EV control systems, a harmonious balance in the energy sector can be achieved, maximizing the utilization of renewable sources such as solar energy. These advancements will facilitate effective communication with clients, ensuring their satisfaction and providing cost-effective charging rates. The optimization of the charging system not only minimizes EV charging time but also ensures a stable DC bus voltage for efficient charging infrastructure operation.

Specifically, the research investigated the application of both droop and master-slave control techniques in off-grid EV charging infrastructure. The implementation of droop control proved effective in maintaining voltage stability and power sharing among multiple charging stations. The decentralized operation enabled by droop control allows for the seamless integration of new charging stations and improved scalability. The study confirms that droop control enables reliable and efficient charging operations, minimizing voltage fluctuations and ensuring a balanced load distribution.

Furthermore, the master-slave control technique was implemented, resulting in improved system stability and load balancing. By leveraging both droop and master-slave control techniques, a robust and efficient charging system was achieved that ensures stable voltage, effective load management, and reliable power sharing.

The combination of droop and master-slave control techniques further enhanced the performance of the off-grid EV charging infrastructure. By leveraging the advantages of both control strategies, a robust and efficient charging system was achieved that ensures stable voltage, effective load management, and reliable power sharing. The integration of these control techniques enables optimized power flow management within the EVCS, maximizing the utilization of available resources and improving overall system efficiency.

Additionally, the research investigated the integration of snubber circuits in BDCs. The study compared various active and passive snubber circuit configurations and evaluated their impact on switching losses, voltage spikes, and electromagnetic interference. The findings demonstrate that the appropriate selection and optimization of snubber circuit components effectively mitigate voltage stress, reduce switching losses, and enhance the overall performance of the off-grid EV charging system.

A comparison of models and efficiencies is summarized in Table 7.1 to provide a better clarity.

Table 7.1 Model Comparison and Efficiency Improvement Summary

Model Comparison	**Control Strategies**	**BDC Configuration**	**Snubber Circuits**	**Efficiency Improvement**
Chapter 4 Model	N/A	Isolated BDC	Active Clamp and Passive Snubber	92%
Chapter 5 Model	N/A	Isolated BDC	RCD, Active Clamp, and Flyback Snubber	92%
Chapter 6 Model	Droop + Master-Slave	Isolated BDC	Flyback and Passive Snubber	96.40%

There are some limitations in the research that are yet to be addressed. Firstly, its applicability is restricted since the findings may not universally apply to all EV charging scenarios, primarily due to a lack of diverse validation. Further, the heavy reliance on simulations in the thesis ignores the potential oversight of real-world implementation and associated complexities. The study has not explored alternative control techniques and their advantages/limitations as they are well beyond the scope of this work. The examination of long-term system performance and sustainability

issues such as wear and tear, maintenance requirements, etc. are not addressed either. Most of these issues could be easily taken up as future research topics and studied further.

7.2 Scope for Further Work

While this thesis has made significant contributions to the field of off-grid EV charging infrastructure, there are several avenues for future research and development. The following areas offer potential for further exploration and improvement:

7.2.1 Advanced Control Techniques

Although this research explored control techniques like droop and master-slave control, further investigation can be conducted to explore advanced control algorithms such as model predictive control (MPC) or artificial intelligence (AI)-based approaches. These techniques have the potential to enhance the dynamic response and efficiency of the EV charging system.

7.2.2 Battery Management Systems (BMS)

Integrating an intelligent BMS into the standalone EVCS can optimize battery charging and discharging operations. Future research can focus on developing advanced BMS algorithms that consider factors such as battery aging, *SOC* estimation, and optimal power flow management.

7.2.3 Grid Interaction and V2G Integration

As the EV market continues to grow, grid interaction and V2G integration become crucial aspects to explore. Further research can investigate the seamless integration of off-grid EVCS with the utility grid, enabling bi-directional power flow between EVs and the grid, and enabling V2G services that allow EVs to supply power back to the grid during peak demand periods.

7.2.4 Scalability and Deployment Strategies

Future research can focus on exploring strategies for scaling up off-grid EV charging infrastructure, particularly in remote locations or areas with limited access to the utility grid. Deployment strategies, including cost-effective installation, system sizing, and maintenance considerations, should be thoroughly investigated to facilitate the widespread adoption of off-grid EVCS.

7.2.5 Economic and Environmental Analysis

Future research can undertake comprehensive economic and environmental analyses to evaluate the feasibility and economic viability of off-grid EV charging infrastructure. This analysis should consider factors such as the total cost of ownership, payback periods, carbon footprint reduction, and potential revenue streams, providing valuable insights for stakeholders and policymakers.

7.2.6 Integration of RES

While this research focused on standalone solar-powered EVCS, future studies can explore the integration of other RES such as wind or hydroelectric power. Investigating hybrid renewable energy systems for off-grid EV charging infrastructure can enhance reliability, reduce dependency on a single energy source, and optimize energy utilization.

7.2.7 Standardization and Regulations

As off-grid EV charging infrastructure evolves, the establishment of standards and regulations becomes essential. Future research can contribute to the development of guidelines and frameworks that ensure the interoperability, safety, and efficiency of off-grid EVCS, promoting uniformity and facilitating the adoption of these systems worldwide.

In conclusion, this thesis has successfully explored the potential of off-grid EV charging infrastructure using standalone solar-powered EVCS equipped with snubber circuits for BDCs. The integration of droop and master-slave control techniques, along with the optimization of snubber circuits, has demonstrated improved system stability, load balancing, and overall charging efficiency. The findings from this research contribute to the development of sustainable transportation systems and support the transition toward a cleaner and greener future. Further research and development are essential to unlock the full potential of off-grid EV charging infrastructure and address the emerging challenges in this field. By continuing to innovate and explore advanced control techniques, battery management systems, grid interaction, and real-world deployment, we can pave the way for a more sustainable and efficient future of EV charging.

References

[1] "First Electric Car: A Brief History of the EV, 1830 to Present." https://www.caranddriver.com/features/g43480930/history-of-electric-cars/ (accessed Apr. 29, 2023).

[2] L. K. Michael, S. K V, S. S. Hungund, and M. Fernandes, "Factors influencing adoption of electric vehicles–A case in India," *Cogent Eng*, vol. 9, no. 1, 2022, doi: 10.1080/23311916.2022.2085375.

[3] "Global Energy Review: CO2 Emissions in 2021 – Analysis - IEA." https://www.iea.org/reports/global-energy-review-co2-emissions-in-2021-2 (accessed Apr. 29, 2023).

[4] "Global CO2 emissions by sector 2021 | Statista." https://www.statista.com/statistics/276480/world-carbon-dioxide-emissions-by-sector (accessed Apr. 29, 2023).

[5] D. K. Nair, K. Prasad, and T. T. Lie, "Design of a PV-fed electric vehicle charging station with a combination of droop and master-slave control strategy," *Energy Storage*, p. e442, 2023, doi: 10.1002/EST2.442.

[6] "EV vs ICE: Are Electric Cars Worth It? | Mer UK." https://uk.mer.eco/news/ev-vs-ice-are-electric-cars-worth-it (accessed Apr. 29, 2023).

[7] "Transport | Ministry for the Environment." https://environment.govt.nz/publications/aotearoa-new-zealands-first-emissions-reduction-plan/transport/ (accessed Apr. 29, 2023).

[8] "What Are the Five Major Types of Renewable Energy?" https://elements.visualcapitalist.com/what-are-the-five-major-types-of-renewable-energy/?fbclid=IwAR2Oc155eRdm4ayXODqxnDPUIgkcvVeO6BxuZWuGyYR_smiv-hg1bU1wl_0 (accessed Apr. 29, 2023).

[9] "Report: Universal Access to Sustainable Energy Will Remain Elusive Without Addressing Inequalities." https://www.worldbank.org/en/news/press-release/2021/06/07/report-universal-access-to-sustainable-energy-will-remain-elusive-without-addressing-inequalities (accessed Apr. 29, 2023).

[10] I. E. Atawi, E. Hendawi, and S. A. Zaid, "Analysis and Design of a Standalone Electric Vehicle Charging Station Supplied by Photovoltaic Energy," *Processes 2021, Vol. 9, Page 1246*, vol. 9, no. 7, p. 1246, Jul. 2021, doi: 10.3390/PR9071246.

[11] "Top 5 Off Grid Solar Projects | Zonna Energy | 2023 List." https://www.zonnaenergy.com/top-off-grid-solar-projects/ (accessed May 23, 2023).

[12] Xianli Zhu and Gabriela Prata Dias, Eds., "BEHAVE 2020-2021 the 6th European Conference on Behaviour Change for Energy Efficiency," Denmark: Fabrice Belaire Infographie, 2021. Accessed: May 30, 2023. [Online]. Available: http://www.energyefficiencycentre.org

[13] "Go Off-Grid | Tesla Support." https://www.tesla.com/support/energy/powerwall/mobile-app/go-off-grid (accessed May 30, 2023).

[14] "BMW Proposes to Use Old Batteries in Off-Grid Solar Charging Stations - autoevolution." https://www.autoevolution.com/news/bmw-proposes-to-use-old-batteries-in-off-grid-solar-charging-stations-167742.html (accessed May 30, 2023).

[15] "Does Solar Energy Allow You to Go Off Grid? | SunPower Solar Blog." https://us.sunpower.com/blog/2022/07/14/does-solar-energy-allow-you-go-grid (accessed May 30, 2023).

[16] "Energy and industry | Ministry for the Environment." https://environment.govt.nz/publications/aotearoa-new-zealands-first-emissions-reduction-plan/energy-and-industry (accessed Apr. 29, 2023).

[17] D. K. Nair, K. Prasad, and T. T. Lie, "Standalone electric vehicle charging station using an isolated bidirectional converter with snubber," *Energy Storage*, vol. 3, no. 5, p. e255, Oct. 2021, doi: 10.1002/EST2.255.

[18] D. K. Nair, K. Prasad, and T. T. Lie, "Implementation of Snubber Circuits in a PV-Based Off-Grid Electric Vehicle Charging Station—Comparative Case Studies," *Energies 2021, Vol. 14, Page 5853*, vol. 14, no. 18, p. 5853, Sep. 2021, doi: 10.3390/EN14185853.

[19] A. Verma, B. Singh, A. Chandra, and K. Al-Haddad, "An Implementation of Solar PV Array Based Multifunctional EV Charger," *IEEE Trans Ind Appl*, vol. 56, no. 4, pp. 4166–4178, Jul. 2020, doi: 10.1109/TIA.2020.2984742.

[20] "History of the electric car | EVBox." https://blog.evbox.com/electric-cars-history (accessed May 06, 2023).

[21] "The ICE age is over: Why battery cars will beat hybrids and fuel cells." https://thedriven.io/2018/11/14/the-ice-age-is-over-why-battery-cars-will-beat-hybrids-and-fuel-cells/ (accessed May 06, 2023).

[22] J. Yuan, L. Dorn-Gomba, A. D. Callegaro, J. Reimers, and A. Emadi, "A review of bidirectional on-board chargers for electric vehicles," *IEEE Access*, vol. 9, pp. 51501–51518, 2021, doi: 10.1109/ACCESS.2021.3069448.

[23] "Electric Vehicle On-board Chargers and Charging Stations." https://circuitdigest.com/article/electric-vehicle-on-board-chargers-and-charging-stations (accessed May 06, 2023).

[24] Z. Qu *et al.*, "Optimization Model of EV Charging and Discharging Price Considering Vehicle Owner Response and Power Grid Cost," *Journal of Electrical Engineering & Technology*, vol. 14, no. 3, pp. 2251–2261, 2019, doi: 10.1007/s42835-019-00264-0.

[25] S. R. Dabbagh, M. K. Sheikh-El-Eslami, and A. Borghetti, "Optimal operation of vehicle-to-grid and grid-to-vehicle systems integrated with renewables," *19th Power Systems Computation Conference, PSCC 2016*, Aug. 2016, doi: 10.1109/PSCC.2016.7540933.

[26] "Electric Vehicle Myths | US EPA." https://www.epa.gov/greenvehicles/electric-vehicle-myths (accessed May 06, 2023).

[27] T. S. Biya and M. R. Sindhu, "Design and Power Management of Solar Powered Electric Vehicle Charging Station with Energy Storage System," *Proceedings of the 3rd International Conference on Electronics and Communication and Aerospace Technology, ICECA 2019*, pp. 815–820, Jun. 2019, doi: 10.1109/ICECA.2019.8821896.

[28] J. Tang, B. Ye, Q. Lu, D. Wang, and J. Li, "Economic Analysis of Photovoltaic Electricity Supply for an Electric Vehicle Fleet in Shenzhen, China," *International Journal of Sustainable Transportation*, vol. 8, no. 3, pp. 202–224, May 2013, doi: 10.1080/15568318.2012.665980.

[29] L. Bokopane, K. Kusakana, and H. J. Vermaak, "Energy Management of a Grid-Intergrated Hybrid Peer-to-Peer Renewable Charging Station for Electric Vehicles," *2018*

Open Innovations Conference, OI 2018, pp. 275–280, Nov. 2018, doi: 10.1109/OI.2018.8535881.

[30] D. B. Richardson, "Electric vehicles and the electric grid: A review of modeling approaches, Impacts, and renewable energy integration," *Renewable and Sustainable Energy Reviews*, vol. 19, pp. 247–254, Mar. 2013, doi: 10.1016/J.RSER.2012.11.042.

[31] S. Khan, A. Ahmad, F. Ahmad, M. Shafaati Shemami, M. Saad Alam, and S. Khateeb, "A Comprehensive Review on Solar Powered Electric Vehicle Charging System," *Smart Science*, vol. 6, no. 1, pp. 54–79, Jan. 2017, doi: 10.1080/23080477.2017.1419054.

[32] P. J. Tulpule, V. Marano, S. Yurkovich, and G. Rizzoni, "Economic and environmental impacts of a PV powered workplace parking garage charging station," *Appl Energy*, vol. 108, pp. 323–332, Aug. 2013, doi: 10.1016/J.APENERGY.2013.02.068.

[33] Y. Zhang and L. Cai, "Dynamic Charging Scheduling for EV Parking Lots with Photovoltaic Power System," *IEEE Access*, vol. 6, pp. 56995–57005, 2018, doi: 10.1109/ACCESS.2018.2873286.

[34] H. Zhao and A. Burke, "An intelligent solar powered battery buffered EV charging station with solar electricity forecasting and EV charging load projection functions," *2014 IEEE International Electric Vehicle Conference, IEVC 2014*, 2014, doi: 10.1109/IEVC.2014.7056169.

[35] N. Chowdhury, C. A. Hossain, M. Longo, and W. Yaïci, "Optimization of Solar Energy System for the Electric Vehicle at University Campus in Dhaka, Bangladesh," *Energies 2018, Vol. 11, Page 2433*, vol. 11, no. 9, p. 2433, Sep. 2018, doi: 10.3390/EN11092433.

[36] M. Yilmaz and P. T. Krein, "Review of battery charger topologies, charging power levels, and infrastructure for plug-in electric and hybrid vehicles," *IEEE Trans Power Electron*, vol. 28, no. 5, pp. 2151–2169, 2013, doi: 10.1109/TPEL.2012.2212917.

[37] C. C. Castello, T. J. LaClair, and L. Curt Maxey, "Control strategies for electric vehicle (EV) charging using Renewables and local storage," *2014 IEEE Transportation Electrification Conference and Expo: Components, Systems, and Power Electronics - From Technology to Business and Public Policy, ITEC 2014*, Jul. 2014, doi: 10.1109/ITEC.2014.6861835.

[38] V. Kumar, V. R. Teja, M. Singh, and S. Mishra, "PV Based Off-Grid Charging Station for Electric Vehicle," *IFAC-PapersOnLine*, vol. 52, no. 4, pp. 276–281, 2019, doi: 10.1016/J.IFACOL.2019.08.211.

[39] H. Doubabi, Y. Oublaid, I. Salhi, M. Chennani, and N. Essounbouli, "A Reliable Power Management Strategy of a PV-Based Electric Scooters Charging Station," *2021 International Conference on Optimization and Applications, ICOA 2021*, May 2021, doi: 10.1109/ICOA51614.2021.9442660.

[40] I. E. Atawi, E. Hendawi, and S. A. Zaid, "Analysis and Design of a Standalone Electric Vehicle Charging Station Supplied by Photovoltaic Energy," *Processes 2021, Vol. 9, Page 1246*, vol. 9, no. 7, p. 1246, Jul. 2021, doi: 10.3390/PR9071246.

[41] Y. Krim, M. Sechilariu, and F. Locment, "PV Benefits Assessment for PV-Powered Charging Stations for Electric Vehicles," *Applied Sciences 2021, Vol. 11, Page 4127*, vol. 11, no. 9, p. 4127, Apr. 2021, doi: 10.3390/APP11094127.

[42] K. Mohamed, H. K. Wolde, A. M. S. Al-Farsi, R. Khan, and S. M. S. Alarefi, "Opportunities for an off-Grid Solar PV Assisted Electric Vehicle Charging Station," *11th*

International Renewable Energy Congress, IREC 2020, Oct. 2020, doi: 10.1109/IREC48820.2020.9310376.

[43] A. Hajimiragha, C. A. Canizares, M. W. Fowler, and A. Elkamel, "Optimal transition to plug-in hybrid electric vehicles in Ontario, Canada, considering the electricity-grid limitations," *IEEE Transactions on Industrial Electronics*, vol. 57, no. 2, pp. 690–701, Feb. 2010, doi: 10.1109/TIE.2009.2025711.

[44] A. H. Hajimiragha, C. A. Cañizares, M. W. Fowler, S. Moazeni, and A. Elkamel, "A robust optimization approach for planning the transition to plug-in hybrid electric vehicles," *IEEE Transactions on Power Systems*, vol. 26, no. 4, pp. 2264–2274, Nov. 2011, doi: 10.1109/TPWRS.2011.2108322.

[45] A. Cabrera-Tobar, A. M. Pavan, N. Blasuttigh, G. Petrone, and G. Spagnuolo, "Real time Energy Management System of a photovoltaic based e-vehicle charging station using Explicit Model Predictive Control accounting for uncertainties," *Sustainable Energy, Grids and Networks*, vol. 31, p. 100769, Sep. 2022, doi: 10.1016/J.SEGAN.2022.100769.

[46] A. Shafiq *et al.*, "Solar PV-Based Electric Vehicle Charging Station for Security Bikes: A Techno-Economic and Environmental Analysis," *Sustainability (Switzerland)*, vol. 14, no. 21, Nov. 2022, doi: 10.3390/SU142113767.

[47] T. V. Thang, A. Ahmed, C. I. Kim, and J. H. Park, "Flexible System Architecture of Stand-Alone PV Power Generation with Energy Storage Device," *IEEE Transactions on Energy Conversion*, vol. 30, no. 4, pp. 1386–1396, Dec. 2015, doi: 10.1109/TEC.2015.2429145.

[48] D. Wu, F. Tang, T. Dragicevic, J. M. Guerrero, and J. C. Vasquez, "Coordinated control based on bus-signaling and virtual inertia for Islanded DC Microgrids," *IEEE Trans Smart Grid*, vol. 6, no. 6, pp. 2627–2638, Nov. 2015, doi: 10.1109/TSG.2014.2387357.

[49] Y. Xia, M. Yu, P. Yang, Y. Peng, and W. Wei, "Generation-Storage Coordination for Islanded DC Microgrids Dominated by PV Generators," *IEEE Transactions on Energy Conversion*, vol. 34, no. 1, pp. 130–138, Mar. 2019, doi: 10.1109/TEC.2018.2860247.

[50] Y. Zhang and W. Wei, "Decentralised coordination control strategy of the PV generator, storage battery and hydrogen production unit in islanded AC microgrid," *IET Renewable Power Generation*, vol. 14, no. 6, pp. 1053–1062, Apr. 2020, doi: 10.1049/IET-RPG.2019.0842.

[51] M. S. Alam, F. S. Al-Ismail, S. M. Rahman, M. Shafiullah, and M. A. Hossain, "Planning and protection of DC microgrid: A critical review on recent developments," *Engineering Science and Technology, an International Journal*, vol. 41, p. 101404, May 2023, doi: 10.1016/J.JESTCH.2023.101404.

[52] E. Hleihe, M. Fadel, and H. Y. Kanaan, "Control and power sharing of an islanded DC microgrid integrating a back-up diesel generator," *2020 5th International Conference on Renewable Energies for Developing Countries, REDEC 2020*, Jun. 2020, doi: 10.1109/REDEC49234.2020.9163831.

[53] "Photovoltaics and electricity - U.S. Energy Information Administration (EIA)." https://www.eia.gov/energyexplained/solar/photovoltaics-and-electricity.php (accessed May 06, 2023).

[54] G. Kavlak, J. McNerney, and J. E. Trancik, "Evaluating the causes of cost reduction in photovoltaic modules," *Energy Policy*, vol. 123, pp. 700–710, Dec. 2018, doi: 10.1016/J.ENPOL.2018.08.015.

[55] M. F. Akorede, "Design and performance analysis of off-grid hybrid renewable energy systems," *Hybrid Technologies for Power Generation*, pp. 35–68, Jan. 2022, doi: 10.1016/B978-0-12-823793-9.00001-2.

[56] "Solar Photovoltaic Cell Basics | Department of Energy." https://www.energy.gov/eere/solar/solar-photovoltaic-cell-basics (accessed May 06, 2023).

[57] A. Alanazi, M. Alanazi, S. Arabi, and S. Sarker, "A New Maximum Power Point Tracking Framework for Photovoltaic Energy Systems Based on Remora Optimization Algorithm in Partial Shading Conditions," *Applied Sciences 2022, Vol. 12, Page 3828*, vol. 12, no. 8, p. 3828, Apr. 2022, doi: 10.3390/APP12083828.

[58] H. Fathabadi, "Novel solar powered electric vehicle charging station with the capability of vehicle-to-grid," *Solar Energy*, vol. 142, pp. 136–143, Jan. 2017, doi: 10.1016/J.SOLENER.2016.11.037.

[59] I. Owusu-Nyarko, M. A. Elgenedy, and K. Ahmed, "Combined Temprature and Irradiation Effects on the Open Circuit Voltage and Short Circuit Current Constants for Enhancing their Related PV-MPPT Algorithms," *IEEE Conference on Power Electronics and Renewable Energy, CPERE 2019*, pp. 343–348, Oct. 2019, doi: 10.1109/CPERE45374.2019.8980007.

[60] S. Siouane, S. Jovanovic, and P. Poure, "Influence of contact thermal resistances on the Open Circuit Voltage MPPT method for Thermoelectric Generators," *2016 IEEE International Energy Conference, ENERGYCON 2016*, Jul. 2016, doi: 10.1109/ENERGYCON.2016.7514002.

[61] D. Baimel, S. Tapuchi, Y. Levron, and J. Belikov, "Improved Fractional Open Circuit Voltage MPPT Methods for PV Systems," *Electronics 2019, Vol. 8, Page 321*, vol. 8, no. 3, p. 321, Mar. 2019, doi: 10.3390/ELECTRONICS8030321.

[62] P. Pillai, S. Sundaresan, P. Kumar, K. R. Pattipati, and B. Balasingam, "Open-Circuit Voltage Models for Battery Management Systems: A Review," *Energies 2022, Vol. 15, Page 6803*, vol. 15, no. 18, p. 6803, Sep. 2022, doi: 10.3390/EN15186803.

[63] N. Díaz, A. Luna, and O. Duarte, "Improved MPPT short-circuit current method by a fuzzy short-circuit current estimator," *IEEE Energy Conversion Congress and Exposition: Energy Conversion Innovation for a Clean Energy Future, ECCE 2011, Proceedings*, pp. 211–218, 2011, doi: 10.1109/ECCE.2011.6063771.

[64] H. A. Sher, A. F. Murtaza, A. Noman, K. E. Addoweesh, K. Al-Haddad, and M. Chiaberge, "A New Sensorless Hybrid MPPT Algorithm Based on Fractional Short-Circuit Current Measurement and P&O MPPT," *IEEE Trans Sustain Energy*, vol. 6, no. 4, pp. 1426–1434, Oct. 2015, doi: 10.1109/TSTE.2015.2438781.

[65] S. Xiao and R. S. Balog, "An improved adaptive perturb & observe maximum power point tracking technique," *2018 IEEE Texas Power and Energy Conference, TPEC 2018*, vol. 2018-February, pp. 1–6, Mar. 2018, doi: 10.1109/TPEC.2018.8312066.

[66] A. Belkaid, I. Colak, and K. Kayisli, "A Novel Approach of Perturb and Observe Technique Adapted to Rapid Change of Environmental Conditions and Load," *Electric Power Components and Systems*, vol. 48, no. 4–5, pp. 375–387, Aug. 2020, doi: 10.1080/15325008.2020.1793842.

[67] A. N. M. Mohammad, M. A. M. Radzi, N. Azis, S. Shafie, and M. A. A. M. Zainuri, "An Enhanced Adaptive Perturb and Observe Technique for Efficient Maximum Power Point

Tracking Under Partial Shading Conditions," *Applied Sciences 2020, Vol. 10, Page 3912*, vol. 10, no. 11, p. 3912, Jun. 2020, doi: 10.3390/APP10113912.

[68] D. Jaraniya, R. K. Nema, and S. K. Gawre, "Design and Simulation of Power Electronics Interface for Modified P & O Maximum Power Point Tracking under Suddenly Varying Irradiance," *2020 IEEE International Students' Conference on Electrical, Electronics and Computer Science, SCEECS 2020*, Feb. 2020, doi: 10.1109/SCEECS48394.2020.110.

[69] R. John, S. S. Mohammed, and R. Zachariah, "Variable step size Perturb and observe MPPT algorithm for standalone solar photovoltaic system," *Proceedings of the 2017 IEEE International Conference on Intelligent Techniques in Control, Optimization and Signal Processing, INCOS 2017*, vol. 2018-February, pp. 1–6, Feb. 2018, doi: 10.1109/ITCOSP.2017.8303163.

[70] C. P. Roy, B. K. Naick, and G. Shankar, "Modified three-point weight comparison method for adaptive MPPT of photovoltaic systems," *IET Conference Publications*, vol. 2013, no. 645 CP, pp. 146–156, 2013, doi: 10.1049/CP.2013.2184.

[71] A. A. A. E. El Baset Halim, N. H. Saad, and A. A. E. Sattar, "Application of a Combined System between Perturb and Observe Method and Incremental Conductance Technique for MPPT in PV Systems," *2019 21st International Middle East Power Systems Conference, MEPCON 2019 - Proceedings*, pp. 103–110, Dec. 2019, doi: 10.1109/MEPCON47431.2019.9008079.

[72] D. Mustafic, D. Jokic, S. Lale, and S. Lubura, "Implementation of Incremental Conductance MPPT Algorithm in Real Time in Matlab/Simulink Environment with Humusoft MF634 Board," *2020 9th Mediterranean Conference on Embedded Computing, MECO 2020*, Jun. 2020, doi: 10.1109/MECO49872.2020.9134356.

[73] M. S. Nkambule, A. N. Hasan, and A. Ali, "MPPT under partial shading conditions based on Perturb & Observe and Incremental Conductance," *ELECO 2019 - 11th International Conference on Electrical and Electronics Engineering*, pp. 85–90, Nov. 2019, doi: 10.23919/ELECO47770.2019.8990426.

[74] O. Tremblay, L. A. Dessaint, and A. I. Dekkiche, "A generic battery model for the dynamic simulation of hybrid electric vehicles," *VPPC 2007 - Proceedings of the 2007 IEEE Vehicle Power and Propulsion Conference*, pp. 284–289, 2007, doi: 10.1109/VPPC.2007.4544139.

[75] P. Singh and J. S. Lather, "Real-Time Simulation and Analysis of Energy Storage System in Standalone PV-Based DC Microgrid," *Advances in Communication and Computational Technology - Proceedings of ICACCT 2019. (Lecture Notes in Electrical Engineering)*, vol. 668, pp. 1019–1032, 2021, doi: 10.1007/978-981-15-5341-7_77.

[76] X. Li *et al.*, "SOC Estimation of Lithium-Ion Battery for Electric Vehicle Based on Deep Multilayer Perceptron," *Comput Intell Neurosci*, vol. 2022, May 2022, doi: 10.1155/2022/3920317.

[77] R. Emamalipour and J. Lam, "A hybrid string-inverter/rectifier soft-switched bidirectional DC/DC converter," *IEEE Trans Power Electron*, vol. 35, no. 8, pp. 8200–8214, Aug. 2020, doi: 10.1109/TPEL.2019.2962518.

[78] J. Zeng, Z. Yan, J. Liu, and Z. Huang, "A High Voltage-Gain Bidirectional DC-DC Converter with Full-Range ZVS Using Decoupling Control Strategy," *IEEE J Emerg Sel Top Power Electron*, vol. 8, no. 3, pp. 2775–2784, Sep. 2020, doi: 10.1109/JESTPE.2019.2911331.

[79] A. Elserougi, I. Abdelsalam, A. Massoud, and S. Ahmed, “A bidirectional non-isolated hybrid modular DC–DC converter with zero-voltage switching,” *Electric Power Systems Research*, vol. 167, pp. 277–289, Feb. 2019, doi: 10.1016/J.EPSR.2018.11.009.

[80] Y. Du, S. Lukic, B. Jacobson, and A. Huang, “Review of high power isolated bi-directional DC-DC converters for PHEV/EV DC charging infrastructure,” *IEEE Energy Conversion Congress and Exposition: Energy Conversion Innovation for a Clean Energy Future, ECCE 2011, Proceedings*, pp. 553–560, 2011, doi: 10.1109/ECCE.2011.6063818.

[81] N. Hou, W. Song, Y. Zhu, X. Sun, and W. Li, “Dynamic and static performance optimization of dual active bridge DC-DC converters,” *Journal of Modern Power Systems and Clean Energy*, vol. 6, no. 3, pp. 607–618, May 2018, doi: 10.1007/S40565-017-0343-7/FIGURES/18.

[82] H. Bai and C. Mi, “Eliminate reactive power and increase system efficiency of isolated bidirectional dual-active-bridge dc-dc converters using novel dual-phase-shift control,” *IEEE Trans Power Electron*, vol. 23, no. 6, pp. 2905–2914, 2008, doi: 10.1109/TPEL.2008.2005103.

[83] D. M. Bellur and M. K. Kazimierczuk, “DC-DC converters for electric vehicle applications,” *2007 Electrical Insulation Conference and Electrical Manufacturing Expo, EEIC 2007*, pp. 286–293, 2007, doi: 10.1109/EEIC.2007.4562633.

[84] N. Guennouni, A. Chebak, and N. Machkour, “Optimal Dual Active Bridge DC-DC Converter Operation with Minimal Reactive Power for Battery Electric Vehicles Using Model Predictive Control,” *Electronics 2022, Vol. 11, Page 1621*, vol. 11, no. 10, p. 1621, May 2022, doi: 10.3390/ELECTRONICS11101621.

[85] K. Bathala, D. Kishan, and N. Harischandrappa, “Soft Switched Current Fed Dual Active Bridge Isolated Bidirectional Series Resonant DC-DC Converter for Energy Storage Applications,” *Energies 2023, Vol. 16, Page 258*, vol. 16, no. 1, p. 258, Dec. 2022, doi: 10.3390/EN16010258.

[86] B. Zhao, Q. Song, W. Liu, and Y. Sun, “Overview of dual-active-bridge isolated bidirectional DC-DC converter for high-frequency-link power-conversion system,” *IEEE Trans Power Electron*, vol. 29, no. 8, pp. 4091–4106, 2014, doi: 10.1109/TPEL.2013.2289913.

[87] X. Pan, H. Li, Y. Liu, T. Zhao, C. Ju, and A. K. Rathore, “An Overview and Comprehensive Comparative Evaluation of Current-Fed-Isolated-Bidirectional DC/DC Converter,” *IEEE Trans Power Electron*, vol. 35, no. 3, pp. 2737–2763, Mar. 2020, doi: 10.1109/TPEL.2019.2931739.

[88] E. E. Henao-Bravo, C. A. Ramos-Paja, A. J. Saavedra-Montes, D. González-Montoya, and J. Sierra-Pérez, “Design Method of Dual Active Bridge Converters for Photovoltaic Systems with High Voltage Gain,” *Energies 2020, Vol. 13, Page 1711*, vol. 13, no. 7, p. 1711, Apr. 2020, doi: 10.3390/EN13071711.

[89] V. Karthikeyan and R. Gupta, “Light-load efficiency improvement by extending ZVS range in DAB-bidirectional DC-DC converter for energy storage applications,” *Energy*, vol. 130, pp. 15–21, Jul. 2017, doi: 10.1016/J.ENERGY.2017.04.119.

[90] V. Karthikeyan and R. Gupta, “Zero circulating current modulation for isolated bidirectional dual-active-bridge DC–DC converter,” *IET Power Electronics*, vol. 9, no. 7, pp. 1553–1561, Jun. 2016, doi: 10.1049/IET-PEL.2015.0475.

[91] V. Karthikeyan and R. Gupta, "FRS-DAB Converter for Elimination of Circulation Power Flow at Input and Output Ends," *IEEE Transactions on Industrial Electronics*, vol. 65, no. 3, pp. 2135–2144, Mar. 2018, doi: 10.1109/TIE.2017.2740853.

[92] T. Prasetya, F. D. Wijaya, and E. Firmansyah, "Design of Full-bridge DC-DC Converter 311/100 V 1kW with PSPWM Method to Get ZVS Condition," *International Journal of Power Electronics and Drive Systems (IJPEDS)*, vol. 8, no. 1, pp. 59–68, Mar. 2017, doi: 10.11591/IJPEDS.V8.I1.PP59-68.

[93] S. Lee, W. Hong, T. Kim, G. D. Kim, E. S. Lee, and S. H. Lee, "Voltage balancing control of a series-resonant DAB converter with a virtual line shaft," *Journal of Power Electronics*, vol. 22, no. 8, pp. 1347–1356, Aug. 2022, doi: 10.1007/S43236-022-00466-2/METRICS.

[94] H. Chen and A. K. S. Bhat, "A bidirectional dual-bridge LCL-type series resonant converter controlled with modified gating scheme," *2016 IEEE 8th International Power Electronics and Motion Control Conference, IPEMC-ECCE Asia 2016*, pp. 3036–3042, Jul. 2016, doi: 10.1109/IPEMC.2016.7512780.

[95] H. Chen and A. K. S. Bhat, "Analysis and design of a dual-bridge series resonant DC-to-DC converter for capacitor semi-Active battery-ultracapacitor hybrid storage system," *IEEE International Symposium on Industrial Electronics*, pp. 1788–1793, 2014, doi: 10.1109/ISIE.2014.6864886.

[96] A. K. S. Bhat and R. L. Zheng, "Analysis and design of a three-phase LCC-type resonant converter," *IEEE Trans Aerosp Electron Syst*, vol. 34, no. 2, pp. 508–519, 1998, doi: 10.1109/7.670332.

[97] X. Li and A. K. S. Bhat, "Analysis and design of high-frequency isolated dual-bridge series resonant DC/DC converter," *IEEE Trans Power Electron*, vol. 25, no. 4, pp. 850–862, 2010, doi: 10.1109/TPEL.2009.2034662.

[98] J. Yang, Y. Zhang, and X. Wu, "Minimum Current Optimization of DBSRC Considering the Dead-Time Effect," *Energies 2022, Vol. 15, Page 8484*, vol. 15, no. 22, p. 8484, Nov. 2022, doi: 10.3390/EN15228484.

[99] M. Biswas, S. P. Biswas, M. R. Islam, M. A. Rahman, K. M. Muttaqi, and S. M. Muyeen, "A New Transformer-Less Single-Phase Photovoltaic Inverter to Improve the Performance of Grid-Connected Solar Photovoltaic Systems," *Energies 2022, Vol. 15, Page 8398*, vol. 15, no. 22, p. 8398, Nov. 2022, doi: 10.3390/EN15228398.

[100] J. Deng and H. Wang, "A Hybrid-Bridge and Hybrid Modulation-Based Dual-Active-Bridge Converter Adapted to Wide Voltage Range," *IEEE J Emerg Sel Top Power Electron*, vol. 9, no. 1, pp. 910–920, Feb. 2021, doi: 10.1109/JESTPE.2019.2949604.

[101] O. M. Hebala, A. A. Aboushady, K. H. Ahmed, I. Abdelsalam, and S. J. Burgess, "A New Active Power Controller in Dual Active Bridge DC-DC Converter with a Minimum-Current-Point-Tracking Technique," *IEEE J Emerg Sel Top Power Electron*, vol. 9, no. 2, pp. 1328–1338, Apr. 2021, doi: 10.1109/JESTPE.2020.3016771.

[102] C. Jiang and H. Liu, "A Novel Interleaved Parallel Bidirectional Dual-Active-Bridge DC-DC Converter with Coupled Inductor for More-Electric Aircraft," *IEEE Transactions on Industrial Electronics*, vol. 68, no. 2, pp. 1759–1768, Feb. 2021, doi: 10.1109/TIE.2020.3018047.

[103] R. Yamada, A. Hino, and K. Wada, "Improvement of Efficiency in Bidirectional DC-DC Converter with Dual Active Bridge Using GaN-HEMT," *2022 International Power*

Electronics Conference, IPEC-Himeji 2022-ECCE Asia, pp. 1398–1403, 2022, doi: 10.23919/IPEC-HIMEJI2022-ECCE53331.2022.9807182.

[104] B. Majmunovic and D. Maksimovic, "400-48-V Stacked Active Bridge Converter," *IEEE Trans Power Electron*, vol. 37, no. 10, pp. 12017–12029, Oct. 2022, doi: 10.1109/TPEL.2022.3160413.

[105] N. Hou, Y. Zhang, and Y. W. Li, "A Load-Current-Estimating Scheme with Delay Compensation for the Dual-Active-Bridge DC-DC Converter," *IEEE Trans Power Electron*, vol. 37, no. 3, pp. 2636–2647, Mar. 2022, doi: 10.1109/TPEL.2021.3111854.

[106] R. Haneda and H. Akagi, "Power-Loss Characterization and Reduction of the 750-V 100-KW 16-KHz Dual-Active-Bridge Converter with Buck and Boost Mode," *IEEE Trans Ind Appl*, vol. 58, no. 1, pp. 541–553, 2022, doi: 10.1109/TIA.2021.3129728.

[107] P. Xuewei and A. K. Rathore, "Comparison of bi-directional voltage-fed and current-fed dual active bridge isolated dc/dc converters low voltage high current applications," *IEEE International Symposium on Industrial Electronics*, pp. 2566–2571, 2014, doi: 10.1109/ISIE.2014.6865024.

[108] P. Xuewei and A. K. Rathore, "Novel interleaved bidirectional snubberless soft-switching current-fed full-bridge voltage doubler for fuel-cell vehicles," *IEEE Trans Power Electron*, vol. 28, no. 12, pp. 5535–5546, 2013, doi: 10.1109/TPEL.2013.2252199.

[109] D. Sha, X. Wang, and D. Chen, "High-Efficiency Current-Fed Dual Active Bridge DC-DC Converter With ZVS Achievement Throughout Full Range of Load Using Optimized Switching Patterns," *IEEE Trans Power Electron*, vol. 33, no. 2, pp. 1347–1357, Feb. 2018, doi: 10.1109/TPEL.2017.2675945.

[110] H. Wu, S. Ding, K. Sun, L. Zhang, Y. Li, and Y. Xing, "Bidirectional Soft-Switching Series-Resonant Converter with Simple PWM Control and Load-Independent Voltage-Gain Characteristics for Energy Storage System in DC Microgrids," *IEEE J Emerg Sel Top Power Electron*, vol. 5, no. 3, pp. 995–1007, Sep. 2017, doi: 10.1109/JESTPE.2017.2651049.

[111] H. Wu, K. Sun, Y. Li, and Y. Xing, "Fixed-Frequency PWM-Controlled Bidirectional Current-Fed Soft-Switching Series-Resonant Converter for Energy Storage Applications," *IEEE Transactions on Industrial Electronics*, vol. 64, no. 8, pp. 6190–6201, Aug. 2017, doi: 10.1109/TIE.2017.2682020.

[112] K. Bathala, D. Kishan, and N. Harischandrappa, "Current Source Isolated Bidirectional Series Resonant DC-DC Converter for Solar Power/Fuel Cell and Energy Storage Application," *IECON Proceedings (Industrial Electronics Conference)*, vol. 2021-October, Oct. 2021, doi: 10.1109/IECON48115.2021.9589693.

[113] K. Bhatt, R. A. Gupta, and N. Gupta, "Design and development of isolated snubber based bidirectional DC-DC converter for electric vehicle applications," *IET Power Electronics*, vol. 12, no. 13, pp. 3378–3388, Nov. 2019, doi: 10.1049/IET-PEL.2019.0111.

[114] I. Ferencz, D. Petreus, and T. Patarau, "Comparative study of three snubber circuits for a phase-shift converter," *2020 International Symposium on Power Electronics, Electrical Drives, Automation and Motion, SPEEDAM 2020*, pp. 763–768, Jun. 2020, doi: 10.1109/SPEEDAM48782.2020.9161962.

[115] X. Pan, H. Li, Y. Liu, T. Zhao, C. Ju, and A. K. Rathore, "An Overview and Comprehensive Comparative Evaluation of Current-Fed-Isolated-Bidirectional DC/DC Converter," *IEEE Trans Power Electron*, vol. 35, no. 3, pp. 2737–2763, Mar. 2020, doi: 10.1109/TPEL.2019.2931739.

[116] H. Asgari, M. Heidari, and E. Adib, “Soft-Switching Isolated Dual Active Bridge Bidirectional DC-DC Converter with Simple Structure,” *2019 10th International Power Electronics, Drive Systems and Technologies Conference, PEDSTC 2019*, pp. 707–712, Apr. 2019, doi: 10.1109/PEDSTC.2019.8697703.

[117] L. Zhu, “A novel soft-commutating isolated boost full-bridge ZVS-PWM DC-DC converter for bidirectional high power applications,” *IEEE Trans Power Electron*, vol. 21, no. 2, pp. 422–429, Mar. 2006, doi: 10.1109/TPEL.2005.869730.

[118] L. Zhou and X. Ruan, “A zero-current and zero-voltage-switching PWM boost full-bridge converter,” *PESC Record - IEEE Annual Power Electronics Specialists Conference*, vol. 2, pp. 957–962, 2003, doi: 10.1109/PESC.2003.1218184.

[119] U. R. Prasanna and A. K. Rathore, “Small signal analysis and control design of current-fed full-bridge isolated dc/dc converter with active-clamp,” *IEEE International Symposium on Industrial Electronics*, pp. 509–514, 2012, doi: 10.1109/ISIE.2012.6237139.

[120] T. F. Wu, J. G. Yang, C. L. Kuo, K. H. Sun, and Y. K. Chen, “Comparison of bi-directional isolated full-bridge converters with combinations of active and passive snubbers,” *IEEE Energy Conversion Congress and Exposition: Energy Conversion Innovation for a Clean Energy Future, ECCE 2011, Proceedings*, pp. 127–133, 2011, doi: 10.1109/ECCE.2011.6063759.

[121] T. F. Wu, Y. C. Chen, J. G. Yang, and C. L. Kuo, “Isolated bidirectional full-bridge DC-DC converter with a flyback snubber,” *IEEE Trans Power Electron*, vol. 25, no. 7, pp. 1915–1922, 2010, doi: 10.1109/TPEL.2010.2043542.

[122] T. F. Wu, J. G. Yang, C. L. Kuo, and Y. C. Wu, “Soft-switching bidirectional isolated full-bridge converter with active and passive snubbers,” *IEEE Transactions on Industrial Electronics*, vol. 61, no. 3, pp. 1368–1376, 2014, doi: 10.1109/TIE.2013.2262746.

[123] J. H. Jung, H. S. Kim, M. H. Ryu, and J. W. Baek, “Design methodology of bidirectional CLLC resonant converter for high-frequency isolation of DC distribution systems,” *IEEE Trans Power Electron*, vol. 28, no. 4, pp. 1741–1755, Apr. 2013, doi: 10.1109/TPEL.2012.2213346.

[124] K. Wang, F. C. Lee, and J. Lai, “Operation principles of bi-directional full-bridge DC/DC converter with unified soft-switching scheme and soft-starting capability,” *Conference Proceedings - IEEE Applied Power Electronics Conference and Exposition - APEC*, vol. 1, pp. 111–118, 2000, doi: 10.1109/APEC.2000.826092.

[125] T. F. Wu, Y. D. Chang, C. H. Chang, and J. G. Yang, “Soft-switching boost converter with a flyback snubber for high power applications,” *IEEE Trans Power Electron*, vol. 27, no. 3, pp. 1108–1119, 2012, doi: 10.1109/TPEL.2011.2126024.

[126] C. Zhang, P. Li, and Y. Guo, “Bidirectional DC/DC and SOC Drooping Control for DC Microgrid Application,” *Electronics 2020, Vol. 9, Page 225*, vol. 9, no. 2, p. 225, Jan. 2020, doi: 10.3390/ELECTRONICS9020225.

[127] J. Lv, X. Wang, G. Wang, and Y. Song, “Research on Control Strategy of Isolated DC Microgrid Based on SOC of Energy Storage System,” *Electronics 2021, Vol. 10, Page 834*, vol. 10, no. 7, p. 834, Mar. 2021, doi: 10.3390/ELECTRONICS10070834.

[128] D. Zammit, C. S. Staines, M. Apap, and A. Micallef, “Control Of Buck and Boost Converters For Stand-Alone DC Microgrids,” in *Eighth International Symposium on Energy, Aberdeen, Scotland, United Kingdom*, Aug. 2018.

[129] R. Haghmaram, F. Sedaghati, and R. Ghafarpour, "Power exchange among microgrids using modular-isolated bidirectional DC–DC converter," *Electrical Engineering*, vol. 99, no. 1, pp. 441–454, Mar. 2017, doi: 10.1007/S00202-016-0437-7/METRICS.

[130] D. S. Abraham *et al.*, "Electric Vehicles Charging Stations' Architectures, Criteria, Power Converters, and Control Strategies in Microgrids," *Electronics 2021, Vol. 10, Page 1895*, vol. 10, no. 16, p. 1895, Aug. 2021, doi: 10.3390/ELECTRONICS10161895.

[131] C. Y. Chung, J. Chynoweth, C. C. Chu, and R. Gadh, "Master-slave control scheme in electric vehicle smart charging infrastructure," *Scientific World Journal*, vol. 2014, 2014, doi: 10.1155/2014/462312.

[132] M. Kamran, "Power electronics for smart grids", *Fundamentals of Smart Grid Systems*, pp. 133-218, Academic Press, Jan.2023. doi: 10.1016/B978-0-323-99560-3.00009-0.

[133] S. Kim, H. Van Quy, and C. W. Bark, "Photovoltaic technologies for flexible solar cells: beyond silicon," *Mater Today Energy*, vol. 19, p. 100583, Mar. 2021, doi: 10.1016/J.MTENER.2020.100583.

[134] "Photovoltaic systems and Renewable energy." https://www.level.org.nz/energy/renewable-electricity-generation/photovoltaic-pv-systems/ (accessed May 07, 2023).

[135] J. Solis-Rodriguez, J. C. Rosas-Caro, A. Alejo-Reyes, and J. E. Valdez-Resendiz, "Optimal Selection of Capacitors for a Low Energy Storage Quadratic Boost Converter (LES-QBC)," *Energies 2023, Vol. 16, Page 2510*, vol. 16, no. 6, p. 2510, Mar. 2023, doi: 10.3390/EN16062510.

[136] A. A. Stephen, K. Musasa, and I. E. Davidson, "Modelling of Solar PV under Varying Condition with an Improved Incremental Conductance and Integral Regulator," *Energies 2022, Vol. 15, Page 2405*, vol. 15, no. 7, p. 2405, Mar. 2022, doi: 10.3390/EN15072405.

[137] S. Jagtap and A. Khandekar, "Implementation of Combined System between Perturb Observe and Incremental Conductance Technique for MPPT in PV System," *2021 2nd Global Conference for Advancement in Technology, GCAT 2021*, Oct. 2021, doi: 10.1109/GCAT52182.2021.9587457.

[138] H. Huang, S. Balasubramaniam, G. Todeschini, and S. Santoso, "A photovoltaic-fed dc-bus islanded electric vehicles charging system based on a hybrid control scheme," *Electronics (Switzerland)*, vol. 10, no. 10, May 2021, doi: 10.3390/ELECTRONICS10101142.

[139] C. Balakishan, N. Sandeep, M. V. Aware, and P. Bauer, "Design and implementation of three-level DC-DC converter with golden section search based MPPT for the photovoltaic applications," *Advances in Power Electronics*, vol. 2015, 2015, doi: 10.1155/2015/587197.

[140] D. Aggeler, F. Canales, H. Zelaya - De La Parra, A. Coccia, N. Butcher, and O. Apeldoorn, "Ultra-fast DC-charge infrastructures for EV-mobility and future smart grids," *IEEE PES Innovative Smart Grid Technologies Conference Europe, ISGT Europe*, 2010, doi: 10.1109/ISGTEUROPE.2010.5638899.

[141] B. Kim, "Smart charging architecture for between a plug-in electrical vehicle (PEV) and a smart home," *2013 International Conference on Connected Vehicles and Expo, ICCVE 2013 - Proceedings*, pp. 306–307, 2013, doi: 10.1109/ICCVE.2013.6799811.

[142] S. Divyapriya, Amutha, and R. Vijayakumar, "Design of Residential Plug-in Electric Vehicle Charging Station with Time of Use Tariff and IoT Technology," *ICSNS 2018 -*

Proceedings of IEEE International Conference on Soft-Computing and Network Security, Dec. 2018, doi: 10.1109/ICSNS.2018.8573637.

[143] M. S. Mastoi *et al.*, "An in-depth analysis of electric vehicle charging station infrastructure, policy implications, and future trends," *Energy Reports*, vol. 8, pp. 11504–11529, Nov. 2022, doi: 10.1016/J.EGYR.2022.09.011.

[144] "Environmental Assessment of Plug-In Hybrid Electric Vehicles," *Volume 1: Nationwide Greenhouse Gas Emissions*. http://mydocs.epri.com/docs/CorporateDocuments/SectorPages/Portfolio/PDM/PHEV-ExecSum-vol1.pdf (accessed May 07, 2023).

[145] J. Babic, A. Carvalho, W. Ketter, and V. Podobnik, "Evaluating Policies for Parking Lots Handling Electric Vehicles," *IEEE Access*, vol. 6, pp. 944–961, Nov. 2017, doi: 10.1109/ACCESS.2017.2777098.

[146] S. Habib, M. M. Khan, F. Abbas, L. Sang, M. U. Shahid, and H. Tang, "A Comprehensive Study of Implemented International Standards, Technical Challenges, Impacts and Prospects for Electric Vehicles," *IEEE Access*, vol. 6, pp. 13866–13890, Mar. 2018, doi: 10.1109/ACCESS.2018.2812303.

[147] "National guidance for public electric vehicle charging infrastructure | Waka Kotahi NZ Transport Agency." https://nzta.govt.nz/planning-and-investment/planning/transport-planning/planning-for-electric-vehicles/national-guidance-for-public-electric-vehicle-charging-infrastructure/ (accessed May 08, 2023).

[148] P. Vishnuram *et al.*, "A comprehensive review on EV power converter topologies charger types infrastructure and communication techniques," *Front Energy Res*, vol. 11, Feb. 2023, doi: 10.3389/FENRG.2023.1103093/FULL.

[149] A. S. Varghese, P. Thomas, and S. Varghese, "An efficient voltage control strategy for fast charging of plug-in electric vehicle," *2017 Innovations in Power and Advanced Computing Technologies, i-PACT 2017*, vol. 2017-January, pp. 1–4, 2017, doi: 10.1109/IPACT.2017.8245074.

[150] S. Arora, A. T. Abkenar, S. G. Jayasinghe, and K. Tammi, "EV Battery Pack Engineering—Electrical Design and Mechanical Design," *Heavy-Duty Electric Vehicles*, pp. 105–134, Jan. 2021, doi: 10.1016/B978-0-12-818126-3.00004-X.

[151] "Market Development for Green Cars - Google Books." https://www.google.co.nz/books/edition/Market_Development_for_Green_Cars/qJKnnQAACAAJ?hl=en (accessed May 08, 2023).

[152] S. M. Arif, T. T. Lie, B. C. Seet, S. Ayyadi, and K. Jensen, "Review of Electric Vehicle Technologies, Charging Methods, Standards and Optimization Techniques," *Electronics 2021, Vol. 10, Page 1910*, vol. 10, no. 16, p. 1910, Aug. 2021, doi: 10.3390/ELECTRONICS10161910.

[153] M. Bashiri and N. Bahadori, "Optimized plan of charging stations for management of demands: An emerging need of hybrid electric vehicle," *FTC 2016 - Proceedings of Future Technologies Conference*, pp. 422–425, Jan. 2017, doi: 10.1109/FTC.2016.7821643.

[154] W. Khan, F. Ahmad, and M. S. Alam, "Fast EV charging station integration with grid ensuring optimal and quality power exchange," *Engineering Science and Technology, an International Journal*, vol. 22, no. 1, pp. 143–152, Feb. 2019, doi: 10.1016/J.JESTCH.2018.08.005.

[155] L. Bokopane, K. Kusakana, and H. J. Vermaak, "Energy Management of a Grid-Intergrated Hybrid Peer-to-Peer Renewable Charging Station for Electric Vehicles," *2018 Open Innovations Conference, OI 2018*, pp. 275–280, Nov. 2018, doi: 10.1109/OI.2018.8535881.

[156] G. Badea *et al.*, "Design and Simulation of Romanian Solar Energy Charging Station for Electric Vehicles," *Energies 2019, Vol. 12, Page 74*, vol. 12, no. 1, p. 74, Dec. 2018, doi: 10.3390/EN12010074.

[157] K. Dimitriadou, N. Rigogiannis, S. Fountoukidis, F. Kotarela, A. Kyritsis, and N. Papanikolaou, "Current Trends in Electric Vehicle Charging Infrastructure; Opportunities and Challenges in Wireless Charging Integration," *Energies 2023, Vol. 16, Page 2057*, vol. 16, no. 4, p. 2057, Feb. 2023, doi: 10.3390/EN16042057.

[158] B. C. Johnson, D. G. Dunn, and R. Hulett, "A comparison of the IEEE and IEC standards processes," *Record of Conference Papers - Annual Petroleum and Chemical Industry Conference*, pp. 1–12, 2002, doi: 10.1109/PCICON.2002.1044979.

[159] "Homepage | IEC." https://iec.ch/homepage (accessed May 08, 2023).

[160] "IEA – International Energy Agency." https://www.iea.org/ (accessed May 08, 2023).

[161] "SAE's Involvement in the Smart Grid - Standards Development - Standards - SAE International." https://www.sae.org/standards/development/sae-involvement-smart-grid (accessed May 08, 2023).

[162] S. Habib, M. M. Khan, F. Abbas, L. Sang, M. U. Shahid, and H. Tang, "A Comprehensive Study of Implemented International Standards, Technical Challenges, Impacts and Prospects for Electric Vehicles," *IEEE Access*, vol. 6, pp. 13866–13890, Mar. 2018, doi: 10.1109/ACCESS.2018.2812303.

[163] S. Pareek, A. Sujil, S. Ratra, and R. Kumar, "Electric Vehicle Charging Station Challenges and Opportunities: A Future Perspective," *Proceedings - 2020 International Conference on Emerging Trends in Communication, Control and Computing, ICONC3 2020*, Feb. 2020, doi: 10.1109/ICONC345789.2020.9117473.

[164] M. S. Mahmoud and Y. Xia, "Smart Grid Infrastructures," *Networked Control Systems*, pp. 315–349, Jan. 2019, doi: 10.1016/B978-0-12-816119-7.00015-0.

[165] M. Kamran, "Electric vehicles and smart grids," *Fundamentals of Smart Grid Systems*, pp. 431–460, Academic Press, Jan. 2023, doi: 10.1016/B978-0-323-99560-3.00002-8.

[166] J. Mullan, D. Harries, T. Bräunl, and S. Whitely, "The technical, economic and commercial viability of the vehicle-to-grid concept," *Energy Policy*, vol. 48, pp. 394–406, Sep. 2012, doi: 10.1016/J.ENPOL.2012.05.042.

[167] M. A. Hannan *et al.*, "Vehicle to grid connected technologies and charging strategies: Operation, control, issues and recommendations," *J Clean Prod*, vol. 339, p. 130587, Mar. 2022, doi: 10.1016/J.JCLEPRO.2022.130587.

[168] "EV charging connector types: How long to recharge electric car UK." https://www.zap-map.com/ev-guides/connector-types/ (accessed Jun. 03, 2023).

[169] "Electric Vehicle On-board Chargers and Charging Stations." https://circuitdigest.com/article/electric-vehicle-on-board-chargers-and-charging-stations (accessed May 08, 2023).

[170] "Charging point connectors and socket outlets | Waka Kotahi NZ Transport Agency." https://www.nzta.govt.nz/planning-and-investment/planning/transport-

planning/planning-for-electric-vehicles/national-guidance-for-public-electric-vehicle-charging-infrastructure/charging-point-connectors-and-socket-outlets/ (accessed May 08, 2023).

[171] "Charging cables for electric cars – mode 2 and mode 3 | MENNEKES." https://www.mennekes.org/emobility/products/ev-charging-cable/ (accessed May 08, 2023).

[172] "Supercharger | Tesla." https://www.tesla.com/supercharger (accessed May 08, 2023).

[173] S. W. Lee and B. H. Cho, "Master-slave based hierarchical control for a small power DC-distributed microgrid system with a storage device," *Energies (Basel)*, vol. 9, no. 12, Oct. 2016, doi: 10.3390/EN9110880.

[174] J. Singh, S. Prakash Singh, K. Shanker Verma, A. Iqbal, and B. Kumar, "Recent control techniques and management of AC microgrids: A critical review on issues, strategies, and future trends," *International Transactions on Electrical Energy Systems*, vol. 31, no. 11, Nov. 2021, doi: 10.1002/2050-7038.13035.

[175] C. Leone, M. Longo, and L. M. Fernández-Ramírez, "Optimal Size of a Smart Ultra-Fast Charging Station," *Electronics 2021, Vol. 10, Page 2887*, vol. 10, no. 23, p. 2887, Nov. 2021, doi: 10.3390/ELECTRONICS10232887.

[176] M. A. S. T. Ireshika, R. Lliuyacc-Blas, and P. Kepplinger, "Voltage-based droop control of electric vehicles in distribution grids under different charging power levels," *Energies (Basel)*, vol. 14, no. 13, Jul. 2021, doi: 10.3390/EN14133905.

[177] H. Pan, X. Feng, F. Li, and J. Yang, "Energy coordinated control of DC microgrid integrated incorporating PV, energy storage and EV charging," *Appl Energy*, vol. 342, Jul. 2023, doi: 10.1016/j.apenergy.2023.121155.

[178] S. Wang, L. Lu, X. Han, M. Ouyang, and X. Feng, "Virtual-battery based droop control and energy storage system size optimization of a DC microgrid for electric vehicle fast charging station," *Appl Energy*, vol. 259, p. 114146, Feb. 2020, doi: 10.1016/J.APENERGY.2019.114146.

[179] M. Nour, J. P. Chaves-Ávila, G. Magdy, and Á. Sánchez-Miralles, "Review of Positive and Negative Impacts of Electric Vehicles Charging on Electric Power Systems," *Energies 2020, Vol. 13, Page 4675*, vol. 13, no. 18, p. 4675, Sep. 2020, doi: 10.3390/EN13184675.

[180] N. Saxena, I. Hussain, B. Singh, and A. L. Vyas, "Implementation of a Grid-Integrated PV-Battery System for Residential and Electrical Vehicle Applications," *IEEE Transactions on Industrial Electronics*, vol. 65, no. 8, pp. 6592–6601, Aug. 2018, doi: 10.1109/TIE.2017.2739712.

[181] "National Renewable Energy Laboratory (NREL) Home Page | NREL." https://www.nrel.gov/ (accessed May 20, 2023).

[182] P. Garcia-Trivino, L. M. Fernandez-Ramirez, J. P. Torreglosa, and F. Jurado, "Control of electric vehicles fast charging station supplied by PV/energy storage system/grid," *2016 IEEE International Energy Conference, ENERGYCON 2016*, Jul. 2016, doi: 10.1109/ENERGYCON.2016.7514120.

[183] J. Liu, Z. Zheng, K. Wang, and Y. D. Li, "Comparison of boost and LLC converter and active clamp isolated full-bridge boost converter for photovoltaic DC system," *The Journal of Engineering*, vol. 2019, no. 16, pp. 3007–3011, Mar. 2019, doi: 10.1049/JOE.2018.8507.

[184] R. Fan, X. Zhang, and S. Bai, "A maximum power point tracking method for photovoltaic systems," *Lecture Notes in Electrical Engineering*, vol. 334, pp. 221–228, 2015, doi: 10.1007/978-3-319-13707-0_25/COVER.

[185] "How to Charge a Nissan LEAF | Charging Times | Electric Battery Type." https://www.wolfchasenissan.com/manufacturer-information/nissan-leaf-charging-guide/ (accessed May 20, 2023).

[186] D. D. Tran, H. N. Vu, S. Yu, and W. Choi, "A Novel Soft-Switching Full-Bridge Converter with a Combination of a Secondary Switch and a Nondissipative Snubber," *IEEE Trans Power Electron*, vol. 33, no. 2, pp. 1440–1452, Feb. 2018, doi: 10.1109/TPEL.2017.2688580.

[187] H. Tao, G. Zhang, Z. Zheng, and C. Du, "Design of Digital Control System for DC/DC Converter of On-Board Charger," *J Adv Transp*, vol. 2019, 2019, doi: 10.1155/2019/2467307.

[188] Y. E. Wu and X. Y. Lin, "A Novel Non-Isolated Three-Port Bidirectional DC/DC Converter for Photovoltaic Electric Scooter Charging Stations," *Electronics 2020, Vol. 9, Page 1741*, vol. 9, no. 10, p. 1741, Oct. 2020, doi: 10.3390/ELECTRONICS9101741.

[189] S. M. Shariff, M. S. Alam, F. Ahmad, Y. Rafat, M. S. J. Asghar, and S. Khan, "System Design and Realization of a Solar-Powered Electric Vehicle Charging Station," *IEEE Syst J*, vol. 14, no. 2, pp. 2748–2758, Jun. 2020, doi: 10.1109/JSYST.2019.2931880.

[190] P. Sharon and S. Paul Sathiyan, "Design and simulation of bidirectional converter with flyback and capacitor diode snubbers," *ICIIECS 2015 - 2015 IEEE International Conference on Innovations in Information, Embedded and Communication Systems*, Aug. 2015, doi: 10.1109/ICIIECS.2015.7193245.

[191] P. C. Todd, "Snubber Theory, Design Circuits and Application." https://www.ee.bgu.ac.il/~dcdc/notes/Additional_2012/Snubbers.pdf (accessed May 22, 2023).

[192] A. R. Vaz and F. L. Tofoli, "In-depth analysis of an RCD snubber applied to a DC-DC boost converter," *International Journal of Circuit Theory and Applications*, vol. 49, no. 2, pp. 283–305, Feb. 2021, doi: 10.1002/CTA.2911.

[193] J. S. Yoo, T. Ahn, G. Yu, J. Lee, and J. Lee, "A study on novel active clamp snubber applied DC-DC quasi resonant flyback converter to effectively reduce switch voltage surge," *2017 20th International Conference on Electrical Machines and Systems, ICEMS 2017*, Oct. 2017, doi: 10.1109/ICEMS.2017.8056280.

[194] Z. Yan, J. Zeng, J. Liu, and W. Lin, "A Novel Soft-Switching Bidirectional DC-DC Converter with High Voltage-Gain for Grid-Connected Energy Storage System," *2019 4th IEEE Workshop on the Electronic Grid, eGRID 2019*, Nov. 2019, doi: 10.1109/EGRID48402.2019.9092762.

[195] G. Balbayev, A. Nussibaliyeva, B. Tultaev, E. Dzhunusbekov, G. Yestemessova, and A. Yelemanova, "A novel regenerative snubber circuit for flyback topology converters," *Journal of Vibroengineering*, vol. 22, no. 4, pp. 983–992, Jun. 2020, doi: 10.21595/JVE.2020.20898.

[196] S. M. Tadvin, S. R. Bin Shah, and M. R. T. Hossain, "A Brief Review of Snubber Circuits for Flyback Converter," *2018 3rd International Conference for Convergence in Technology, I2CT 2018*, Nov. 2018, doi: 10.1109/I2CT.2018.8529494.

[197] J. S. Daza O., A. C. Cristancho B., M. Restrepo, and A. Arango-Manrique, "Application software for studying the impact of electric vehicle charging stations in distribution systems," *2021 IEEE PES Innovative Smart Grid Technologies Conference - Latin America, ISGT Latin America 2021*, Sep. 2021, doi: 10.1109/ISGTLATINAMERICA52371.2021.9543084.

[198] "Electric Vehicles – Analysis - IEA." https://www.iea.org/reports/electric-vehicles (accessed May 23, 2023).

[199] B. Grasel, J. Baptista, and M. Tragner, "Supraharmonic and Harmonic Emissions of a Bi-Directional V2G Electric Vehicle Charging Station and Their Impact to the Grid Impedance," *Energies 2022, Vol. 15, Page 2920*, vol. 15, no. 8, p. 2920, Apr. 2022, doi: 10.3390/EN15082920.

[200] S. Paul Sathiyan *et al.*, "Comprehensive Assessment of Electric Vehicle Development, Deployment, and Policy Initiatives to Reduce GHG Emissions: Opportunities and Challenges," *IEEE Access*, vol. 10, pp. 53614–53639, 2022, doi: 10.1109/ACCESS.2022.3175585.

[201] K. Sheng, M. Dibaj, and M. Akrami, "Analysing the Cost-Effectiveness of Charging Stations for Electric Vehicles in the U.K.’s Rural Areas," *World Electric Vehicle Journal 2021, Vol. 12, Page 232*, vol. 12, no. 4, p. 232, Nov. 2021, doi: 10.3390/WEVJ12040232.

[202] S. Mamidala, A. K. Prajapati, and S. Ravada, "Modeling of Buck Converter Charging Station to Improve the Power Quality using Three Phase Single Tuned Harmonic Filter for Electric Transportation," *2022 IEEE 2nd International Conference on Sustainable Energy and Future Electric Transportation, SeFeT 2022*, 2022, doi: 10.1109/SEFET55524.2022.9909306.

[203] Y. Zou, J. Zhao, X. Gao, Y. Chen, and A. Tohidi, "Experimental results of electric vehicles effects on low voltage grids," *J Clean Prod*, vol. 255, p. 120270, May 2020, doi: 10.1016/J.JCLEPRO.2020.120270.

[204] Z. Wang, P. Jochem, and W. Fichtner, "A scenario-based stochastic optimization model for charging scheduling of electric vehicles under uncertainties of vehicle availability and charging demand," *J Clean Prod*, vol. 254, p. 119886, May 2020, doi: 10.1016/J.JCLEPRO.2019.119886.

[205] A. Girard, C. Roberts, F. Simon, and J. Ordoñez, "Solar electricity production and taxi electrical vehicle conversion in Chile," *J Clean Prod*, vol. 210, pp. 1261–1269, Feb. 2019, doi: 10.1016/J.JCLEPRO.2018.11.092.

[206] J. Dave, H. Ergun, and D. Van Hertem, "Incorporating DC Grid Protection, Frequency Stability and Reliability into Offshore DC Grid Planning," *IEEE Transactions on Power Delivery*, vol. 35, no. 6, pp. 2772–2781, Dec. 2020, doi: 10.1109/TPWRD.2020.3011897.

[207] E. C. Mathew and A. Das, "A New Isolated Bidirectional Switched Capacitor DC-DC Converter For Exchanging Power with MVDC Grid," *2022 IEEE IAS Global Conference on Emerging Technologies, GlobConET 2022*, pp. 974–980, 2022, doi: 10.1109/GLOBCONET53749.2022.9872374.

[208] A. Leippi, M. Fleschutz, and M. D. Murphy, "A Review of EV Battery Utilization in Demand Response Considering Battery Degradation in Non-Residential Vehicle-to-Grid Scenarios," *Energies 2022, Vol. 15, Page 3227*, vol. 15, no. 9, p. 3227, Apr. 2022, doi: 10.3390/EN15093227.

[209] G. Sasikumar and A. Sivasangari, “Design and development of solar charging system for electric vehicles: An initiative to achieve green campus,” *Nature Environment and Pollution Technology*, vol. 20, no. 2, pp. 801–804, Jun. 2021, doi: 10.46488/NEPT.2021.V20I02.042.

[210] S. Ayyadi and M. Maaroufi, “Optimal Framework to Maximize the Workplace Charging Station Owner Profit while Compensating Electric Vehicles Users,” *Hindawi Mathematical Problems in Engineering*, vol. 2020, no. Article ID 7086032, pp. 1–12, May 2020, doi: 10.1155/2020/7086032.

[211] Azaroual M, Ouassaid M, and Maaroufi M, “Optimum Energy Flow Management of a Grid-Tied Photovoltaic-Wind-Battery System considering Cost, Reliability, and CO2 Emission,” *International Journal of Photoenergy*, vol. 2021, no. Article ID 5591456, pp. 1–20, Sep. 2021, Accessed: May 23, 2023. [Online]. Available: https://downloads.hindawi.com/journals/ijp/2021/5591456.pdf

[212] R. Liemthong, C. Srithapon, P. K. Ghosh, and R. Chatthaworn, “Home Energy Management Strategy-Based Meta-Heuristic Optimization for Electrical Energy Cost Minimization Considering TOU Tariffs,” *Energies 2022, Vol. 15, Page 537*, vol. 15, no. 2, p. 537, Jan. 2022, doi: 10.3390/EN15020537.

[213] V. T. Tran, M. R. Islam, K. M. Muttaqi, and D. Sutanto, “An Efficient Energy Management Approach for a Solar-Powered EV Battery Charging Facility to Support Distribution Grids,” *IEEE Trans Ind Appl*, vol. 55, no. 6, pp. 6517–6526, Nov. 2019, doi: 10.1109/TIA.2019.2940923.

[214] F. Spertino *et al.*, “A Smart Battery Management System for Photovoltaic Plants in Households Based on Raw Production Forecast” Green Energy Advances. Intech Open, Feb. 20, 2019, doi: 10.5772/INTECHOPEN.80562.

Appendix

Check for updates

Received: 15 January 2021 | Revised: 5 May 2021 | Accepted: 9 May 2021

DOI: 10.1002/est2.255

RESEARCH ARTICLE

ENERGY STORAGE WILEY

Standalone electric vehicle charging station using an isolated bidirectional converter with snubber

Divya Krishnan Nair | **Krishnamachar Prasad** | **Tek T. Lie**

School of Engineering, Computer and Mathematical Sciences, Auckland University of Technology, Auckland, New Zealand

Correspondence
Divya Krishnan Nair, School of Engineering, Computer and Mathematical Sciences, Auckland University of Technology, Auckland, New Zealand.
Email: divya.krishnan.nair@autuni.ac.nz

Abstract

The rise of green technologies in transportation requires electric vehicles (EV) as a prominent solution for reducing greenhouse gas emissions. An off-grid EV charging station plays a significant role in remote regions leading to increased use of EVs. Solar energy promises to be the best solution due to its abundance and simple installation. As solar energy is not constant over a 24-hour period, there is a need for an energy storage unit (ESU) along with a photovoltaic array. In this paper, we present an efficient design approach that uses a fast-charging station with a maximum power point tracking boost converter, a bidirectional DC-DC converter with a snubber circuit, and ESU. The power electronic converters with an active snubber and two capacitive-diode snubbers act as the energy sources that interface with the ESU. The snubber circuits achieve near zero voltage switching and zero current switching for the converter, thus improving overall efficiency. ESU meets the energy demand for EVs when there is insufficient generated solar energy. On the other hand, during the excess generation of solar energy, ESU utilizes this energy to develop an optimal power management system. This results in a green, reliable, and efficient off-grid EV charging station. The proposed method is validated using the MATLAB/Simulink environment to verify system performance.

KEYWORDS

electric vehicles, energy storage unit, off-grid charging station, snubber circuit

1 | INTRODUCTION

Electric vehicles (EVs) guarantee a large-scale reduction of greenhouse gas emissions and fossil fuel depletion issues. Presently, internal combustion engines is the commonly used form to drive the vehicles. However, there is a necessity to find a solution for cars independent of non-renewable energy sources. Therefore, a flexible solution can use electricity generated from solar, wind, nuclear, geothermal, natural gas, and fossil fuels. The transport sector serves as the second-largest contributor to carbon emission and global warming. EVs extract electricity from renewable energy sources resulting in overall emission-free transportation. Although EVs came into existence in the early 20th century, the revolutionary transition from gasoline to EVs occurred in the 21st century due to the increased global concerns regarding climate change and the rising price of crude oil. Nevertheless, numerous challenges obstruct massive-scale adoption of EVs, and one of the significant challenges is the lack of infrastructure for the fast charging of EVs.[1]

Charging EVs requires an adequate number of charging stations with maximum climate benefits, economic

 © 2021 John Wiley & Sons Ltd.

profit, and public acceptance. The electricity produced from renewable energy sources, especially solar energy, makes charging stations active participants in the power market. Therefore, charging from renewable energy sources make EVs entirely free from exhaust gases. Hence, for feeding non-urban and farm areas, a solar-based remote EV charging station, where grid availability is nil, is considered. However, the available power for charging the EVs may be uncertain and unreliable due to the inconsistency of solar irradiance. Hence during the unevenness of solar irradiance conditions, a photovoltaic (PV) source incorporated with an energy storage unit (ESU) needs to be efficiently implemented. During excess power conditions and the absence of EVs, ESU gets charged from solar energy. The power electronic equipment used in the EV charging station is responsible for charging and discharging the ESU. Batteries are essential to back-up power, and a bidirectional DC-DC converter (BDC) used in this system can execute the charging and discharging of ESU.

In previous studies, EV charging stations consisting of bridge-type bidirectional converters have been widely applied.[2] Kumar et al[2] used a bridge-type bidirectional converter where the charging station could not achieve near zero voltage switching (ZVS) and zero current switching (ZCS). Further, the voltage and current stresses on the converter's main switches reduced the EV charging station's overall efficiency. The present work proposes a clean and efficient off-grid EV charging station that includes a BDC with an active snubber and two passive capacitive—diode snubbers. It will be shown that the use of the snubber enables to attain near ZVS and ZCS for the switches on either side of the transformer. This was accomplished by both developing and simulating various EV charging stations for optimized energy extraction. The results obtained from the study support the selection for PV-enabled EV charging stations. In addition, comparisons will be drawn with existing charging facilities and the potential of the off-grid EV charging systems to reduce stresses in the long run, in order to improve the overall efficiency.

2 | ARCHITECTURE OF THE PROPOSED SYSTEM

A block diagram representing the PV-charged EV charging station proposed in this work is shown in Figure 1.

The proposed charging station is typically located in non-urban areas where there are no grid facility provisions. This station uses a PV system with a total capacity of 100 kW, and the maximum power of the PV system is

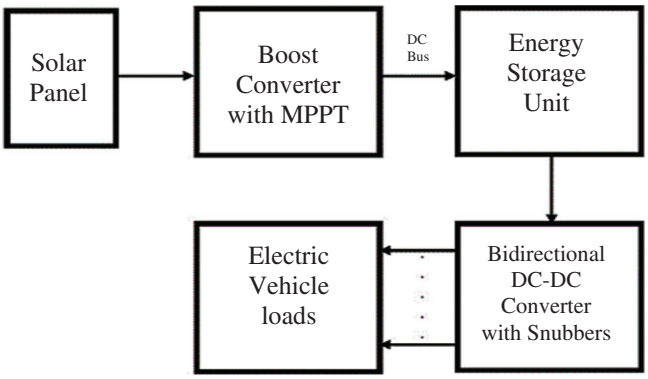

FIGURE 1 Block diagram of the proposed charging station

continuously tracked and fed to the integrated DC bus. Hence, the charging station is a DC microgrid with the generation from the PV system, and the ESU stores the power/energy. The maximum capacity of the proposed ESU is 80 kW. The charging station is connected to the EV load through a BDC with an active and passive snubber circuit. A bidirectional converter controls the total amount of power for charging and discharging the ESU. The modeling of each component of the proposed system is discussed below.

2.1 | Modeling of PV panel with boost converter

In the present scheme, the PV array acts as the primary source of power. The amount of real-time available output power is calibrated before the charging station's simulation. The modeling of output power uses a single diode model of the PV cell.[3] Hence the model utilizes PV module parameters such as solar irradiance (G) and the module temperature (T). The National Renewable Energy Laboratory[4] provides meteorological data to extract the operating parameters of the PV model. A boost converter steps up the PV array voltage to the required DC voltage, and the PV panel is designed to load two EVs.

2.2 | Modeling of ESU

The ESU is commissioned as a back-up option when there is insufficient power from the PV array. A lithium-ion battery pack works as the ESU in the present work. The upper and lower constraints of the state of charge (SOC) are set at 95% and 20%, respectively, to bypass the over-charging and over-discharging of the battery pack, such that

$$SOCL \leq SOC \leq SOC \quad (1)$$

where SOCL is the lower SOC limit value of 20% and SOCU is the upper SOC limit of 95%. The battery pack charges the PV array until the SOC reaches the upper limit (SOCU) of 95%, whereas the ESU supplies the energy for EV charging till the lower limit (SOCL) of SOC of 20%. In the proposed work, SOC is initially assumed to be a random value between SOCL and SOCU and gradually updated as the charging process continues. The estimation of obtainable energy within the battery pack is obtained from the SOC of the ESU. ESU can deliver the energy to EV load when the current SOC is higher than SOCL.[5]

2.3 | Modeling of BDC with snubber circuit

ESU discharges when the EV loads are connected. There are two charging units, and each charging unit functions as a current source to regulate the EV charging current. Thus, a current control strategy is utilized for the charging and discharging of ESU. The bidirectional converter uses the buck mode while the ESU is charging, whereas boost mode is used when the ESU discharges and supplies the power needed for the EV loads. An active snubber and two passive capacitor-diode snubbers with the BDC can reduce the high current and high voltage stress occurring at the converter's main switches during turn-on or turn-off transitions.[6] This bidirectional converter model with the snubber circuits can achieve ZVS and ZCS on either side, thereby significantly improving system reliability. Figure 2 shows the implementation of the overall arrangement.

The converter consists of a current-fed bridge, an active snubber circuit at the low-voltage side, a voltage-fed bridge and passive snubber pair at the high voltage side. Inductor L performs the output filtering when power flows from the high voltage side to the low voltage side, denoted as a buck operation. On the other hand, it works in the boost operation when power is transferred from the low-voltage side to the high voltage side. The active snubber recycles the absorbed energy stored in the snubber capacitor C, and it also clamps the voltage to a value slightly higher than the voltage across the low side of the transformer. The current stress across the main switches can be reduced under heavy load conditions as the snubber current cannot circulate through the main switches.

In boost mode, first of all, switches S, M_1, and M_4 are turned on and M_2 and M_3 are turned off. The energy stored in the inductor and clamp capacitor is discharged to the output. Then S is switched off suddenly making the transformer leakage current higher than inductive current, i_L. The surplus current discharges the capacitor across the clamp branch and switches M_2 and M_3, resulting in clamp branch voltage resonating down to zero. When the transformer current becomes equal to i_L, the switches M_2 and M_3 are turned on with ZVS

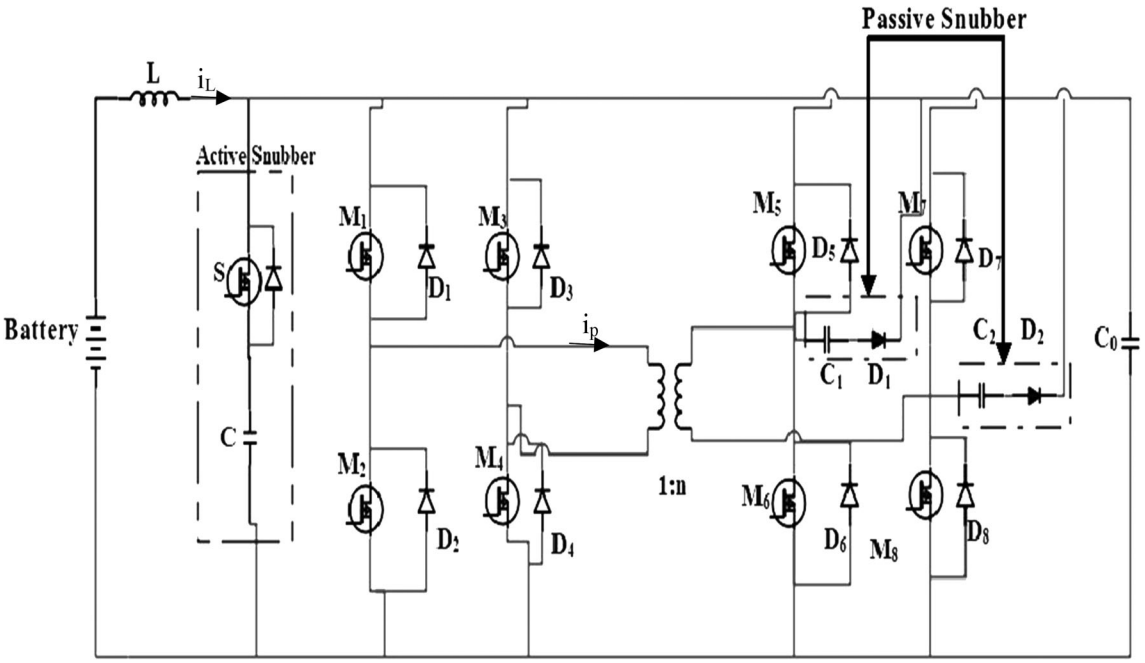

FIGURE 2 Bidirectional DC-DC converter with a combination of active and passive snubber circuits

characteristics as a result of antiparallel diodes that are conducting. With all the switches on and transformer current drops to zero, the inductor L gets charged. Next, the switches M_1 and M_4 are turned off, and inductive current charges the clamp branch voltage until the clamping capacitor clamps it. The voltage difference between the clamp capacitor and the reflected output voltage is exerted on the transformer's leakage inductance. Clamp switch, S, is turned off and it initiates the next half-cycle of operation.

Now the switch M_5, which is already in buck mode, allows the load current to be freewheeling on the current fed bridge. The switch M_8 is turned on and the output voltage is fed to the transformer. As the other side of the transformer is shorted, the whole voltage is exerted on the leakage inductance and causes the current to rise. With the transformer current increasing linearly to the load current, the voltage across the transformer terminals on the low voltage side changes immediately to the reflected voltage from the high voltage side. Once the transformer current reaches the load current, clamp branch voltage rises to the reflected voltage. The clamp switch's antiparallel diode starts to conduct the resonant current between the leakage inductance and clamping capacitor, which charges the inductor L. Now M_5 gets turned off. D_7 then starts to conduct the freewheeling leakage current.

Meanwhile, the clamp branch voltage is held high as the switch S is turned on. This reflected voltage at the transformer terminals of the voltage fed side is exerted on the leakage inductance, making the current fall. Then M_7 conducts with ZVS. D_1 and D_2 start to reverse block and prevent leakage current from going into the other direction. The clamp branch increases the load current. Now S is turned off and clamp branch voltage drops immediately to zero. There is no current freewheeling on the high voltage side during this time and M_8 is turned off with complete ZCS. Subsequently, M_7 is turned on and the circuit assumes the same operation as in the previous half-cycle. The voltage on the transformer reverses its polarity to exercise flux balance.[6,7]

The snubber capacitor C absorbs the current difference between the current fed inductor current and the leakage inductance current of the isolation transformer during switching commutation. Additionally, the active snubber provides the initial charge to the capacitor's high-voltage side to avoid any inrush current during the start-up period. But the high-voltage side switches experience a hard switching turn-off in step-down mode. Therefore, two passive capacitive-diode snubbers are connected in parallel with the voltage-fed bridge. Thus, the main switches operate near ZVS and ZCS turn-off transitions. The active snubber transfers the energy stored in the snubber capacitor C to buffer capacitors C1 and C2. Hence, the snubber capacitor voltage drops to zero. Thus, the voltage stresses of the switches M_1-M_4 can be limited to a lower level, achieving near ZCS turn-off. For alleviating the leakage inductance effect on the voltage spike, high-voltage side switches are operated with phase-shift control, achieving ZVS turn-on features. With two capacitor-diode snubbers, high-voltage side switches achieve near ZVS turn-off characteristics.[6]

The switching condition of the proposed converter is illustrated in Table 1. It is clear from the table that all switches achieve ZVS turn-on features for the proposed converter. It is also evident that the switches M1-M4 achieve ZCS turn-on characteristics, whereas switches M5-M8 achieve ZCS turn-off features.

The inductor is designed large enough to restrain the exciting current and reduce the transformer loss determined by the following equation,

$$l_r = \frac{I_{in} \times {}^{V_0}/_{n}}{t_d} \tag{2}$$

where l_r is the critical point of leakage inductance to attain ZVS and t_d is the dead time considered as 500 ns.

The voltage stress on the rectifier diodes is the output voltage, and the voltage stress on the primary side switches of the proposed converter is the reflecting output voltage $({}^{V_0}/_{n})$. Inductors are not commercially available readymade for these power levels and they must be designed for this application. The maximum discharging current is assumed to be 2 A.[7] The allowed ripple is about 10% of the maximum discharging current. Therefore, inductor is given by

$$L = \frac{[|V_{bat} - V_c|(1-D)T_s]}{\Delta i_L} \tag{3}$$

where duty cycle is $D = \frac{2\Delta t}{T_s}$,

Δt is the time during which the primary side of the voltage across the transformer is equal to $\pm V_i$ and T_s is the period of the driving signal for each bridge switch. The leakage inductance and the output capacitor provide a resonant transition switching which creates a large ringing voltage spike across the switches. The ringing will

TABLE 1 Switching condition of proposed converter

Switches	ZVS turn ON	ZCS turn ON	ZCS turn OFF
M1-M4	Yes	Yes	No
S	Yes	No	No
M5-M8	Yes	No	Yes

Abbreviations: ZCS, zero current switching; ZVS, zero voltage switching.

be well damped by using a snubber resistor equal to the ringing's characteristic impedance. The snubber capacitor is used to minimize dissipation at the switching frequency while allowing the resistor to be effective at the ringing frequency. The best design point to start with is the capacitor's impedance at the ringing frequency equal to the resistor value.

$$\text{Clamping capacitor}, C \geq \frac{(T_s/4\pi)^2}{L_k} \tag{4}$$

Transformer turns the formula gives the ratio as

$$\frac{N_p}{N_s} = \frac{V_i}{V_0} \tag{5}$$

T_{DR} is the conducting time of rectifier diode given by,

$$T_{DR} = \frac{V_{in}}{2f_s V_0/n} \tag{6}$$

where f_s is the switching frequency and the duty ratio, D_{clamp} calculated as

$$\left(1 - D_{clamp}\right)T + \frac{2I_{in} \times l_r}{V_0/n} = T_{DR} \tag{7}$$

2.4 | Modeling of EV load demand

It is essential to expand the power demand model of EV to avoid damage to the batteries. Hence, we assume that an 80% SOC of full battery capacity at departure time has to be achieved, and the EV battery should not be over-discharged. Therefore, on attaining a SOC of 10% of rated battery capacity, EV stops utilizing the EV battery's electric energy. On achieving SOC of 70% of total battery capacity during the next charging from ESU, the EV starts using electric energy.[8] The calculation of EV power demand is described by the equation

$$P_{EV_i} = P_{EV_{req}} \times S_i \times w_i \tag{8}$$

where P_{EV_i} is the demand of EV power at time slot i in kW, $P_{EV_{req}}$ is the maximum required EV power in kW at the time of plug-in, corresponding to the maximum SOC difference (80%) and current SOC_0. S_i is the EV connectivity status at time slot i, and w_i, the EV charging status at time slot i. The required EV power, $P_{EV_{req}}$ is calculated as

$$P_{EV_{req}} = (SOCU - SOC_0) \times C_{battery} \tag{9}$$

where SOCU is the maximum SOC required by each EV and $C_{battery}$ is the EV battery capacitance.[8]

3 | CONTROL AND FORMULATION OF THE PROPOSED SYSTEM

The proposed work presents a PV array delivering a maximum of 100 kW at a solar irradiance of 1000 W/m^2 and a temperature of 40°C. This PV block consists of 64 parallel strings, each having 5 SunPower SPR-315E modules in series. The PV array output is connected to the boost converter and then to a common DC bus of 400 V. DC-DC converter control uses the maximum power point technique (MPPT), especially the "Perturb and Observe" technique,[9] to attain maximum power by varying the voltage across the PV array terminal. The ESU consisting of the lithium-ion battery inputs the energy from the boost converter with MPPT through the common DC bus. The battery SOC limits are always maintained within the 20% to 95% range to extend its life cycle. The following operational ESU scenarios are possible.

- *Scenario 1*: $E_{PV} > E_{TOT}$ and $SOC_{ESU} \geq \max SOC_{ESU}$
  With the solar energy E_{PV}, EVs get charged, but when SOC_{ESU} reaches its maximum, ESU gets disconnected from the DC bus for the power balance. E_{TOT} is the total energy capacity of all the connected EVs.
- *Scenario 2*: $E_{PV} > E_{TOT}$ and $SOC_{ESU} < \max SOC_{ESU}$
  If the delivered solar energy E_{PV} is more than the required energy capacity of all the connected EVs (E_{TOT}), EVs get charged from the solar energy. If the current SOC of the charging station battery is lower than its maximum SOC, the additional power from solar energy is used to charge the ESU by connecting to its bus.
- *Scenario 3*: $E_{PV} \leq E_{TOT}$ and $SOC_{ESU} > \min SOC_{ESU}$
  During the night or rainy/cloudy conditions, when there is no or reduced solar output, ESU supplies the energy for charging the EVs in the charging station by maintaining the minimum SOC in the battery.

The BDC with the snubber circuits helps charge or discharge the ESU. An isolated BDC with snubber circuits at a switching frequency of 50 kHz acts as the charging unit. The battery provides nominal input voltage, and the EV voltage is in the range of 250 to 450 V.

The EV current is within the range of 200 to 500 A. Each of the two charging units interfaces an EV with the DC bus. Each charging unit operates as a current source to control EV charging to balance the power supply with the power demand; thus, the DC-DC converter feeds energy to the EV loads when they are connected to the charging station.

For the ideal case, assuming a charging current of 11 A, the charging time of the 100 Ah battery is 9.09 hours. For example, the Nissan Leaf Acenta Auto model with 40kWh battery capacity can have a charging time between 29 minutes and 5 hours depending on whether it uses a DC rapid charger or fast charger at a public charging station.[10] Based on the assumed scenarios, the performance of the proposed charging station is analyzed. The characteristics and analysis of the station during each considered scenario is discussed and described in below section.

4 | SIMULATION RESULTS

The proposed PV based off-grid EV charging station consists of 100kWh solar generation to charge EV battery of 40kWh capacity and ESU of 80 kWh capacity. ESU acts as an auxiliary supply to the EV batteries during low solar generation and saves power at the peak generation of solar energy. The simulation study of the proposed charging station is carried out using MATLAB/Simulink by considering three cases of EV requirements—EVs are charged (a) with the PV array only, (b) with both PV array and ESU, and (c) with the ESU only. The performance of ESU and solar generation varies with the increase or decrease in the power demand. The maximum power point (MPP) is 96.24 kW at 1000 W/m^2 solar irradiance and 40°C temperature.

The DC-link voltage is usually more than the voltage levels of the batteries. Thus, the BDC comes into practical use to charge/discharge the batteries in the EVs and charging stations. The proposed converter performance, with and without snubber circuits, is compared. The voltage waveform of the transformer's primary side of the BDC is shown in Figure 3. A parasitic ringing with voltage spikes are seen in the BDC without snubber. These voltage spikes can damage the diodes. When the proposed snubber circuits are implemented with BDC, the voltage is clamped at the desired level. This helps in selecting smaller rating diodes and can lead to an increased lifetime of the diodes compared to BDC without a snubber circuit.[11]

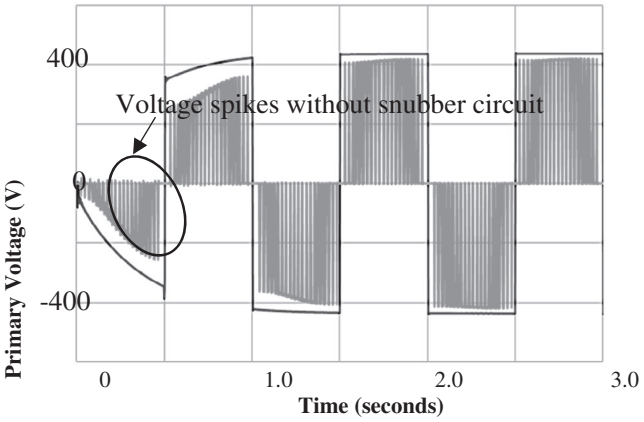

FIGURE 3 Voltage across the primary side of the transformer of the proposed bidirectional DC-DC converter (BDC)

4.1 | Charging of EV with the PV array only

Figure 4 shows the solar irradiance graph for generating the solar irradiance test data at 1000 W/m^2 and the PV panel's power response curve. In this particular scenario, the EV batteries get charged only from solar power. The constant DC voltage provides the required terminal voltage to the EV loads continuously. Figure 5 shows the SOC of EV load and the EV load's power response curve with the BDC with and without snubber circuits. The power response curve of BDC with snubber circuit shows that it obtains the designed output power based on the available solar irradiance. This converter can also clamp the voltage and remove the voltage spikes, thus improving the converter's lifecycle and increase overall efficiency.[11]

4.2 | Charging of EV with both PV array and ESU

This particular scenario works when solar energy adequately charges the connected EV loads and ESU. In practical applications, the excess solar energy gets utilized for residential or commercial applications. When the PV generation is not sufficient to meet the EV charging demand, ESU starts discharging the stored energy and feeds to the EV battery, thus providing continuous charging of the EV battery. The charging and discharging of ESU is possible because of the BDC with snubber circuits. Figure 6 shows the response curves for ESU and SOC. Figure 7 shows the EV load's power response curve, with the BDC, with and without snubber circuits. The

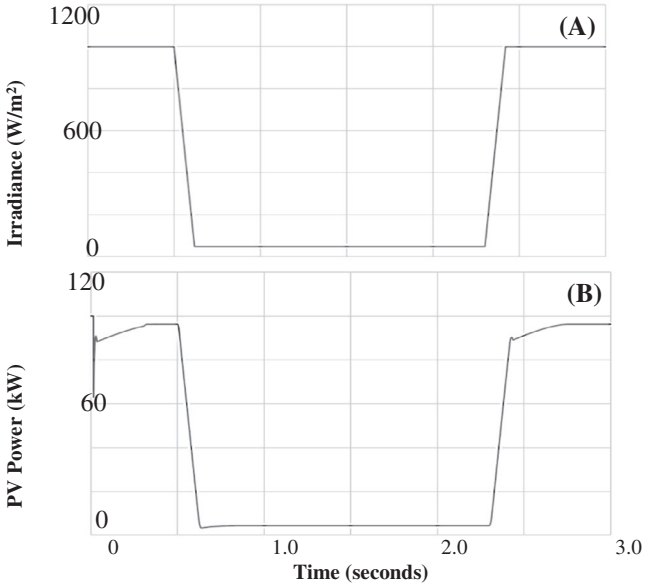

FIGURE 4 A, Solar irradiance data used for generating the test data and B, power response curve of photovoltaic (PV)

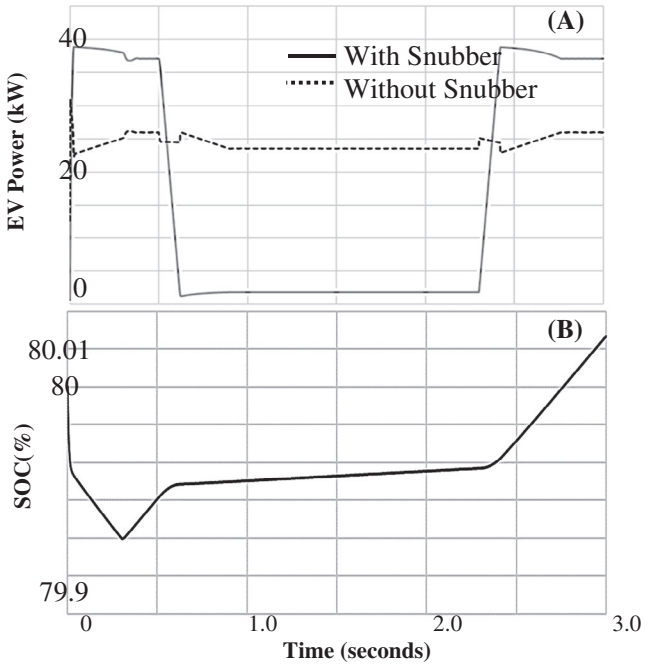

FIGURE 5 A, Power response curve for electric vehicles (EV) load with and without snubber circuit and B, state of charge (SOC) of EV load

output power ringing in the power response curve of EV load attenuates more rapidly for fewer seconds when the BDC without snubber circuit is used. This ringing or surge attributes minimum efficiency for the EV charging station. This can be eliminated when the BDC with active and passive snubbers are implemented, thus obtaining a

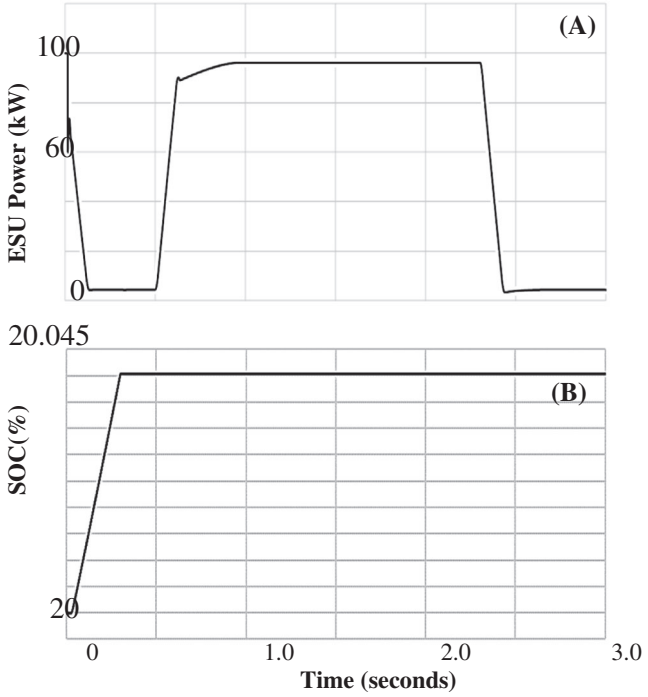

FIGURE 6 A, Power response curve of energy storage unit (ESU) and B, state of charge (SOC) response of electric vehicles (EV) load

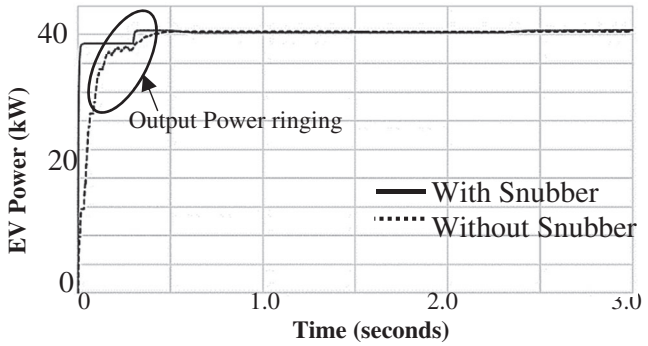

FIGURE 7 Power response curve of electric vehicles (EV) load with and without snubber circuits

smooth output power as depicted in Figure 7. The worst-case scenario is during the complete absence of solar generation. In such a case, ESU alone should meet the energy demand for the EV load.

4.3 | Charging of EV with the ESU only

This scenario presents the charging of EV loads from ESU only. At this condition, the power for the EV loads is fed only from ESU. ESU starts discharging the stored energy to the load providing a continuous supply of

energy. Figure 8 shows the power response curves of the PV and SOC response of the EV load. Figure 9 shows the power response curve of EV load with and without snubber circuits and the ESU response. This scenario also shows an output power ringing when the BDC without snubber circuits are used. The BDC with active and passive snubber circuit eliminates the ringing, thus improving the converter's lifecycle and improving the EV charging station's overall efficiency.

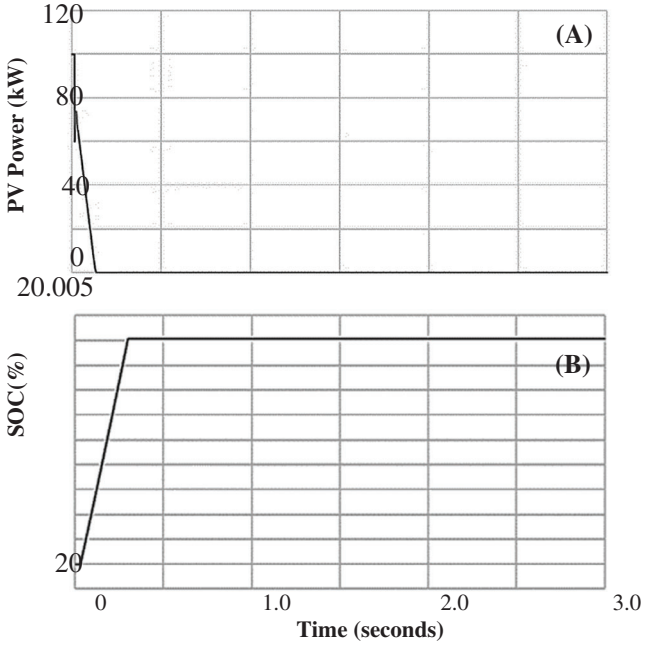

FIGURE 8 A, Power response curve for photovoltaic (PV) and B, state of charge (SOC) response of electric vehicles (EV) load

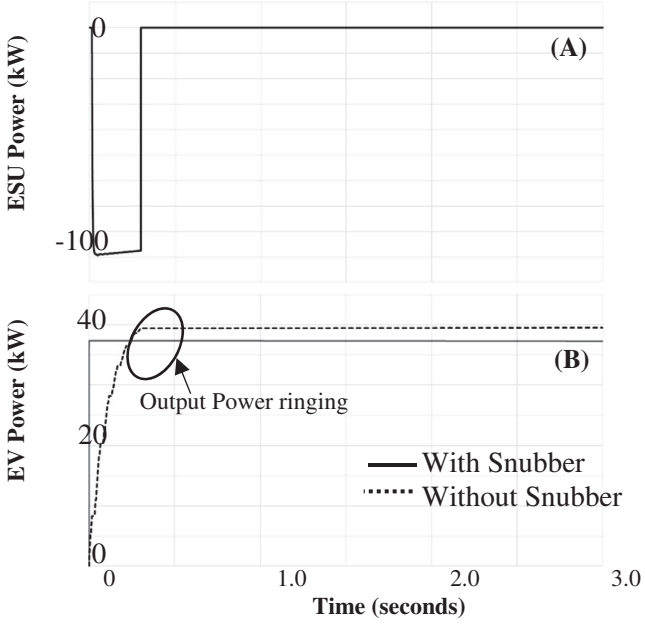

FIGURE 9 A, Power response curves of energy storage unit (ESU) and B, electric vehicles (EV) load using bidirectional DC-DC converter (BDC) with and without snubber circuits

These scenarios demonstrate that the proposed off-grid EV charging station based on PV generation is competent for charging the EVs under any circumstance. The use of snubber circuits in the BDC also implies a maximum energy-efficient charging station and the system is protected from high voltage and high current stresses. The efficiency curve is obtained by maintaining the input voltage constant. Figure 10 shows the efficiency curves for the inductor current variation ranges from 5 to 30 A with a fixed value of input voltage of 400 V. The maximum efficiency secured by the BDC without a snubber circuit is ~88.7%, whereas the maximum efficiency of the BDC with the snubber circuit is ~92%. Thus, the BDC with active and passive snubber circuit obtains higher efficiency compared to BDC without snubber circuits.

A comparative analysis between different converter topologies for DC fast chargers is shown in Table 2. As it can be observed from Table 2 the most of the topology described is bidirectional, provides grid support and employs battery storage. Therefore choosing the most suitable topology is a compromise between other factors such as the realization of ZVS and ZCS, number of passive components, conduction losses and complexity. Non-isolated three-port BDC is the least complex among all the converters. It requires fewer diodes/switches than all the other converters due to the dissipative energy element, and it offers low efficiency. Compared to all the other converters, the proposed converter offers and realizes both ZVS and ZCS. Circulating current causes conduction losses in the system. However, the proposed converter reduces the circulating current and voltage spike at a particular level.

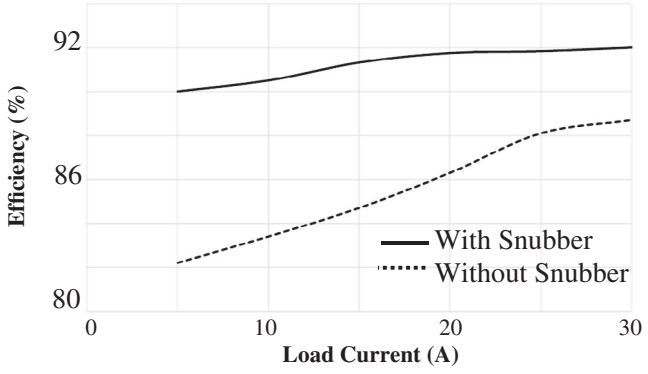

FIGURE 10 Plot of conversion efficiency of the proposed converter

TABLE 2 Comparative analysis between different converter topologies for DC fast chargers

References	[12]	[13]	[2]	Proposed converter
DC-DC Converter	Phase-shift full-bridge unidirectional DC-DC converter	Non-isolated three-port bidirectional DC-DC converter	Non-isolated bidirectional DC-DC converter	Isolated bidirectional DC-DC converter with active and passive snubber
Use of snubber circuit	Clamp diode at primary side	No	No	Active clamp snubber circuit at LV side and passive snubber circuits at HV side
Grid support	Yes	Yes	No	No
RES Integration	No	Yes	Yes	Yes
BES Integration	No	Yes	Yes	Yes
Number of switches/ diodes/ capacitors	8/1/7	3/1/3	7/1/3	8/2/4
Conduction loss	High	High	High	Low
Realization of ZVS and ZCS	ZVS	Near ZVS	No	Both ZVS and ZCS
Complexity	Very high	Low	High	Medium
Features	Due to the presence of circulating current, conduction loss is high Low efficiency at light load conditions	Due to the presence of circulating current, conduction loss is high	Due to the presence of circulating current, conduction loss is high	Low conduction loss using the snubber circuit Less switching stress

Abbreviations: ZCS, zero current switching; ZVS, zero voltage switching.

Kumar et al[2] proposed an off-grid EV charging station capable of charging the EV battery under any circumstance and using renewable energy resources to their maximum extent., The system was able to minimize the grid burden. However, they did not show results on the elimination of any voltage stress developed at the BDC used in the charging station. These stresses reduce the overall efficiency of the converter. By employing an additional active snubber circuit, the converter in the present work has the following advantages: (a) ZVS turn on for the main switches of the converter and the elimination of the reverse recovery problem, (b) No conduction losses, (c) No duty cycle loss caused by the energy transfer of the clamp capacitor, (d) Higher efficiency, and (e) Simple switching and control scheme.

Figure 11 shows that the clamp branch voltage obtained with an active clamp snubber for the BDC provides a zero voltage within 4 to 6 seconds. The stresses are eliminated with the implementation of a snubber. ZVS characteristics make the converter in the present work effectively reduce the losses and increase the EV charging station power.

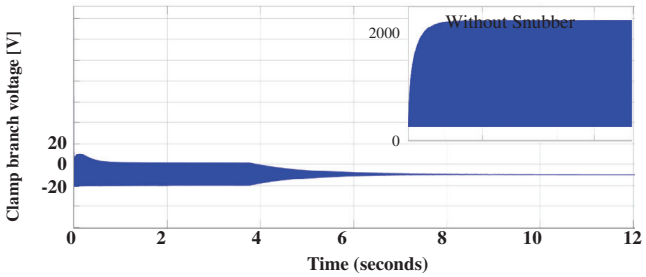

FIGURE 11 Clamp branch voltage of bidirectional converter with active clamp snubber (inset shows the clamp branch voltage without snubber)

5 | CONCLUSION

We have developed a standalone EV charging station based on PV generation and have validated it through MATLAB/Simulink simulation. An isolated BDC configuration with a combination of active and passive snubber circuits stands between the EV and ESU. The proposed isolated BDC with active and passive snubber circuit

successfully overcomes the problems encountered with classical techniques and offers an effective solution to minimize circulating current issues and voltage spikes. The active clamp and passive snubber used in the converter in the present work reduce the spikes at the primary side of the transformer and rapidly attain ZVS and ZCS characteristics. Compared to the existing topology of an off-grid EV charging station, the proposed converter with a snubber circuit reduces the stresses across the main switches, yielding an increase in efficiency. The combination of active and passive snubbers with BDC and an additional energy storage device provides an excellent option for PV-dependent EV charging stations with a conversion efficiency of 92%. The proposed EV charging station also minimizes the grid burden and improves its utilization in remote areas. The PV array and the ESU suitably supply the power to the EV loads depending on or absence or reduced solar energy. The end result is a more ecological and energy-efficient PV-based EV charging station.

DATA AVAILABILITY STATEMENT

The data that support the findings of this study are available on request from the corresponding author. The data are not publicly available due to privacy or ethical restrictions.

ORCID

Divya Krishnan Nair https://orcid.org/0000-0001-7416-4188

REFERENCES

1. Nour M, Chaves-Ávila JP, Magdy G, Sánchez-Miralles Á. Review of positive and negative impacts of electric vehicles charging on electric power systems. *Energies*. 2020;13(18):4675-4709. https://doi.org/10.3390/en13184675.
2. Kumar V, Teja VR, Singh M, Mishra S. PV based off-grid charging station for electric vehicle. *IFAC-PapersOnLine*. 2019;52(4):276-281. https://doi.org/10.1016/j.ifacol.2019.08.211.
3. Saxena N, Hussain I, Singh B, Vyas AL. Implementation of a grid-integrated PV-battery system for residential and electrical vehicle applications. *IEEE Trans Ind Electron*. 2018;65(8):6592-6601. https://doi.org/10.1109/TIE.2017.2739712.
4. National Renewable Energy Laboratory (NREL) Home Page | NREL. https://www.nrel.gov/. Accessed December 30, 2020.
5. Garcia-Trivino P, Fernandez-Ramirez LM, Torreglosa JP, Jurado F. Control of electric vehicles fast charging station supplied by PV/energy storage system/grid. Paper presented at: 2016 IEEE International Energy Conference (ENERGYCON); July 2016. https://doi.org/10.1109/ENERGYCON.2016.7514120.
6. Wu TF, Yang JG, Kuo CL, Sun KH, Chen YK. Comparison of bidirectional isolated full-bridge converters with combinations of active and passive snubbers. Paper presented at: Proceeedings of IEEE Energy Conversion Congress and Exposition: Energy Conversion Innovation for a Clean Energy Future. ECCE 2011; 2011:127-133. https://doi.org/10.1109/ECCE.2011.6063759.
7. Liu J, Zheng Z, Wang K, Li YD. Comparison of boost and LLC converter and activew clamp isolated full-bridge boost converter for photovoltaic DC system. *Inst Eng Technol Int J*. 2019;2019(16):3007-3011. https://doi.org/10.1049/joe.2018.8507.
8. Khan W, Ahmad F, Alam MS. Fast EV charging station integration with grid ensuring optimal and quality power exchange. *Eng Sci Technol Int J*. 2019;22(1):143-152. https://doi.org/10.1016/j.jestch.2018.08.005.
9. Fan R, Zhang X, Bai S. A maximum power point tracking method for photovoltaic systems. *Lect Notes Electr Eng*. 2015;334:221-228. https://doi.org/10.1007/978-3-319-13707-0_25.
10. Nissan Leaf Charging Guide - How to charge a Nissan Leaf. https://www.zap-map.com/charge-points/nissan-leaf-charging-guide/. Accessed December 30, 2020.
11. Tran DD, Vu HN, Yu S, Choi W. A novel soft-switching full-bridge converter with a combination of a secondary switch and a nondissipative snubber. *IEEE Trans Power Electron*. 2018;33(2):1440-1452. https://doi.org/10.1109/TPEL.2017.2688580.
12. Tao H, Zhang G, Zheng Z, Du C. Design of digital control system for DC/DC converter of on-board charger. *J Adv Transport*. 2019;2019:2019-2019. https://doi.org/10.1155/2019/2467307.
13. Wu Y-E, Lin X-Y. A novel non-isolated three-port bidirectional DC/DC converter for photovoltaic electric scooter charging stations. *Electronics*. 2020;9(10):1741. https://doi.org/10.3390/electronics9101741.

How to cite this article: Krishnan Nair D, Prasad K, Lie TT. Standalone electric vehicle charging station using an isolated bidirectional converter with snubber. *Energy Storage*. 2021;3(5):e255. https://doi.org/10.1002/est2.255

energies

MDPI

Article

Implementation of Snubber Circuits in a PV-Based Off-Grid Electric Vehicle Charging Station—Comparative Case Studies

Divya Krishnan Nair *, Krishnamachar Prasad and Tek Tjing Lie

School of Engineering, Computer and Mathematical Sciences, Auckland University of Technology, 1010 Auckland, New Zealand; krishnamachar.prasad@aut.ac.nz (K.P.); tek.lie@aut.ac.nz (T.T.L.)
* Correspondence: divya.krishnan.nair@autuni.ac.nz

Abstract: With the penetration of electric vehicles (EVs), there have been paradigm shifts in the transportation sector. EVs are ideally considered to be clean and eco-friendly, but they can overload the existing grid infrastructure and significantly contribute towards carbon emissions depending on the source of charging. The ideal solution is to develop a charging infrastructure for EVs that is integrated with solar energy technology. This paper presents the design of a zero-voltage switching snubber-based bidirectional converter for an off-grid charging station for EVs. The proposed system includes a solar array with a boost converter, a bidirectional converter with snubber circuits and an energy storage unit. A comprehensive comparison between various types of snubbers, such as the resistive capacitive diode snubber, active clamp snubber and flyback snubber, is presented. This type of system configuration clamps the rail voltage, due to the difference in current between leakage inductance and low voltage side-fed inductor currents, resulting in reduced current spikes at the converter's switches. Such a converter, therefore, leads to higher efficiency of the charging station for EVs. The design of a snubber-based off-grid charging station for EVs is formulated and validated in the MATLAB/Simulink environment.

Keywords: resistive capacitive diode snubber; active clamp snubber; flyback snubber; bidirectional converter; off-grid charging station

check for updates

Citation: Krishnan Nair, D.; Prasad, K.; Lie, T.T. Implementation of Snubber Circuits in a PV-Based Off-Grid Electric Vehicle Charging Station—Comparative Case Studies. *Energies* **2021**, *14*, 5853. https://doi.org/10.3390/en14185853

Academic Editors: Islam Safak Bayram and Enrique Romero-Cadaval

Received: 26 June 2021
Accepted: 14 September 2021
Published: 16 September 2021

Publisher's Note: MDPI stays neutral with regard to jurisdictional claims in published maps and institutional affiliations.

Copyright: © 2021 by the authors. Licensee MDPI, Basel, Switzerland. This article is an open access article distributed under the terms and conditions of the Creative Commons Attribution (CC BY) license (https://creativecommons.org/licenses/by/4.0/).

1. Introduction

Electric vehicles (EVs) are more environmentally friendly than the current internal combustion engine (ICE) vehicles, as they have the potential to dramatically reduce greenhouse gases and global warming. The electrification of transport sector promotes sustainable energy development. Even though EVs may not emit CO_2 or other noxious gases when in use, they create a burden on the grid. Therefore, the coupling between the photovoltaics (PV) and charging stations for EVs is beneficial, as it allows greater usage of both EVs and solar energy without interrupting the grid's capacity and provides better power quality. The solar-based charging station is primarily applicable on highways and remote locations to successfully charge EVs [1]. Kumar et al. [2] proposed a PV-based off-grid charging station in which the solar source is coupled with an energy storage unit (ESU) efficiently for variable irradiance conditions. The system enhances the reliability of the off-grid charging station for EVs. However, they used a non-isolated bidirectional converter with no capability of attaining zero-voltage switching (ZVS) characteristics. This is likely to result in a decrease in the overall efficiency of the charging station. Therefore, in this paper, we present a bidirectional DC–DC converter (BDC) with snubber circuits and demonstrate that a near ZVS across BDC switches is achieved for an off-grid charging station for EVs. This is expected to yield a higher efficiency PV-based charging station for EVs.

Since EVs are operated at low voltage levels, there is a need for an interface between the BDC and the charging station. Isolated BDC offers many advantages over non-isolated

BDC: for example, bidirectional energy flow, electrical isolation, high reliability, etc. This BDC will be used for both stepping up and stepping down the voltage. Thus, charging and discharging can be combined in one circuit topology. Moreover, a full-bridge BDC is popular, due to its high power-handling capacity. However, the leakage inductance of the isolation transformer will result in high voltage and current spikes during switching transitions.

Additionally, the freewheeling current increases the conduction losses and reduce the effective duty cycle, due to the effect of leakage inductance. An alternative method is to charge the leakage inductance to the current level of the current-fed inductor, thereby reducing the current difference as well as reducing the voltage and current spikes. However, it is difficult to tune the switching diagram to match these two currents, as the current level varies with the load conditions [3].

The aforementioned problems can be overcome by using different types of snubber circuits. The snubber circuits provide an alternate path for the circulating current across BDC switches. The snubber is used to control the effect of the reactance of the circuit. It improves the switching circuit's performance overall. The snubber absorbs the energy from the reactive elements in the circuit. As a result, the stress across the switch is reduced. This automatically increases the converter's reliability [4,5]. Snubbers may be either passive or active networks. Passive snubbers are made of resistors, inductors, capacitors, or diodes, whereas active snubbers use transistors or other types of active switching elements. A conventional passive approach is to employ a resistive capacitive diode (RCD) snubber to clamp the voltage and the resistor limits the capacitor discharge current. The active clamped snubber used for BDC recycles the energy stored in the leakage inductance, thereby improving the converter efficiency. Another type of snubber is a flyback snubber in which the voltage spike across the switches gets clamped by a capacitor-diode circuit and is recovered. This snubber also provides an effective solution to reduce the circulating current across the BDC switches [6].

The implementation and benefits of snubber based BDCs in EVs were reported in the recent past [6,7]. However, there are negligible data on the use of snubber based BDCs for use in off-grid charging stations for EVs. Kumar et al. [2] described a standalone charging station, but this station does not use any snubber circuit. In the previous study [3], the beneficial effects of using a flyback snubber were reported. However, a systematic comparison of the performance of the off-grid EVs charging station with various available snubber circuit configurations was not performed. Hence, in this paper, RCD, active clamp, and flyback snubbers for the BDC in terms of the overall performance off-grid charging station for EVs are compared. Such a study was carried out on the BDCs in EVs which operate at low-voltage levels only [6,7]. However, there have been no reported results on either off-grid or grid-connected charging stations for EVs. In this paper, the proposed configuration of BDC with snubber circuits effectively reduces the impact of circulating current on the main switches, thereby effectively clamping the voltage spikes across the switches. This leads to an improved performance of the off-grid charging station for EVs. Furthermore, it is cheaper and cost-effective to have just one snubber circuit in the charging station instead of having one in each electric vehicle. Hence, a study of the performance of charging stations for EVs with various snubber circuit configurations is both meaningful and important.

2. Analyses of the Snubbers

The BDC used in [2] consists of a voltage source as a DC link capacitor and MOSFET switches for step-up and step-down modes. The load source is inductive, as the converter is a voltage source. When the switch's state changes from turn-off or turn-on, the time lapse for transition can cause an overvoltage condition. Additionally, due to the reverse recovery of the free-wheeling diode, the switches show a current spike at turn-on, leading to high switching losses, especially at turn-off. These problems can be minimized/eliminated with the introduction of snubber circuits.

The proposed system [2] consists of a BDC model, which operates both in charging (buck) and discharging (boost) modes as shown in Figure 1. In the charging mode, DC-link acts as an input of BDC and the battery acts as a load on the output side. The battery's voltage level is achieved at the output side when BDC operates in buck mode with component as an inductor (L_{buck}). This value is calculated as follows:

$$L_{buck} = \frac{[|V_{DC} - V_{bat}|(1 - D)]}{\Delta i_L f_s} \quad (1)$$

where Δi_L and f_s are the ripple current switching frequency of the buck mode, respectively. V_{DC} and V_{bat} are input and output voltages of the bidirectional converter, respectively, and D is the converter's duty ratio.

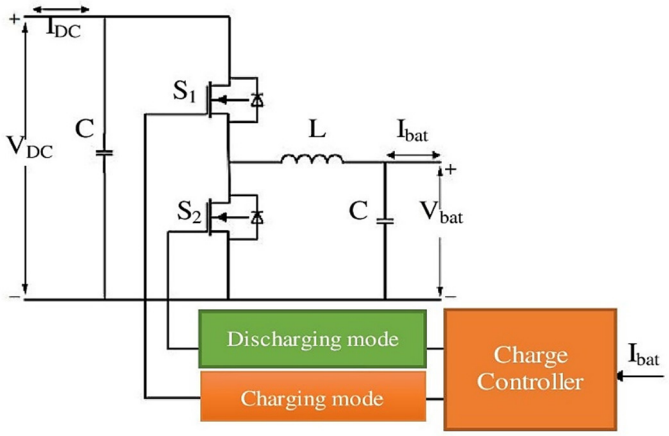

Figure 1. Circuit diagram of the bidirectional converter [2].

In the discharging mode, the battery is connected as an input and DC-link connected as the output and the DC-link voltage is more than the battery terminal voltage. The component inductor (L_{boost}) in boost mode is calculated as follows:

$$L_{boost} = \frac{V_{bat} D}{\Delta i_L f_s} \quad (2)$$

Since the BDC is operating in both boost and buck modes, the value of L is chosen as follows:

$$L = \max(L_{buck},\ L_{boost}) \quad (3)$$

For comparison, the converters with an RCD passive snubber, an active clamping circuit, and a flyback snubber were simulated.

2.1. RCD Snubber

RCD snubber or RCD clamp limits any sharp voltage fluctuations across the switches. The three main components of RCD snubber are resistor R_s, the capacitance C_s, and diode D_s for as shown in Figure 2. The stored leakage energy is dissipated through the resistor while the capacitor acts as a filter to and guarantees a low ripple DC source. The diode here is nothing but a unidirectional switch. The clamping of the spikes using an RCD snubber requires calculating the resonant circuit's characteristic impedance, given by the following equation:

$$Z = 2\pi f_s L \quad (4)$$

$$C_s = \frac{1}{2\pi f_s R} \quad (6)$$

where f_s is the switching frequency of the converter.

The RCD snubber works by absorbing the inductor's current when the switch's drain voltage exceeds the clamp capacitor voltage. The relatively large capacitor used in the circuit manages to keep the voltage constant over a switching cycle. By using a larger capacitor value, the peak power will increase while the switching loss will decrease [8].

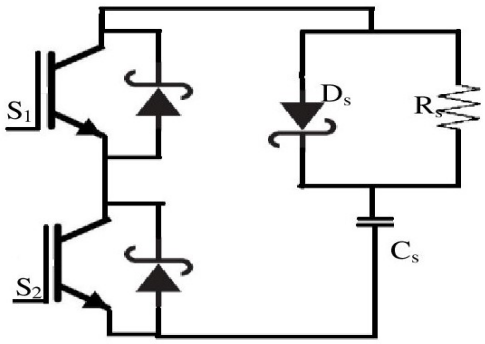

Figure 2. Circuit diagram of the RCD snubber [8].

2.2. Active Clamp Snubber

An active clamp for the BDC's higher power applications is a good choice. It limits the overshoot of the bridge switch's turn-off voltage, thus enabling the energy stored for ZVS. The output diode's reverse-recovery problem can partly be overcome by utilizing an appropriate design for the leakage inductance. However, the switches in these converters work under hard switching conditions. The active clamp circuit replaces the role of the passive lossless clamp circuit. The primary and the clamp switches turn ON under the ZVS condition, and the use of parallel capacitors help significantly reduce the turn OFF losses.

As shown in Figure 3, the coupled inductor included in the topology is used to recycle the leakage inductance energy and achieve the ZVS condition for the main and clamp switches. The switches and diodes' voltage stresses are lower than the output voltage. Thus, by using an active clamp circuit with an active switch M_c, and a capacitor, $C_{c''}$ conduction losses and cost can be significantly reduced.

The design is based on the resonant tank circuit formed by the clamping capacitor C_c and the leakage inductance L_k. Resonance occurs during the off-stage of the boost mode operation. The criterion to select C_c is such that the following holds:

$$C_c \geq \frac{(T_s/4\pi)^2}{L_k} \quad (7)$$

where T_s is the period of the driving signal for each bridge switch of the converter [9,10].

In the snubber resistor value is equal to the characteristic impedance, the ringing effect is reduced. Therefore, to select the resistor, the following equation is used:

$$R_s = Z \quad (5)$$

The snubber capacitor, C_s, allows the resistor to be most effective at the ringing frequency by reducing the dissipation to a minimum at the switching frequency. The capacitor is designed so that the impedance of the capacitor at the clamping frequency is considered equal to the resistor, as shown in the following equation:

$$C_s = \frac{1}{2\pi f_s R} \quad (6)$$

where f_s is the switching frequency of the converter.

The RCD snubber works by absorbing the inductor's current when the switch's drain voltage exceeds the clamp capacitor voltage. The relatively large capacitor used in the circuit manages to keep the voltage constant over a switching cycle. By using a larger capacitor value, the peak power will increase while the switching loss will decrease [8].

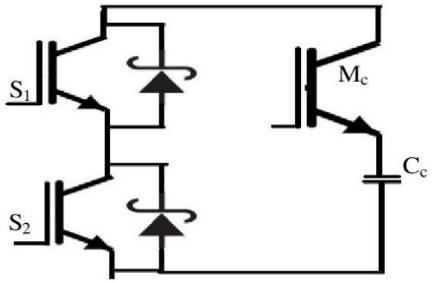

Figure 3. Circuit diagram of the active clamp snubber [9,10].

2.3. Flyback Snubber

A flyback snubber is suitable for high power applications and is shown in Figure 4. This snubber circuit enables the main switch to achieve a ZVS turn-on or a ZCS turn-off process as a result of short time interval of ZVS or ZCS characteristics. The use of the series inductor results in slowing down the diode's reverse recovery current. However, these inductors increase the switching loss, due to additional voltage stress on the main switch at turn-off transition. The snubber capacitor enables to clamp the switch voltage by absorbing the stored energy of the snubber inductor. However, the converter reliability and life span deteriorate as a result of the snubber capacitor's energy reprocessing through the main switch, resulting in high current stress. The use of flyback snubber helps overcome this problem through its ability to attain soft-switching features and thus, significantly reduces both the voltage and current stresses. The flyback snubber can also achieve near ZVS and ZCS. It also significantly reduces any current and voltage stresses on the main switch. The output voltage ripple in flyback converter is given by the following:

$$\frac{\Delta V_0}{V_0} = \frac{DT_s}{C_f} \tag{8}$$

where C_f is the capacitor of the flyback converter, and the output voltage ripple ($\Delta V_0/V_0$) is considered to be 3%. Thus, the snubber capacitor for the flyback snubber can be calculated using Equation (8) [11,12].

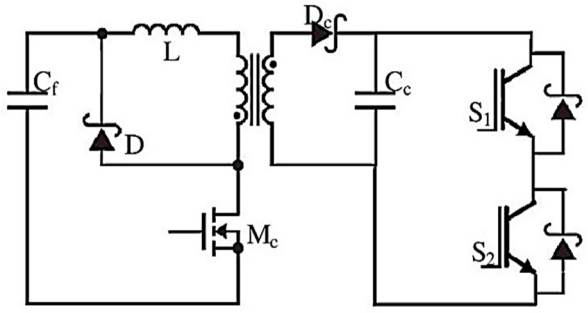

Figure 4. Circuit diagram of the flyback snubber [11,12].

3. Simulation Results

CASE 1 Using model proposed by Kumar et al. [2]

The system presented in [2] consists of a 24 kW PV generation for the 15 kWh battery (of EVs) coupled with an ESU of 15 kWh capacity. The ESU acts as a reserve for the batteries of EVs during times when PV generation is low and stores the energy during excess PV energy generation. Three modes for electrical vehicle battery charging were considered: (i) with PV energy only, (ii) with both PV energy and ESU energy, and (iii) with ESU energy only. The three modes are simulated using MATLAB/Simulink and the results are compared for each snubber circuit for the BDC in the charging station in the following sub-sections.

compared for each snubber circuit for the BDC in the charging station in the following sub-sections.

3.1. Charging Battery of EVs with PV Energy Only

In this mode, the PV generation is in abundance and is adequate to charge the battery of EVs. Figure 5 shows the PV generation power. The DC-link voltage is maintained constant and supplies the required terminal voltage for the batteries continuously. Figure 6 shows the power variations in EVs using three different snubber circuits with the BDC in this mode.

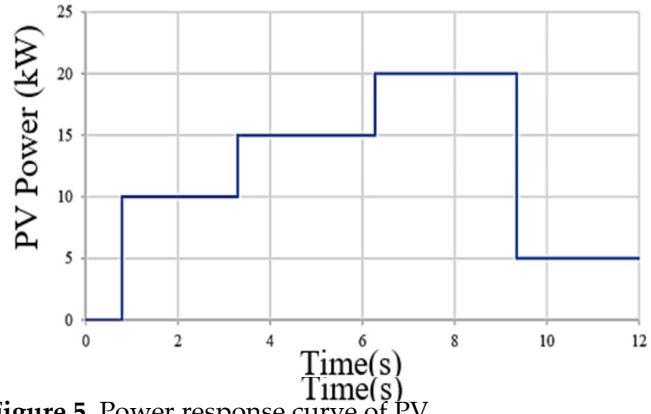

Figure 5. Power response curve of PV

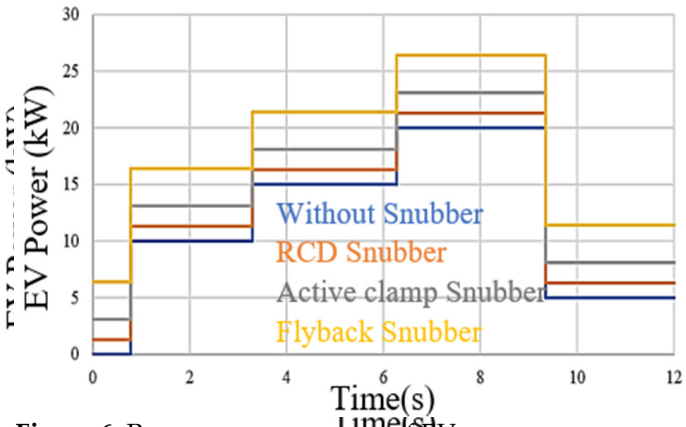

Figure 6. Power response curve of EVs.

3.2. Charging Battery of EVs with PV Energy and ESU Energy

In this mode, the PV energy alone is insufficient to charge the EVs (Figure 7). An additional energy is supplied by the ESU to charge the battery of EVs. Figure 8 shows the power variations of EVs when using three different snubber circuits with the BDC in this mode.

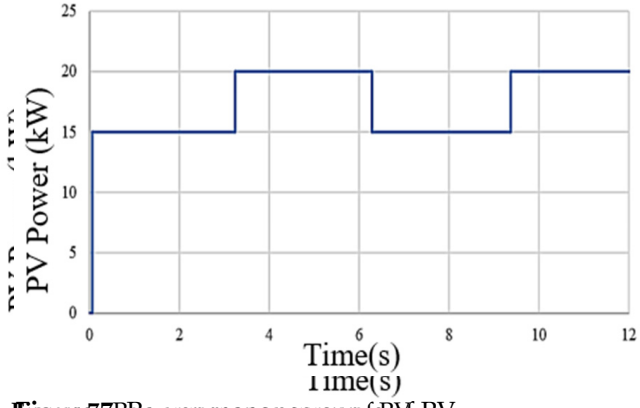

Figure 7. Power response curve of PV.

Energies 2021, 14, x FOR PEER REVIEW 7 of 12

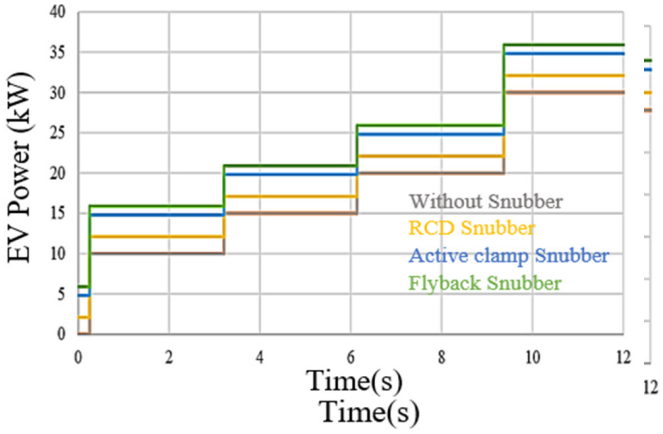

Figure 8. Power response curve of EVs

Figure 8. Power response curve of EVs

3.3. Charging Battery of EVs with ESU Only

3.3. Charging Battery of EVs with ESU Only

In this mode, the battery of EVs is charged only from the ESU. The PV generation is almost zero. Figure 9 shows the power variations of EVs when using three different snubber circuits for the BDC in this mode.

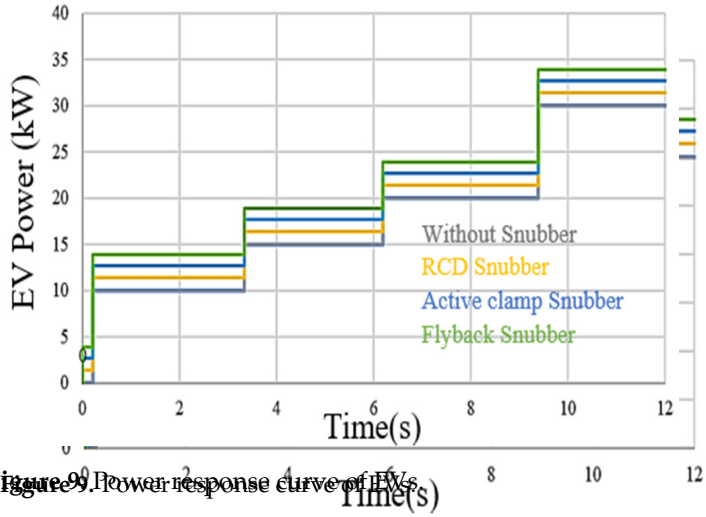

Figure 9. Power response curve of EVs

Figure 9. Power response curve of EVs

The results presented in these three cases clearly show that this standalone charging station can charge the battery of EVs under any circumstance. It is an attractive way of using renewable energy. Figure 10 shows the clamp branch voltage across the main switches of the BDC.

It is evident from the graph that without a snubber circuit possessing higher voltage stress across the switch, it does not achieve the ZVS condition. In contrast, the three proposed snubber circuit attain ZVS condition rapidly. The RCD snubber circuit attains ZVS within six seconds. Using the active clamp snubber results in a significantly smaller voltage stress, and using the flyback snubber attains ZVS almost instantaneously. It is evident from the graph that the flyback snubber is the best option, as it can achieve ZVS by mitigating the voltage stresses. It is also clear from Figures 6, 8 and 9 that the power of EVs improves when snubber circuits are implemented. Additionally, the power waveforms clearly show that the use of the flyback snubber in the charging station results in the highest output power, compared to the other two snubber circuits.

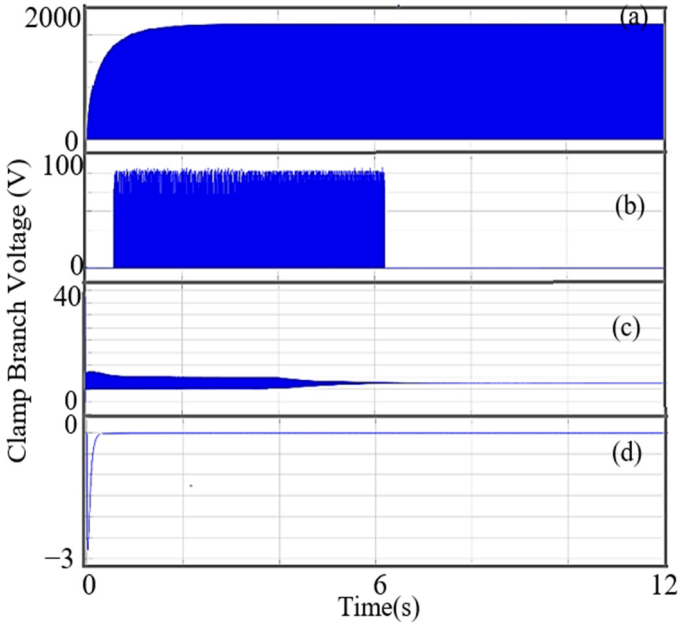

Figure 10. Clamp branch voltage of BDC (**a**) without snubber (**b**) RCD Snubber (**c**) active clamp snubber (**d**) flyback snubber.

CASE 2 Using Model proposed previously by the authors [3]

We used a standalone charging station for EVs [3]. It consists of a PV panel, ESU, BDC with a snubber circuit—the EVs act as the load. The system uses a PV panel with a capacity of 100 kWh. An ESU with a capacity of 80 kWh stores the power to charge 40 kWh EVs. The performance of the proposed charging station was carried out using MATLAB/Simulink by considering three cases—EVs are charged (i) with the PV array only, (ii) with both PV array and ESU, and (iii) with the ESU only [3]. Figure 11 shows the clamp branch voltage across each active snubber circuit. There is a power dissipation in the resistor of the RCD snubber. This means a reduced efficiency and is ideal for high-power operations. The burden of high current stress and associated thermal issues of the active switches and the capacitor limits the use of an active clamp snubber circuit in the BDC topology, as it switches at a frequency that is two times the switching frequency. From the voltage-clamp branch waveform, BDC using the RCD snubber and active clamp snubber causes more voltage transients. Meanwhile, the BDC with the flyback snubber can clamp the voltage better than all the other snubber circuits. Thus, transients can be avoided in the circuit. Figures 12 and 13 show the output voltage obtained for the BDC using three different snubber circuits and the power of EVs. The BDC with the flyback snubber attains the steady state faster when compared to the other snubber circuits. Once again, the power waveforms clearly show that the use of the flyback snubber in the charging station results in the highest output power, compared to the other snubber circuits.

A comparative analysis between the various snubber circuits is shown in Table 1. From the table, it is clear that all three snubber topologies can be used successfully with the BDC for an off-grid charging station for EVs. Therefore, choosing the most suitable snubber circuit depends on voltage ripple, ability to achieve ZVS, and conduction losses. Thus, the flyback snubber provides the best option, compared to other snubber circuits while considering the aforementioned factors. However, the flyback snubber has the drawback of a complex structure, being more difficult to implement with the BDC, compared to other snubbers, and its cost is somewhat higher than the other snubber circuits. Nevertheless, one can ignore these disadvantages, as it offers superior performance with the BDC for the off-grid charging station, achieving ZVS, mitigating the voltage spikes and providing better efficiency than the other snubber circuits.

Energies **2021**, *14*, x FOR PEER REVIEW 9 of 12

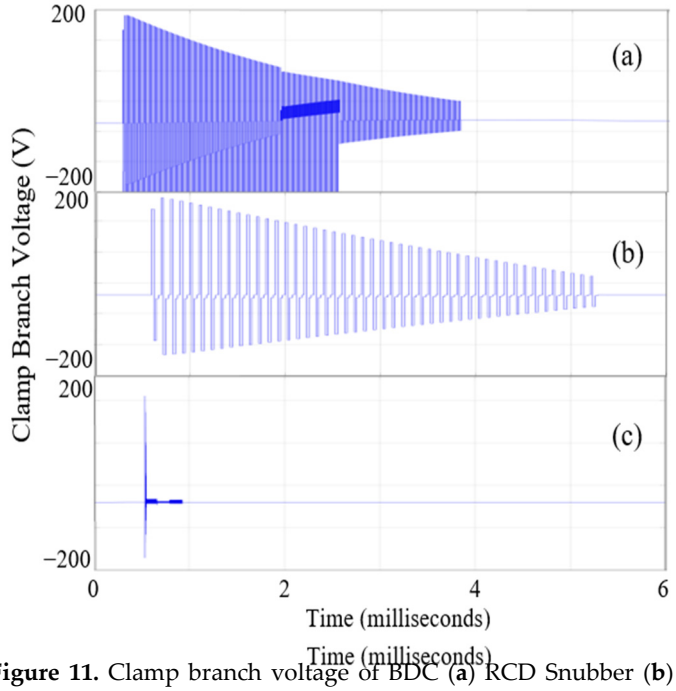

Figure 11. Clamp branch voltage of BDC (**a**) RCD Snubber (**b**) active clamp snubber (**c**) flyback snubber.

Figure 11. Clamp branch voltage of BDC (**a**) RCD Snubber (**b**) active clamp snubber (**c**) flyback snubber.

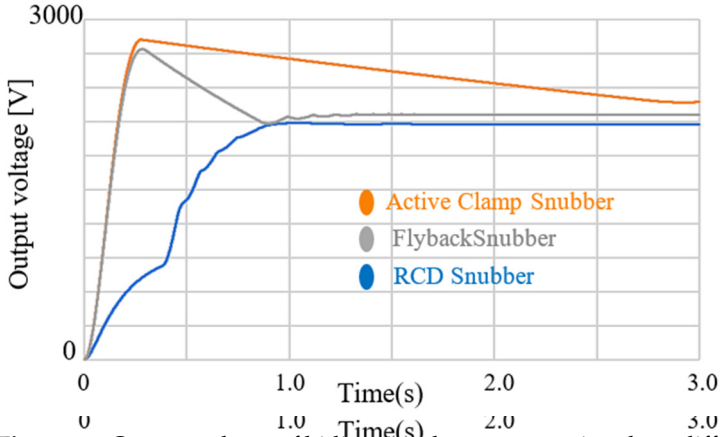

Figure 12. Output voltage of bidirectional converter, using three different snubber circuits.

Figure 12. Output voltage of bidirectional converter, using three different snubber circuits.

These scenarios clearly demonstrate that a stand-alone PV-based charging station is equipped to successfully charge EVs under any condition. The snubber circuit in the BDC results in a system free from any high voltage stresses, which is energy efficient. The proposed isolated BDC with flyback and passive snubbers offers a viable solution to significantly reduce any circulating current issues and voltage spikes. Using a BDC with no snubber circuit will always suffer from voltage spikes, due to the presence of the inductor. The flyback snubber successfully reduces this voltage spike. Additionally, the flyback snubber, in addition to exhibiting excellent reliability and efficiency, can be controlled to attain a soft start-up feature. Figure 14 shows the plot of the efficiency curve, while maintaining a constant input voltage for the two case studies described in this paper. This curve was obtained with a fixed input voltage of 400 V. The maximum efficiency for case 1, having BDC with flyback snubber and passive snubber, is 90%, whereas for case 2, it is about 92%. It was previously shown in [3] that the efficiency of BDC without the snubber circuit was less than the BDC with a snubber circuit. The efficiency curves shown in Figure 14 indicate that an off-grid charging station for EVs by using a BDC with snubber circuits is improved.

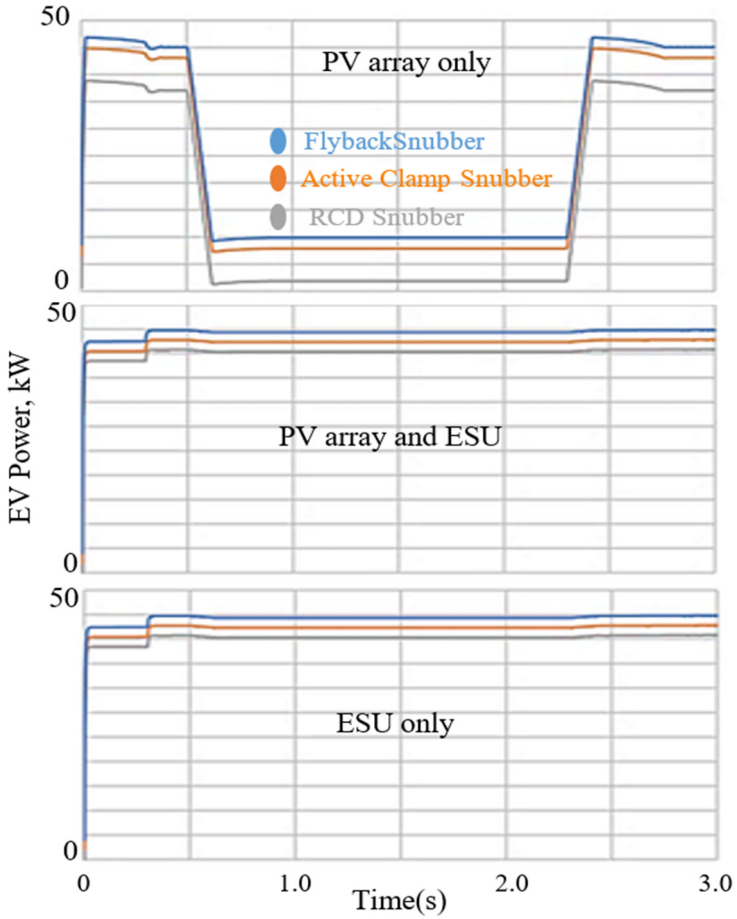

Figure 13. Output voltage of EVs load, using three different snubber circuits.

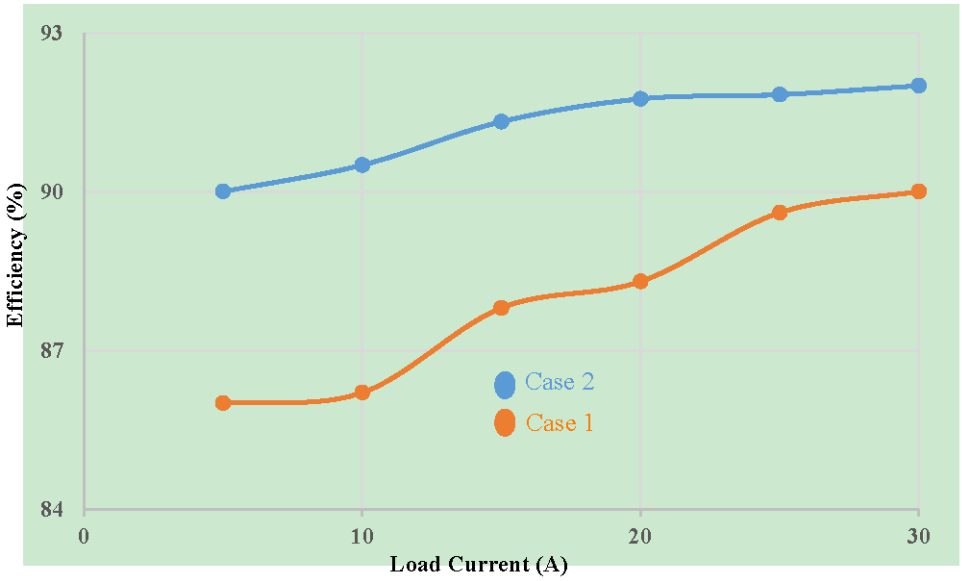

Figure 14. Plot of conversion efficiency of the proposed converter.

Table 1. Comparative analysis of various snubber circuits.

Parameters	RCD Snubber	Active CLAMPING SNUBBER	Flyback Snubber
Number of switches/diodes/capacitors	0/1/1	1/0/1	1/1/2
Conduction loss	Moderate	Low	Very low
Voltage ripple	Moderate	Low	Negligible
Attaining speed of ZVS	Very slow	Slow	Fast
Ease of implementation in BDC	Much easier	Easy	Difficult
Complexity	Smooth	Bit complex	Complex
Cost	Inexpensive	Reasonable	Bit expensive
Efficiency	Low	Moderate	High

4. Conclusions

In this paper, various snubber circuits for the BDC of two different models of an off-grid solar-based charging station for EVs were implemented and studied. A performance comparison of the charging station was carried out. The use of PV to charge EVs in an off-grid charging station will help to achieve clean energy generation and reduce the grid burden. Thus, the use of EVs in remote locations can be significantly increased. An ESU is coupled with the system to work under any circumstances. The proposed BDC incorporates either RCD snubber or active clamp snubber or flyback snubber to reduce the voltage spike caused by the current fed inductor. The proposed station's design using various snubber circuits was explained and validated in MATLAB/Simulink. It was successfully tested on two independent models, thus making the method both credible and robust. The efficiency of the proposed converter with the snubber circuits in both the cases is higher, compared to the converter without snubbers. The converter can achieve ZVS conditions more rapidly than a converter without the snubber. Thus, the use of an appropriate snubber enhances the system reliability efficiency. In both the models reported here, the flyback snubber consistently offered the best possible results.

Author Contributions: Conceptualization, D.K.N. and K.P.; methodology, D.K.N.; software, D.K.N.; validation, D.K.N., K.P. and T.T.L.; formal analysis, D.K.N.; investigation, D.K.N.; resources, D.K.N.; data curation, D.K.N.; writing—original draft preparation, D.K.N.; writing—review and editing, D.K.N. and K.P.; visualization, D.K.N.; supervision, K.P. and T.T.L.; project administration, K.P. and T.T.L. All authors have read and agreed to the published version of the manuscript.

Funding: This research received no external funding.

Conflicts of Interest: The authors declare no conflict of interest.

References

1. Shariff, S.M.; Alam, M.S.; Ahmad, F.; Rafat, Y.; Asghar, M.S.J.; Khan, S. System Design and Realization of a Solar-Powered Electric Vehicle Charging Station. *IEEE Syst. J.* **2020**, *14*, 2748–2758. [CrossRef]
2. Kumar, V.; Teja, V.R.; Singh, M.; Mishra, S. PV Based Off-Grid Charging Station for Electric Vehicle. *IFAC-PapersOnLine* **2019**, *52*, 276–281. [CrossRef]
3. Nair, D.K.; Prasad, K.; Lie, T.T. Standalone electric vehicle charging station using an isolated bidirectional converter with snubber. *Energy Storage* **2021**, e255. [CrossRef]
4. Sharon, P.; Sathiyan, P.S. Design and simulation of bidirectional converter with flyback and capacitor diode snubbers. In Proceedings of the 2015 International Conference on Innovations in Information, Embedded and Communication Systems (ICIIECS), Coimbatore, India, 19–20 March 2015; pp. 1–5.
5. Todd, P.C. Snubber Theory, Design Circuits and Application. Available online: https://www.ee.bgu.ac.il/~dcdc/notes/Additional_2012/Snubbers.pdf (accessed on 13 September 2021).
6. Bhatt, K.; Gupta, R.A.; Gupta, N. Design and development of isolated snubber based bidirectional DC–DC converter for electric vehicle applications. *IET Power Electron.* **2019**, *12*, 3378–3388. [CrossRef]
7. Wu, T.-F.; Chen, Y.-C.; Yang, J.-G.; Kuo, C.-L. Isolated Bidirectional Full-Bridge DC–DC Converter With a Flyback Snubber. *IEEE Trans. Power Electron.* **2010**, *25*, 1915–1922. [CrossRef]

8. Vaz, A.R.; Tofoli, F.L. In-depth analysis of an RCD snubber applied to a DC-DC boost converter. *Int. J. Circuit Theory Appl.* **2021**, *49*, 283–305. [CrossRef]
9. Yoo, J.S.; Ahn, T.; Yu, G.; Lee, J.; Lee, J. A study on novel active clamp snubber applied DC-DC quasi resonant flyback converter to effectively reduce switch voltage surge. In Proceedings of the 2017 20th International Conference on Electrical Machines and Systems (ICEMS), Sydney, Australia, 11–14 August 2017; pp. 1–5. [CrossRef]
10. Yan, Z.; Zeng, J.; Liu, J.; Lin, W. A Novel Soft-Switching Bidirectional DC-DC Converter with High Voltage-Gain for Grid-Connected Energy Storage System. In Proceedings of the 2019 4th IEEE Workshop on the Electronic Grid (eGRID), Xiamen, China, 11–14 November 2019; pp. 1–6. [CrossRef]
11. Balbayev, G.; Nussibaliyeva, A.; Tultaev, B.; Dzhunusbekov, E.; Yestemessova, G.; Yelemanova, A. A novel regenerative snubber circuit for flyback topology converters. *J. Vibroengineering* **2020**, *22*, 983–992. [CrossRef]
12. Tadvin, S.M.; Bin Shah, S.R.; Hossain, M.R.T. A Brief Review of Snubber Circuits for Flyback Converter. In Proceedings of the 2018 3rd International Conference for Convergence in Technology (I2CT), Pune, India, 6–7 April 2018; pp. 1–5. [CrossRef]

Check for updates

Received: 10 June 2022 | Revised: 5 December 2022 | Accepted: 11 December 2022

DOI: 10.1002/est2.442

RESEARCH ARTICLE

ENERGY STORAGE WILEY

Design of a PV-fed electric vehicle charging station with a combination of droop and master-slave control strategy

Divya Krishnan Nair | **Krishnamachar Prasad** | **Tek T. Lie**

School of Engineering, Computer and Mathematical Sciences, Auckland University of Technology, Auckland, New Zealand

Correspondence
Divya Krishnan Nair, School of Engineering, Computer and Mathematical Sciences, Auckland University of Technology, Auckland, New Zealand.
Email: divya.krishnan.nair@autuni.ac.nz

Funding information
School of Engineering, Computer and Mathematical Sciences, Auckland University of Technology, Auckland, New Zealand

Abstract

Electric vehicles (EVs) are becoming essential elements for both the transport and power sectors. Consequently, they need a suitable charging infrastructure at the same time. Electric vehicle charging stations (EVCS) assisted by photovoltaic (PV) panels draw attention due to minimal expenditure, increased environmental awareness, and a consistent increase in the effectiveness of the PV modules. In this paper, a combination control scheme utilizing the merits of both droop and master-control strategies for the EVCS is proposed. In addition, an isolated bidirectional DC-DC converter combined with the snubber circuits and a three-level boost converter that utilizes a capacitance-voltage control design is used to further enhance the system stability. The design of the EVCS is formulated and validated through MATLAB/Simulink.

KEYWORDS

bidirectional converter, droop control, electric vehicle charging station, master-slave control, photovoltaic, snubber circuit

1 | INTRODUCTION

Electric vehicles (EVs) has led to a paradigmatic change in the electric and transportation sectors. In recent years, EVs have become a viable alternative due to the transport sector's contribution of 23% to worldwide emissions of greenhouse gases (GHG) connected to energy. The percentage of renewable energy used in transportation is quite low currently but is experiencing a tremendous transformation, especially in the wagon category where EVs are gaining ground.[1] According to the IEA reports, the number of electric vehicles sold worldwide reached 10 million in the year 2020. The greatest fleet is in China, where there are 4.5 million electric vehicles, but in 2020, Europe saw the largest yearly growth, rising to 3.2 million. If most cars built after 2040 are electric, more than

Abbreviations: A, ampere; AC, alternating current; CO_2, carbon dioxide; DC, direct current; D_C, duty ratio generated from capacitor voltage; D_{PV}, duty ratio generated from solar panels; ESU, energy storage unit; EV, electric vehicle; EVCS, electric vehicle charging station; G', slope of solar irradiance; G_{avg}, disable function based on the average sun irradiance; GHG, greenhouse gases; ICE, internal combustion engines; IEA, international energy agency; $I_{ESU\text{-}ref}$, storage current reference; $I_{EV\text{-}ref}$, reference charging current; IGBT, insulated gate bipolar transistor; K_{ESU}, ESU droop gain; MATLAB, matrix laboratory; MOSFET, metal-oxide-semiconductor field-effect transistor; MPPT, maximum power point tracking; MW, megawatt; P_{ESU}, ESU power; P_{EV}, maximum consumption from the EVs; PI, proportional integral controller; P_{mpp}, maximum output power from the PVs; PV, photovoltaic; *SOC*, state-of-charge; V, voltage; V2G, vehicle to grid; V_{PV}, solar panel voltage; V_{ref}, reference voltage; W, watts; ΔI_{EV}, droop control's output.

This is an open access article under the terms of the Creative Commons Attribution-NonCommercial-NoDerivs License, which permits use and distribution in any medium, provided the original work is properly cited, the use is non-commercial and no modifications or adaptations are made.
© 2023 The Authors. *Energy Storage* published by John Wiley & Sons Ltd.

25784862, 0, Downloaded from https://onlinelibrary.wiley.com/doi/10.1002/est2.442, Wiley Online Library on [21/01/2023]. See the Terms and Conditions (https://onlinelibrary.wiley.com/terms-and-conditions) on Wiley Online Library for rules of use; OA articles are governed by the applicable Creative Commons License

1 billion people might have access to EVs by 2050.[2] Electricity is an ideal low-cost fuel for the transportation sector due to the cost reduction in renewable energy generation. The increasing deployment of EVs provides a great scope for the power sector as these vehicles have the potential to reduce emissions and save energy. EVCS has the potential to provide massive amounts of storage capacity for electricity. Uncontrolled charging of EVs on the grid might result in system overload, thus necessitating upgrades to the distribution and transmission as well as in the generation capacity.[3,4] Private investments are necessary to develop charging infrastructure, but currently, few business models make sense for them. Government can provide incentives for the installation of EVCS in both residential and public access areas. Furthermore, a crucial and ongoing challenge is to optimize the charging, aggregation, and overall management of EVs on the grid. As a result, crucial decisions about where to place charging points, which technologies to utilize, and to optimize slow smart charging and rapid charging to best serve consumers will have to be addressed while establishing charging infrastructure.[5]

The demand for charging infrastructure is projected to rise as the number of electric vehicles grows, placing additional strain on the grid. EV charging patterns are unpredictable and erratic, as well as the rising deployment of rapid charging systems that take significant grid power for shorter durations exacerbates this situation.[4-6] Major and costly renovations will be required for both the transmission and distribution systems, as well as associated components of the energy network. The impact of EV charging on the low voltage network was investigated by Zou et al[7] who discovered that overloading on the transformers had a detrimental impact on the power quality. To safeguard the network, grid charging points must manage EV charge characteristics like time and demand for charging when they arrive at a charging point. These responses, on the other hand, are unpredictable and difficult to assess.[8] Girard et al[9] found that charging EVs via the grid has no environmental benefits. Using the off-grid method to charge EVs, on the other hand, results in a significant reduction in CO_2 emissions. As a result, building stand-alone off-grid charging stations would be an ideal approach for promoting EV adoption globally while minimizing the impact on the current power grid.[10]

In an earlier publication,[11] it has been shown that an off-grid EVCS using PV energy can be effectively installed in remote locations. The most common renewable sources of energy are solar and wind. However, wind energy consists of multiple conversion stages to produce power compared to PV energy. Therefore the feasibility of PV-based EVCS is more attractive.

Compared with more common AC grid-connected EV charging stations, the benefits of DC off-grid connected EVCS include the following[12,13]:

- Minimal energy conversion losses in systems that include DC sources.
- Continuous supply of high-quality power and free from skin effect and reactive power losses.
- Less expensive and fewer power-electronic gadgets.
- No need to consider utility grid synchronization.

So, there is a great trend in PV-fed DC fast-charging stations in the literature. A typical PV-fed DC fast charging station consists of solar arrays, EV chargers, energy storage unit (ESU), and numerous DC-DC power converters. A microgrid charging station may offer charging facilities in remote areas. Multiple applications have made use of off-grid charging stations. The world's biggest off-grid solar project, the DeGrussa Solar farm in Australia, uses a 10.6 MW solar PV panel and a 6 MW battery system to supplement a 23 MW diesel-fired power station, saving an estimated 5 million liters of diesel fuel each year. It also saves 12 million tons of CO_2 emissions. Since 2017, Robben Island has been cut off from the mainland's electricity system; however, it is equipped with a 666.4 kW solar PV system and a battery energy storage microgrid. It may save 275 000 gal of diesel every year, and 820 t of CO_2 emissions are eliminated from the air each year, helping to protect the island's ecosystem and wildlife.[14]

The published work on PV-based charging systems covers system design, vehicle-to-grid (V2G) operations, power management, and electricity bill reduction in smart homes.[15-21] Because all these methods involve a greater standard over a long duration, they cannot tolerate unexpected system perturbations such as rapid irradiance shifts. It has been demonstrated by Thang et al[22] that a sliding-mode control can be used to enhance the robustness of the output voltage of the DC bus to bridge this gap. However, the coordination of EVs and ESU is absent. To prevent the ESU from being overcharged and overdischarged, Wu et al[23] develop a coordinated control in the islanded mode. Although, there is no evidence of transient PV generating interruption that would compromise system stability. According to Xia et al,[24] a decentralized control system for synchronizing solar power with ESU charging/discharging is proposed. They employ a droop control-based technique for the ESU, and adaptive power regulation for the PV generator. Furthermore, the EV chargers were depicted simplistically and were not included in the synchronization. This prevented any investigation into the impact of failures on the EV side.

25784862, 0, Downloaded from https://onlinelibrary.wiley.com/doi/10.1002/est2.442, Wiley Online Library on [21/01/2023]. See the Terms and Conditions (https://onlinelibrary.wiley.com/terms-and-conditions) on Wiley Online Library for rules of use; OA articles are governed by the applicable Creative Commons License

Global EV makers have increased their investments to create and market contemporary EV models because of concerns over climate change, the shortage of fossil fuels, and advances in battery technology. Compared to cars powered by ICEs, EVs produce much fewer GHG emissions. Most nations have started to encourage the use of electric vehicles by implementing specific programs like tax incentives, reduced parking fees, etc. Range anxiety, often known as the restricted range with a fully charged battery, is one of the key issues preventing customers from converting to EVs. The range typically ranges from 100 km to 500 km. A battery may be recharged in anywhere from 30 minutes to 10 hours, depending on the quality of the charging stations. By offering a charge duration of between 30 and 60 minutes, installed fast charging stations distributed in appropriate areas might alleviate this issue. The features of the charger circuit affect the battery charging profile, including the charging time, battery life, and efficiency. The charger circuit's functionality is influenced by the type, components, control strategies, switching methods, and total cost of the converter implementation. The control circuit should be easy to construct and versatile.[25] Therefore, the isolated bidirectional DC-DC converter in the ESU's control circuit is snubber-equipped and is used to regulate the battery's charging and discharging. Since the leakage inductance and low voltage side-fed inductor currents have different current densities, this form of system layout clamps the rail voltage, reducing current spikes at the converter's switches.

However, depending on the electricity generation source, the charging stations have their own drawbacks, including the overloading of the current grid infrastructure and the potential to drastically increase carbon emissions. The development of an off grid charging infrastructure coupled with PV panels is the appropriate remedy to address the serious inadequacies. The PV-ESU-EV coordination along with snubbers in the isolated bidirectional converters is mostly the focus of solutions for decentralized control of islanded EV charging infrastructure. However, it has received little attention as shown in the small number of published research work. Unfortunately, the adoption of PV-ESU-EV systems has been significantly hampered by the restricted access to charging infrastructure and growing driving range anxiety. Additionally, societal, and political constraints impede the advancement of these technologies in the general market, particularly in developing nations where there is a wide range of application. Meanwhile, several in-depth studies have been conducted in recent years to address the problems related to the adoption of PV based charging infrastructure installations by using a variety of charging system designs. Since it is stated that the night is darkest before the sunrise, filling the dispersed PV-ESU-EV infrastructure appears to be the best alternative for boosting economic growth, generating jobs, promoting sustainability, and improving climatic conditions.

The DC system is disconnected from the network, thus more sophisticated management techniques must be utilized to keep the system stable in the face of erratic operating situations such unexpected ESU disconnections or sharp fluctuations in the PV generating power owing to irradiance. The controllers of the converters should therefore be able to maintain coordination among them and handle these transients through combined droop and master-slave control scheme. Although both droop control and master control can deliver precise current sharing under steady-state and transient situations, the fundamental disadvantage of both control methods is that the ESU is crucial to the stability and dependability of the overall system.[26] In this regard, sluggish charging circumstances are not acceptable for the charging/discharging controller, as it cannot switch off the ESU, nor can it regulate the current through it based on the *SOC* value falling below or rising above a certain level. A fast disturbance in the system makes it impossible for the EVs to connect to the bus frequently and disconnect from it within a brief period of time. EVs may suffer harm in this operating mode, so a control scheme that takes advantage of both the droop control system and the master-slave control system is proposed to overcome this issue.

This paper describes a PV-based EVCS using droop and master-slave control techniques to maintain system stability by coordinating PV arrays, EVs, and ESU. The present work also proposes an ESU that includes an isolated bidirectional DC-DC converter with passive and active snubbers. This configuration effectively achieves zero-voltage switching conditions across the switches leading to an enhanced performance of the PV-based EVCS. Moreover, it is economical and reliable to have a single snubber circuit topology in the EVCS rather than one in each EV. It was proposed by Huang et al[26] that an off-grid EVCS based on PV arrays, EVs, and ESUs could be coordinated and maintained by a hybrid control scheme. It is designed to maintain stability in the system by employing both the master slave and droop control schemes. There was, however, no capability to achieve zero voltage switching characteristics since they were using a non-isolated bidirectional DC-DC converter. This will very certainly reduce the EVCS's overall efficiency. Furthermore, there are relatively no data from studies concerning a snubber-based bidirectional DC-DC converter in conjunction with a master-slave as well as droop control technique for the implementation of an EVCS. Thus, in this paper, an isolated bidirectional DC-DC converter with active and passive snubber circuits and a

25784862, 0, Downloaded from https://onlinelibrary.wiley.com/doi/10.1002/est2.442, Wiley Online Library on [21/01/2023]. See the Terms and Conditions (https://onlinelibrary.wiley.com/terms-and-conditions) on Wiley Online Library for rules of use; OA articles are governed by the applicable Creative Commons License

master - slave control scheme combined with a droop control scheme to reduce the impact of circulating current on the main switches is proposed. In addition, the proposed technique can clamp voltage spikes across those switches to achieve maximum efficiency. The combination of droop and master-slave control technique for the PV-based EVCS and the snubber circuits attain minimal voltage fluctuation in the DC bus voltage, thus enabling the ESU to slowly access the maximum allowable number of charge/discharge cycles, thereby enhancing the service life. The proposed work is simulated and validated through MATLAB/Simulink.

In summary, the objectives of the proposed work are:

- Developing a stand-alone off-grid EVCS is a plausible way to promote EV adoption all around the world while minimizing the impact on the present power grid and a considerable decrease in CO_2 emissions.
- Designing the charging station components with the help of derived equations and the control strategies.

2 | DC OFF-GRID STRUCTURE

The DC off-grid system fed by a photovoltaic system uses droop and master-slave control schemes that coordinate PV, EVs, and ESU. In addition, a battery storage system is utilized to offer off-grid electricity continually. When the PV arrays' power is limited, the battery storage system steps in to fill the gap. On the other hand, when the amount of solar power generated exceeds the amount required for off-grid operation, the battery is used to store the extra power. Figure 1 shows the overview of the PV-based off-grid EVCS architecture.

2.1 | System power and energy analysis

Energy and power relations are calculated during the design process to aid in the development of the system.[27,28] Specifically, the following premises are made:

- The initial energy of the storage battery is "E_t" in watthour (Wh).
- The amount of solar power "P_{PV}" emitted from a PV panel changes with time and is determined by:

$$P_{PV} = \frac{P_{mpp}}{36}\left(36 - t^2\right) \quad (1)$$

where P_{mpp} is the maximum output power from the PVs and "t" is the time in hours. In Figure 2, the origin of the time axis of the chart is usually set at noon that is when the irradiation level is at its maximum.[27] A 12-hour period of solar energy is assumed to begin at 6:00 AM and to end at midnight. According to the principle of power balance, the power consumption of EV, P_{EV} is given by,

$$P_{EV} = P_{PV} - P_{BATTERY} \quad (2)$$

where $P_{BATTERY}$ is the instantaneous battery power.

The average battery power is assumed to be zero during a day (T = 24 hours).

Hence,

$$\int_0^T P_{BATTERY} dt = 0 \quad (3)$$

Therefore,

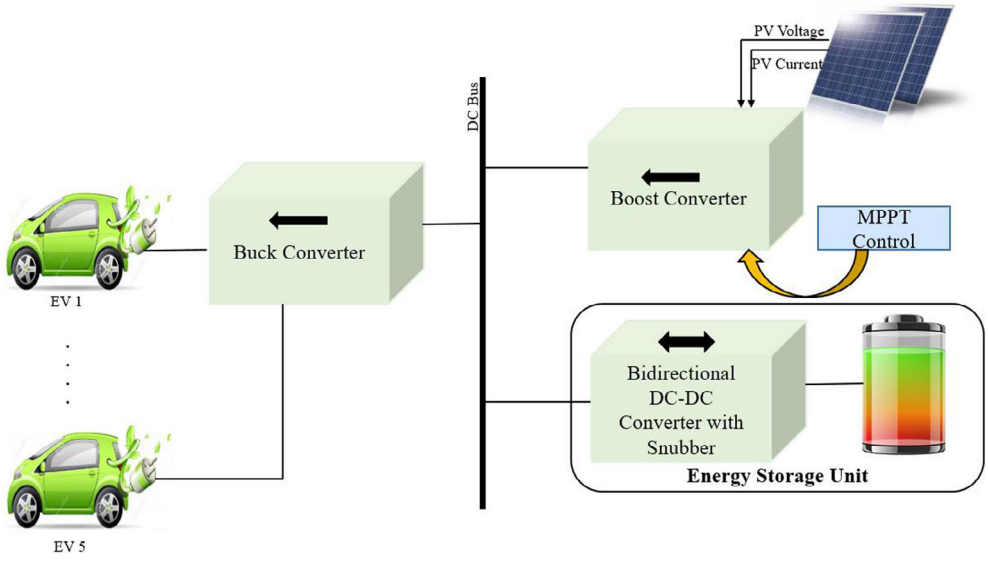

FIGURE 1 Architecture of the off-grid EVCS

25784862, 0, Downloaded from https://onlinelibrary.wiley.com/doi/10.1002/est2.442, Wiley Online Library on [21/01/2023]. See the Terms and Conditions (https://onlinelibrary.wiley.com/terms-and-conditions) on Wiley Online Library for rules of use; OA articles are governed by the applicable Creative Commons License

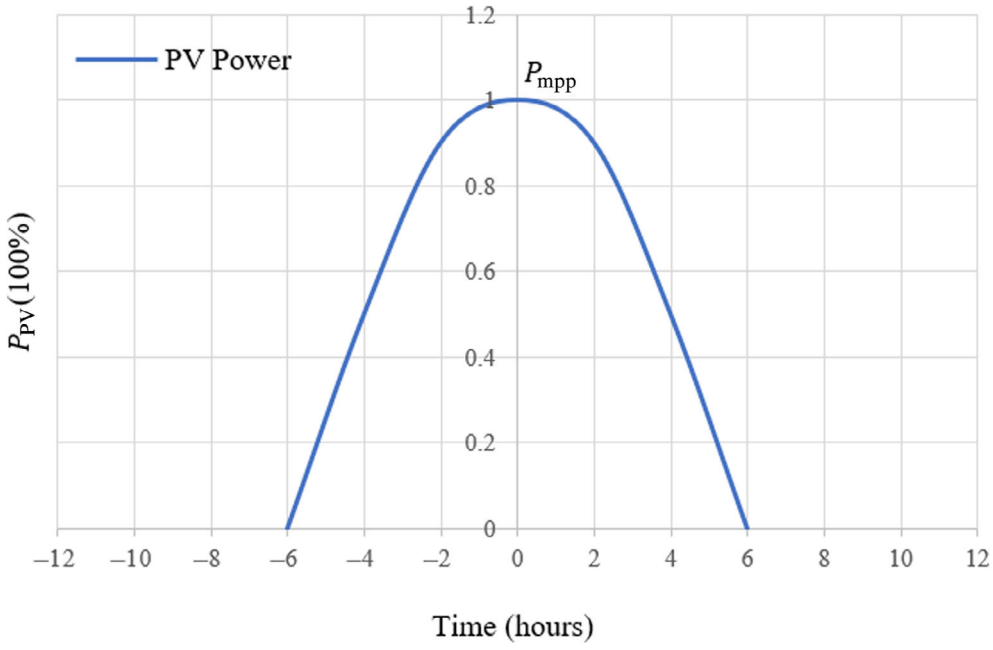

FIGURE 2 PV power distribution for a day[27]

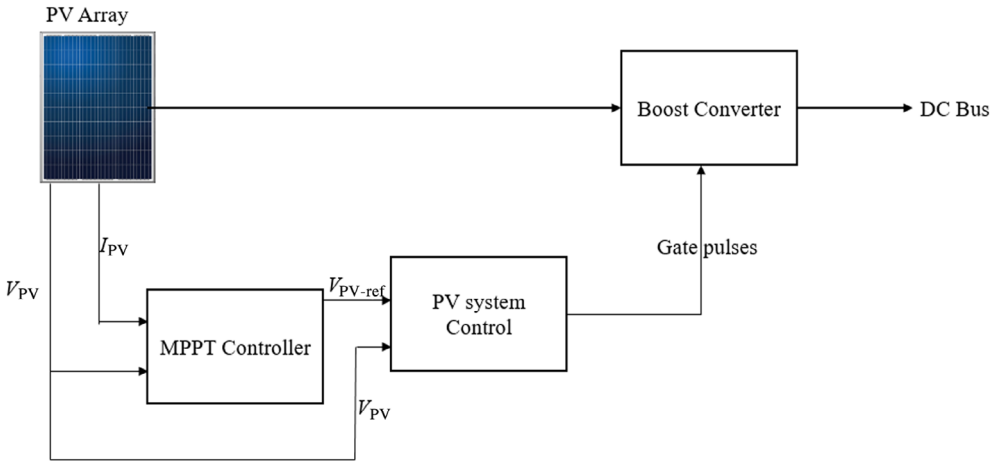

FIGURE 3 Block diagram of PV system control[29,30]

$$\int_{-6}^{6}\left[\frac{P_{mpp}}{36}\left(36-t^2\right)-P_{EV}\right]dt-\int_{6}^{18}P_{EV}dt=0 \quad (4)$$

$$P_{mpp}=3P_{EV} \quad (5)$$

The EV charging station is designed to charge 5 EVs simultaneously. A DC-DC boost converter connects the PV system to a 400 V DC bus. An isolated bidirectional DC-DC converter with an active and passive snubber assists power transfer between the battery and the PV system. The ESU includes a battery storage system and an isolated bidirectional DC-DC converter with an active and passive snubber that can store and release energy which is accomplished by maintaining the DC bus voltage within a reasonable range regardless of the conditions under which it is used. The PV system, which consists of two panels each with 50 kW of electricity, is the primary energy source for the DC off-grid system, providing a total of 100 kW. The PV system's maximum power is actively monitored and transferred to the DC bus. The ESU stores/releases energy from the PV system with a maximum capacity of 80 kW. The charging station's power consumption is around 24 kW.

2.2 | PV panel with a boost converter

The link between the solar array and the DC bus is provided by a three-level boost converter. The maximum power point tracking (MPPT) mode is used by the PV boost converter. The PV system's MPPT control architecture is shown in Figure 3. Using the Incremental Conductance Method,[29,30] the maximum power point of the PV array is determined by measuring its current and

25784862, 0, Downloaded from https://onlinelibrary.wiley.com/doi/10.1002/est2.442, Wiley Online Library on [21/01/2023]. See the Terms and Conditions (https://onlinelibrary.wiley.com/terms-and-conditions) on Wiley Online Library for rules of use; OA articles are governed by the applicable Creative Commons License

voltage. The PV voltage traces the optimal operating voltage using a PV system control. The three-level boost converter (Figure 4) consists of an inductor, two IGBTs with antiparallel diodes, two capacitors, and two diodes. Such a converter provides higher efficiency and double voltage gain as compared to a conventional boost converter.[26]

2.3 | Energy storage unit converter

The ESU consists of a battery and an isolated bidirectional DC-DC converter with a flyback and passive snubber circuit. The bidirectional converter (see Figure 5) provides the battery charging in buck mode and discharging operation in the boost mode, and provides power for the EV loads.[10,11]

When the PV system's generated power exceeds the needed load power, the ESU's primary function is to charge the battery and discharge the battery when the generated power is inadequate to charge the EVs. The configuration of the isolated bidirectional converter with flyback and passive snubber circuit significantly lowers the influence of circulating current on the main switches, thus voltage spikes across the main switches are efficiently clamped. The bidirectional converter uses a flyback snubber and two passive capacitor-diode snubbers to mitigate the high current and high voltage stress that occurs at the main switch during turn-on or turn-off transitions. When compared to a converter without snubber circuits, the efficiency of the converter with snubber circuits is superior.[10,11] The converter attains zero voltage switching conditions faster than a converter without the snubber. This design provides improved performance of the off-grid EVCS. Furthermore, using a snubber circuit in EVCS rather of having one in each EV is less expensive and more cost-effective.

2.4 | EV charger converter

The buck converter (shown in Figure 6) is the EV charger, which consists of a MOSFET switch, an inductor, a diode, and a capacitor.[26] The charger's primary duties

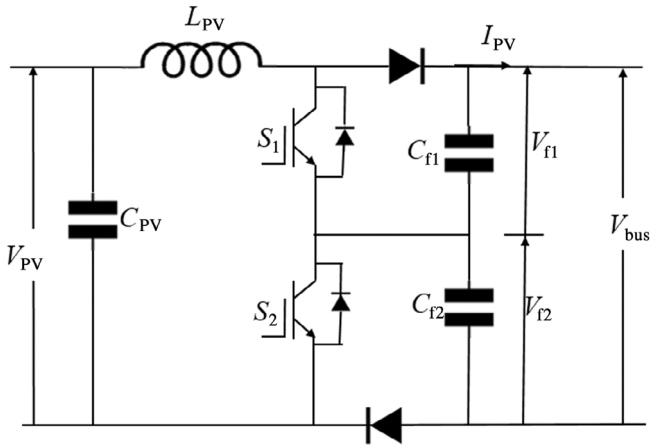

FIGURE 4 PV boost converter[26]

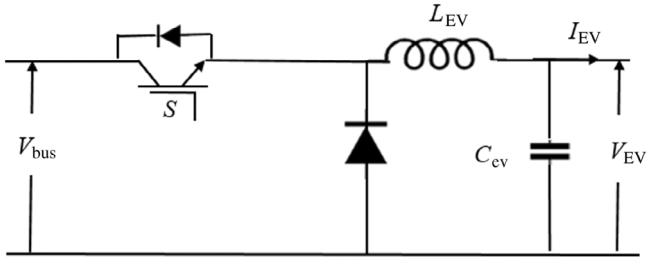

FIGURE 6 EV buck converter[26]

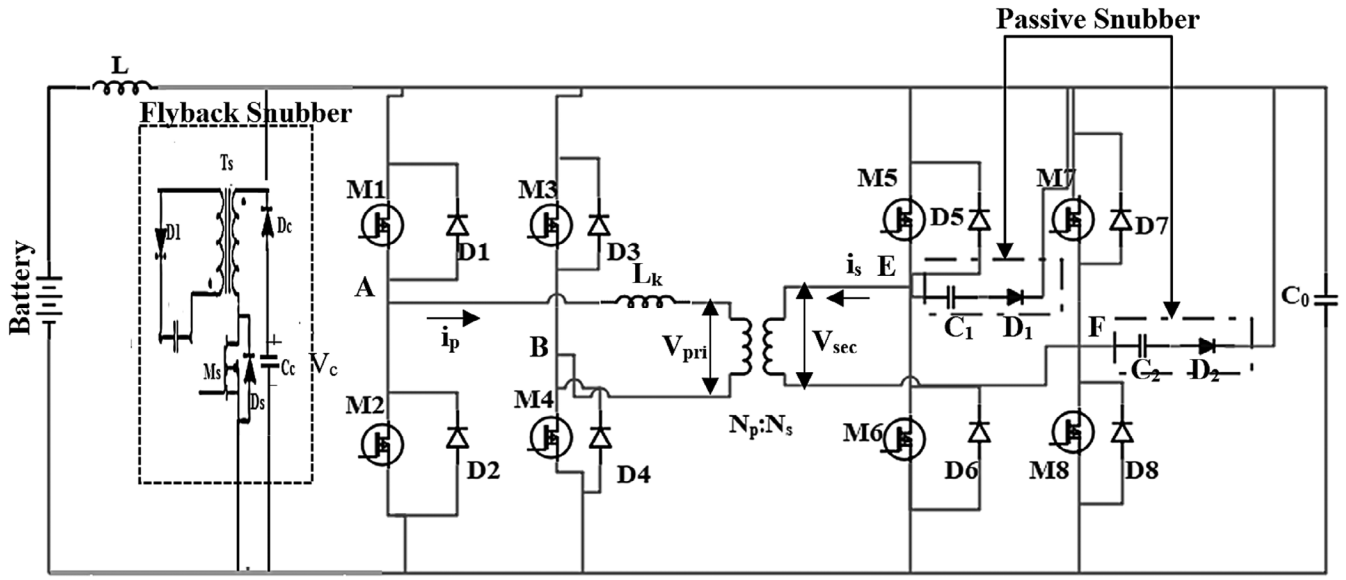

FIGURE 5 Isolated bidirectional DC-DC converter with a flyback snubber and a passive snubber[10,11]

25784862, 0, Downloaded from https://onlinelibrary.wiley.com/doi/10.1002/est2.442, Wiley Online Library on [21/01/2023]. See the Terms and Conditions (https://onlinelibrary.wiley.com/terms-and-conditions) on Wiley Online Library for rules of use; OA articles are governed by the applicable Creative Commons License

include connecting the DC bus to the EV battery terminals and controlling the charging current. In this work, the charging current is limited to 100A.

3 | CONTROL STRUCTURE

The control structure of the DC off-grid system comprises three major algorithms. This includes PV system droop control, ESU converter control, and EV charger converter control and is discussed below in sub-sections.

3.1 | PV system droop control

Through the three-level boost converter, the PV system droop control manages the PV array terminal voltage, extracting the maximum power from the PV arrays. In the PV system droop control, the reference voltage $V_{\text{PV-ref}}$ is obtained from the MPPT algorithm using the Incremental Conductance method.[29,30] The difference between $V_{\text{PV-ref}}$ and V_{PV} is used to calculate the error term, which is then applied to the proportional-integral (PI) controller to provide the duty ratio, D_{PV} for the boost converter. This D_{PV} is then altered by the duty ratio D_C derived from the error term received as the difference between capacitor voltages of the boost converter, V_{f1} and V_{f2}, applied to the secondary PI controller, thereby balancing the two capacitor voltages. Figure 7 shows the control algorithm of the PV boost converter.[26]

3.2 | ESU converter control

The ESU bidirectional converter is controlled to regulate the nominal value of the DC bus voltage, V_{bus}. The battery is charged and discharged by the ESU converter in boost and buck modes, respectively. Figure 8 shows the flowchart to manage the changeover between the two modes.[26]

There will be continuous monitoring of the reference voltage and bus voltage within the system, which enables the converter's operating scheme to be determined by the contrast between the maximum output power from PVs (P_{mpp}) and the maximum consumption from EVs (P_{EV}).

The ESU converter control, shown in Figure 9, consists of a reference charging current, $I_{\text{ESU-ref}}$, and a disable function based on the average sun irradiance, G_{avg}. This disable function allows to limit the ESU discharging current and to coordinate ESU and EV chargers. All EV chargers are turned off when ESU goes below the minimum state-of-charge (*SOC*) level and G_{avg} remains zero until power is generated again by the PV arrays. Since the ESU is so important to the overall system's stability and dependability, it cannot be turned off nor the current through it can be adjusted when *SOC* goes below or climbs above a specific threshold. However, by combining droop control with the master-slave technology,

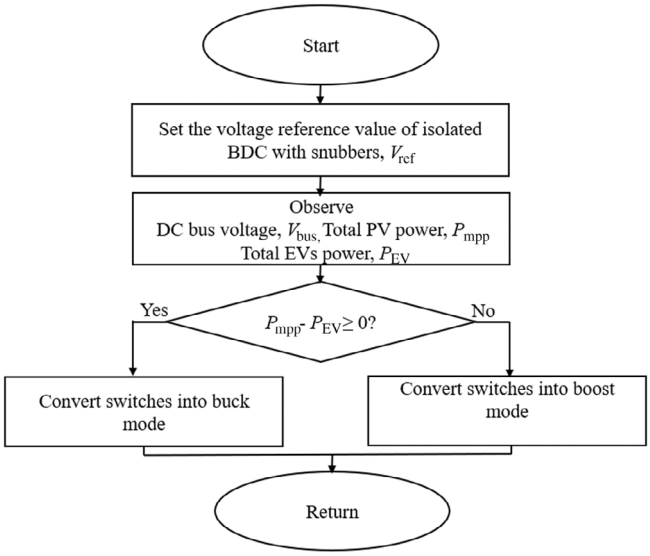

FIGURE 8 Flowchart for the detection of buck/boost mode in isolated bidirectional converter[26]

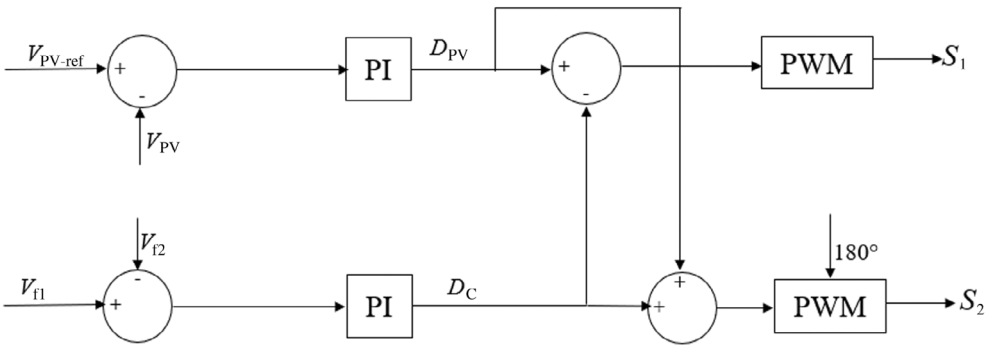

FIGURE 7 Control algorithm of PV boost converter[26]

25784862, 0, Downloaded from https://onlinelibrary.wiley.com/doi/10.1002/est2.442, Wiley Online Library on [21/01/2023]. See the Terms and Conditions (https://onlinelibrary.wiley.com/terms-and-conditions) on Wiley Online Library for rules of use; OA articles are governed by the applicable Creative Commons License

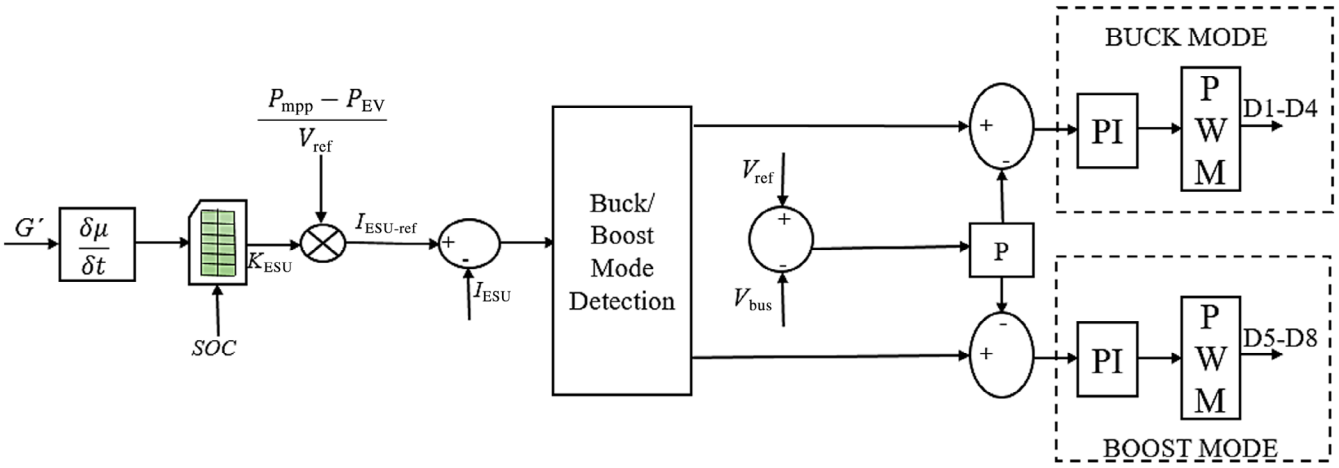

FIGURE 9 ESU converter control[26]

which provides variable current sharing and great reliability, this flaw may be solved. Therefore, the additional droop control adapts to the slope of solar irradiance $G'\left(\frac{dG_{avg}}{dt}\right)$, changes in *SOC*, and the demand. The updated storage current reference $I_{ESU\text{-}ref}$ can then be computed as follows:

$$I_{ESU-ref} = \frac{P_{mpp} - P_{EV}}{V_{ref}} \times K_{ESU} \quad (6)$$

where K_{ESU} stands for the ESU droop gain, which ranges from 0 to 1. The droop gain is calculated using a look-up table depending on G' and *SOC* levels.

3.3 | EV charger converter control

The EV Charger Converter control deploys 5 EVs and a buck converter. The EV charger converter control is shown in Figure 10. The reference charging current is $I_{EV\text{-}ref}$. The disable function is controlled by the controller based on the average value of solar irradiation, G_{avg}. The disable function is activated when G_{avg} falls below a particular threshold, thereafter $I_{EV\text{-}ref}$ approaches zero, and the charger gently disconnects from the DC bus.

The number of unconnected EVs rises as G_{avg} drops. Figure 9 shows the EV Charger converter control in which the EVs are provisioned with a voltage-based droop control structure. This EV charger converter control regulates the DC-bus voltage. The droop control's output, ΔI_{EV} may be stated as follows:

$$\Delta I_{EV} = K_{droop}(V_{ref} - V_{bus}) \quad (7)$$

Where K_{droop} represents the EVs adaptive droop gain calculated from G' and *SOC*.

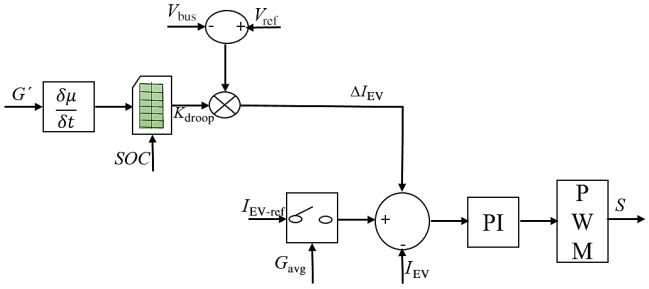

FIGURE 10 EV charger converter control[26]

3.4 | Modes of operation

Mode 1: $P_{mpp} > P_{EV}$ and $K_{ESU} = 1$, $K_{droop} = 0$, *SOC* and G' are within the specified limits.

If the PV panels' provided power exceeds the necessary power of all connected EVs, the EVs are solely charged from the PV panel. The isolated bidirectional DC-DC converter charges the battery with excess power from the PV panel. The surplus energy may be used for a variety of applications (both domestic and commercial).

Mode 2: $P_{mpp} < \sim 0$ and $0 \le K_{ESU} \le 1$, $0 < K_{droop} \le 1$ and *SOC* and G' fall outside the specified limits.

If the PV panels' power output is lower (or nil) than the power required by the EVs for charging during rainy and/or no/low sunlight conditions, the extra required power will be captured from the battery through the isolated bidirectional DC-DC converter while retaining a minimum SOC in the battery.

Mode 3: $K_{ESU} < 1$ and $K_{droop} = 0$ and *SOC* reaches the maximum limit.

When no EVs are plugged into the charging station and the battery charging reaches its *SOC* maximum limit of 90%, the PV panels are unplugged from the bus to preserve the overall system stability.

25784862, 0, Downloaded from https://onlinelibrary.wiley.com/doi/10.1002/est2.442, Wiley Online Library on [21/01/2023]. See the Terms and Conditions (https://onlinelibrary.wiley.com/terms-and-conditions) on Wiley Online Library for rules of use; OA articles are governed by the applicable Creative Commons License

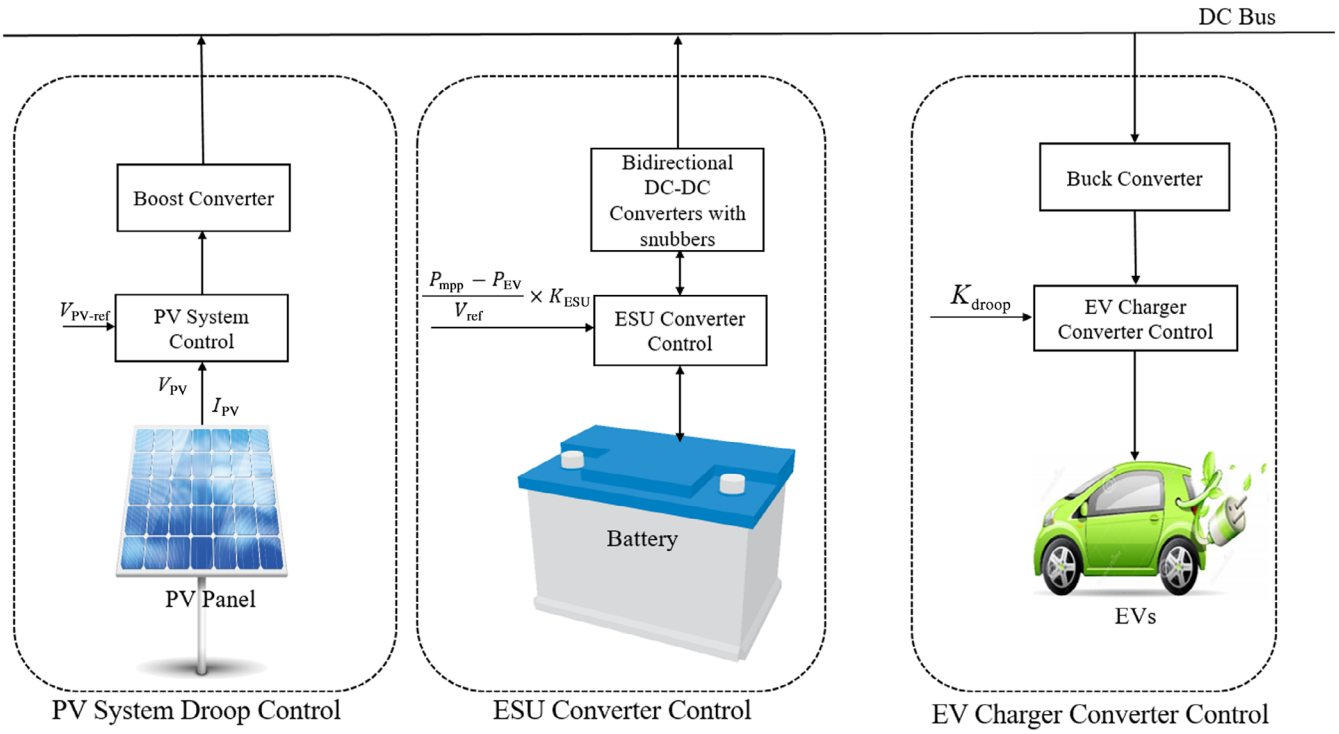

FIGURE 11 Schematic view of the overall control strategy of the off-grid EVCS

Thus the EVCS comprises PV system boost converter droop control, EV charger buck converter droop control and ESU isolated bidirectional converter using both droop and master-slave control along with the PV-ESU-EVs coordination.

4 | SIMULATION RESULTS

The system, as shown in Figure 11, is simulated on the MATLAB/Simulink platform, and the simulated results are obtained under different modes of operation.

The battery's initial *SOC* is set to 20%, with a nominal operating range of 20% to 80%. The PV panels generate the rated electricity initially, with no EVs connected. Therefore the maximum power tracked from the boost converter flows to the ESU. The overall system stability is affected by one of the most important factors, the rate of change of irradiance, G'. In the proposed work, we consider the irradiance G as 1 kW/m^2 at the outset and gradually reduce it to 600 W/m^2 at 3 s, further drops to 0 kW/m^2 at 5 s as shown in Figure 12.

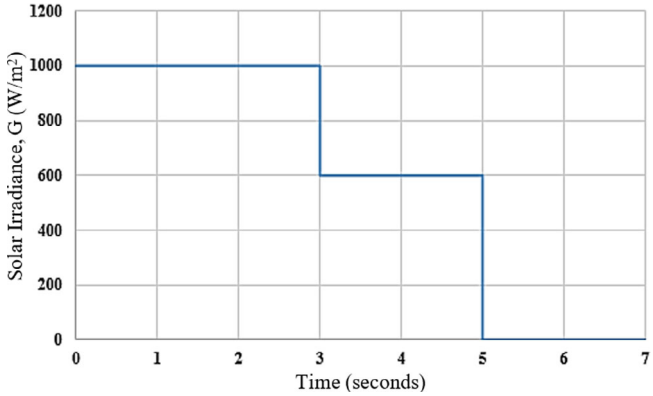

FIGURE 12 Solar irradiance data

4.1 | Mode 1

The EV's *SOC* ranges from 20% to 90%. The solar output in mode 1 is more than the total power required for all EVs, and the battery is charged via an isolated bidirectional converter connected to the PV boost converter. Using the extra power from the PV array, the battery is charged until it reaches its maximum *SOC*. The DC bus voltage is kept constant at 400 V, and the solar array current is 650 A using the droop control and master-slave control. Figure 13 shows the array current drops at t = 3 s when the irradiance falls from 1 kW/m^2 to 600 W/m^2. The current level is similar to the MPPT conditions. In this mode, $K_{droop} = 0$ and $K_{ESU} = 1$, and the *SOC* and G' are defined within the limits. Therefore, the PV panels provide more electricity than is required for all the EVs, and the excess energy is utilized to charge the battery to its maximum *SOC*. In Figure 14A, with the

25784862, 0, Downloaded from https://onlinelibrary.wiley.com/doi/10.1002/est2.442, Wiley Online Library on [21/01/2023]. See the Terms and Conditions (https://onlinelibrary.wiley.com/terms-and-conditions) on Wiley Online Library for rules of use; OA articles are governed by the applicable Creative Commons License

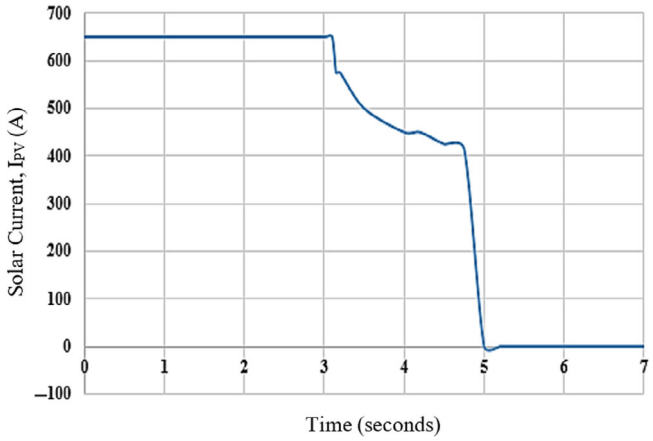

FIGURE 13 Solar array current

surplus ESU power, P_{ESU}, that is, 2500 W − 400 W = 2100 W, the ESU charges from 20% to 34% *SOC* (Figure 14B). The battery of EVs will gradually charge from 20%, 30%, 50%, and 70% to 80% *SOC* are shown in Figure 14C. The current is negative since the EV battery is charging, as shown in Figure 14D.

4.2 | Mode 2

As the solar power is less or absent, the battery discharges from the maximum *SOC*, and this energy is used to charge the EVs as shown in Figure 15A,B. EV charger converter control implements the droop control to maintain the voltage stability. When the change in irradiance G' exceeds a threshold value and the combined droop and master-slave control is enabled for the ESU converter control, the gain droop, K_{droop} changes from 0 to 1. The gain K_{ESU} and K_{droop} are changed from 1 to 0.9 and 0 to 1, respectively (Figure 15D). Thus the ESU and all linked EVs share the PV power, and the ESU's charging current reduces (Figure 15C).

4.3 | Mode 3

When there are no EVs connected, the battery *SOC* is at its maximum of 90% (Figure 16) with the help of energy from the solar array, and the gain $K_{ESU} < 1$ and $K_{droop} = 0$. The PV panels then get disconnected from the overall system to maintain system stability.

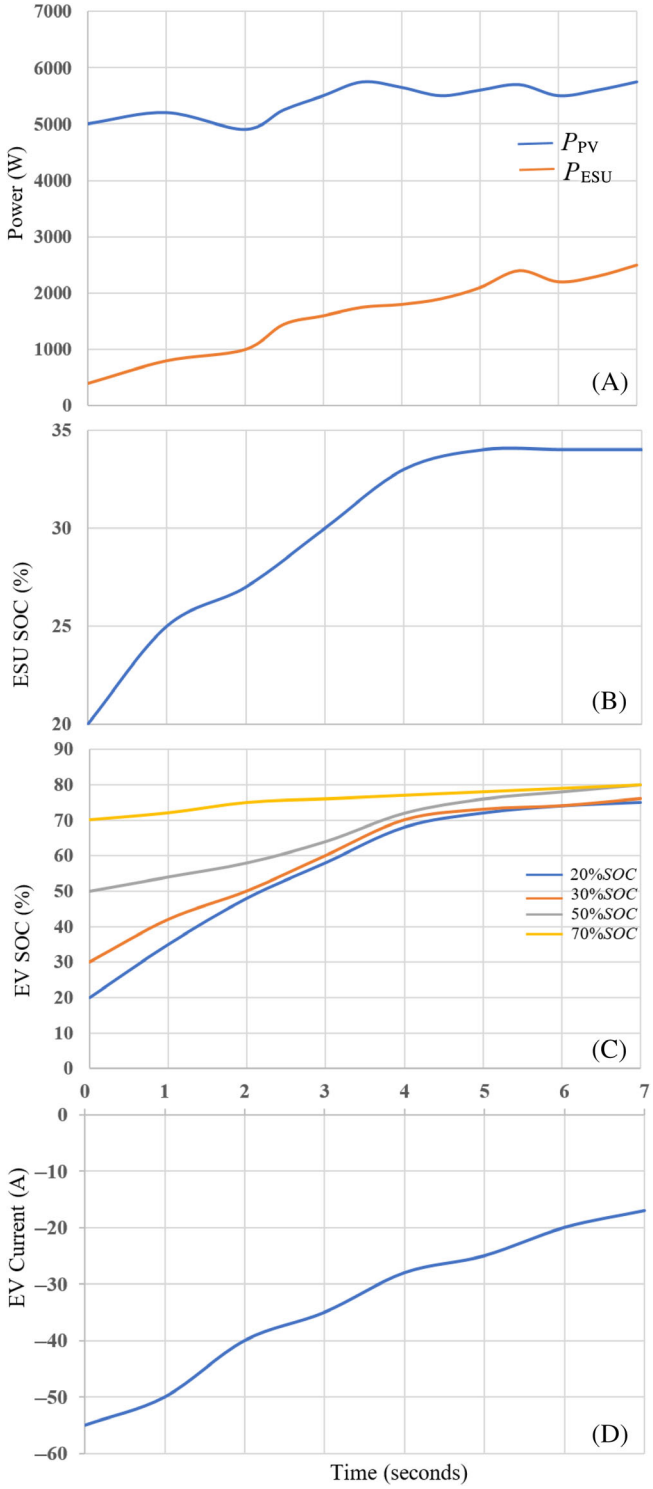

FIGURE 14 A, Solar power and ESU power. B, *SOC* of ESU. C, SOC of EV charging. D, Current drawn by EV Schematic view of the overall control strategy of the off-grid EVCS

5 | COMPARATIVE ANALYSIS

In the proposed PV-based EVCS, ESU plays an important role in stabilizing the DC bus voltage. The ESU's bidirectional converter is designed to keep the voltage level within the certain limits of *SOC* and *G′*. It is insufficient to regulate the voltage or the current through ESU with droop control or master-slave control alone while

25784862, 0, Downloaded from https://onlinelibrary.wiley.com/doi/10.1002/est2.442, Wiley Online Library on [21/01/2023]. See the Terms and Conditions (https://onlinelibrary.wiley.com/terms-and-conditions) on Wiley Online Library for rules of use; OA articles are governed by the applicable Creative Commons License

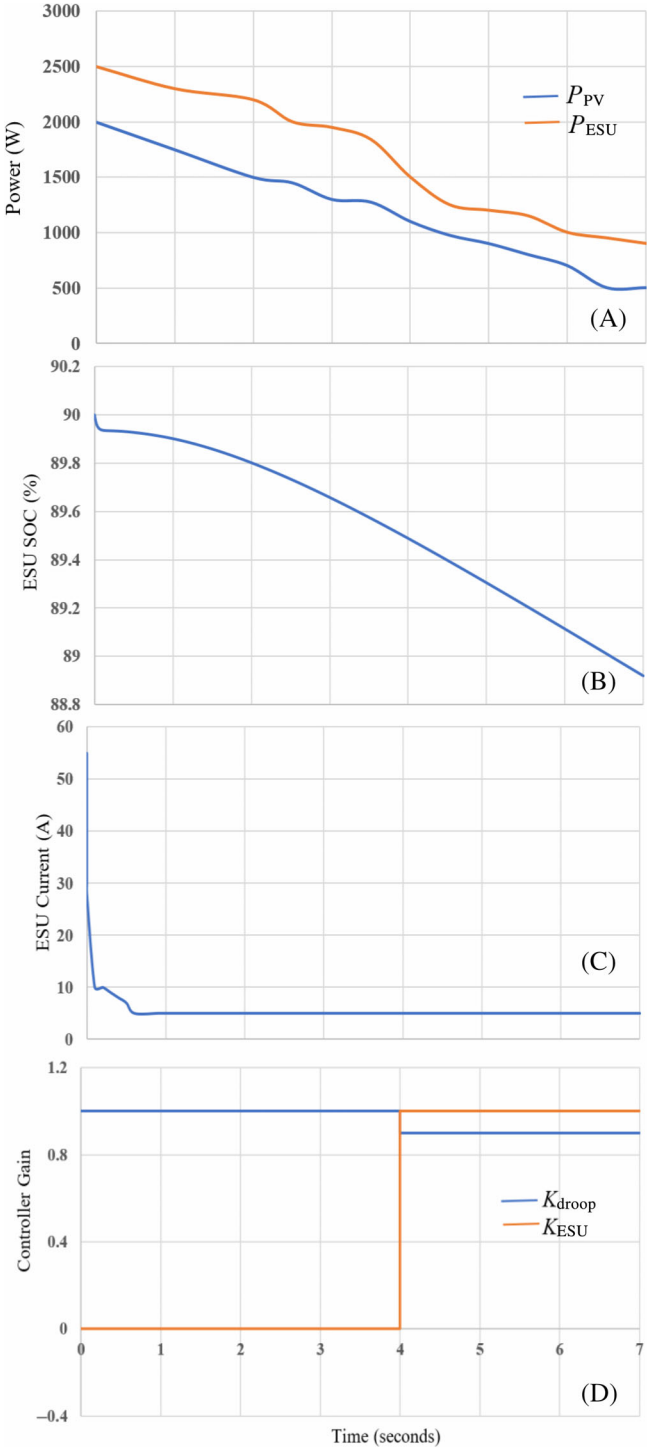

FIGURE 15 A, Solar power and ESU power. B, *SOC* of ESU. C, Charging current of ESU. D, Controller gain, K_{ESU} and K_{droop}

SOC is out of the limits. The larger gain of the control techniques causes more voltage deviation. To address the aforementioned problems, an extra control loop is necessary. Hence we implement both control techniques in the proposed PV-based EVCS which utilizes the merits of both droop and master-slave control techniques.

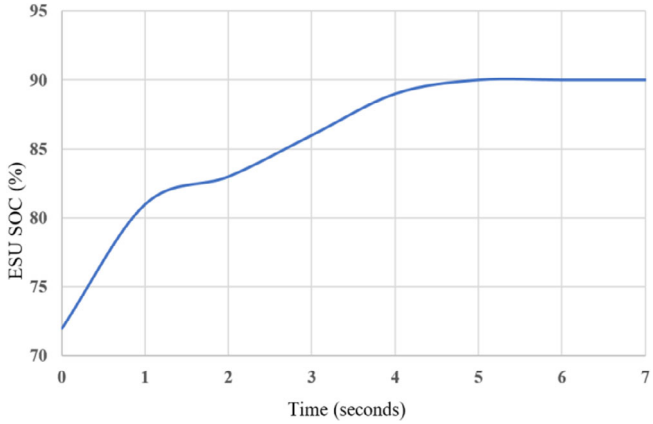

FIGURE 16 *SOC* of ESU

Figure 17A,B depicts DC bus voltage variations with master-slave control and droop control with active and passive snubber circuit in the proposed work alone, respectively. The DC bus voltage is shown in Figure 17C using a combination of master-slave and droop control approaches with active and passive snubber circuit in the proposed work. The bus voltage shifts down from the rated value while using the master-slave control technique alone or droop control alone. Note the fluctuations in the DC voltage in both these cases. However, the combination of the master-slave and droop control techniques along with active and passive snubber circuit provides a stable and uniform DC bus voltage. The combination of droop and master-slave control technique for the PV-based EVCS achieves the lowest voltage fluctuation in the DC bus voltage, thus enabling the ESU to slowly access the maximum allowable number of charge/discharge cycles, thereby enhancing the service life. Figure 17D depicts the DC bus voltage proposed by Huang et al.[26] Huang et al[26] reported a failure in achieving a uniform and stable DC bus voltage using a combination of master-slave and droop control techniques without active and passive snubber circuits, despite efforts. As a result, the service quality of ESU is declining over time.

The key device connecting the ESU and the DC bus is the bidirectional converter requiring a stable, reliable, and efficient topology. However, the bidirectional converter used by Huang et al,[26] results in significant voltage and current spikes during the connect/disconnect of the EVs to the system frequently. Moreover, the freewheeling current raises conduction losses and reduces the effective duty cycle. These problems are overcome with the help of an isolated bidirectional converter with active and passive snubber circuits in this paper. This converter achieves zero-voltage switching conditions quickly and effectively clamps the voltage spikes across the switches

25784862, 0, Downloaded from https://onlinelibrary.wiley.com/doi/10.1002/est2.442, Wiley Online Library on [21/01/2023]. See the Terms and Conditions (https://onlinelibrary.wiley.com/terms-and-conditions) on Wiley Online Library for rules of use; OA articles are governed by the applicable Creative Commons License

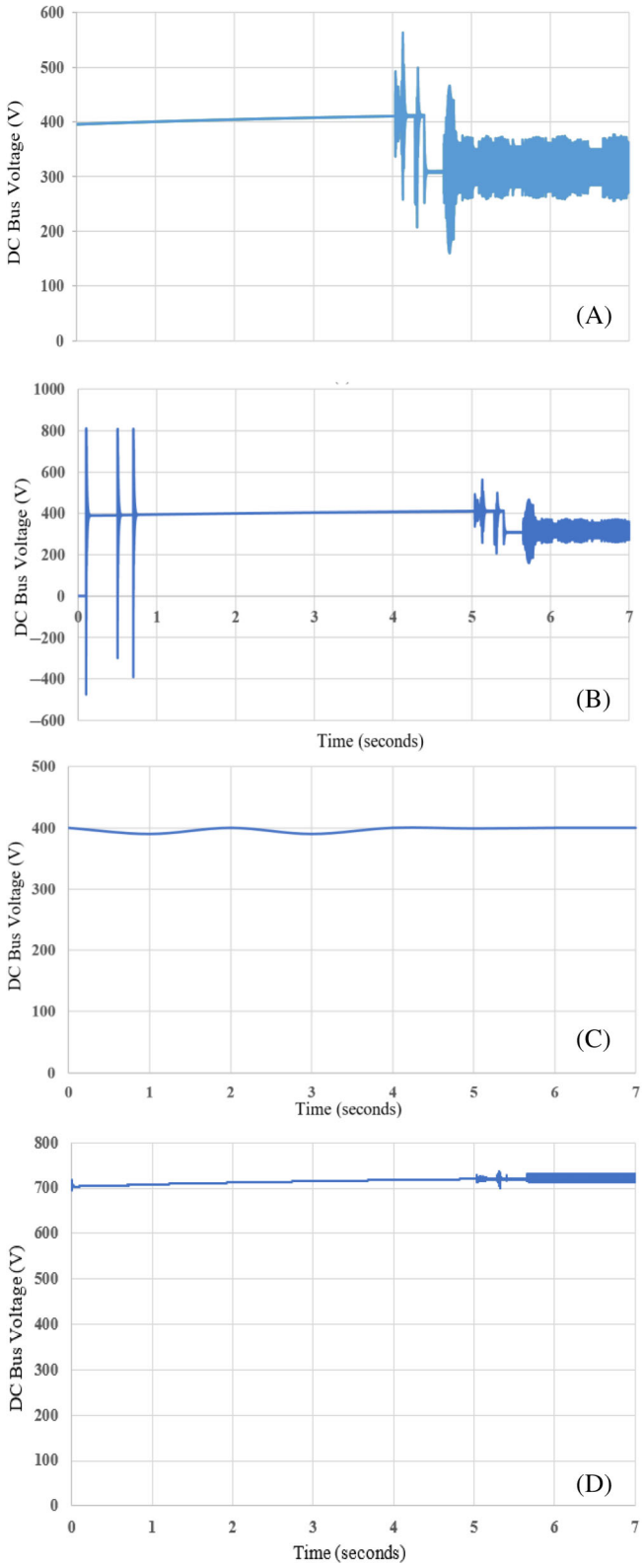

FIGURE 17 A, DC Bus voltage with master-slave control with active and passive snubber circuit in the proposed work. B, DC Bus voltage with droop control with active and passive snubber circuit in the proposed work. C, DC Bus voltage with the combination of master-slave and droop control with active and passive snubber circuit in the proposed work. D, DC bus voltage without active and passive snubber circuit used by Huang et al[26]

as compared to the bidirectional converter used by Huang et al,[26] thus improving the total efficiency of the PV-based EVCS.

Figure 18A,B shows the clamp branch voltage across the switches of the bidirectional converter used by Huang et al[26] and this work, respectively. It is clear from Figure 18A that the bidirectional converter used by Huang et al[26] creates high voltage stress across the switch, due to the presence of an inductor and does not attain zero-voltage switching conditions. However, in Figure 18B, the usage of an isolated bidirectional converter with snubber circuits in this work attains zero-voltage switching conditions instantaneously within a fraction of seconds. Thus, the isolated bidirectional converter with snubber circuits is the best option as it achieves zero-voltage switching by alleviating the voltage stresses across the main switches. It can be concluded from the above scenarios that the proposed off grid EV charging station utilizing PV generation will be competent to charge EVs under any conditions. Snubber circuits are used in the bidirectional DC-DC converter to ensure that the charging station is as energy-efficient as possible and to safeguard the system from high voltage and high

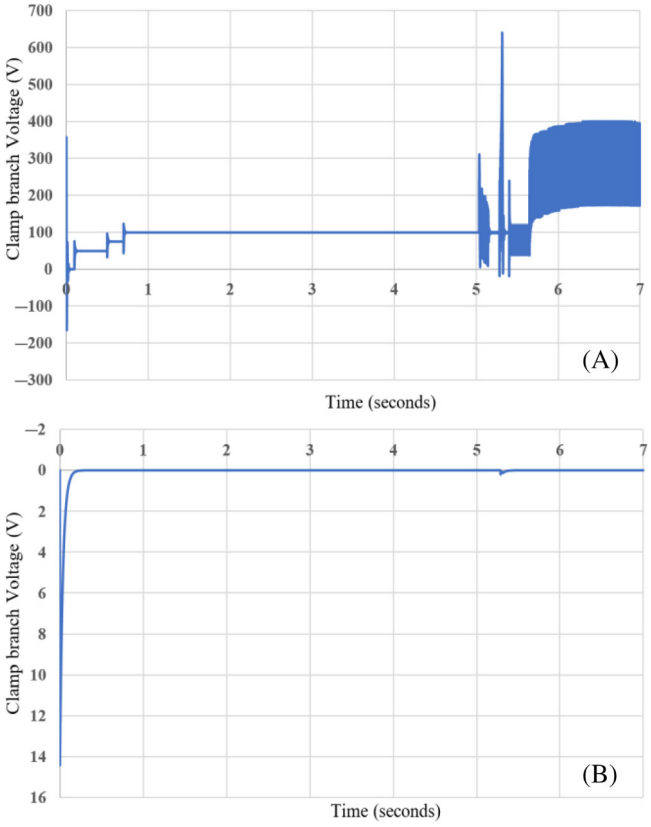

FIGURE 18 A, Clamp branch voltage of the bidirectional converter used by Huang et al.[26] B, Clamp branch voltage of the isolated bidirectional converter with active and passive snubber circuits in this work

25784862, 0, Downloaded from https://onlinelibrary.wiley.com/doi/10.1002/est2.442, Wiley Online Library on [21/01/2023]. See the Terms and Conditions (https://onlinelibrary.wiley.com/terms-and-conditions) on Wiley Online Library for rules of use; OA articles are governed by the applicable Creative Commons License

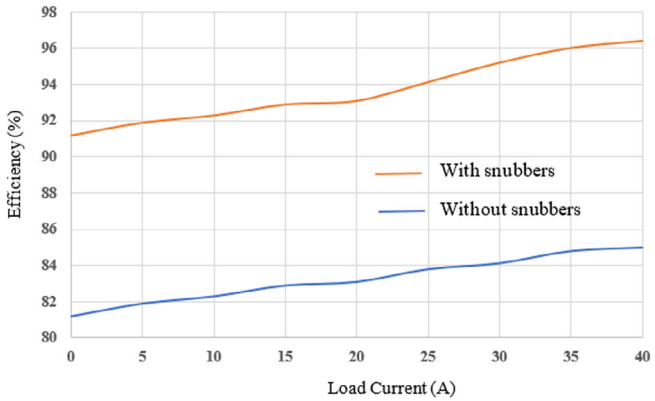

FIGURE 19 Plot of conversion effeciency of the proposed work

current strains. By keeping the input voltage constant, the efficiency curve is produced. With a fixed amount of input voltage of 400 V, Figure 19 displays the efficiency curves for inductor current fluctuation ranges of 2 to 40 A. As a result of the occupancy advantages of active and passive snubber circuits coupled with dual control schemes, the maximum efficiency of a bidirectional DC-DC converter without a snubber circuit is approximately 85%, whereas the highest efficiency of a bidirectional DC-DC converter with an active and passive snubber circuit combined with dual control schemes is 96.4%. Consequently, with active and passive snubber circuits, the bidirectional DC-DC converter achieves a higher efficiency than the bidirectional DC-DC converter without snubber circuits, in that the latter achieves lower efficiency.

6 | CONCLUSION

The paper proposes a combination control scheme for a PV-based EVCS with improved system stability as compared to a conventional master-control only or conventional droop control scheme only. The three-level boost converter designed to provide higher efficiency for PV generation is controlled by incremental and conductance MPPT and a capacitor voltage balance controller. The control schemes for the EV chargers and ESU with an isolated bidirectional DC-DC converter along with active and passive snubbers are also described. The combination of droop control and master-control scheme with active and passive snubber circuits maintains the DC bus voltage stable and constant at 400 V while obtaining the desired power. The proposed station's design is validated using MATLAB/Simulink, taking into account three alternative modes of EV operation. The design and control scheme is shown to be robust. The EVCS were also compared in terms of performance. The isolated bidirectional converter with snubber circuits achieves zero-voltage switching conditions more rapidly as compared to the converter without snubber circuits. This will enhance the system's reliability. An outstanding solution for PV-dependent EV charging stations with a conversion efficiency of 96.4% is provided by the combination of active and passive snubbers with a bidirectional DC-DC converter, a dual control system with master slave droop control technique, and an energy storage device. Using solar energy to electrify road transportation as well as deploys them in remote rural areas without access to the grids is within the scope of the proposed design.

There have been a number of observations made in the proposal that have been discussed below:

- EVCS based on DC supply technology is more suitable since there is less conversion loss involved.
- The charging station's ESU enables the efficient use of solar energy while ensuring that EVs can charge continuously.
- Through the use of master-slave and droop control techniques along with snubber circuits in the control of the EVCS, fast charging and discharging of the batteries can be accomplished as well as better regulation of DC bus voltages can be achieved.

By implementing new technologies for charging EVs, such as off-grid EVCS, smart charging techniques, electric vehicle control systems, and many more, a balance will be maintained in the energy sector, which in turn will maximize the use of renewable energy such as solar energy. Additionally, it will assist in communicating with the clients and ensuring that they are satisfied in addition to ensuring cost-effective charging rates. An optimized charging system will reduce the charging time for EVs, along with a stable DC bus voltage, which is very crucial for the efficient operation of the charging infrastructures for EVs. It is possible to promote a stable DC based off-grid EVCS system with the highest energy generation from renewable energy sources soon to meet the goals of reducing the dependency on fossil fuels. In addition, it can achieve zero emissions of environmentally harmful gases to provide electricity to expanding and dynamic electrical loads, such as the increasing popularity of electric vehicles.

ACKNOWLEDGMENT

The authors acknowledge gratefully for the support of School of Engineering, Computer and Mathematical Sciences, Auckland University of Technology, Auckland, New Zealand. Open access publishing facilitated by Auckland University of Technology, as part of the Wiley -

25784862, 0, Downloaded from https://onlinelibrary.wiley.com/doi/10.1002/est2.442, Wiley Online Library on [21/01/2023]. See the Terms and Conditions (https://onlinelibrary.wiley.com/terms-and-conditions) on Wiley Online Library for rules of use; OA articles are governed by the applicable Creative Commons License

Auckland University of Technology agreement via the Council of Australian University Librarians.

DATA AVAILABILITY STATEMENT

The data that support the findings of this study are available from the corresponding author upon reasonable request.

ORCID

Divya Krishnan Nair https://orcid.org/0000-0001-7416-4188

REFERENCES

1. Daza, JSO, Cristancho ACB, Restrepo M, Arango-Manrique A. Application software for studying the impact of electric vehicle charging stations in distribution systems. 2021 IEEE PES innovative smart grid technologies conference—Latin America, ISGT Latin America 2021 (2021). doi:10.1109/ISGTLATINAMERICA52371.2021.9543084
2. Electric Vehicles – Analysis - IEA. https://www.iea.org/reports/electric-vehicles. Accessed December 5, 2022.
3. Grasel B, Baptista J, Tragner M. Supraharmonic and harmonic emissions of a Bi-directional V2G electric vehicle charging station and their impact to the grid impedance. *Energies*. 2022;15:2920.
4. Paul Sathiyan S, Pratap CB, Stonier AA, et al. Comprehensive assessment of electric vehicle development, deployment, and policy initiatives to reduce GHG emissions: opportunities and challenges. *IEEE Access*. 2022;10:53614-53639.
5. Sheng K, Dibaj M, Akrami M. Analysing the cost-effectiveness of charging stations for electric vehicles in the U.K.'s rural areas. *World Electr Veh J*. 2021;12:232.
6. Mamidala S, Prajapati AK, Ravada S. Modeling of buck converter charging station to improve the power quality using three phase single tuned harmonic filter for electric transportation. Paper presented at: 2022 IEEE 2nd International Conference on Sustainable Energy and Future Electric Transportation, SeFeT 2022, Institute of Electrical and Electronics Engineers Inc., 2022. doi:10.1109/SeFeT55524.2022.9909306
7. Zou Y, Zhao J, Gao X, Chen Y, Tohidi A. Experimental results of electric vehicles effects on low voltage grids. *J Clean Prod*. 2020;255:120270.
8. Wang Z, Jochem P, Fichtner W. A scenario-based stochastic optimization model for charging scheduling of electric vehicles under uncertainties of vehicle availability and charging demand. *J Clean Prod*. 2020;254:119886.
9. Girard A, Roberts C, Simon F, Ordoñez J. Solar electricity production and taxi electrical vehicle conversion in Chile. *J Clean Prod*. 2019;210:1261-1269.
10. Krishnan Nair D, Prasad K, Lie TT. Standalone electric vehicle charging station using an isolated bidirectional converter with snubber. *Energy Stor*. 2021;3:e255.
11. Nair DK, Prasad K, Lie TT. Implementation of snubber circuits in a PV-based off-grid electric vehicle charging station—comparative case studies. *Energies*. 2021;14:5853.
12. Dave J, Ergun H, van Hertem D. Incorporating DC grid protection, frequency stability and reliability into offshore DC grid planning. *IEEE Trans Power Deliv*. 2020;35:2772-2781.
13. Mathew EC, Das A. A new isolated bidirectional switched capacitor DC-DC converter for exchanging power with MVDC grid. Paper presented at: 2022 IEEE IAS Global Conference on Emerging Technologies, GlobConET 2022 974–980, Institute of Electrical and Electronics Engineers Inc., 2022. doi:10.1109/GlobConET53749.2022.9872374
14. Top 5 Off Grid Solar Projects | Zonna Energy | 2022 List. https://www.zonnaenergy.com/top-off-grid-solar-projects/. Accessed December 5, 2022.
15. Leippi A, Fleschutz M, Murphy MD. A review of EV battery utilization in demand response considering battery degradation in non-residential vehicle-to-grid scenarios. *Energies*. 2022;15:3227. doi:10.3390/en15093227
16. Sasikumar G, Sivasangari A. Design and development of solar charging system for electric vehicles: an initiative to achieve green campus. *Nat Environ Pollut Technol*. 2021;20:801-804.
17. Ayyadi S, Maaroufi M. Optimal framework to maximize the workplace Charging Station owner profit while compensating electric vehicles users. *Math Probl Eng*. 2020;2020:1-12.
18. Azaroual M, Ouassaid M, Maaroufi M. Optimum energy flow management of a grid-tied photovoltaic-wind-battery system considering cost, reliability, and CO_2 emission. *Int J Photoenergy*. 2021;2021:1-20.
19. Shariff SM, Alam MS, Ahmad F, Rafat Y, Asghar MSJ, Khan S. System design and realization of a solar-powered electric vehicle Charging Station. *IEEE Syst J*. 2020;14:2748-2758.
20. Liemthong R, Srithapon C, Ghosh PK, Chatthaworn R. Home energy management strategy-based meta-heuristic optimization for electrical energy cost minimization considering TOU tariffs. *Energies*. 2022;15:537.
21. Tran VT, Islam MR, Muttaqi KM, Sutanto D. An efficient energy management approach for a solar-powered EV battery charging facility to support distribution grids. *IEEE Trans Ind Appl*. 2019;55:6517-6526.
22. Thang T, Ahmed A, Kim CI, Park JH. Flexible system architecture of stand-alone PV power generation with energy storage device. *IEEE Trans Energy Convers*. 2015;30:1386-1396.
23. Wu D, Tang F, Dragicevic T, Guerrero JM, Vasquez JC. Coordinated control based on bus-signaling and virtual inertia for islanded DC microgrids. *IEEE Trans Smart Grid*. 2015;6:2627-2638.
24. Xia Y, Yu M, Yang P, Peng Y, Wei W. Generation-storage coordination for islanded DC microgrids dominated by PV generators. *IEEE Trans Energy Convers*. 2019;34:130-138.
25. Mohamed K, Wolde HK, Al-Farsi AMS, Khan R, Alarefi SMS. Opportunities for an off-grid solar PV assisted electric vehicle charging station. Paper presented at: 11th International Renewable Energy Congress, IREC 2020, Institute of Electrical and Electronics Engineers Inc., 2020. doi:10.1109/IREC48820.2020.9310376
26. Huang H, Balasubramaniam S, Todeschini G, Santoso S. A photovoltaic-fed dc-bus islanded electric vehicles charging system based on a hybrid control scheme. *Electronics*. 2021;10:1142.
27. Atawi IE, Hendawi E, Zaid SA. Analysis and design of a standalone electric vehicle charging station supplied by photovoltaic energy. *Processes*. 2021;9:1246.
28. Spertino F, Ciocia A, di Leo P, Malgaroli G, Russo A. A smart battery management system for photovoltaic plants in households based on raw production forecast. http://www.intechopen.com. Accessed December 5, 2022.

25784862, 0, Downloaded from https://onlinelibrary.wiley.com/doi/10.1002/est2.442, Wiley Online Library on [21/01/2023]. See the Terms and Conditions (https://onlinelibrary.wiley.com/terms-and-conditions) on Wiley Online Library for rules of use; OA articles are governed by the applicable Creative Commons License

29. Jagtap S, Khandekar A. Implementation of combined system between perturb observe and incremental conductance technique for MPPT in PV system. Paper presented at: 2021 2nd Global Conference for Advancement in Technology, GCAT 2021, Institute of Electrical and Electronics Engineers Inc., 2021. doi:10.1109/GCAT52182.2021.9587457
30. Stephen AA, Musasa K, Davidson IE. Modelling of solar PV under varying condition with an improved incremental conductance and integral regulator. *Energies*. 2022;15:2405.

How to cite this article: Krishnan Nair D, Prasad K, Lie TT. Design of a PV-fed electric vehicle charging station with a combination of droop and master-slave control strategy. *Energy Storage*. 2023;e442. doi:10.1002/est2.442

25784862, 0, Downloaded from https://onlinelibrary.wiley.com/doi/10.1002/est2.442, Wiley Online Library on [21/01/2023]. See the Terms and Conditions (https://onlinelibrary.wiley.com/terms-and-conditions) on Wiley Online Library for rules of use; OA articles are governed by the applicable Creative Commons License